NOVEL ANALYTICAL APPROACHES FOR STUDYING DEGRADATION IN POLYPROPYLENE AND PROPYLENE-1-PENTENE COPOLYMERS

by

STEFAN DE GOEDE

Dissertation presented for the degree of
Doctor of Science (Polymer Science)

at the
University of Stellenbosch

Promoter: Prof. H Pasch
Co-promoter: Prof. R D Sanderson

University of Stellenbosch
April 2006

DECLARATION

I, the undersigned, hereby declare that the work contained in this dissertation is my own original work and has not previously been submitted in its entirety or in part at any university for a degree.

Signature:_____ Date:_____

ABSTRACT

Commercial polyolefins degrade under the influence of light, heat, chemical and mechanical factors. They are therefore stabilised to ensure that they maintain performance characteristics during their service life. Degradation results in changes in the molar mass, molar mass distribution, chemical composition and chemical composition distribution. Classical analytical techniques only provide averaged values of these properties. Much information is available in the open literature on the changes in molar mass, molar mass distribution and chemical composition of polypropylene upon degradation, but no information was available on the changes in chemical composition distribution (CCD) during degradation.

This study describes the use of the following analytical techniques to study this: temperature rising elution fractionation (TREF), crystallisation analysis fractionation (CRYSTAF) and coupled size exclusion chromatography-Fourier transform infrared analysis (SEC-FTIR). The CRYSTAF results complimented those obtained by classical techniques: there was a broadening of the crystallisation peak (CCD), an increase in the soluble fraction and a decrease in crystallisation temperatures. SEC-FTIR analysis showed that most of the degraded products were concentrated in the low molar mass regions. TREF analysis was used to separate a degraded sample into fractions of different degrees of degradation. It was then possible to study the spatial heterogeneity in a thick, degraded polypropylene sample using SEC, FTIR and CRYSTAF.

The degradation behaviour of selected Sasol propylene-1-pentene random copolymers was investigated. CRYSTAF, SEC-FTIR and TREF analyses provided information on the thermo-oxidative degradation behaviour differences between unstabilised polypropylene homopolymers and these propylene-1-pentene copolymers. It was found that the pentene copolymers degraded significantly faster compared to the homopolymers, even at low levels of pentene (< 3%). The reduction in stability was virtually linear with an increase in pentene content (up to 8 mol% pentene), indicating that higher levels of primary stabilisers are needed to ensure similar life spans for the Sasol propylene-1-pentene copolymers. The extrusion stability of the propylene-1-pentene copolymers was, however, similar to that of the polypropylene homopolymers, indicating that similar processing stabiliser packages may be used.

OPSOMMING

Kommersieële poli-olefiene degradeer onder die invloed van lig, hitte, chemiese en meganiese faktore. Poli-olefiene word om die rede gestabiliseer om the verseker dat die poli-olefien sy verrigtingseienskappe behou gedurende sy diensleeftyd. Degradasie lei tot veranderinge in die molekulere massa, molekulere massaverspreidings, chemiese samestelling en chemiese samestellings-verspreiding van n poli-olefien produk. Klassieke analitiese tegnieke verskaf slegs gemiddelde waardes van die eienskappe. n Groot hoeveelheid informasie beskikbaar aangaande die veranderinge in molekulere massa, molekulere massaverspreiding en chemiese samestelling gedurende die degradasie van polipropileen. maar geen informasie was beskikbaar aangaande die veranderinge in chemiese samestellings-verspreiding gedurende die degradasie proses.

Die studie beskryf die gebruik van die volgende analitiese tegnieke om die eienskappe te bestudeer: “temperature rising elution fractionation” (TREF), “crystallisation analysis fractionation” (CRYSTAF) en “size exclusion chromatography-Fourier transform infrared spectroscopy” (SEC-FTIR). Die CRYSTAF analises het inligting gekomplimenteer wat met klassieke analitiese tegnieke verkry is: daar was n verbreding van die kristallisasiepiek, n verhoging in die oplosbare fraksie en n afname in die kristallisasietemperature. SEC-FTIR analise het bewys dat meeste van die degradasieprodukte in die lae molekulere massagebied gekonsentreer was. TREF analise is gebruik om die gedegradeerde monster in fraksies van verskillende degradasievlakke te skei.

Die degradasie-gedrag van geselekteerde Sasol propileen-1-penteen ko-polimere is bestudeer. CRYSTAF, SEC-FTIR en TREF analises het meer informasie aangaande die verskille in die termo-oksidatiewe degradasieprosesse tussen polipropileen homopolimere en propileen-1-penteen kopolimere. Dit is bevind dat die penteen kopolimere heelwat vinniger degradeer as die homopolimere, selfs by lae penteeninhoud (<3%). Die verlaging in stabiliteit was omtrent lineêr met n verhoging in penteenvlakke (tot 8 mol%), n aanduiding dat hoër vlakke van primêre stabilisering benodig word om leeftye soortgelyk aan die van die Sasol homopolimeer te verseker. Die ekstrusieverrigting van die propileen-1-penteen kopolimere was soortgelyk aan die van die homopolimeer, sodat soortgelyke vlakke van die sekondêre stabiliseerders benodig word om ekstrusieverrigting te verseker.

DEDICATION

To my parents

ACKNOWLEDGEMENTS

I wish to express my sincerest gratitude to the following people and institutions:

My study leader Prof. Dr. H Pasch for his endless patience and guidance with this work and for organising my experimental work in Germany

My co-promoter Prof R.D. Sanderson for his help with this study

Dr. Niall Marshall for his help with the conceptualisation of the project and his valuable insight throughout this project

Dr. R Brüll for his help with the experimental work at the Deutsches Kunststoff-Institut (DKI) in Darmstadt, Germany

Dr. Margie Hurndall for her help with editing this thesis. Thanks for your endless time and patience.

Dr. Udo Wahner for his help with the interpretation of the NMR spectra and the synthesis of the samples used in Chapter 6

Heidi Assumption (Sastech) and Dr. Wolf Hiller (DKI) for their help with the NMR investigations

Christoph Brinkmann at the DKI for his help with the SEC investigations in Chapter 6 and 7

Dr. L Siphuma for his help with the CRYSTAF analyses in Chapter 6

To my parents for their love, trust and support through my study career

Karol Cameron and Dr. John Mellor at Sasol Polymers for their guidance, financial support and assistance with this work

My friends, Jerrie, Henk, Anita, Robert, Sven, Dawid, Udo, Aletti, Udo, Malcolm, David, Marietjie, Marissa and Thalma for their support throughout my study career

Robert, Jerrie, Rishi, Heidi, Elias and Recardo for their assistance with this work

Sasol Polymers for financial support with this work

I would also like to thank the German Ministry of Education and Research (BMBF, Jülich), for a research grant (Project-Code 39.6.L2A.7.A)

LIST OF CONTENTS

LIST OF FIGURES

Chapter 7

Chapter 8

LIST OF TABLES

LIST OF ABBREVIATIONS

A	Absorbance
AO	Anti-oxidant
ASTM	American Society of Testing Materials
ATR	Attenuated total reflectance
BHT	Butylated hydroxy toluene
c	The concentration of the absorbing species
CCD	Chemical composition distribution
CFB	Continuous fluidised bed
CL-OIT	Chemiluminescence oxidation induction time
Cr	Chromium
CRYSTAF	Crystallisation analysis fractionation
CSDF	Chain scission distribution function
DEGMBE	Diethylene glycol monobutyl ether
DNPH	Dinitrophenylhydrazine
DtBpC	Di-tertiary butyl para-cresol
DRI	Differential refractive index
DSC	Differential scanning calorimetry
DSC-OIT	Differential scanning calorimetry oxidation induction time
d-TCE	Deuterated tetrachloroethane
ε	Absorptivity or extinction coefficient
EPDM	Ethylene propylene diene monomer
EPR	Ethylene propylene rubber
ESCR	Environmental stress cracking resistance
ESR	Electron spin resonance
FTIR	Fourier-transform infrared
GC	Gas chromatograph
GC-MS	Gas chromatography-mass spectrometry
g/mol	Grams per mol
GPC	Gel permeation chromatography
G(t)	Relaxation modulus
G'(ω)	Storage modulus
G"(ω)	Loss modulus
HAS	Hindered amine stabiliser
HALS	Hindered amine light stabiliser
HDPE	High-density polyethylene
HT-FT	High-temperature Fischer Tropsch
HT-SEC	High-temperature size exclusion chromatography
IR	Infrared
l	The length of the optical path through the sample
LDPE	Low density polyethylene
LLDPE	Linear low density polyethylene
LTTS	Long-term thermal stability
M_e	Molar mass between entanglements
MFI	Melt flow index
MMD	Molar mass distribution
M_n	Number average molar mass
M_w	Weight average molar mass
MWDCA	Molecular weight distribution computer analysis
M_z	z-average molar mass
NBS	National Bureau of Standards
NMR	Nuclear magnetic resonance

$NO^{\cdot}$	Nitroxyl radical
ODCB	Ortho- dichlorobenzene
OIT	Oxidation induction temperature
OIt	Oxidation induction time
PE	Polyethylene
PET	Polyethylene terephthalate
PI	Polydispersity index
PP	Polypropylene
Prep-TREF	Preparative-temperature rising elution fractionation
Pyrolysis-GC	Pyrolysis gas chromatography
R·	Alkyl radical
RI	Refractive Index
ROOH	Hydroperoxide
ROO·	Peroxy radical
SAS	Sasol Advanced Synthol
SAXS	Small angle X-ray scattering
SCB	Short-chain branching
SCBD	Short-chain branching distribution
SEC	Size exclusion chromatography
SEC-FTIR	Size exclusion chromatography-Fourier transform infrared
T_c	Temperature of crystallisation
TCB	1,2,4 trichlorobenzene
$TiCl_3$	Titanium chloride
T_m	Melting temperature
TREF	Temperature rising elution fractionation
UK	United Kingdom
ULDPE	Ultra low-density polyethylene
UV	Ultraviolet
WAXS	Wide angle X-ray scattering
XRD	X-ray diffraction
YI	Yellowness index

LIST OF REACTION SCHEMES

Chapter 2

Chapter 5

Chapter 6

Chapter 8

Chapter One

Introduction and objectives

1.1 Introduction

Polyolefins are the most widely used class of synthetic polymers in the world and constitute more than 50% of all synthetic polymers produced worldwide. Polyolefin consumption is growing at a substantial rate and will continue to grow over the next decades [1]. Polyolefins are synthesised under specific conditions to yield polymer molecules with well-defined structures. The polymer structure can be described in terms of the molar mass properties (molar mass and molar mass distribution). However, this is not sufficient to fully describe the molecular heterogeneity. The chemical composition and chemical composition distribution as well as the molecular topology are also important parameters in describing the polymer structure.

Polyolefins degrade under the influence of light, heat and several other factors. Degradation of polyolefins may take place during processing, application and recycling. Degradation is initiated by the formation of a radical (initiation) and is followed by propagation, branching and termination reactions. The study of polymer degradation is a field of immense interest to the polymer scientist and has received significant attention in literature [2, 3, 4].

During degradation of polyolefins, the polymer structure changes to a significant extent. The changes in the polymer structure influence the polymer performance properties, thereby usually limiting the lifetime of the materials and leading to economic restrictions [5, 6]. In particular, the increasing importance of polymer recycling is a strong motivation to search for new analytical methods to analyse the degradation of polyolefins [7]. One can distinguish photo-oxidative and thermo-oxidative degradation. Polyolefins can also be attacked by strong acids and bases [8]. Polyolefin samples may, under the influence of external factors, degrade via chain scission or crosslinking mechanisms. Over the past decades, very few new approaches for studying degradation in polyolefins have been developed. Most studies have focused on the changes in molar mass and molar mass distribution, as determined by high-temperature size-exclusion chromatography (HT-SEC) or melt flow index (MFI) measurements. The bulk chemical composition has also received significant attention and can be studied by several techniques, like nuclear magnetic resonance spectroscopy (NMR) and Fourier-transform infrared spectroscopy (FTIR). However, prior to the present study, no data were available on changes in the chemical composition and chemical composition distribution during degradation as a function of molar mass.

The chemical composition distribution (CCD) can be quantified by temperature-rising elution fractionation (TREF). There are two types of TREF, analytical TREF and preparative TREF. In a TREF experiment, a polymer is slow crystallised at a controlled rate. The subsequent slow dissolution is then monitored (for analytical-TREF) or samples are collected (preparative-TREF). The time required for a TREF separation is, however, excessive. This subsequently resulted in the development of crystallisation fractionation (CRYSTAF), a relatively new analytical approach to the quantification of the chemical composition distribution in polyolefin samples [9, 10]. In a CRYSTAF experiment, a polyolefin sample is dissolved at elevated temperatures. The slow cooling step is then followed and the concentration of the polymer in solution is plotted. A CRYSTAF crystallisation curve provides useful information on the chemical composition distribution of polyolefins and results are obtained in a significantly shorter time span compared to TREF. The coupling of SEC and FTIR (SEC-FTIR) through the LC transform approach has also recently received much attention [11]. The advantage of SEC-FTIR is that it can provide chemical composition (FTIR) data as a function of polymer molar mass.

In this dissertation, a very significant change in the CCD in a polypropylene homopolymer sample during the degradation process is reported. Differences between the CCD changes of polypropylene homopolymers and propylene-1-pentene copolymers are also reported. The changes in molecular heterogeneity upon degradation were monitored using novel techniques for polyolefin analysis.

1.2 Objectives and methodology

The main objectives of this study, and relevant methodology, were the following:

1. The main objective of the first section of the study was to investigate the use of hyphenated (SEC-FTIR) and fractionation (CRYSTAF and TREF) analytical techniques to compliment the information obtained from the classical analytical techniques (SEC, FTIR and DSC) in studying degradation in polypropylene. This was carried out to provide more information on the changes in the chemical composition distribution of polyolefin samples with degradation. An unstabilised, commercial Ziegler-Natta polypropylene homopolymer sample was to be used to evaluate the applicability of novel analytical approaches to studying degradation in polyolefins. Samples were to be analysed by the classical techniques for studying polyolefin degradation: SEC (decrease in molar mass) and FTIR (increase in carbonyl

functionalities). Subsequently, SEC-FTIR analysis was to be carried out to establish the distribution of the degradation products as a function of molar mass. CRYSTAF was then to be used to establish the effect of thermo-oxidative degradation on the chemical composition distribution. A degraded sample was then to be subjected to TREF to establish whether a degraded sample can be successfully separated by TREF. A degraded sample was to be microtomed to determine the spatial heterogeneity of a degraded sample. The microtomed layers were then to be subjected to SEC, FTIR and CRYSTAF analyses to study the differences in chemical composition and chemical composition distribution of these layers.

2. The second overall objective was to evaluate the degradation behaviour of an unstabilised commercial polypropylene homopolymer sample with an MFI of 4 and a density of around 0.910 (produced using a Ziegler-Natta catalyst system) and contrast the degradation behaviour with that of two commercial unstabilised propylene-1-pentene copolymer samples with MFI's of 11 and 14 respectively (see Chapter 6 for more details on the samples). The most important question to be answered here was how the incorporation of an intrinsically less stable comonomer into a polypropylene chain would influence the degradation behaviour of the unstabilised copolymer. This information is considered essential in order to establish the stabiliser requirements of the polypropylene homopolymer and copolymer systems (will not be covered in this thesis). The changes in polymer chemical composition distribution with thermo-oxidative degradation were to be investigated at two temperatures: 70 ºC and 90 ºC. Another objective was to study the effect of pentene incorporation on the degradation behaviour.
3. The third overall objective was to evaluate the degradation behaviour of laboratory-synthesised propylene-1-pentene copolymer samples, containing up to 8 mol% pentene.
4. The fourth objective was to evaluate the multiple extrusion behaviour of a polypropylene homopolymer and contrast the behaviour with that of a propylene-1-pentene sample. This was, again, to be carried out using the classical analytical techniques (SEC and FTIR) as well as fractionation techniques. A new model, developed by Canevarolo [12], was to be used to evaluate the number of scissions as a function of molar mass. This was to be carried out to see if any differences observed in the thermo-oxidation behaviour of the polypropylene homopolymer sample and the propylene-1-pentene sample under thermo-oxidative degradation (see objective 3) would also be valid for oxygen deficient degradation under high shear conditions.

1.3 Motivation for this study

Sasol Polymers recently introduced a range of random propylene-1-pentene copolymers into the marketplace. These copolymers are unique to Sasol Polymers and are not produced on a commercial scale by any other company. Due to the uniqueness of these polymers, not much information is available in the open literature on their molecular structure. It was also found that the stabiliser requirements of these copolymers were higher compared to the polypropylene homopolymers. The stabilised copolymers, however, showed a tendency to yellow during normal use. Although the degradation behaviour of stabilised propylene-1-pentene samples has been studied in depth [13], the degradation behaviour of the unstabilised propylene-1-pentene copolymers has not yet been studied. The extrusion behaviour of the propylene-1-pentene copolymers has also not yet been studied.

1.4 Layout of this dissertation

This dissertation is divided into nine chapters and is presented in such a way that the individual experimental chapters (Chapters 5-8) can stand alone, i.e. they can be read with minimal knowledge required from previous chapters. Therefore, there may be some unavoidable repetition in some chapters.

- All experimental chapters (Chapters 5-8) are divided into the following sections: background (and/or introduction), objectives, experimental, results and conclusions. The overall conclusions are summarised in Chapter 9.
- Chapter 1 provides a brief introduction to this dissertation, as well as the objectives and methodology, and motivations for this study.
- Chapter 2 provides a background on the current state of knowledge on the degradation of polyolefins. The effect of different stabiliser systems is also to be briefly reviewed.
- In Chapter 3 some of the classical methodologies used to evaluate polyolefin degradation are discussed. Oven aging, multiple extrusions and photo-degradation of polymers are discussed in terms of applicability and the information obtained from these techniques. The classical analytical techniques used for monitoring degradation in polyolefins, including FTIR, DSC, chemiluminescence, and the determination of mechanical properties and the yellowness index are also reviewed.
- In Chapter 4, newer analytical methods for determining the chemical composition distribution in polyolefins namely TREF, SEC-FTIR and CRYSTAF, are discussed.

- In Chapter 5 the abovementioned novel analytical approaches for studying degradation in polyolefins are evaluated and discussed.
- In Chapter 6 the degradation behaviours of a polypropylene homopolymer and two commercial propylene-1-pentene copolymers are determined and discussed.
- In Chapter 7 the degradation behaviour of propylene-1-pentene copolymers, with higher pentene contents (up to 8%), is determined and discussed.
- In Chapter 8 the multiple extrusion behaviour of a commercial propylene-1-pentene sample is determined and compared with that of a polypropylene homopolymer.
- Overall conclusions are presented in Chapter 9.

1.5 References

[1] Maack Business Services, Polypropylene 2003 Conference, Zürich, 15-17 September 2003

[2] Colom, X., Canavate, J., Sunol, J.J., Pages, P., Saurina, J. Carrasco, F., *Journal of Applied Polymer Science* **2003**, 87, 1685-1692

[3] Gugumus, F., *Polymer Degradation and Stability* **1998**, 62, 403-406

[4] Gugumus, F., *Polymer Degradation and Stability* **2000**, 68, 21-33

[5] Struik, L.C.E., *Polymer* **1987** 28, 1521-1533

[6] Halim Hamid, S., *Handbook of Polymer Degradation,* Marcel Dekker Inc., New York **2000**

[7] Michaeli, W., Bittner, M., in “Recycling von Kunststoffen”, editors: Menges, G., Michaeli, W., Bittner, M., Carl Hanser Verlag, München, **1992**

[8] “Encyclopedia of Polymer Science”, Editor: Korschwitz, J., J Wiley, New York **1986**

[9] Monrabal, B., Presentation at the GPC conference, Waters 2000

[10] Monrabal, B., *Macromolecular Symposia* **1996**, 110, 81-86

[11] Willis, J.N., Dwyer, J.L., Liu, X., Dark, W., *ACS Symposium* **1999**, 226-231

[12] Canevarolo, S.V., *Polymer Degradation and Stability,* Volume 70, Issue 1, **2000**, 71-76

[13] Marshall, N., PhD thesis, University of Sussex, **December 2001**

Chapter Two

Degradation in polyolefins: A literature review

2.1 Introduction

2.1.1 Polyolefins: An overview

Polyolefins are the most widely used synthetic polymers in the world, constituting more than 50% of all the synthetic polymers produced worldwide [1]. In numerous applications, polyolefins have replaced traditional materials like wood and metal. Their light weight and relatively low cost make them suitable for use in applications where high strength and durability are required. There are two major classes of polyolefins:

1. Polyethylene (PE) and copolymers of ethylene
2. Polypropylene (PP) and copolymers of propylene

Of a worldwide polyolefin capacity of approximately 107 megatons per annum in 2002, polyethylene constituted approximately 60% of the world market (68 megatons per annum) and polypropylene 27% (39 megatons per annum) [1]. It is predicted that in 2005, in Western Europe alone, 11 megatons polypropylene will be consumed. These two classes of polyolefins are used for thousands of applications, varying from the manufacture of small plastic bags to large rotomoulded tanks with a capacity of more than 20,000 litres.

Polyethylenes differ in branching type and branching distribution. Low density polyethylene (LDPE) is characterised by a long-chain randomly branched structure with short-chain branches of different lengths. The short-chain branches are mostly between two and four carbons long, and are responsible for the control of the density in LDPE. LDPE is usually made in a high-pressure and high-temperature process and oxygen or peroxides are used as initiators. Commercially, there are two fabrication processes, namely the autoclave (vessel) process and the tubular process. These two processes (autoclave and tubular processes) yield LDPE resins with slightly different properties. The molar mass distribution (MMD) of LDPE is usually broad. LDPE is used in several applications, especially where optical properties and ease of processing are of importance.

In linear low density polyethylene (LLDPE) the short-chain branching is introduced into the polymer chain by the addition of a comonomer. Commercially, butene, hexene and octene are used to modify the density of LLDPE. All the branches are similar in length (for example, with butene added, the side chains will be two carbons in length while the other two carbons will be incorporated in the main chain). Supported Ziegler-Natta catalysts are typically used. Characteristic of this catalyst system is an uneven distribution of the branching as a function

of molar mass, with the incorporation of much branching in the low molar mass region. Production conditions are mild in comparison with LDPE and moderate pressures and temperatures are employed during synthesis.

Newer metallocene-based systems can be used to make the branching distribution more uniform and to narrow the molar mass distribution. This, however, makes metallocene-LLDPE more difficult to process compared to Ziegler-Natta-LLDPE.

High-density polyethylene (HDPE) is also a major polyethylene family and is characterised by the absence of long- and short-chain branches. Small amounts of short-chain branches are usually incorporated (by addition of a comonomer) to modify the density. Two catalyst systems are used for the synthesis of HDPE: Ziegler-Natta (giving relatively narrow MMD) and chromium catalysts (giving relatively wide MMD).

In industry, two types of polypropylene polymers are produced: polypropylene homopolymers and polypropylene copolymers. Homopolymers can further be described in terms of tacticity [2]. In isotactic polypropylene all methyl groups are distributed evenly along the polymer chain, and is the result of head-to-tail addition of the monomer units. The methyl group always has the same configuration in relation to the polymer backbone. Syndiotacticity is also the result of head-to-tail additions, but the methyl group has an alternating configuration with regards to the polymer backbone. In an atactic polypropylene sample there is no consistent placement and distribution of the methyl group.

There are two classes of polypropylene copolymers. Random copolymers are manufactured by the same process as the homopolymer, but instead of the pure monomer, a mixture of propylene and a comonomer is introduced into the reactor (usually between 2 and 6 weight % of the comonomer). The incorporation of a comonomer results in a lowering in the melting point and the density. Random copolymers are usually higher in clarity compared to the homopolymers.

Impact block copolymers are made in a two-stage process and contain phase-separated areas of ethylene-propylene elastomer in the polypropylene matrix. This improves impact strength significantly and is responsible for increased toughness.

2.1.2 Polyolefins and degradation

Already in 1946, Bolland and Gee described possible degradation mechanisms and reactions in polymers [3]. Polyolefins are unstable towards environmental factors and need to be properly stabilised to maintain their properties through their lifetime. If the preferential route of degradation is known, a stabiliser package can be added to ensure the properties of the polyolefin are maintained during their lifetime. The degradation of polyolefins is a complex process involving many possible reactions. It has been studied extensively by several classical techniques. Degradation can be initiated by several processes, the only requirement is the formation of a radical which is able to initiate the degradation process. Any process that results in the formation of reactive alkyl radicals can activate a polymer towards degradation. Thermal factors (thermal degradation), light-induced degradation (photo-oxidation), mechanical factors (mechanical degradation) are all possible initiators of the degradation process. Even during initial extrusion (on the production plant) a polyolefin needs to be stable towards thermo-mechanical and thermo-oxidative degradation.

Alkyl radicals can react with oxygen or undergo reactions of disproportionation or recombination to form crosslinks or chain branches. The preferential route of degradation (disproportionation or recombination) will depend on several factors, including the polymer composition and degradation conditions. For example, HDPE (made with a chromium catalyst) will degrade preferentially through crosslinking, while HDPE (made with a Ti catalyst) degrades through chain scission reactions [4].

When polyolefins are exposed to shear, stress, mechanical factors, heat, light, water and radiation, chemical reactions may start in the polymer that may change the chemical composition and the molar mass of the polymer. Typical changes in the polymer mechanical properties include a decrease in strength, stiffness or flexibility, discolouration and scratching, and a loss of gloss.

Polymer oxidation (also referred to as oxidative degradation) takes place when the polymer reacts with molecular oxygen. A prerequisite for oxidation is, therefore, the presence of oxygen, dissolved in the polymer. Degradation will result in a polymer with inferior properties compared to the original unaged material. Several factors may contribute to the degradation of polyolefins:

1. Conditions during synthesis. Exposure to very high temperatures during synthesis may result in degradation of the polymer.
2. Post-synthesis processing. If the polymer is not adequately stabilised it may already start degrading during processing, leading to changes in the optical, mechanical and other performance properties.
3. Environmental factors; polyolefins degrade during normal use.

2.2 Mechanisms of degradation in polyolefins

There are a few main mechanisms for the degradation of polyolefins [5]:

1. Thermal degradation
2. Photo-degradation
3. Oxidative degradation
4. Mechanical degradation

The reaction of a polyolefin with oxygen will lead to the formation of oxygen-containing functionalities through a sequence of reactions, known as auto-oxidation. During outdoor exposure, light initiated breakdown (photo-degradation or photo-oxidation) predominantly takes place, followed by thermally initiated reactions. High temperatures are usually not encountered during normal exposure and temperatures above the crystalline melting points are not encountered for extended periods of time. Irradiation can also lead to the degradation of polymers. γ-Irradiation may result in crosslinking or scission of polyethylene chains, depending on the conditions of degradation [6].

Polyolefins may degrade in the absence of light if they are exposed to extreme temperatures. However, thermally initiated oxidation of isotactic polypropylene can occur at temperatures as low as room temperature if the sample is unstabilised. Adams and others [7] attributed the decrease in the molar mass of polypropylene to monomolecular breakdown (β-scission) of alkoxy radicals that form during oxidative degradation. Degradation in polyolefins can be described by a simplified degradation cycle. The Ciba cycle [8] for the thermo-oxidation of polyolefins is given in Figure 1.

The formation of a polymer (alkyl) radical by hydrogen abstraction or chain scission will initiate the degradation cycle. In polypropylene, the tertiary hydrogen atom can be easily abstracted during degradation.

The general degradation mechanism of polyolefins will now be reviewed. The degradation reactions can be divided into initiation, propagation, branching and termination reactions.

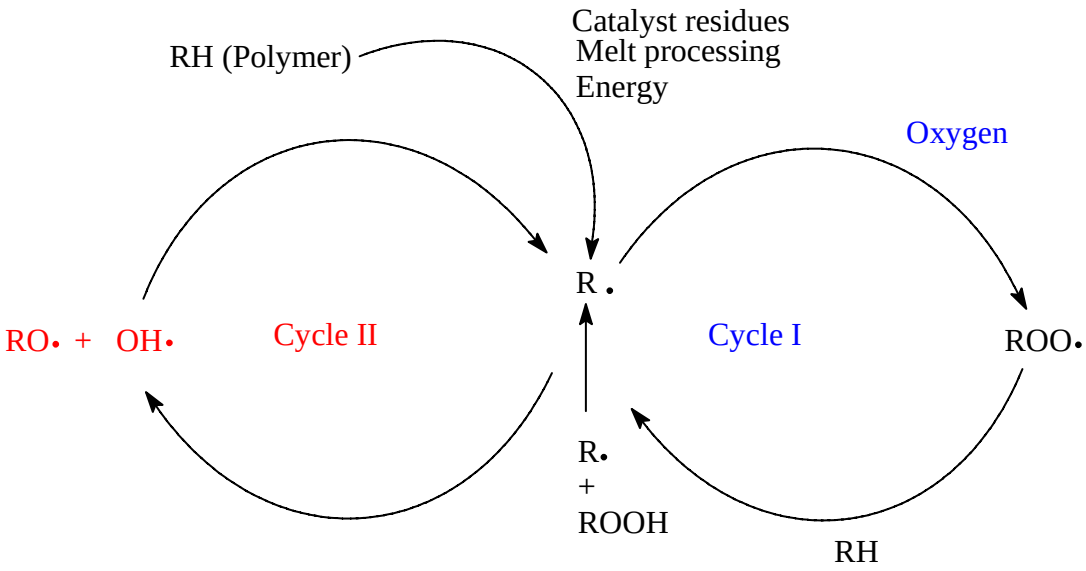

Figure 1: The simplified Ciba cycle for the degradation of polyolefins.

2.2.1 Initiation

During the initiation reaction of polymer degradation, polymer radicals are formed [9]. These radicals can be the result of any of the processes listed earlier (thermal, photo-oxidative, shear, etc). On a molecular level, the three most likely routes for the formation of radicals are the abstraction of a hydrogen atom from a polymer backbone or the cleavage of a polymer chain to form terminal radicals. The possible initiation reactions are given in Scheme 1. Radicals formed on the polymer chains may react with each other (for example during crosslinking) or with other molecules absorbed in the polymer matrix (for example molecular oxygen).

$$\text{R-H} \longrightarrow \text{R}\bullet + \text{H}\bullet \qquad (1.1)$$

$$\text{R-R} \longrightarrow \text{R}\bullet + \text{R}\bullet \qquad (1.2)$$

$$\text{R-H} \xrightarrow{{}^1O_2} \text{R}\bullet + \bullet\text{OOH} \qquad (1.3)$$

Scheme 1: Possible reactions in the initiation of polyolefin degradation

The cleavage of a polymer chain (Scheme 1, reaction 1.2) is usually caused by severe deformation of the polymer or high temperatures experienced in the molten state (for

example during extrusion) or in the solid state (by physical processes). This process is less likely to occur and most of the degradation in a polyolefin is by the scission of a carbon-hydrogen bond. This could be the result of a chemical or radiation attack, and this process occurs more readily at elevated temperatures. A reaction of an oxy-radical with the polyethylene chain may result in the abstraction of a hydrogen atom by the homolysis of the carbon-hydrogen bond. This may form an alcohol and an alkyl radical.

High energy radiation may also lead to the breaking of a carbon-hydrogen bond. This produces an alkyl radical and a hydrogen atom, which may be trapped close to the area of formation. The hydrogen atom may recombine with the alkyl radical to reform the original carbon-hydrogen (C-H) bond or it may diffuse through the polymer matrix to combine with another radical.

Trapping of radicals may be due to the slow motions of chain segments in the crystalline phases. Radicals formed in the crystalline phases by irradiation have a high probability of recombination. Radicals can also migrate intra- and inter-molecularly by a process named hydrogen transfer. Hydrogen transfer may, therefore, lead to migration of the radicals formed in the crystalline phase to a non-crystalline phase. Here they could participate in reactions with other radicals or absorbed molecules.

Each radical produced in this process may be responsible for hundreds of subsequent reactions. Hydrogen atoms formed may participate in three possible reactions: reactions with alkyl radicals, reactions with alkoxy radicals or reactions with another hydrogen radical to form molecular hydrogen that will migrate through the polymer matrix.

Photo-oxidation, for example, cannot be initiated in a polymer matrix consisting of only saturated carbon-carbon bonds or carbon-hydrogen bonds. The presence of a molecule containing a UV absorbing group is a requirement for this type of degradation to progress. Initiation will, therefore, be promoted by the presence of unsaturation, carbonyl groups, catalyst residues, dyes, and certain anti-oxidant molecules.

2.2.2 Propagation

During propagation, the alkyl radicals react with molecular oxygen to transform it into hydroperoxides. Two processes are responsible for this transformation (Scheme 2). In the first reaction, the alkyl radical reacts with molecular oxygen to form a peroxy radical (Scheme

2, reaction 2.1). In the subsequent reaction, this peroxy radical abstracts a hydrogen atom from another polymer molecule (Scheme 2, reaction 2.2). This will lead to the formation of a hydroperoxide and another alkyl radical. The possible reactions during propagation are given in Scheme 2.

The net result of ß-scission (Scheme 2, reaction 2.7) will be a decrease in the molar mass of the polymer. ß-scission also has an influence on the crystallinity of the sample, resulting in an effect called chemi-crystallization [10]. This is the result of the oxygen-induced cleavage of tie molecules or entangled chains in the amorphous regions of the polymer and the incorporation of the free segments into new crystalline domains at the lamellar surfaces or within the amorphous regions [11]. The scission of these tie molecules will have a drastic influence on the polymer mechanical properties. Tie molecules link two crystalline phases together. Oxygen solubility in the crystalline regions is low, leading to a very low level of degradation in the crystalline phase. With orientation of a polypropylene film, the oxygen uptake decreases and the film is more resistant to degradation. In thick samples, a degradation profile develops. The process is diffusion controlled and the molecules closer to the surface will show a higher level of degradation.

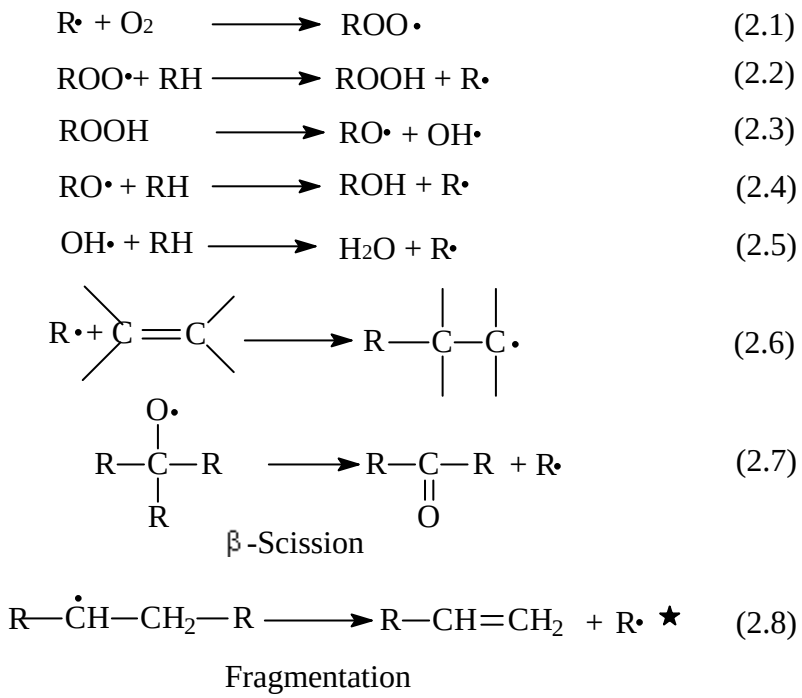

Scheme 2: Possible reactions in the propagation and branching of polyolefin degradation

*Occurs more often in stressed samples [12]

Propagation of degradation will mainly take place in the non-crystalline regions, as oxygen can diffuse freely through this region. Without oxygen being present, the alkyl radicals will migrate until they react with another radical species. This process is referred to as autocatalytic, as an alkyl radical is needed for the process to progress, but the reaction also produces a radical that can lead to further reactions.

2.2.3 Branching

Several reactions may occur during branching. Each hydroperoxide molecule will result in two new radicals. Hydroperoxides may cleave homolytically to yield alkoxy and hydroxyl radicals (Scheme 2, reaction 2.3). These two radicals may then each abstract a hydrogen atom from an adjacent polymer chain. This will result in the formation of an alcohol, water and more alkyl radicals, which may participate in further reactions. There are several more complex reactions which may also take place.

2.2.4 Termination

During termination, several reactions may take place. For example, the alkoxy and alkyl radical species may react with atomic hydrogen. If two alkyl radicals react with each other, crosslinking will result. This is common in polyethylene and will lead to the formation of gels (highly crosslinked materials). This will be highly possible at low oxygen concentrations. The following reactions are possible during termination (Scheme 3):

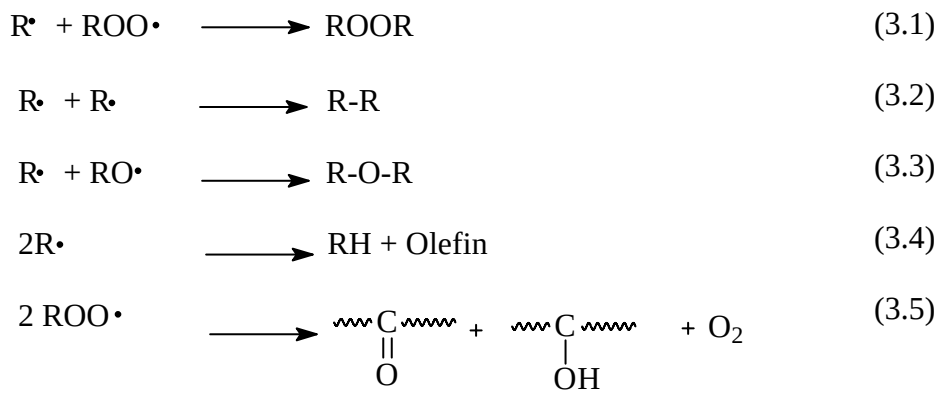

<u>Scheme 3:</u> Possible reactions in the termination of polyolefin degradation

2.3 The degradation of polyethylene

Polyethylene degradation has been studied extensively. There are several excellent articles by Gugumus on the mechanisms of and factors influencing polyethylene degradation [13-15]. Under normal circumstances polyethylene is relatively inert. This is due to the polymer having only carbon-carbon and carbon-hydrogen bonds. In the synthesis and processing of polyethylene, however, unsaturation may develop. Other factors may also result in the formation of active sites (radicals) where degradation could initiate. Commonly, degradation refers to chain scission reactions, but degradation can be due to any of the following reactions:

1. Chain scission
2. Crosslinking
3. Insertion of chemical groups

The possibility of these competing reactions taking place will depend on several factors, including temperature, chemical environment, oxygen availability, and the presence and effectiveness of stabilisers.

Chain scission will result in a decrease in the molar mass averages and the molar mass distribution. This will dramatically affect the rheological properties, as well as tear strength and other mechanical properties. Under oxidative breakdown of polyethylene, the optical properties will also be negatively affected.

In a review article by Gugumus [14], the influence of several factors on the degradation of polyethylene is considered. He reviewed the work by Rideal and Padget [16], who considered the thermo-mechanical degradation of high density polyethylene. A nitrogen blanketed Brabender extruder was used for the experiments and several temperature regions were considered. They found that there were two distinct temperature regions with respect to the effect on the polymer. Below 290 °C the melt viscosity increased. This is indicative of crosslinking and chain branching. Above 290 °C the melt viscosity decreased. This is indicative of chain scission. They attributed the increase in viscosity in the lower temperature region to the formation of long-chain branching. This was confirmed by measuring the melt elasticity and the intrinsic viscosity.

The mechanism proposed for this phenomenon postulates that at lower temperatures the chains undergo scission due to shear and will yield two radicals in a cage structure. Due to the relatively higher melt viscosity at lower temperatures, the cage structure will be disrupted. These radicals will not recombine but rather abstract a hydrogen atom from another polymer chain and will form a secondary alkyl radical. This alkyl radical will combine with another alkyl radical to form long-chain branching. The alkyl radical may also react with vinyl groups to form long-chain branching.

At higher temperatures (> 290 °C) the melt viscosity is lower, resulting in a lower shear on the polymer. The radical pair may, therefore, recombine or disproportionate to a methyl and a vinyl end group. The radical may also react with oxygen and form an oxygen-functionalised polymer chain, again leading to a reduction in the molar mass of the polymer. Secondary reactions may take place, leading to the formation of long-chain branching. It was found that in spite of using a nitrogen blanket, both shear and thermal degradation that lead to a decrease in molar mass resulted in the formation of carbonyl functionalities. A small increase in the concentration of the vinyl end group was also detected.

2.4 The thermo-oxidative degradation of unstabilised isotactic polypropylene

The general degradation mechanism discussed in Section 2.2 will now be investigated in more detail for polypropylene. The oxidative degradation of polypropylene can also be divided in the general steps: initiation, propagation, branching and termination. The whole process is known as auto-oxidation, as initial degradation activates the polymer for further degradation.

2.4.1 Initiation

The formation of a tertiary radical in polypropylene will take place under the influence of shear, heat or photo-initiation. The formation of a secondary polymer radical is also possible, but is not favoured to the same extent as the formation of the tertiary radical (Scheme 4).

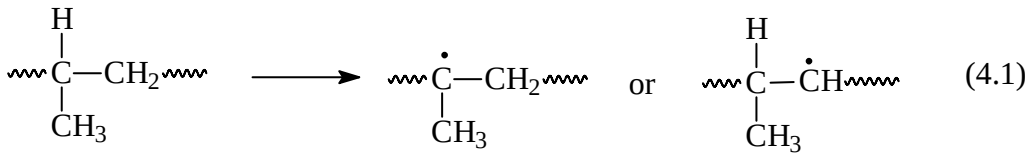

(4.1)

Tertiary radical Secondary radical

Scheme 4: Formation of secondary and tertiary alkyl radicals during initiation of polypropylene degradation

2.4.2 Propagation and branching reactions

The secondary and the tertiary alkyl radicals will now follow two separate paths, leading to the formation of different degradation products. The mechanisms for the degradation of the tertiary and the secondary alkyl radicals will, therefore, be considered separately. Due to the relative importance and the higher concentration of the tertiary radical during degradation, the reaction path of this species will be considered first.

2.4.2.1 Propagation involving the tertiary alkyl radical

In the propagation step, the tertiary alkyl radical will react with oxygen to form a tertiary peroxide (Scheme 5).

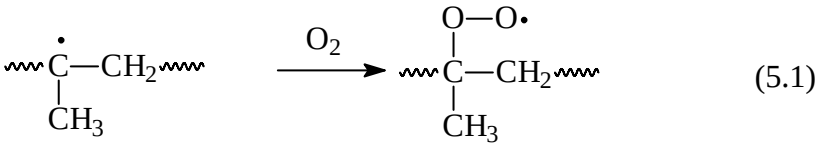

Scheme 5: Formation of a tertiary peroxide during polypropylene degradation

This peroxide will be converted into a hydroperoxide. The hydroperoxide may then decompose via two avenues: it may react with a hydrogen atom to form a tertiary alcohol (III) or it may undergo ß-scission to form a ketone (IV) and a macroalkyl radical (V) [11]. The decomposition of the tertiary hydroperoxide is given in Scheme 6.

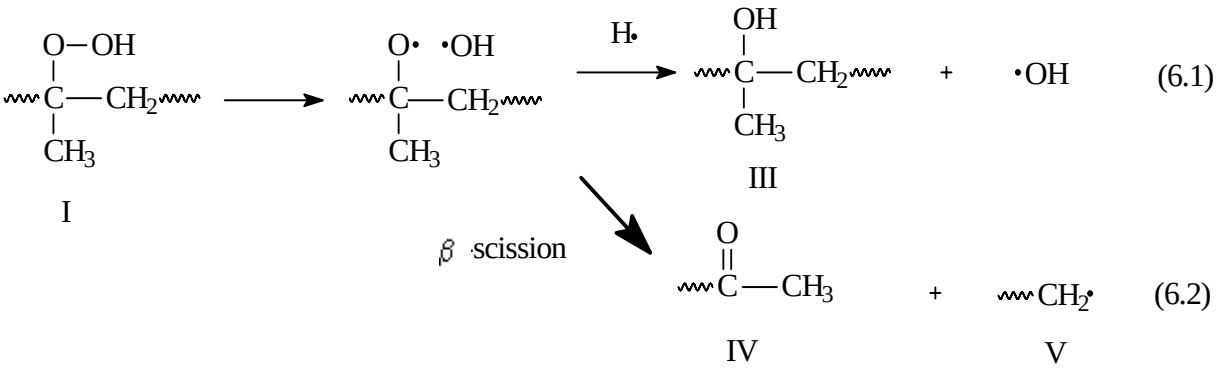

Scheme 6: Decomposition of a tertiary hydroperoxide during polypropylene degradation

The primary chain end (V) that forms during hydroperoxide decomposition can be oxidised further (Scheme 7) [11].

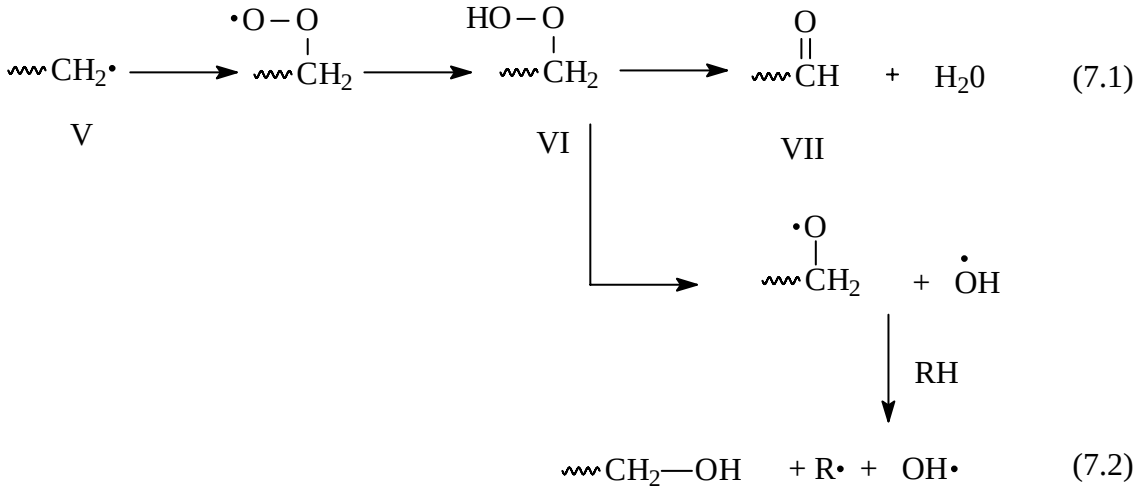

Scheme 7: Oxidation of the chain ends during polypropylene degradation

The end products of the chain-end oxidation reaction will be an aldehyde or alcohol and water.

2.4.2.2 Propagation involving the secondary alkyl radical

A secondary hydroperoxide may also form but this is less likely than the formation of a tertiary peroxide. The formation of the secondary hydroperoxide is given in Scheme 8 [11].

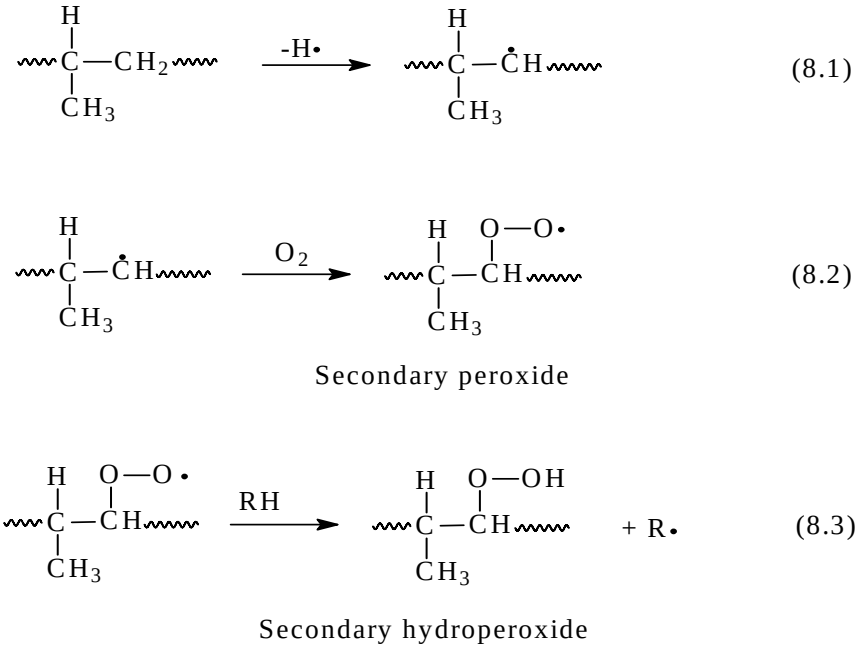

Scheme 8: Formation of a secondary hydroperoxide during polypropylene degradation

In the first propagation reaction, the secondary alkyl radical reacts with oxygen to form a secondary peroxide. The peroxide will then react with another polymer chain to form a secondary hydroperoxide. Secondary hydroperoxides can decompose in a similar fashion to tertiary hydroperoxides: They can react with a hydrogen atom to form a secondary alcohol (VI) or undergo ß-scission to yield an aldehyde (VII) and a macroalkyl radical (Scheme 9) [11]. Secondary radical formation will occur most infrequently in polypropylene homopolymers and co-polymers

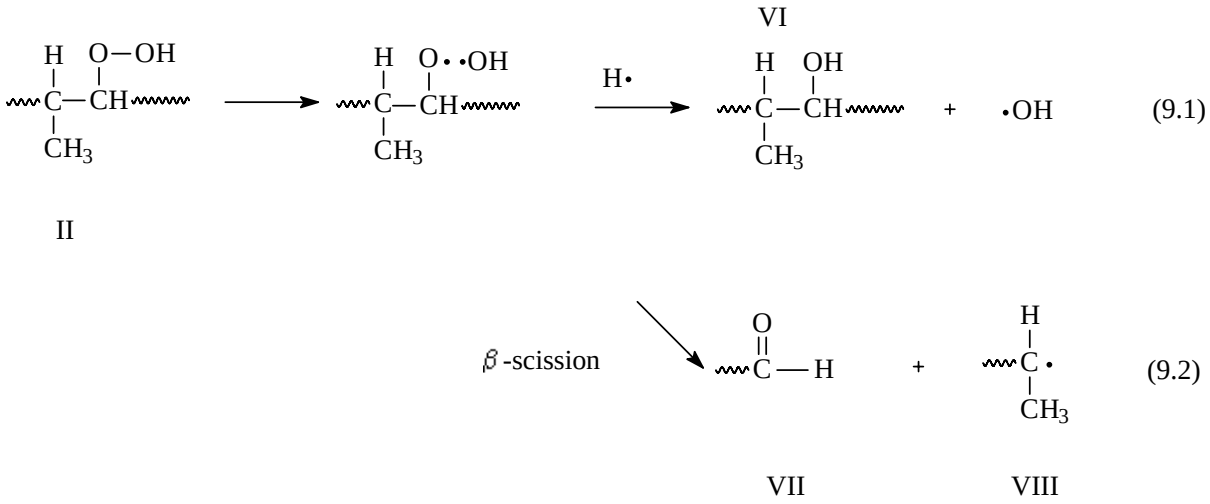

Scheme 9: Decomposition of the secondary hydroperoxide to alcohol and aldehyde degradation products during polypropylene degradation

The secondary chain ends that form during the decomposition of secondary hydroperoxides can be oxidised further (Scheme 10).

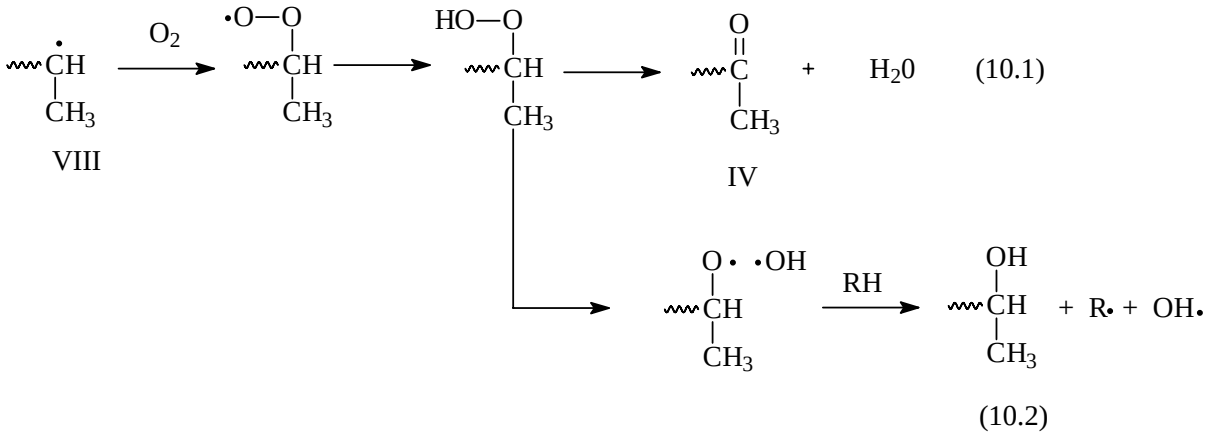

Scheme 10: Oxidation of chain ends to ketones, alcohols and water during PP degradation

According to Adams [7], these degradation cycles should lead to equal amounts of methyl ketone and aldehyde groups. Costa [17], however, using a combination of infrared spectroscopy and derivatization techniques, has shown that the main degradation products detected are secondary and tertiary hydroperoxides (Scheme 6, 8), alcohols (Scheme 6, 7, 9, 10), ketones (Scheme 10), carboxylic acids (Scheme 11), γ-lactones and γ-perlactones. A very low percentage of aldehydes was detected. The reason for this is that aldehydes are highly reactive and can be further oxidised to yield peracid groups (Scheme 11).

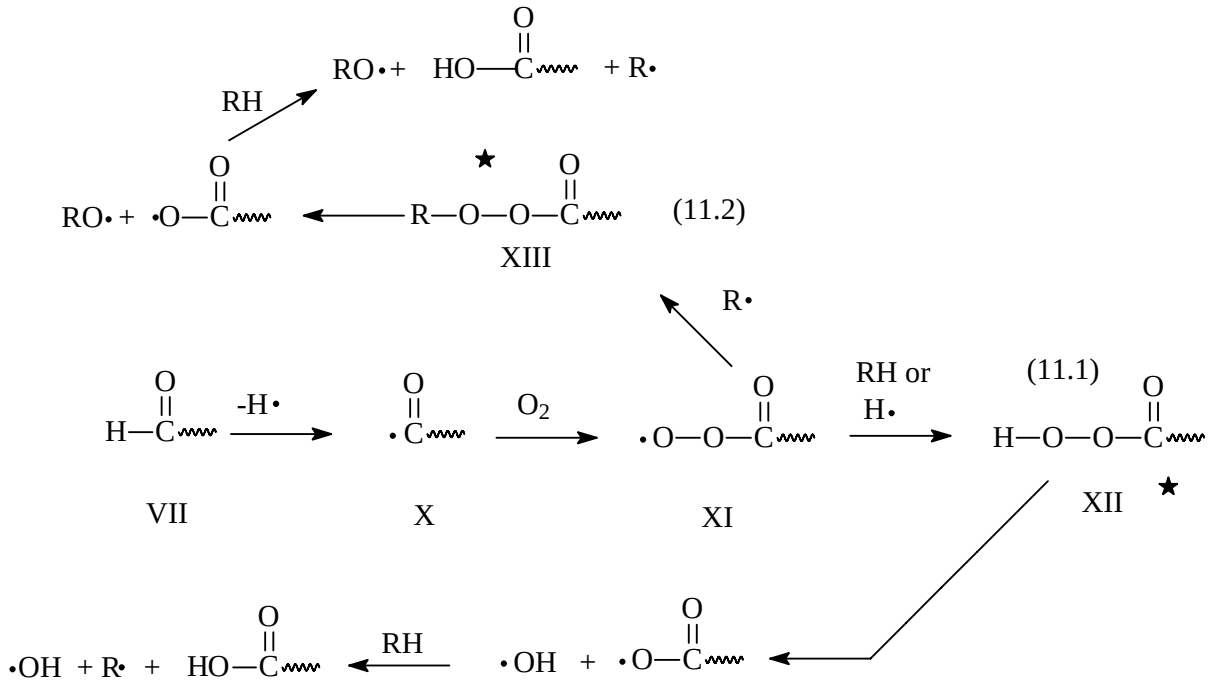

Scheme 11: *Oxidation of aldehydes during polyolefin degradation to peracids and peresters*

*These can and will decompose as do the peroxides and hydroperoxides into two radicals.

2.4.3 Termination reactions in polypropylene

During termination in polyolefin degradation mechanisms, several reactions may take place. In polyethylene, termination is usually a combination of crosslinking and disproportionation reactions. Polypropylene, however, degrades preferentially via scission reactions. In Schemes 9, 10 and 11 the formation of ketones, alcohols and peracids and acids is shown. There are, however, several other disproportionation reactions that may take place. Terminal vinylidene groups form during decomposition reactions in polypropylene (Scheme 12).

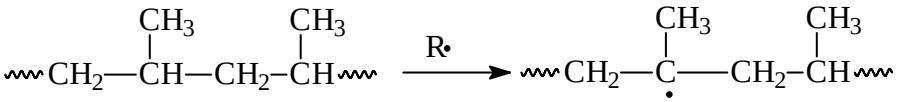

(12.1)

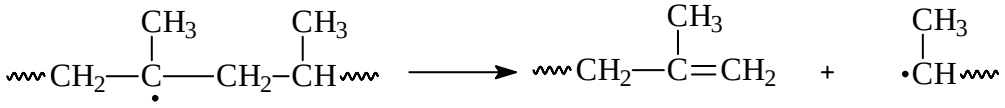

(12.2)

Terminal vinylidene

Scheme 12: Formation of terminal vinylidene groups during radical decomposition in polypropylene

2.5 Factors influencing the degradation of polypropylene

Apart from the conditions of exposure (heat, shear, irradiation, oxygen concentration etc.) that can have a severe influence on polypropylene degradation, there are several chemical factors that can also have an influence on the degradation of the polymer. These include the influence of stereoregularity, chemical heterogeneity, presence of pigments and the effect of catalyst residues on the breakdown of polypropylene.

2.5.1 Influence of the stereoregularity of polypropylene on its degradation behaviour

Isotactic polypropylene was first prepared in 1953 by Natta's group using modified Ziegler catalysts. In 1960 they prepared syndiotactic polypropylene but this had to be purified by extracting the isotactic part. In 1988, using metallocene catalysts with a high stereoregularity, Ewen et al. [18] finally prepared syndiotactic polypropylene.

The difference in oxidisability between isotactic polypropylene and atactic polypropylene was studied [19, 20 and 26] and atactic polypropylene was found to be more stable than isotactic polypropylene. At temperatures below the melting point, it is possible that the structure of isotactic polypropylene is more susceptible to degradation through changes in the crystalline morphology where the amorphous inter-crystalline regions offer easier access to oxygen or place stress on the molecules. Hatanaka [26] also compared the degradation behaviour of atactic and syndiotactic PP. He speculated that, due to the location of all methyl groups on one side of the plane of the carbon-to carbon main chain in isotactic PP, mainly meso-dyads are present, while in atactic PP, a mix of racemic structures exists, and it is thought that this racemic mixture improves the thermo-oxidative stability of the atactic PP.

Kato et al. [21, 22] also investigated the influence of the stereoregularity of polypropylene on its degradation behaviour. They studied the degradation of isotactic and syndiotactic polypropylene and compared it to the degradation behaviour of HDPE. Both photo-oxidative and weathering of the samples were considered. It was found that both photo-irradiation and weathering caused earlier failure in the isotactic polypropylene samples compared to the syndiotactic polypropylene. Kato ascribed the higher stability of the syndiotactic polypropylene to the favourable configuration of the isotactic polypropylene towards auto-oxidation, through a backbiting mechanism in which a formed peroxy radical easily abstracts an adjacent tertiary hydrogen atom in the same polymer chain. This allows the photostability of syndiotactic polypropylene to be explained.

2.5.2 Influence of catalyst residues on degradation

Some studies suggest that the degradation in the amorphous region is initiated around the catalyst residues [23, 24]. Metal contamination and catalyst residues have been shown to promote polyolefin degradation [23]. In Ziegler-Natta catalysed polymers (LLDPE and PP), catalyst residues typically consist of titanium, magnesium and aluminium containing compounds. This could result in a localised high level of degradation around the catalyst residues, which could promote auto-oxidation of the polymer. A metallic residue will promote the breakdown of hydroperoxides to free radicals, which will accelerate the auto-oxidation cycle. Gijsman and Hennekens [25] investigated the effect of catalyst residues on polypropylene degradation. They showed that at 50 ºC, two polymers with respectively 2 and 8 ppm of a $TiCl_3$-based catalyst had longer induction periods compared to polymers containing 64 or 180 ppm of the same catalyst. At 130 ºC all four polymers degraded at similar rates. It was postulated that at low temperature the degradation of the samples was probably catalysed by the catalyst residues, while at high temperatures the process was probably catalysed by temperature (high thermal energy).

Gugumus [13] found a very small difference in the degradation behaviour of conventional high-pressure polyethylene (LDPE) and a titanium-catalysed polyethylene (LLDPE). He, however, found that the presence of chromium catalyst residues significantly increased the degradation rate in LLDPE (Phillips catalysed). He speculated that this was due to the catalytic activity of chromium (Cr) in the decomposition of hydroperoxides, which would result in faster chain branching at an earlier stage. Titanium has a lower activity towards the decomposition of hydroperoxides. He found, however, that Cr residues had no such effect in the degradation of stabilised polyethylene samples.

Hatanaka et al. [26] investigated the influence of stereroregularity, molar mass and catalyst residues on the degradation of isotactic, atactic and syndiotactic polypropylene. Hatanaka et al. found that catalyst residues only had a slight influence on the degradation of isotactic polypropylene. Metallic residues are also known to act as photo-sensitisers, leading to a higher possibility of polymer breakdown. An important fact is that the effect of the catalyst residues on polyolefin degradation is dependent on the activity of the residue. He also found that the molar mass only has a slight influence on the polymer stability. The influence of tacticity of the polypropylene had a much more significant influence on the degradation behaviour.

2.5.3 Influence of heterogeneity and thickness of a polyolefin sample on the degradation process

Oxidation of polyolefins is known to be heterogeneous due to the presence of amorphous and crystalline regions in the polymer. The amorphous regions will be more susceptible towards degradation due to the exclusion of oxygen from the crystalline phases. A semi-crystalline polymer can be described as a heterogeneous system, where the crystalline and amorphous phases differ significantly in their physical and chemical properties. Studies indicate that when a crystalline polymer is cooled from the melt, any impurities will be pushed aside by the lamellae to become interlamellar amorphous zones or ahead of the growing spherulite to form an interspherulite boundary [27]. Impurities are classified as any material that is kinetically or thermodynamically excluded from the crystal phase, including additives, oxygenates, solid particles (like catalyst residues) and short polymer chains, branched and atactic molecules. This will result in low concentrations of impurities in the spherulitic regions and a high concentration in the amorphous phase [27]. Evidence suggests that degradation is even non-homogeneous in the amorphous phase, particularly due to the presence of catalyst residues that could catalyse degradation.

According to Kato et al. [21, 22] the stereoregularity of polypropylene plays a role in degradation. The thickness of the sample can, however, also play a role in the degradation of a film: the oxygen availability will be lower towards the internal layers of the film. Castejon et al. [28] investigated the degradation rates in thick and thin polypropylene films and found that there is a significant difference between the degradation kinetics in thick and thin films.

Rincon-Rubio et al. [29] postulated that the degradation of films will be oxygen-diffusion limited even at film thicknesses lower than 100 microns. Billingham [30] showed that oxygen

diffusion plays a role in the degradation of poly(4-methyl pentene-1) at film thicknesses greater than 40 microns.

2.5.4 Influence of pigments and stabilisers

The presence of pigments and stabilisers was found to change the degradation profile to a significant extent [31,32]. Pigments (for example titanium dioxide) were found to limit the depth of degradation. Pigments may reflect or scatter UV light and this may limit the exposure of deeper layers to the ultraviolet (UV) light. Carbon black also effectively decreases photo-oxidation [31].

The presence of a photo-stabiliser will also reduce the rate of oxidation [32] and will prevent the consumption of oxygen close to the surface. Oxygen will, therefore, be allowed to diffuse deeper into a thick sample compared to an unstabilised sample. The degradation profile in a stabilised sample is, therefore, not as steep as in an unstabilised sample.

The addition of silica-coated titanium dioxide causes a reduction in the number of chain scissions at all depths into the sample mainly because of scattering and reflectance effects as discussed above. Uncoated titanium dioxide has, however, been shown to promote polyolefin breakdown [32].

Turton and White [32] investigated the degradation profiles in unstabilised, hindered amine stabilised (HAS) and pigmented samples. Samples of 3-mm thickness were selected for this study and the degradation profiles in these samples were investigated as a function of exposure time. All samples were exposed to photo-degradation in a UV weatherometer (with Q panel UVA 340 tubes). The degradation profile through a sample that was exposed to UV light is usually quite steep. This is partially due to the high UV intensity close to the sample surface but mainly due to the oxygen diffusion effects. Oxygen is consumed close to the surface and therefore it cannot penetrate to deeper layers. Microtoming was used to determine the degradation profile and the microtomed fractions were analysed by UV spectrophotometry, molar mass determinations and microscopy techniques.

2.6 Effect of degradation on the mechanical properties

The mechanical properties of samples will change significantly during degradation. Polyolefins will show a dramatic loss in mechanical properties with progressing degradation.

This includes a loss of tensile strength, toughness and other properties. This is primarily due to the scission of tie molecules (discussed in Section 2.2.2) during the thermo-oxidative process. With the destruction of the tie molecules, on a molecular level, there is nothing to link the crystalline regions together, which ultimately results in failure of the polymer. The reduction in molar mass is also an important consideration in this decrease in mechanical properties. Gensler et al. [11] found that isotactic polypropylene has highly ductile behaviour in the undegraded state. This was still valid in the degraded state in the case of phenolic stabilised isotactic PP. In the case of HAS-stabilised PP, however, this was slightly different, polyolefin tensile strength decreased significantly with degradation. Other properties like tear strength also decreased.

2.7 Preventing oxidation in polyolefins

There are several ways to prevent polyolefin degradation [9]. Without the addition of any anti-oxidant, the polymer stability can be improved by choice of optimum processing conditions, control of the polymer structure and removal of oxygen and oxidation catalysts from the polymer. The simplest way to prevent oxidation, theoretically, is to prevent contact between the polymer and oxygen. This approach is, however, not practical. The addition of anti-oxidants or oxidation inhibitors can prevent polymer degradation [33]. These additives diffuse almost exclusively through the amorphous phase [34].

As mentioned earlier, polymer degradation comprises the following steps:

1. Initiation
2. Propagation
3. Branching
4. Termination

Preventing or retarding any one of the steps in polymer degradation can be effective in retarding polymer degradation.

2.7.1 Stabilisation of a polymer by preventing the initiation step of oxidation

The initiation step in polymer degradation is the least understood. In this reaction a polymer radical is formed by:

$$RH + O_2{}^1 \longrightarrow R\cdot + \cdot OOH$$

$$R\text{-}H \longrightarrow R\cdot + H\cdot$$

This is due to the negligible interaction between polymer and oxygen, which only occurs in a free-radical self-accelerated chain reaction or if the oxygen is in the singlet state. Polymer processing (even during the compounding step when additives are added to the polymer) is also responsible for imparting shear on the polymer, which can lead to ß-scission of the polymer.

2.7.2 Deactivation of chain-scission initiating impurities

The effect of metallic residues on polyolefin degradation has been discussed in Section 2.5. High levels of catalyst residues will, therefore, contribute to polypropylene breakdown. The interaction of polymers and metallic residues is extremely complex. Metal deactivators can be added to polymers to inhibit the catalytic activities of metals in polymer degradation. Typically these compounds contain ligand atoms like N, S, O and P. These atoms can act as chelating agents for the metallic residues. The structure of a typical metal deactivator is given in Figure 2.

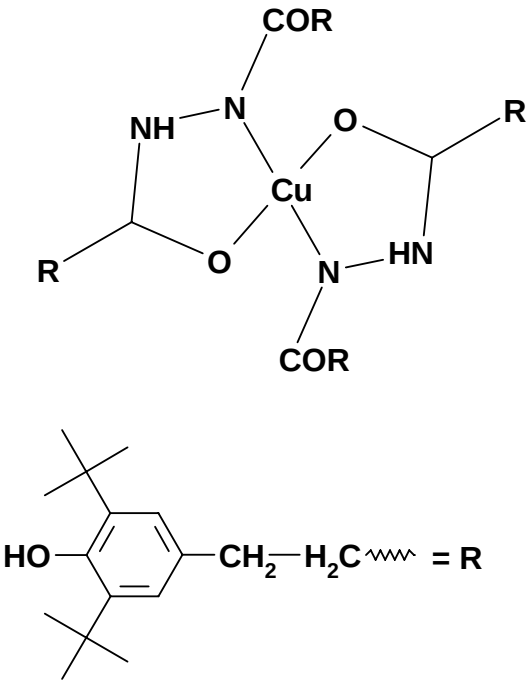

Figure 2: Structure of a typical metal deactivator.

Other initiators of degradation include hydroperoxides, peroxides and aldehydes, that form during polymer production and processing. These compounds may form radicals especially

under UV or sunlight irradiation and can then accelerate degradation. Removing these compounds from the polymer matrix will reduce their availability for the initiation of degradation.

2.7.3 Removing oxygen from the polymer

Oxygen will be predominantly present in the amorphous parts of the polymer. With an increase in the crystallinity, the oxygen concentration that can be absorbed in the polymer matrix will decrease. Additives are needed to reduce the singlet oxygen concentration in the polymer during thermo-oxidative degradation.

2.7.4 Retarding the oxidation at the chain propagation step

The chain propagation step can be written as follows:

$$R\bullet + O_2 \longrightarrow ROO\bullet \qquad (1)$$

$$ROO\bullet + RH \longrightarrow ROOH + R\bullet \qquad (2)$$

There are two possible ways of preventing the propagation step:

1. Inhibition with compounds reacting with ROO·
2. Inhibition with compounds reacting with R·

2.7.4.1 Inhibition of propagation with species reacting with a peroxy radical

Due to the high concentration of peroxy radicals (ROO·) in the polymer during degradation, an effective inhibitor of degradation will target the peroxy radicals and not alkyl radicals (R·). A peroxyradical is also more reactive towards phenols and amines than an alkyl radical is. The rate constants of these inhibitors have been proven to be much higher compared with the chain propagation rate. The mechanism of this type of inhibition will be discussed under ‘hindered phenol stabilisers’ (Section 2.8.2).

2.7.4.2 Inhibition of propagation with radicals reacting with an alkyl radical

Reaction (1) above will proceed at temperatures as low as 0 ºC. Therefore, at room temperature there will be a high concentration of ROO· and a low concentration of R· radicals present in the polymer. Nitroxyl radicals (NO·) can react with the polymer chain radical and

form a stable species (Scheme 13). These are found in hindered amine light stabilisers (HALS), and the addition of HALS will inhibit photo-oxidation (Section 2.8.2).

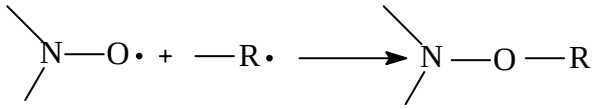

Scheme 13: Reaction of an NO· radical with a polymer radical to form a stable product

2.7.5 Inhibition of the chain branching step

The hydroperoxides formed during degradation are unstable in the presence of metallic impurities, UV irradiation or excessive heat and will decompose, resulting in the formation of radicals.

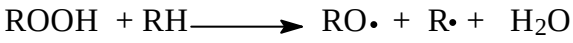

This step can be inhibited by the addition of compounds that will react with hydroperoxides, with a low yield of radicals. As the free radicals initiate further oxidation of chains, the decrease in radicals will result in lower degradation levels.

Organosulphur compounds (including sulphides, disulphides and thiodipropionates) have also been found to reduce the level of hydroperoxides [5]. A reduction in hydroperoxide yield was found for sulphides containing at least one alkyl group. Aromatic sulphides did not have this effect. Sulphur-containing compounds have also been shown to be effective in polymer stabilisation [7]. The current view is that sulphur compounds do not play a role in stabilisation during processing, but only improve the long-term thermal stability.

Several phosphorous-containing compounds have also been shown to reduce the levels of hydroperoxides [7]. Phosphites have been used extensively as hydroperoxide decomposers.

2.8 Typical anti-oxidative stabilisation packages

BHT (butylated hydroxy toluene, see Appendix 1) is a phenolic anti-oxidant that is commonly used as a primary anti-oxidant in polyolefins. It is a relatively cheap and effective anti-oxidant. It was, however, shown that BHT at low concentrations can contribute to gel formation. At low concentrations of butylated hydroxyl toluene (BHT), the polymer may be more sensitive to the formation of gels compared to polymer containing no BHT.

Mixtures of phosphites, hindered phenols and lactones are commonly used in industry to stabilise commercial polyolefins [8]. Hindered phenols are very effective in improving the long-term heat stability of polyolefins [11]. Some of the transformation products may, however, result in discolouration of the polymer during its service life [11].

2.8.1 Hindered phenol stabilisers and phosphite stabilisers

The stability of polypropylene towards oxidative degradation is low and, therefore, polypropylene needs to be stabilised against processing, heat and light to maintain its performance. Hindered phenols are effective long-term heat stabilisers. In Appendix 1 the structures of several phenolic stabilisers are given.

Phenolic anti-oxidants act as radical scavengers [11]. During degradation, a peroxy radical forms. The main reaction in the anti-oxidative stabilisation is the transfer of a hydrogen atom from the phenoxyl group of the stabiliser to a peroxy radical, forming a hydroperoxide (Figure 2). Hydroperoxides are stable up to temperatures as high as 150 ºC. This prevents the acceleration of the auto-oxidation cycle (intra-molecular H-abstraction).

The effect of the hindered phenols and the phosphites on the degradation of polyolefins can be seen in the modified Ciba cycle (Figure 3).

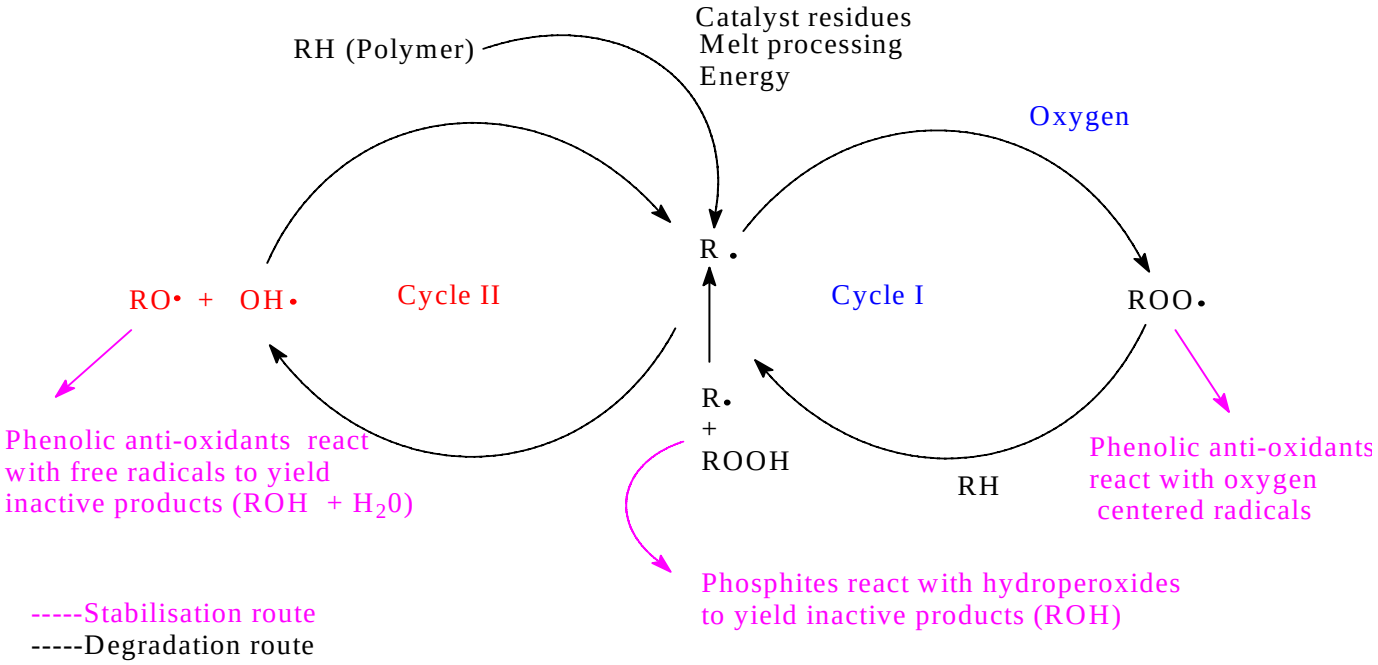

Figure 3: The modified Ciba cycle for the stabilisation of polyolefins showing possible stabilisation routes of phenolic and phosphite stabilisers.

In an unstabilised polypropylene molecule, the tertiary peroxide may abstract a tertiary hydrogen atom to form a hydroperoxide and a peroxide.

Phosphite stabilisers can also react with peroxy radicals, alkoxy radicals and unsaturated vinyl groups, thereby stabilising a polyolefin against degradation. Additionally, the phosphite stabiliser protects the hindered phenols during extrusions, it can co-ordinate with transition metal residues and react with the quinoidal breakdown components [23].

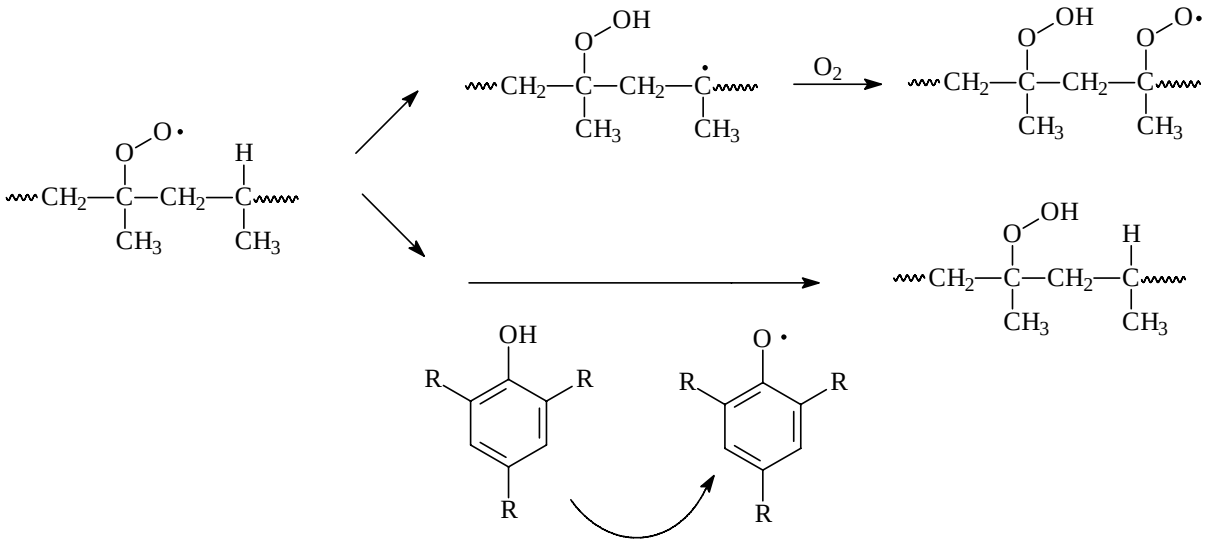

Scheme 14: The stabilising effect of hindered phenols, by donation of a hydrogen atom, resulting in the formation of a stable hydroperoxide.

By stabilising the system with a hindered phenol, the hindered phenol will donate a hydrogen atom to the radical, thereby preventing the abstraction of a hydrogen atom from a polymer chain. It will, therefore, disrupt the degradation cycle by forming a stable hydroperoxide.

It has also been proven that, using an antioxidant with a propionate group in the para-position (for example Irganox 1010: Appendix 1), the degradation products can also contribute to stabilisation. Klemchuck [35], however, found that the transformation products can contribute to yellowing of the polymer.

Phosphite stabilisers are added to polyolefins to provide stability to the polymer at elevated temperatures (Scheme 15). The mechanism of phosphite stabilisers is not totally resolved, but generally it can be written as [36]:

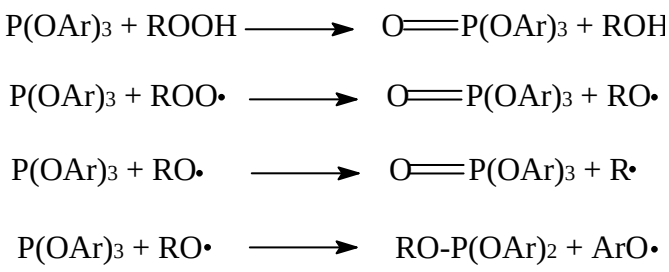

Scheme 15: Reaction of peroxyradicals and hydroperoxide with a phosphite stabiliser

The phosphite will react with the hydroperoxide to form an alcohol and a phosphorous containing compound. Phosphites may also react with oxy- and peroxyradicals.

2.8.2 Hindered amine stabilisers

Hindered amine stabilisers (HAS) were introduced commercially in 1975 and are used to stabilise polymers against UV radiation-induced degradation [29]. They are so effective in light stabilisation that they are commonly referred to as hindered amine light stabilisers. A hindered amine stabiliser acts as an anti-oxidant by the formation of nitroxyl radicals (NO·). It is known that the oxidation of HAS to the nitroxyl radical by peroxy radicals or hydroperoxides is a slow process, but the presence of peracids and acylperoxy radicals will accelerate this process. HAS do not act as H· donors, and will, therefore, not prevent the build-up of intramolecular hydroperoxide sequences. Although HAS have been used for stabilisation against photo-oxidative degradation, they have been shown to stabilise polyolefins against thermo-oxidative degradation. Typical structures of HAS are shown in Appendix 1.

NO· radicals will scavenge alkyl radicals and yield a hydroxylamine ether which will react with a variety of compounds. According to the Denisov cycle (Scheme 16), the hydroxylamine ether will transfer its alkyl group to a peroxy radical and will regenerate the NO· radical.

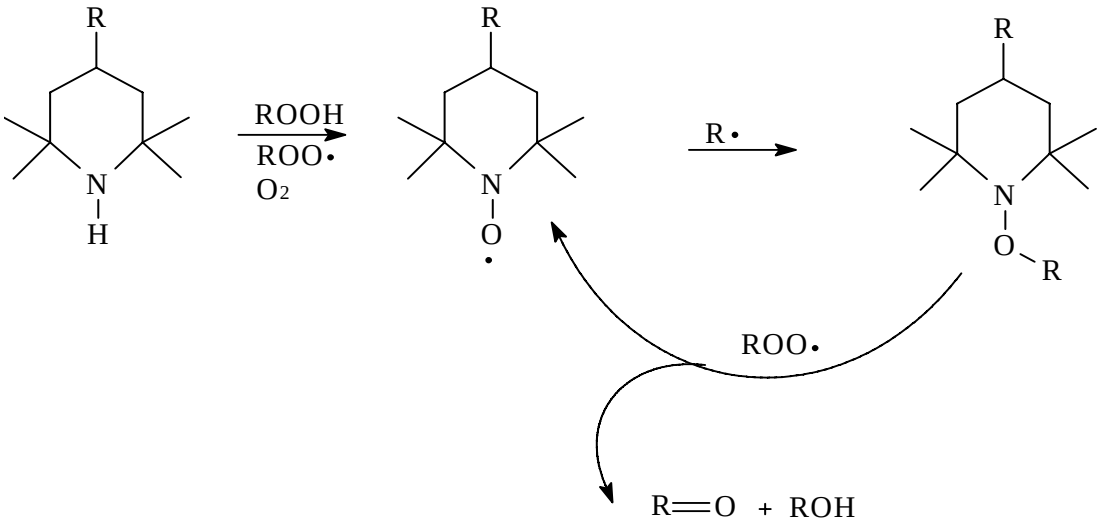

Scheme 16: The stabilising effect of HAS by reacting with peroxides

HAS stabilisers can also serve as heat stabilisers. The mechanism of heat stabilisation by HAS is significantly different to that of a phenolic anti-oxidant. When an isotactic polypropylene is stabilised with a phenolic anti-oxidant, it typically shows a catastrophic failure after the induction period, depending on the stabiliser concentration, sample geometry and aging temperature [11]. A HAS stabilised sample of isotactic polypropylene showed a more gradual decrease in performance properties [11].

2.9 Conclusions

Polyolefins are synthesised in reactions involving chain initiation, chain propagation and chain termination reactions. This results in a polymer with a well-defined composition. The polymer may, however, be subjected to conditions like high temperatures, shear, irradiation, light etc. Such conditions will induce chemical changes in the polymer, which can result in a change in the physical properties of the polymer. The initiation of polymer degradation starts with the abstraction of a hydrogen atom from a polymer molecule by singlet oxygen or the homolysis of a polymer chain. The alkyl radical formed can now react with oxygen to form a peroxide. This peroxide can react with another polymer molecule to form a hydroperoxide. This can then decompose to form alcohols, ketones and aldehydes. Aldehydes will, however, be further oxidised to peracids. Peracids and lactones also form during the degradation process. Species like ketones, aldehydes, peracids, lactones, and free and associated hydroperoxides can be detected by FTIR.

The tacticity of polypropylene has an influence on the stability of the polymer. Isotactic polypropylene has the lowest stability, atactic PP is more stable and syndiotactic

polypropylene is the most stable. The heterogeneity of a polymer sample has been shown to contribute to degradation. Oxygen diffusion will take place through the amorphous part of the polymer. The morphology (number, location and orientation of crystallites) is therefore important in determining the thermo-oxidative stability. This is especially important in thicker objects, where the surface and the inner morphology may differ. For example, in a thick injection moulded object, the surfaces may be quench cooled (in contact with the mould), resulting in smaller spherulites, while the inner layer may form larger sperulites (longer time allowed to crystallise).

Catalyst residues can also contribute to degradation by accelerating the decomposition of the hydroperoxides and therefore the decomposition of hydroperoxides accelerates degradation.

There are several ways of preventing or limiting degradation. These include removing catalyst residues and removing other degradation precursor species from the polymer. The most effective is, however, to add stabilisers to the polymer. Commercial polymers are commonly stabilised by a combination of hindered phenols, phosphites and lactones. Hindered phenols act as radical scavengers and, therefore, slow down the degradation cycles. Phosphites react with hydroperoxides to form inactive products (ROH). Choosing the optimum stabiliser package will ensure a long service lifetime for a polymer.

2.10 References

[1] Maack Business Services, Polypropylene 2003 Conference, Zürich, 15-17 September 2003

[2] Moore, E.P., *Polypropylene Handbook* Hanser, München**, 1996**, 113-117

[3] Bolland, J.L., Gee, G., *Transactions of the Faraday Society* **1946**, 42, 236-243

[4] Moss, S., Zweifel, H., *Polymer Degradation and Stability* **1989**, 25, 217-245

[5] Marshall, N., PhD thesis, University of Sussex, **December 2001**

[6] Singh, A., *Radiation Physics and Chemistry* **1999**, 56, 375-380

[7] Adams, J.H., *Journal of Polymer Science Part A1: Polymer Chemistry* **1970**, 8, 1077-1090

[8] Pauquet, J.R., King, R., Krohnke, C., *World Congress on Polyethylene*, Milan, Italy, May 6-7, 1997

[9] Shlyapnikov, Y.A., Kyrushkin, S.G., Mar'in, A.P., *Antioxidative Stabilisation of Polymers* **1996**, Taylor and Francis. ISBN 0 7484 0577 1

[10] Rabello, M.S., White, J.R., *Polymer* **1997**, 38, 6379-6387

[11] Gensler, R., Plummer, C.J.G., Kausch, H.H, Kramer, E., Paquet, J-R., *Polymer Degradation and Stability* **2000**, 67, 195-208

[12] Kausch, H. H., *Polymer Fracture* **1987** Springer-Verlag, Berlin

[13] Gugumus, F., *Polymer Degradation and Stability* **1997**, 55, 21-43

[14] Gugumus, F., *Polymer Degradation and Stability* **1999**, 66, 161-172

[15] Gugumus, F., *Polymer Degradation and Stability* **2000**, 68, 21-33

[16] Rideal, G.R., Padget, *Journal of Polymer Science Symposia* **1976**, 57, 1-13

[17] Costa, L., Luda, M.P., Trossarelli, L., *Polymer Degradation and Stability* **1997** 55, 329-338

[18] Ewen, J.A., Jones, R.L., Razavi, A., Ferrara, J.D., *Journal of the American Chemical Society* **1988**, 110, 6255-

[19] Dulog, L.O., Radlmann, E. Kern, W., *Macromolecular Chemistry* **1963**, 60, 1-17

[20] Dulog, L.O., Radlmann, E. Kern, W., *Macromolecular Chemistry* **1964**, 80, 67-73

[21] Kato, M., Tsuruta S., Osawa, Z., *Polymer Degradation and Stability* **2000**, 67, 1-5

[22] Kato, M., Osawa, Z., *Polymer Degradation and Stability* **1999**, 65, 457-461

[23] Scheirs, J., Pospisil, J, O'Connor, M.J., Bigger, S.W., *Polymer Durability* **1993**, 359-374

[24] Goss, B.J.S., Nakatani, H., George, G.A., Terano, M., *Polymer Degradation and Stability* **2003**, 82, 119-126

[25] Gijsman, P., Hennekens, J., *Polymer Degradation and Stability* **1993**, 39, 271-277

[26] Hatanaka, T., Mori, H., Terano, M., *Polymer Degradation and Stability* **1999**, 64, 313-319

[27] Ryan, T.G., Calvert, P.D., Billingham, N.C., *Adv. Chem. Ser.* **1978,** 169, 261-272

[28] Castejon, M.J., Tiemblo, P., Gomez-Elvira J-M., *Polymer Degradation and Stability* **2000**, 70, 357-364

[29] Rincon-Rubio L.M., Fayolle, B., Audouin, l., Verdu, J., *Polymer Degradation and Stability* **2001**, 74, 177-188

[30] Billingham, N.C., Prentice, P., Walker, T.J., *Journal of Polymer Science:* **1996**, Symposium no 57, 287

[31] Lemaire, J., Arnaud, R., Gardette, J-l., *Polymer Degradation and Stability* **1991**, 33, 277-294

[32] Turton, T.J., White, J.R., *Polymer Degradation and Stability* **2001**, 74, 559-568

[33] Zweifel, H., *Stabilization of Polymeric Materials* 1997, Springer ISBN 3-540-61690-x

[34] Foldes, E., Turcsanyi, B., *Journal of Applied Polymer Science* **1992**, 46, 507-515

[35] Klemchuck, P., *Polymer Degradation and Stability* **1991**, 34, 333-346

[36] Gijsman, P., Gitton, M., *Polymer Degradation and Stability* **1999**, 66, 365-371

Chapter Three

Classical techniques for studying degradation in polyolefins

3.1 Background

Over the past decades, several analytical and physical techniques have been used to study degradation in polyolefins. By monitoring the concentration of the various species formed during degradation it is possible to determine the mechanisms and kinetics of degradation. In the previous chapter it was shown that oxidative degradation involves the reaction of molecular oxygen with polymer radicals. Oxidation usually starts with an induction period [1]. This is characterised by the build-up of microscopic domains that are highly oxidised. These domains grow rapidly and display radial cracks.

Due to the stability of stabilised samples it may take years to degrade a sample under natural exposure, although natural exposure is still frequently used [2, 3]. Accelerated degradation of polyolefins is therefore of importance and may be carried out in the laboratory.

3.2 Accelerated degradation of polyolefins

There are three techniques that are frequently used to study accelerated degradation of stabilised and unstabilised polyolefins:

1. Oven aging
2. Multiple extrusions
3. UV exposure

These techniques have distinct advantages and disadvantages.

3.2.1 Oven aging of polyolefin samples

Oven aging is commonly used to study the thermo-oxidative degradation of polyolefins and to predict lifetimes of polyolefins [1, 4-6]. The reason for this is twofold: the long lifetime of stabilised samples during outdoor exposure (several years) and the difficulty in controlling the parameters responsible for degradation during outdoor exposure. Oven aging is a convenient technique for assessing the lifespan of a polymer sample. There are, however, several differences between the kinetics of oven aging and normal outdoor exposure. The high temperatures employed during oven aging could, for example, result in the volatilisation of certain stabilisers. This could lead to a depletion of the stabiliser and a subsequent faster degradation of the polymer.

Another concern is the conditions inside the oven. Meijers [4] investigated the effect of higher concentrations of ozone in the oven during degradation. Gugumus [7] showed that oven aging experiments carried out during summer resulted in some samples degrading three times as fast as samples aged during winter (at the same oven temperature). Gugumus speculated that this was due to the effect of ozone variations but Meijers proved that ozone concentration does not influence the life span of samples during oven aging. The reason for this difference between summer and winter degradation behaviour could not be found, but it was speculated that this could be due to other gaseous species present in air in summer or more likely to humidity effects.

Oven aging can be carried out at different temperatures, depending on whether the polymer is stabilised or not. Degradation temperatures also depend on the type of polymer. Polypropylene degradation studies are usually carried out at lower temperatures than polyethylene due to the lower stability of polypropylene compared to polyethylene. Gugumus [7] investigated the degradation of HDPE, LLDPE and LDPE at elevated temperatures. He performed most of his research at 80 ºC, but found that 90 ºC and 100 ºC could also be used for degradation studies. Marshall [9] performed degradation studies on unstabilised polypropylene samples and found that 70 ºC and 90 ºC were suitable for studying the degradation of polypropylene. He found that degradation at 110 ºC and 130 ºC was too rapid and not very suitable for studying the degradation kinetics of polypropylene.

3.2.2 Multiple extrusions of polyolefin samples

Multiple extrusions is another experimental way of assessing the degradation behaviour of polyolefin samples [10-12]. During multiple extrusions the polymer is extruded a few times to assess the effectiveness of the stabiliser package and to predict changes to the polymer structure under conditions of high shear and temperatures. Unstabilised samples can also be evaluated using this methodology.

Fearon [11] used multiple extrusions to compare different stabiliser packages and the effect on mechanical and chemical properties. Gonzales-Gonzales et al. [12] investigated the effect of multiple polymer extrusions at different temperatures on polymer stability. He found that during mechanical degradation chain scission occurs close to the centre of the macromolecule. The temperature of extrusion was found to have a significant effect on the degradation behaviour. Epacher [13] used multiple extrusions to study the effect of processing on stabilised HDPE samples.

In industry, reactive extrusion is used to manipulate the molar mass of PP: A low melt flow index (MFI) polymer (high molar mass) can be extruded with peroxides to decrease the molar mass of the polymer (increase the MFI). Oxygen concentration is usually limited during reactive extrusion compared to oven aging that usually takes place under oxygen-rich conditions. This may have an influence on the degradation mechanism. In polypropylene, ß-scission is the dominant mechanism, and in polyethylene both crosslinking and scission may take place.

3.2.3 Photodegradation of polyolefin samples

Polymers can degrade under the influence of sunlight. This is mainly due to oxygen activation in the singlet state which can be accelerated by the presence of chromophoric groups in the polymer that can be excited by UV light. Pure polyethylene and polypropylene do not contain strong chromophoric groups, but the presence of catalyst residues, contaminants and oxidation products formed during the synthesis of the polymer will sensitise the polymer towards photo-oxidation.

Photo-oxidation is typically studied using weatherometers. Xenon lamps are commonly used to simulate UV exposure.

Several authors used a combination of natural exposure and UV exposure to investigate the suitability of stabilisation packages to protect a polymer against UV degradation [8]. In the present study aging was performed on a propylene-ethylene copolymer.

3.3 Analytical techniques for studying degradation in polyolefins

The following analytical techniques have been used to study polyolefin degradation:

3.3.1 Chemiluminescence

Chemiluminescence is a technique that has used been extensively for the detection of degradation [1, 14-18]. It was found that chemiluminescence is more sensitive to oxidative changes than spectroscopic techniques [18]. Typically a polymer is heated in nitrogen up to the required temperature. Oxygen is then introduced into the system and the chemiluminescence is followed. The luminescence is thought to be due to the bimolecular reaction of two alkylperoxyradicals (ROO·). This reaction results in the formation of singlet

molecular oxygen and a triplet carbonyl group. The transition of the triplet carbonyl group to the ground state results in the emission of weak light. This can be detected by, for example, a photonmultiplier tube. It is possible that the singlet oxygen may also contribute to chemiluminescence. The technique is highly sensitive, but concerns were raised regarding the data obtained from these experiments. The mechanism of chemiluminescence during degradation is not fully understood. There are thousands of reactions that can take place during degradation, and several of these may contribute to chemiluminescence. The technique is also very dependent on sample dimensions.

Chemiluminescence is frequently applied to the bulk polymer and highly sensitive detectors enable studies of the polymer degradation on a molecular level. Through chemiluminescence it was indicated that even at the early stages of degradation, there are highly oxidised domains on the nanoscopic scale. Chemiluminescence during polymer degradation is generally believed to be due to the termination of two alkyl peroxyl radicals. Chemiluminescence intensity is, therefore, proportional to the termination rate of degradation.

Fearon [11] used a combination of differential scanning calorimetry (DSC) and chemiluminescence to study polymer degradation. In his experimental setup a Mettler DSC was fitted with a photomultiplier tube. A normal oxidation induction time (OIT) experiment at 150 °C was performed on the DSC, using the DSC and the photomultiplier tube as detectors. The DSC-OIT curve and the chemiluminescence were then studied as a function of time at 150 °C. The chemiluminescence method was found to be more reliable than normal DSC: a sharper onset of degradation could be seen. Fearon found that in cases where the normal DSC could not detect the onset in degradation, the chemiluminescence detector could detect the onset.

3.3.2 UV spectroscopy

UV spectroscopy can also be used for studying stabilised samples. Fayolle et al. [1] used UV spectroscopy to study the consumption of the phenolic anti-oxidant Irganox 1010 during degradation. He used plaques of 100-micrometers thickness. Irganox 1010 has a strong absorption in the UV region (at around 280 nm) and the concentration of Irganox 1010 can, therefore, be measured by UV spectroscopy. With consumption of the anti-oxidant the peak intensity at 280 nm will decrease.

3.3.3 Molar mass determinations

Synthetic polymers can be seen as a mixture of molecules of various molar masses or chain lengths. Only a few analytical techniques can provide information on this distribution of chains of different molar masses. Size exclusion chromatography (SEC) and gel permeation chromatography (GPC) are comparative terms given to the liquid chromatographic separation of macromolecules in solution.

Molar mass and molar mass distribution data can be obtained directly from SEC. Typically, SEC analyses of polyolefins are carried out at elevated temperatures (usually between 130 ºC and 150 ºC). 1,2,4-Trichlorobenzene is commonly used as a solvent for high temperature SEC analyses of polyolefins. Crosslinked divinylbenzene columns are commonly used for SEC measurements. The results typically obtained from a SEC instrument are the M_n (number-average molar mass), M_w (weight-average molar mass) and M_z (z-average molar mass). These averages all describe different moments in the molar mass distribution curve. Theoretically, the molar mass distribution curve can be divided into segments. These segments can be used to estimate the relative amounts of polymer eluting in each molar mass increment (Figure 1). Taking the amount of polymer of a given molar mass fraction as H_i and the molar mass of this fraction as M_i, equations can be formulated for the different molar mass averages.

The number-average molar mass is given by:

$$M_n = \frac{\Sigma H_i}{\Sigma (H_i/M_i)} \qquad (3.1)$$

The number average molar mass has a value on the low molar mass side of the molar mass distribution.

Molar mass determinations by SEC are commonly used to follow the degradation of polyolefins [1, 12, 19], where SEC results indicate the changes in chain lengths with degradation. During the degradation of polyolefins, chain scission or crosslinking may occur. Chain scission (also called ß-scission) will result in a reduction in the molar mass of polypropylene.

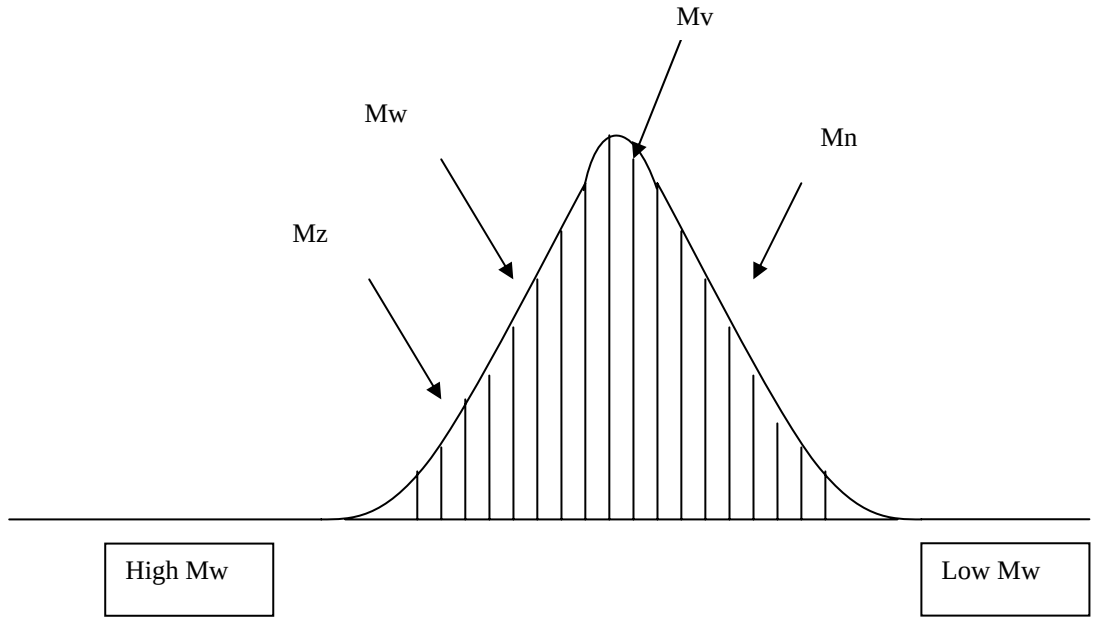

Figure 1: The position of the different molar mass averages on a typical molar mass distribution curve obtained from a HT-SEC instrument.

The weight-average molar mass can be calculated by:

$$M_w = \frac{\Sigma H_i M_i}{\Sigma H_i} \qquad (3.2)$$

The z-average molar mass can be described by:

$$M_z = \frac{\Sigma H_i M_i^2}{\Sigma H_i M_i} \qquad (3.3)$$

The z-average molar mass is characteristic of the high molar mass end of the distribution. The polydispersity index (PDI) can be defined as:

$$PDI = \frac{M_w}{M_n} \qquad (3.4)$$

Canevarolo [10] defined two molar mass-based parameters to describe the number of chain scissions:

$$n_R = \left(\frac{M_{no}}{M_{nf}} \right) - 1 \qquad (3.5)$$

where: n_R is the number of chain scissions

M_{no} is the initial M_n value

M_{nf} is the final M_n value (after scission)

and:

$$n_R = \frac{MWD_i - 1}{MWD_f} \qquad (3.6)$$

n_R is the number of chain scissions
MWD_i is the initial molar mass distribution
MWD_f is the final molar mass distribution (after scission)

Using these definitions, he then developed a model to predict number of chain scissions [10]. This model is called the chain scission distribution function (CSDF) (more about this model in Chapter 6).

3.3.4 Melt flow index measurements

The melt flow index (MFI) of a polymer is closely related to the molar mass of the polymer. Several authors used MFI measurements to follow the degradation of polyolefins [13]. In an MFI test a constant weight (e.g. 2,16kg) is applied to a polymer and the weight of polymer passing through a small die in 10 minutes is measured. In polyethylene degradation, crosslinking reactions can take place. This will increase the molar mass and consequently the viscosity of the polymer. The higher viscosity will result in less polymer passing through the die, resulting in a lower MFI value. In polypropylene, ß-scission will result in a decreased molar mass and therefore a higher MFI.

3.3.5 Mechanical testing

During polymer degradation the polymer mechanical properties may decrease drastically with an increased level of degradation in the sample. The decrease in toughness of a polyolefin sample can be monitored by tensile testing [9]. There are several standard techniques for the testing of tensile strength (ASTM 882-2 and ASTM D-638). Typically, samples of accurate dimensions are prepared for tensile testing. Samples are usually notched before tensile testing to ensure that analyses are reproducible.

As degradation predominantly takes place in the amorphous regions, a significant amount of scission will result in a significant reduction in tensile strength, elongation at break and toughness of a sample [9]. The fracture toughness will also decrease. This is predominantly due to the formation of micro-cracks, resulting in embrittlement of the sample. These cracks are the result of the changes in macroscopic properties of the polymer (chain scission and the incorporation of oxygen-containing functionalities).

3.3.6 Yellowness index

The yellowness index (YI) is commonly determined during polymer degradation [13]. This index gives an indication of polymer breakdown and also changes in the transformation products from phenolic anti-oxidants. ASTM D-1925 deals with the determination of the yellowness index. The assumption for many yellowness index measurements is that the discolouration (or colouration) is primarily caused by the reactions of the phenolic anti-oxidant during its stabilisation reactions. Reactions of the anti-oxidant result in the formation of coloured products (mainly quinones).

3.3.7 Apparent density measurements

Apparent density is another analytical method used for studying the degradation of polyolefin samples. During degradation, the apparent density of samples increases. This is attributed to increases in crystallinity and crosslinking reactions. The incorporation of oxygen into the molecules can also result in an increase in the density of the samples. In LDPE the amorphous content is higher than in LLDPE, rendering the material more susceptible to oxidative degradation and crosslinking.

3.3.8 Infrared spectroscopy

The chemical changes occurring during the degradation of polyolefins have been discussed in chapter 2. Infrared spectroscopy has been widely used for qualitative and quantitative analysis of these degradation products [3, 5, 13, 17, 20-24]. The Lambert-Beer law applies to infrared absorption:

At a constant sample thickness and a constant wavelength, the concentration of a certain chemical species will be directly proportional to the IR absorbance of the absorbing species.

$$A = \varepsilon lc \qquad (3.7)$$

where:

A is the absorbance

ε is the absorptivity or extinction coefficient

l is the length of the optical path through the sample

c is the concentration of the absorbing species

This can be used for quantitative analysis of the degradation products. During the induction phase of thermo-oxidative degradation, no changes are observed in the infrared spectra. The average concentration of the carbonyl species is, therefore, lower than the detection limit of the Fourier-transform infrared (FTIR) spectrophotometer. There may, however, be highly oxidised regions, but this will not be detected by the FTIR should the volume fraction be very low. The same is true for the formation of the hydroxyl (OH) groups, because the sensitivity is approximately five times lower than for the carbonyl groups.

FTIR has been shown to be useful in determining the changes in unsaturation during degradation of HDPE and LDPE [2, 13, 17, 20, 21]. The changes in the vinylidene (determined at 888 cm^{-1}), terminal vinyl (determined at 909 cm^{-1}) and trans-vinylene groups (determined at 964 cm^{-1}) were considered [2]. The degradation behaviours of a stabilised and an unstabilised HPDE sample under natural exposure were compared. Mendes [2] found that the initial vinylidene concentration of the unstabilised sample was higher that in the stabilised sample. This was attributed to β-scission of the unstabilised sample during extrusion (Figure 2).

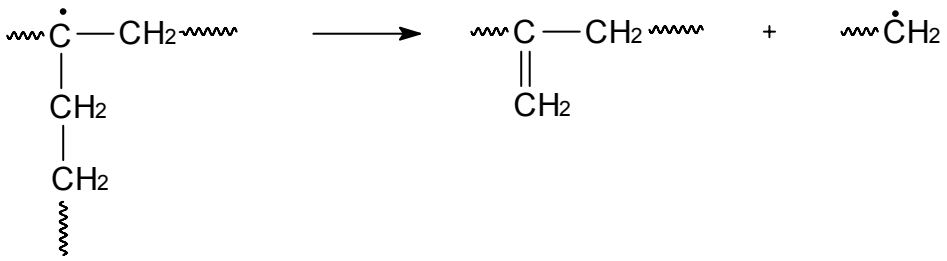

Figure 2: Effect of ß-scission on the formation of the vinylidene group and a radical chain end in HDPE.

The vinylidene concentration decreased during the initial stages of degradation. This was linked to the formation of macroperoxy radicals [2]. The effect of photodegradation on the terminal vinyl group was also studied. It was found that the terminal vinyl index increased during degradation. This was ascribed to Norrish type II reactions during photo-oxidation. The

trans-vinylene groups also showed an increase during degradation of HDPE and this was attributed to a bimolecular reaction between a hydroperoxide and another polymer chain segment (Figure 3).

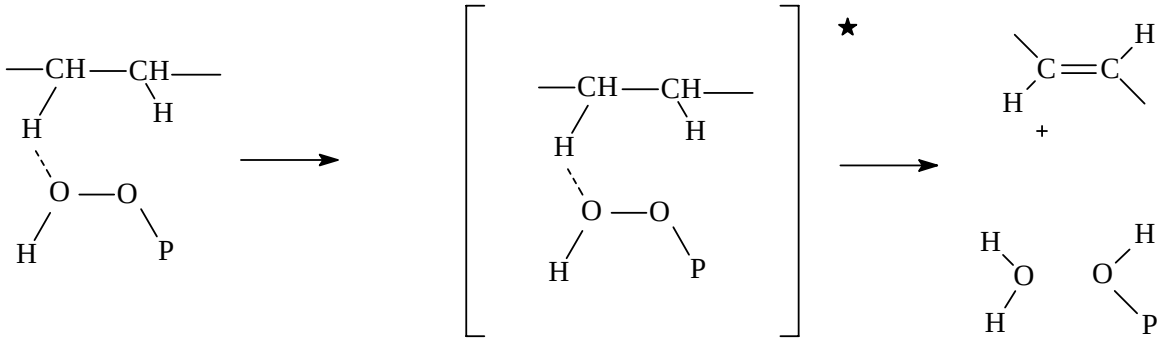

Figure 3: Increase in the trans-vinylene concentration during polyethylene degradation (determined by FTIR spectroscopy at 964 cm^{-1}).

In Figure 4 the relative positions of the three unsaturated groups in the FTIR spectrum of a LLDPE sample can be seen.

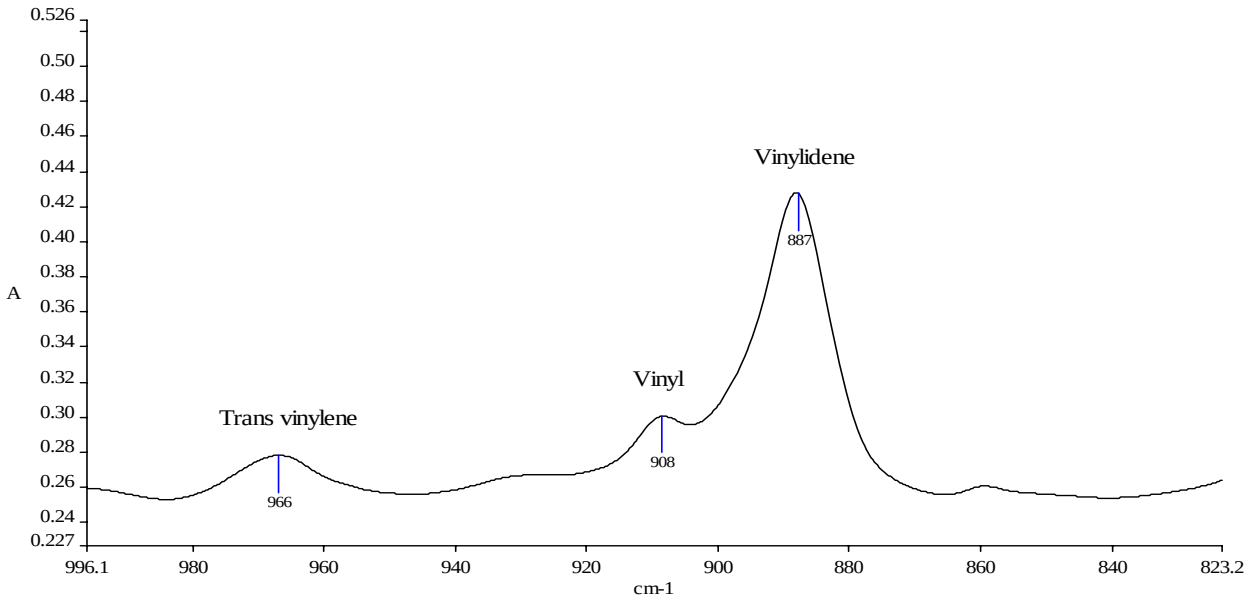

Figure 4: FTIR spectrum indicating the relative positions of the three unsaturated groups present in a typical LLDPE sample.

The carbonyl index, as determined by FTIR, is commonly used to determine the level of degradation in a sample [2, 5, 20]. The carbonyl index is defined as the ratio between the integrated band absorbance of the carbonyl around 1714 cm^{-1} and that of the polyethylene or polypropylene polymer bands. Any characteristic polymer band that is not influenced by degradation can be used for this calculation. In polyethylene the band around 1470 cm^{-1} is commonly used.

Mendes [2] found that the determination of carbonyl indices could be useful in studying polyethylene degradation. He found a significant increase in the carbonyl concentration during outdoor (natural) exposure testing. Gugumus [5] showed that the IR spectrum of a degraded LLDPE is similar to the spectrum of a degraded LDPE sample, with increases in the hydroxyl and carbonyl absorbance regions. He also found significant changes in the double bond concentrations as determined by FTIR during degradation. He associated the increase in the hydroperoxides with the formation of free (3550 cm^{-1}) and associated peroxides (3410 cm^{-1}). In the initial phases of degradation, mainly free peroxides will be detected in the FTIR spectrum, while in the later stages, associated peroxides form [23]. Gugumus showed that aldehydes and ketones will form preferentially trans-vinylene groups [16]. He concluded that trans-vinylene groups originated from free peroxides rather than associated peroxides. Ketones appear to develop from free and associated peroxides.

During polyolefin degradation, peaks can be detected in the FTIR spectrum at 1040 cm^{-1} and 1010 cm^{-1} in the infrared spectrum. These peaks could be attributed to the stretching of the CO grouping, a primary alcohol, or the OH deformation in an alcohol, peroxide or hydroperoxide.

Gulmine et al. [3] used attenuated total reflectance (ATR) FTIR to study surface degradation in polyolefins. In this study the degradation profiles of aged polyethylene samples (LDPE, LLDPE and HDPE) were studied, using the full capability of ATR. ATR analysis was used to supplement microtoming. By microtoming thin layers of a sample the degradation profile through the sample can be studied. Microtoming will, however, be complicated when thin layers (10 micron and less) are studied. During degradation, polyolefin samples become brittle, making microtoming extremely difficult. Gulmine proved that using different reflection angles and different crystal materials, layers as thin as 2 microns can be studied. This involves mathematical treatment of the spectra to calculate the spectra at a certain depth. This is necessary as the spectra recorded at different penetration depths will be a sum of all the layers up to that depth.

Several authors showed that during degradation several carbonyl containing species may be detected in the FTIR spectrum [3, 4, 5, 7, 8, 10, 14, 25, 26, 32]. There is speculation that more than 11 different carbonyl containing species may form during degradation. At the start of degradation, an absorption band can be detected at 1714 cm^{-1}. This can be either due to the formation of carboxylic acids or ketones. Konar and Ghosh [20] boiled a sample in sodium hydroxide and showed that the peak height did not change. If the peak was due to a

carboxylic acid, it would decrease after NaOH exposure (salt formation) and washing. Therefore, this band was assigned to the C=O stretching vibration of a ketone group. The concentration of the ketone group in aged samples can be taken as an indicator of the number of scission events. The intensity of this group grows with an increased level of degradation. Several other bands also appear at higher levels of degradation. These peaks are mainly assigned to the C=O stretching vibrations of aldehydes and esters (both detected at 1733 cm^{-1}), carboxylic acids (1700 cm^{-1}) and γ-lactones (1780 cm^{-1}).

Further information on the degradation products can be obtained by derivatisation techniques, followed by FTIR analysis. Costa et al. [22] showed that derivatisation techniques can be used to selectively convert certain degradation products into groups that can be easily identified by FTIR. Derivatisation can be performed with SF_4, ammonia, KOH (or NaOH) or reaction with 2,4-dinitrophenylhydrazine.

SF_4 will react with the OH groups present in alcohols and hydroperoxides and convert them into alkyl fluorides, which can then be detected at 1080 cm^{-1}. Carboxylic acids will be converted into acyl fluorides, which can be detected at 1847 cm^{-1}, 1842 cm^{-1} and 1815 cm^{-1}. Carboxylic acids can also be derivatised with KOH to form carboxylate salts. A reaction of the degraded polymer with DNPH (di-nitrophenyl hydrazine) in isopropanol will lead to the disappearance of the ketone group in the infrared spectrum.

3.3.9 Differential scanning calorimetry

Differential scanning calorimetry is another technique that can provide more information on the degradation process [13, 27-29]. A broadening in the endotherm graph may be seen upon degradation. This can be attributed to changes in crystallite sizes, and molar mass differences. Olivares et al. [27] found that the crystallinity of isotactic polypropylene increases with degradation while the melting point decreases slightly.

DSC can also be used to study the degradation temperature or degradation time of stabilised polymer samples. Oxidation induction temperature analysis can be used to determine the level of hindered phenolic anti-oxidants in polyolefins. A linear correlation exists between the level of hindered phenol antioxidant in a polymer and the OIT of the polymer. Paquet [28], however, showed that OIT cannot be used to predict long-term thermal or processing stability of polyolefin compounds, particularly in the case of HALS stabilised samples, where the OIT cannot be correlated with the actual thermal stability of the polymer at lower temperatures.

OIT generally leads to an overestimation of the life time compared to data obtained from oven aging. Rosa et al. [29] investigated several parameters that could influence the OIT measurements and found that sample preparation and the temperature of OIT measurements had a significant influence on these measurements. This may be due to the high temperature of OIT measurements (in the molten state- typically 180 ºC and above) compared to oven aging. Oven aging may be performed at the temperature that the polymer will be exposed to during its service lifetime and is dependent on the crystalline morphology.

3.3.10 Gas chromatography-mass spectrometry measurements of degradation products

Gas chromatography-mass spectrometry (GC-MS) can be used for the detection and identification of degradation products [25]. This is especially useful for the identification of volatile products formed during the degradation process. A setup where a trap is connected to the GC-MS enables the volatile products to be introduced into the carrier gas stream. Focusing techniques (for example cryo-focusing) can be used to focus the degradation products onto the capillary column.

Dolezal and Pacanova [26] used pyrolysis-GC to study degradation in polyolefins. Samples were heat-aged in a laboratory oven (in air) and the compositions of the pyrolysis products were evaluated at regular intervals. They proved that the aging of well stabilised HDPE and polypropylene had no effect on the composition of the pyrolysis products. Hoff and Jacobsson [30] carried out an extensive GC-MS investigation into the volatile products formed during the degradation of polypropylene, at temperatures ranging from 120 ºC to 280 ºC. He indicated that although most traditional degradation studies were performed at temperatures below the melting point, significant degradation may occur during the extrusion process which typically takes place at temperatures exceeding 280 ºC. At 280 ºC the major degradation products were: acetaldehyde, formaldehyde, acetone, methacrolein and acetic acid. At lower temperatures (120 ºC), the major products were 3,5-di-substituted dimethylhexanal, dimethylheptanal and dimethyloctanal. In Table 1, the major volatile hydrocarbons, alcohols, ethers, ketones, aldehydes and carboxylic acids are given.

Table 1: Volatiles formed during the high temperature thermo-oxidation of polypropylene and methods of classification

Volatile compound	Type	Identification: GC*	Identification: MS*
Ethene/ethane	Hydrocarbon	a	b
Propene/propane	Hydrocarbon	a	b
Isobutene	Hydrocarbon		c
Butane	Hydrocarbon	a	b
Pentadiene	Hydrocarbon		c
2-methyl-1-pentene	Hydrocarbon		c
2,4-dimethyl-1-pentene	Hydrocarbon		c
5-methyl-1-heptene	Hydrocarbon		c
Dimethylbenzene	Hydrocarbon		c
Methanol	Alcohol	a	b
Ethanol	Alcohol	a	b
2-methyl-2-propen-1-ol	Alcohol	a	b
2-methylfuran	Ether		c
2,5-dimethylfuran	Ether	a	b
Formaldehyde	Aldehyde	a	b
Acetaldehyde	Aldehyde	a	b
Acrolein	Aldehyde	a	b
Propanal	Aldehyde	a	b
Methacrolein	Aldehyde	a	b
2-methylpropanal	Aldehyde		c
Butanal	Aldehyde		c
2-vinylcrotonaldehyde	Aldehyde		c
3-methyl-pentanal	Aldehyde		c
3-methylhexanal	Aldehyde		c
Octanal	Aldehyde		c
Nonanal	Aldehyde		c
Decanal	Aldehyde		c
Ethenone	Ketone		c
Acetone	Ketone	a	b
3-buten-2-one	Ketone		c
2-butanone	Ketone	a	b
1-hydroxy-2-propanone	Ketone	a	b
1-cyclopropylethanone	Ketone	a	b
3-methyl-3-buten-2-one	Ketone		c
3-pentene-2-one	Ketone		c
2-pentanone	Ketone	a	b
2,3-butanedione	Ketone		c
1-cyclopropyl-ethanone	Ketone		c
2,4-pentanedione	Ketone	a	b
4-methyl-2-pentanone	Ketone		c
4-methyl-2-heptanone	Ketone		c
Formic acid	Carboxylic acid	a	b
Acetic acid	Carboxylic acid	a	b
Propanic acid	Carboxylic acid	a	b

**(a) determined by GC retention time, (b) determined by mass spectroscopy analysis of compounds and (c) was determined based on a match with the MS library.*

In samples where (a) is given in the GC classification, it indicates that the identification was based on GC retention time. In samples where (b) is given, it means that identification was based on the mass spectra of individual compounds, while (c) indicates that the classification was based on a match with the spectra in the MS library [30]. At lower temperatures a significant amount of long-chain volatiles were formed, while at higher temperatures a significant amount of shorter-chain volatiles were formed. During the reaction, water and carbon oxides were also detected.

3.3.11 Electron spin resonance

Electron spin resonance (ESR) analysis can be used to monitor the concentration of the NO· radicals in samples stabilised by HAS (Section 2.8.2). HAS stabilises the sample by the formation of the nitroxyl group. The process of oxidation of HAS to the NO· species is a slow process and is temperature dependent [31]. The formation and depletion of the nitroxyl group can be used to follow the stabilisation process. It was shown that the depletion of the nitroxyl radical in a HAS stabilised isotactic polypropylene sample can be correlated with the embrittlement of the sample [31].

3.4 Conclusions

The degradation of polyolefins has been an area of huge scientific interest for many decades. Polyolefins require stabilisation to maintain their performance characteristics during their service lifetime. Three techniques are commonly used to evaluate the effectiveness of stabilisers and/or the degradation of polyolefins:

1. Oven aging at elevated temperatures (to evaluate high temperature stability)
2. Multiple extrusions (to evaluate shear and temperature stability)
3. UV exposure (to evaluate photostability).

The degradation process can be followed by several techniques. Chemiluminescence is used to detect the weak proton emission from hydroperoxides in degraded samples. Chemiluminescence is very useful in investigating the concentration of the active species during degradation.

Molar mass determinations by SEC have also been commonly used to study degradation in polyolefins. The molar mass of polypropylene will decrease during degradation, while the

molar mass of polyethylene could decrease or increase during degradation, depending on the conditions of exposure.

Fourier-transform infrared spectroscopy is a very powerful technique used to study degradation. During degradation several changes in the molecular structure of polyolefins take place and these can be detected by FTIR. Free and associated hydroperoxides and carbonyl species form during degradation. The changes in unsaturation can also be measured by FTIR.

Differential scanning calorimetry is another important method used to study the degradation process. OIT measurements by DSC are very effective in following the concentration of a residual phenolic stabiliser in a polymer sample.

Gas chromatography- mass spectrometry, apparent density, electron spin resonance spectroscopy (ESR) and mechanical testing are additional techniques that have been used to study degradation [24, 25, 29].

3.5 References

[1] Fayolle, B., Audouin, L., Verdu, J., *Polymer Degradation and Stability* **2002**, 75, 123-129

[2] Mendes, L.C., Rufino, E.S., de Paula, O.C., Torres, J.R., *Polymer Degradation and Stability* **2003**, 79, 371-383

[3] Gulmine, J.V., Janissec, P.R., Heise, H.M., *Polymer Degradation and Stability* **2003**, 79, 385-397

[4] Meijers, G., Gijsman, P., *Polymer Degradation and Stability* **2001**, 47, 387-391

[5] Gugumus, F., *Polymer Degradation and Stability* **1997**, 55, 21-43

[6] Chirinos-Padron, A.J., Hernandez, P.H., Allen, N.C., Vasilion, C., Marshall, G.P., *Polymer Degradation and Stability* **1987**, 19, 177-189

[7] Gugumus, F., *Polymer Degradation and Stability* **1998**, 62, 403-406

[8] Colom, X., Canavate, J., Sunol, J.J., Pages, P., Saurina, J., Carrasco, F., *Journal of Applied Polymer Science* **2003**, 87, 1685-1692

[9] Marshall, N., PhD thesis, University of Sussex, **December 2001**

[10] Canevarolo, S., *Polymer Degradation and Stability* **2000**, 70, 71-76

[11] Fearon, P.K., Marshall, N., Billingham, N.C., Bigger, S.W., *Journal of Applied Polymer Science* **2001**, 79, 733-741

[12] Gonzales-Gonzales, V.A., Neira-Velasquez, G., Angulo-Sanchez, J.L., *Polymer Degradation and Stability* **1998**, 60, 33-42

[13] Epacher, E., Tolveth, J., Stoll, K., Pukansky, B., *Journal of Applied Polymer Science* **1999**, 74, 1595-1605

[14] Kato, M., Osawa, Z., *Polymer Degradation and Stability* **1999**, 65, 457-461

[15] Fleming, R.H., Craig, A.Y., *Polymer Degradation and Stability* **1992**, 37, 173-180

[16] Gugumus, F., *Polymer Degradation and Stability* **2000**, 68, 21-33

[17] Setnescu, R., Jipa, S., Setnescu, T., Podina, C., Osawa, Z., *Polymer Degradation and Stability* **1998**, 61, 109-117

[18] Pospisil, J., Horak, Z., Pilar, J., Billingham, N.C., Zweifel, H., Nespurek, S., *Polymer Degradation and Stability* **2003**, 82, 145-162

[19] Iedema, P.D., Willems, C., van Vliet, G., Bunge, W., Mutsers, S.M.P., Hoefsloot, H.C.J., *Chemical Engineering Science* **2001**, 56, 3659-3669

[20] Konar, J., Ghosh, R., *Polymer Degradation and Stability* **1988**, 21, 263-275

[21] Xingzhou, H., *Polymer Degradation and Stability* **1996**, 55, 131-134

[22] Costa, L., Luda, M.P., Trossarelli, L., *Polymer Degradation and Stability* **1997**, 55, 329-338

[23] Al-Madfa, H., Mohamed, Z., Kassem, M.E., *Polymer Degradation and Stability* **1998**, 97, 105-109

[24] La Mantia, F.P., *Polymer Degradation and Stability* **1985**, 13, 297-304

[25] Shlyapnikov, Y.A., Kyrushkin, S.G., Mar'in, A.P., *Antioxidative stabilisation of Polymers* 1996. Taylor and Francis. ISBN 0 7484 0577 1

[26] Dolezal, Z., Pacanova, *Journal of Analytical and Applied Pyrolysis* **2001**, 57, 177-185

[27] Olivares, N., Tiemblo, P., Gomez-Elvira, J.M., *Polymer Degradation and Stability* **1999**, 65297-302

[28] Paquet, J.R., Todesco, R.V., Drake, W.O., Paper presented at the 42th International Wire and Cable Symposium, November 15-18, 1993

[29] Rosa, D.S., Sarti, J., Mei, L.H.I., Filho, M.M., Silveira, S., *Polymer Testing* **2000**, 19, 523-531

[30] Hoff, A., Jacobsson, S., *Journal of Applied Polymer Science* **1984**, 29, 465-480

[31] Gensler, R., Plummer, C.J.G., Kausch, H-H., Kramer, E., Paquet, J-R., *Polymer Degradation and Stability* **2000**, 67, 195-208

[32] He, P., Xiao, Y., Zhang, P., Xing, C., Zhu, N., Zhu, X., Yan, *Polymer Degradation and Stability **2005**, 88, 473-479*

Chapter Four

Fractionation techniques for studying chemical composition distribution in polyolefins

4.1 Introduction

The molecular properties of polyolefins can be analysed by several classical analytical techniques as described in chapter 3, but the results obtained from these techniques are averages, and do not provide information on the chemical heterogeneity or chemical composition distribution of a polyolefin sample. Either the synthesis of polyolefins or the aging thereof gives chains of different lengths and chemical compositions.

During the past few decades several new analytical techniques have been developed to study the chemical heterogeneity and the chemical composition distribution of polyolefin samples. Temperature-rising elution fractionation (TREF) is the oldest of these fractionation techniques. SEC-FTIR and crystallisation analysis fractionation (CRYSTAF) were developed more recently. These techniques will now be discussed.

4.2 Temperature rising elusion fractionation

4.2.1 Background

The TREF technique for the fractionation of polyolefins was developed in the 1970's by Wild [1] although preliminary investigations were already performed as early as the 1950's by Desreux and Spiegels [2]. They realised that different fractionation temperatures can be used to separate a semi-crystalline polymer according to its crystallisability from solution. Amorphous polymers can also be fractionated at different temperatures, but this fractionation is on the basis of molar mass. TREF was initially developed to fractionate low density polyethylene according to the degree of short-chain branching. To a significant degree, polymer properties depend on the molar mass and molar mass distribution. This can be measured directly by SEC. The molar mass data obtained by SEC can, however, not explain all the properties of semi-crystalline polymers. Crystallinity measurements were thus shown to be important in determining the properties of a polyolefin.

The TREF technique separates a polymer sample into fractions on the basis of crystallinity differences between the fractions, or the temperature-solubility relationship. The technique is, therefore, sensitive to and based on the relationship between molecular structure, chain crystallinity, and dissolution temperature. Different molecular structures will be reflected in distinct crystallinities, that will translate to dissimilar dissolution temperatures.

During early fractionation studies of polyethylene it was realised that there are two possible ways of separation or fractionation of polyethylene. In the first, solvent/non-solvent mixtures are used to separate according to molar mass (above the melting point). In the second method, separation is based on the difference in solubility of polymer fractions at different temperatures [1].

Crystallinity in polyethylene and polypropylene is the result of strong van der Waal's forces between neighbouring polymer chains. The linear structure of HDPE (and the absence of significant amounts of branching) allows for the tight packing of the chains and, therefore, results in high crystallinity. With the introduction of side branches, for example by polymerisation under high pressure (like in LDPE) or by the incorporation of comonomers (LLDPE), the degree of crystallinity will decrease. HDPE, for example, crystallises as a hard polymer due to its structural regularity. When a comonomer, for example 1-butene, 1-hexene or 1-octene, is introduced, it results in a disruption of the crystalline structure.

In polypropylene, the crystallinity depends on the position of the methyl group in relation to the polymer main chain (tacticity). Due to the stereo-isomerism, the position of the methyl group can influence the crystallinity. In atactic polypropylene the irregular distribution of methyl groups results in a non-crystalline product. Comonomers as well as polymerisation conditions can also modify the crystallinity.

Several TREF setups were investigated over the years. Initially the support material was considered crucial for the technique, although Holtrup [3] showed that non-supported TREF can also be successful in separating a sample according to crystallisability. Supports include glass beads, Chromosorb P, silica gel or stainless steel balls [1, 4].

4.2.2 Theoretical considerations

Polymer fractionation by crystallisation in solution (TREF and CRYSTAF) can be explained in terms of the Flory-Huggins statistical thermodynamic analysis [1, 5]. The theory explains the depression in melting points as a function of the presence of diluents. Non-crystallising units, comonomer units, diluents and polymer end groups all have an equivalent effect on the melting point depression when the concentration of each is low and the units do not enter into the crystal lattice [6].

The reduction in the melting point as a result of the incorporation of a diluent can be calculated by:

$$\frac{1}{T_m} - \frac{1}{T_m^0} = \frac{R}{\Delta H_u}\left(\frac{V_u}{V_1}\right)(\upsilon_1 - \chi_1 \upsilon_1^2) \qquad (4.1)$$

where:

T_m^0 is the melting point of the pure polymer
T_m is the equilibrium melting point of the polymer/diluent mixture
ΔH_u is the heat of fusion per polymer repeating unit
V_u and V_1 are the molar volumes of the polymer repeating unit and the diluent
υ_1 is the volume fraction of the diluent
χ_1 is the Flory Huggins thermodynamic interaction parameter

The melting point of a polymer decreases with the incorporation of a diluent (for example a comonomer). In a random copolymer the equation can be written as:

$$\frac{1}{T_m} - \frac{1}{T_m^0} = -\frac{R}{\Delta H_u} \ln(p) \qquad (4.2)$$

where:
ΔH_u is the heat of fusion per homopolymer repeating unit
p is the molar fraction of the crystallising unit

4.2.3 The TREF experiment

The TREF setup employs the principle of dissolving polymer from a support at successively higher temperatures. This dissolution step is preceded by a controlled crystallisation step (Figure 1, step 1), taking a considerable amount of time. The hot polymer solution is introduced into the column and cooled slowly. Typically the sample is cooled at a rate of 6 ºC or less per hour. The polymer dissolution phase may be carried out as a stepwise process, or as a continuous temperature gradient (Figure 1, step 2).

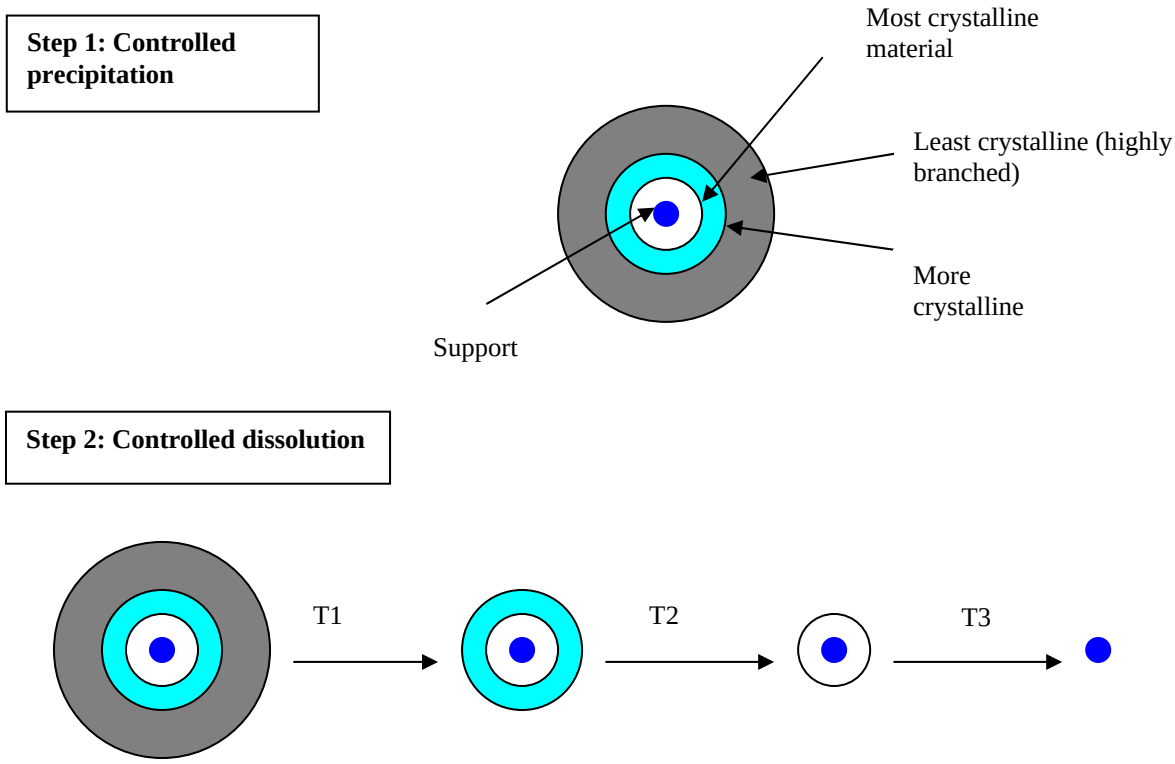

Figure 1: The proposed mechanism of a TREF fractionation, consisting of a controlled crystallisation and a controlled dissolution step.

Mirabella et al. [7], Glöckner [4] and Wild [1] all proposed that the polymer coats the support in layers of different crystallinities. This can be referred to as an onion layer structure. The layers on the surface of the support structure are precipitated at higher temperatures, and are more crystalline (low branching content).

At lower temperatures the chains of increasing branching levels will crystallise. With further cooling the rest of the polymer precipitates, and this leads to a crystallinity gradient over the support material. The less crystalline or amorphous material will precipitate last.

Several authors compared TREF experiments for the determination of chemical composition distribution with conventional DSC analysis [7, 8]. Mirabella [7] and other authors [9] showed that analytical TREF of poly (ethylene-α-olefins) was virtually a diluent DSC melting experiment. This implies that the mechanism of melting in a DSC analysis containing TCB as a diluent is similar to the result obtained from an analytical TREF experiment. There are, however, several differences between these two approaches and these techniques cannot be considered as fully similar. In A-TREF the longest sequences in a chain dominate the dissolution process. So the chain is dissolved at one temperature. DSC is based on the detection of heat flow as a function of temperature, and detects melting of all crystallised

sequences irrespective of their lengths. So in DSC you actually see all melting processes at their characteristic, different temperatures. Starck [8] showed that the results obtained by a stepwise DSC crystallisation experiment were similar to results obtained from an analytical TREF experiment.

Over the years two TREF setups were developed, an analytical TREF setup and a preparative TREF setup. The two techniques will be discussed separately. In the preparative TREF setup larger quantities of the polymer are fractionated for further analysis, while in the analytical TREF the concentration in solution is monitored.

4.2.4 Preparative TREF

In preparative TREF (prep-TREF) the polymer is slowly crystallised and then fractionated and collected at predetermined temperature intervals. Preparative TREF requires larger columns for the fractionation of larger samples than in analytical TREF. These fractions can then be analysed off-line. Typically NMR, FTIR, DSC and SEC analyses can be performed on these fractions. Preparative TREF is, however, more time consuming than analytical TREF. In Table 1, a comparison of analytical and preparative TREF is given.

Table 1: Comparison of preparative and analytical TREF

Preparative TREF	Analytical TREF
Collection of fractions at temperature intervals	Continuous fractionation
Off-line measurements possible (NMR, DSC, GPC, etc)	On-line measurement of polymer concentration
Larger columns and sample sizes required	Smaller columns and smaller sample sizes required
Time consuming, but through additional techniques much information is obtained	Faster, but less information obtained

4.2.5 Analytical TREF

The principles of analytical and prep-TREF are similar, the only difference is that in analytical TREF sufficient quantities of the fractions are not obtained for further off-line analysis. In analytical TREF, the concentration of the polymer in solution is measured as a function of

temperature. Similar to prep-TREF, in an analytical TREF experiment the polymer is slowly crystallised, followed by a slow, controlled dissolution step. At lower temperatures, the highly branched material is dissolved. The less branched material is dissolved at higher temperatures. The concentration of the polymer in solution is obtained continuously by an in-line IR cell. Generally no further analysis is possible.

Analytical TREF data can be converted to branching distribution using a calibration curve relating the number of branches to elution temperature [7]. This is done by analysing narrow chemical composition distribution (CCD) samples. Traditionally, samples with narrow CCDs were obtained by preparative fractionation of a polyolefin sample. The short-chain branching content of these fractions were analysed by NMR or FTIR. The fractions were subsequently analysed by analytical TREF and the crystallisation temperatures of these samples were then related to the short-chain branching content. A more recent development is the synthesis of metallocene (narrow CCD) samples for calibration. These samples are generally narrow in CCD and can be used to calibrate the TREF setup.

Hyphenated techniques, based on TREF, have been developed over the years [1]. One of the most significant hyphenated techniques is TREF-SEC. This prototype automated instrument, designed by Nakano and Goto [described by Wild in reference 1], is able to determine the branching distribution as a function of molar mass. In this setup, fractions from the analytical TREF instrument are introduced into the SEC apparatus. SEC chromatograms can be obtained directly across the fractionation range. This is, however, a very complicated and expensive setup and has not been developed further. The experiment is also limited by the speed of the SEC analysis. Problems were experienced with the cooling step in the TREF experiment due to diffusion of polymer species outside the column. This was solved by fast cooling, but this leaves concern about the efficiency of fractionation. Another approach is to consider SEC-TREF, which is superior to the TREF-SEC setup. This is, however, complicated and requires preparative SEC separations.

4.2.6 Molar mass dependence of TREF separation

Wild [1] performed studies to determine the molar mass dependence of TREF data. In principle there are two main parameters that affect crystallisation: chemical composition and molar mass. In his experimental setup, Wild aimed to separate LLDPE samples according to branching (chemical composition). He found that the molar mass effect can be neglected when MM> 10,000 g/mol. The molar mass of most commercial polyolefins is above 10,000

g/mol hence the separation will be with regard to chemical composition (molar mass effects can be ignored). The CCD across the MMD is more important for effective fractionation in TREF than the absolute molar mass.

4.2.7 Applications of TREF

4.2.7.1 Polyethylene

To understand the performance of polyethylene in end-use applications, the chemical composition and the molar mass distributions need to be considered. Two polyethylene samples may have similar molar masses and molar mass distributions, but significantly different end-use properties. The chemical composition distribution of polyethylene has been extensively analysed by analytical- and prep-TREF [1, 7, 8, 10-15]. TREF is especially useful for the analysis of LLDPE, where the fractionation according to short-chain branching can provide valuable information on the chemical composition distribution. Ziegler-Natta LLDPE resins are typically characterised by a broad, multimodal chemical composition distribution [11]. This broad distribution showed the presence of highly crystalline chains with little or no branching and chains of low crystallinity, highly-branched material. This is ascribed to the presence of two types of active sites on a Ziegler-Natta LLDPE catalyst [1].

Preparative fractionations of polyethylene, followed by FTIR, ^{13}C NMR and/or DSC analyses can provide more information on the CCD of these polymers [10, 11]. Neves et al. [11] found that an ethylene-butene copolymer consisted of a mix of ethylene-butene copolymer molecules with different butene contents, as well as an ethylene homopolymer fraction. TREF can also be used to study short-chain branching in LDPE [1]. The short-chain branching in LDPE mainly arises from the Roedel backbiting mechanism and is influenced by the polymerisation conditions. With an increase in reactor temperature or a decrease in the pressure, the level of short-chain branching in the polymer will increase. The TREF separation in LDPE was found to be dependent on the short-chain branching and not the long chain branching, which is the dominant branching type in LDPE.

Xu and Feng [16] fractionated several metallocene-LLDPE copolymers prepared with the same catalyst, but different feed ratios and polymerisation conditions. They found that the short-chain branching distribution became significantly broader at higher comonomer contents. The polymerisation process (gas phase vs slurry phase) had a significant influence

on the short-chain branching distribution. Samples made via the gas phase process were generally more homogenous than samples made via the slurry process.

TREF can also be used in conjunction with FTIR. FTIR analyses can be performed on the TREF fractions to determine the short-chain branching. With decreasing short-chain branching, the 720 cm^{-1} peak splits and the intensity of the 730 cm^{-1} peak increases. Of the two bands, the 720 cm^{-1} band is the least affected by crystallinity and the ratio of the peaks at 730 cm^{-1} and 720 cm^{-1} may be used to determine the degree of crystallinity.

4.2.7.2 Polypropylene

Similar to polyethylene, polypropylene has been extensively studied by analytical and preparative TREF [1, 4, 5, 16-20]. Several block copolymers and random copolymers have been studied by TREF. In an ethylene-propylene block copolymer, TREF fractionation indicated the existence of a propylene homopolymer phase, a high density polyethylene phase, and an ethylene-propylene copolymer phase containing different ratios of ethylene to propylene [20]. In a propylene-1-butene random copolymer it was shown that the random copolymer is actually a blend of nearly random copolymers with different butene contents [17]. A polypropylene homopolymer made with a magnesium catalyst was shown to consist of an atactic fraction, a fraction of low tacticity and a fraction of high tacticity [16].

Wild [1] found the fractionation of PP by TREF was mainly dependent on the stereo-regularity (tacticity), implying that the TREF fractionation will be influenced by all factors that disrupt the crystalline structure. The nature of the catalyst, the polymerisation conditions and the incorporation of a comonomer will all influence the crystallisation behaviour of polypropylene.

TREF, in summary, is a good technique for the fractionation of semi-crystalline polymers according to their crystallisability.

4.2.8 Shortcomings of the TREF technique

The major disadvantage of traditional TREF analysis of polyolefins is that it is a very slow, time consuming technique. The controlled crystallisation and dissolution steps can take in excess of 36 hours to complete. A second major problem is that it is difficult to automate the system, so it is very labour intensive in setting temperature profiles, draining fractions, precipitating fractions and filtering fractions. The solvent consumption of these setups is also

high. Depending on the number of fractions taken for analysis, up to 4 litres of xylene and 8 litres of acetone are required per fractionation.

4.3 Crystallisation analysis fractionation

4.3.1 Background

CRYSTAF is a relatively new technique for the analysis of the chemical heterogeneity (chemical composition distribution) of semi-crystalline samples. The CRYSTAF technique was invented by Monrabal [6, 21-23]. CRYSTAF uses the opposite approach to the TREF technique: the analysis is carried out during the crystallisation step and not during the dissolution step as with a TREF analysis. In a typical CRYSTAF analysis the sample is dissolved at elevated temperature, followed by a slow cooling step. The concentration of the polymer in solution is monitored during this cooling step. The technique is less time consuming than TREF, as the controlled dissolution step is unnecessary. In CRYSTAF the concentration of the polymer in solution is measured continuously, using an infrared detector. The crystallisation process in CRYSTAF is dominated by the longest crystalline sequences.

4.3.2 CRYSTAF setup

In a CRYSTAF analysis the sample is dissolved at temperatures above the crystallisation point of the polymer. The dissolution of the sample and the crystallisation step is performed in 60-ml stainless steel vessels. A vessel contains a stainless steel cap with three stainless steel lines entering the vessel. A typical crystallisation setup can be seen in Figure 3. The one line entering the reactor is a nitrogen line, used to pressurise the vessel during sampling. The second line is a sampling line, equipped with a porous glass frit at the bottom of the line, and the third line is used for filling the reactors with solvent. Five reactors can be run simultaneously. The CRYSTAF setup is housed in a Hewlett Packard GC oven. Compared to TREF experiments, where oil is typically used as the heating medium, the heat transfer medium in CRYSTAF is air. The five reactors are sampled continuously, based on a sampling interval set on the software program. The reactors are cleaned automatically. In Figure 2 a typical CRYSTAF instrument can be seen. Figure 3 shows the construction of a typical reactor.

Figure 2: A typical CRYSTAF instrument showing the position of the five reactors inside the temperature-controlled oven.

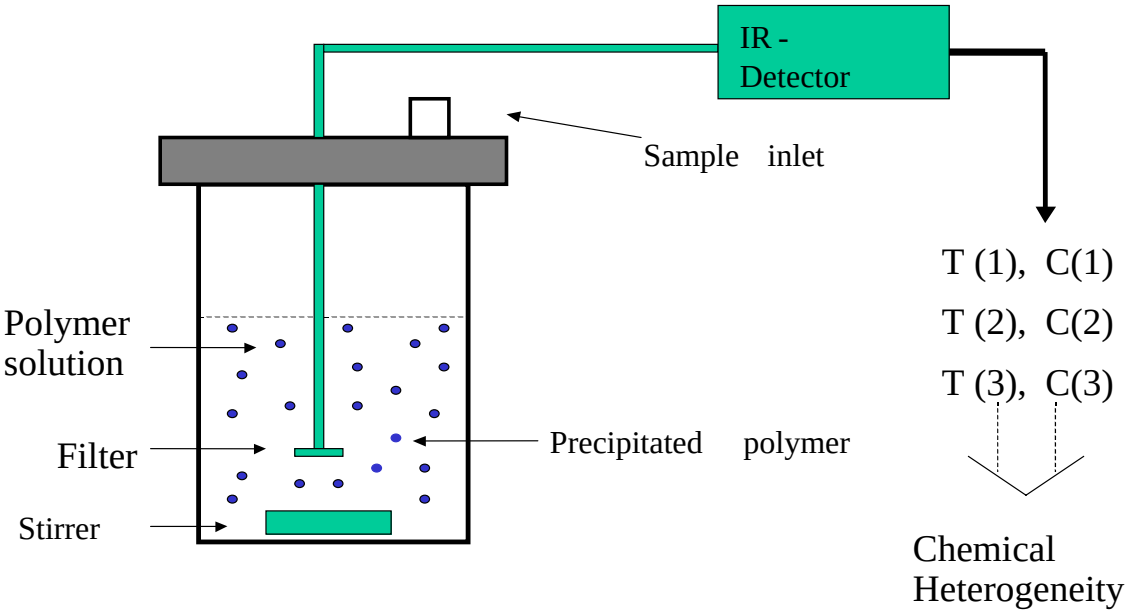

Figure 3: Schematic of a CRYSTAF reactor setup.

4.3.3 The CRYSTAF analysis experiment

CRYSTAF analysis of polyolefins can be performed with 1,2,4-trichlorobenzene (TCB) or ortho-dichlorobenzene (ODCB) as the solvent. Sampling at regular intervals is carried out by the application of nitrogen pressure to the reactor. A small part of the sample in solution is filtered and then passed through a flow-through IR cell in the CRYSTAF instrument. The first few aliquots provide information on the polymer concentration in solution before any crystallisation from solution. Typically for polyethylene, the sample is dissolved at temperatures above 150 ºC. On slow cooling the highest crystallinity material (least amount of branching) will crystallise first, followed by the more branched material. The crystallised material will precipitate and the concentration of the polymer in solution decreases. The process will continue until only highly branched (amorphous) material remains in solution. This will remain in solution and will be integrated and reported as the non-crystalline material. In a CRYSTAF analysis of LLDPE, the curve corresponds to cumulative short-chain branching distribution (SCBD). The temperature axis can be transferred to branches per 1000 C atoms using a similar procedure to the analytical TREF calibration (Section 3.2.5).

Several articles describe the effect of operating conditions on CRYSTAF analysis [24, 25]. It was found that the typical cooling rates used in CRYSTAF and TREF are far from the thermodynamic equilibrium. Crystallisation is, therefore, strongly dependent on the cooling rate. The results of CRYSTAF at fast cooling rates (24 ºC per hour) are similar to the results obtained from TREF at heating rates of 6 ºC per hour. Monrabal [6] found that the results obtained by the two techniques are comparable. A difference is, however, noted in crystallisation temperatures. This is due to the supercooling effect. Supercooling can be described as the difference between the dissolution temperature as determined by TREF and the crystallisation temperature as determined by CRYSTAF. Typically the crystallisation temperatures determined by TREF will be significantly lower than those determined by CRYSTAF. This effect is found in the analysis of all semi-crystalline polymers.

4.3.4 Applications of CRYSTAF

CRYSTAF is a valuable tool in the correlation of the microstructure of a polyolefin with product properties (structure-property relationship). Analytical CRYSTAF has been used extensively in the analysis of the short-chain branching distribution in LLDPE [6, 21, 22, 26, 27]. It has also been used to study blends of isotactic, syndiotactic and atactic polypropylene [23]. Monrabal et al. [6, 21-23] found that the CRYSTAF results for commercial polyolefin

samples are independent of molar mass. They also found a good correlation with a reduction in crystallisation temperatures and the amount of comonomer incorporated. Similar to TREF, the solution crystallisation of polyethylene is independent of molar mass if the molar mass of the sample is above 15,000 g/mol. LLDPE made with Ziegler-Natta type catalysts shows a very characteristic broad and multimodal chemical composition distribution. Typical of Ziegler-Natta catalysed products, the polymer contains a fraction of highly branched material of low crystallinity and a significant amount of lowly branched, high crystallinity material. The low crystallinity fraction (amorphous material), produced by highly active catalyst sites, is generally unacceptable. Large crystallinity fractions on the other hand can result in unacceptable haze values. Metallocene-based LLDPEs are characterised by a narrower MMD and CCD than comparable Ziegler-Natta based LLDPE products. This has, for example, resulted in very low quantities of soluble fractions. One expects a narrow chemical composition distribution when using a single-site catalyst, but this is not always the case as found by, for example, Monrabal et al. [6, 21-23] and Wild [1]. It was found that broad CCDs tailing and shoulders are very common for metallocene LLDPE.

Pasch et al. [28] performed analysis on PE/PP blends and found that SEC was unable to resolve the two components. The two components could, however, be resolved by DSC on condition that the concentration of the PP was above 20%. Quantification of the blend ratio by DSC was problematic as the crystallinity of PP is significantly lower than that of PE and, therefore, the sensitivity for PP in a blend is relatively low. CRYSTAF was, however, able to separate the PE/PP components successfully.

Brüll et al. [29] investigated the CRYSTAF behaviour of several isotactic/syndiotactic polypropylene blends. With DSC, two melting points were detected for syndiotactic polypropylene, at 138.8 ºC and 145.5 ºC. A single melting point was detected for isotactic polypropylene, at 149.1 ºC. In a blend these melting points overlap, making it impossible to quantify the blending ratios. These two components can, however, be successfully separated by CRYSTAF, enabling the quantification of the blending ratios. Brüll also investigated blends of syndiotactic polypropylene and HDPE. Again, CRYSTAF was able to separate these two components successfully. Even ternary blends of isotactic polypropylene, syndiotactic polypropylene and HDPE could be separated successfully by CRYSTAF. In newer developments CRYSTAF has been combined with viscometry. This can be used for molar mass detection [44].

4.4 Size exclusion chromatography-Fourier-transform infrared spectroscopy

Size exclusion chromatography-Fourier-transform infrared spectroscopy is a hyphenated technique that has become increasingly popular in polymer analysis over the past few years [30-43]. It combines the separation capability of SEC with the identification capability of FTIR. There are two main experimental setups [30, 31]: flow cells and LC transform (offline SEC-FTIR).

4.4.1 Flow cell technology

In a flow cell setup the outlet of the SEC instrument is connected via a heated transfer line to the FTIR. A special flow cell is installed in the FTIR and the mobile phase from the SEC instrument passes through this cell. The windows of the flow cell are made from materials that are transparent in the IR region. When only the solvent passes through, the FTIR instrument will only detect the characteristic IR frequencies of the solvent, but when the polymer elutes, it will detect the polymer as well. By using the solvent as a background, the differential spectrum of the solvent/polymer mix will give the polymer spectrum. The only requirement is that there must be certain characteristic frequencies for the polymer where the polymer and the solvent do not overlap.

The use of this method is, however, restricted by two problems:

1. The strong absorption of the solvent in the IR region. Most organic solvents absorb quite intensely in the IR region [40].
2. The relative insensitivity of the FTIR technique. To obtain reasonable spectra, the concentration of the polymer in solution must be increased to levels higher than the concentrations normally used for SEC. This will give the required sensitivity but may lead to a deterioration in the quality of the chromatography.

4.4.2 LC transform (offline SEC-FTIR)

LC transform (offline SEC-FTIR) has become the standard technique for the coupling of FTIR and SEC [28]. In this technique the outlet from the SEC is connected to the LC transform setup (Lab Connections). The low volatility of the solvent 1,2,4-trichlorobenzene necessitates the use of vacuum to remove it [40]. The sample to be analysed must be non-volatile and the

solvent may not contain any buffer that could precipitate with the sample [38]. The setup contains an ultrasonic nebuliser to aid uniform deposition of the polymer layer and removal of the solvent. A rotating Germanium disc is used for deposition of the polymer (Figure 4). The material eluting from the SEC instrument is sprayed continuously onto the rotating Germanium disk, the solvent evaporates under the vacuum conditions and the polymer is deposited continuously as a thin film on the Germanium disk. After the SEC analysis is completed, the Germanium disk is removed and IR spectra can be obtained off-line over the whole disc.

4.4.3 Applications of SEC-FTIR in high temperature measurements

One of the most important uses of SEC-FTIR in polyolefin analysis is the analysis of short-chain branching in polyethylene as a function of molar mass [13, 34, 37]. Willis studied the distribution of butene in an ethylene-butene copolymer [37]. The incorporation of butene will result in the formation of ethyl side branches. These ethyl side branches were detected at 770 cm^{-1}. From his results it was evident that there was a low concentration of ethylene side branches in the high molar mass region and a high concentration of ethylene side branches in the low molar mass region. The unsaturation of polyolefin samples can also be determined using SEC-FTIR. An overview of the SEC-FTIR process is given in Figure 4.

In a study performed by Tackx and Bremmers [42] the LC transform was used in the analysis of EPDM. They used SEC-FTIR to determine the composition as a function of molar mass. Graef et al. [33] used SEC-FTIR to study the chemical heterogeneity of metallocene catalysed copolymers of ethylene and higher α-olefins.

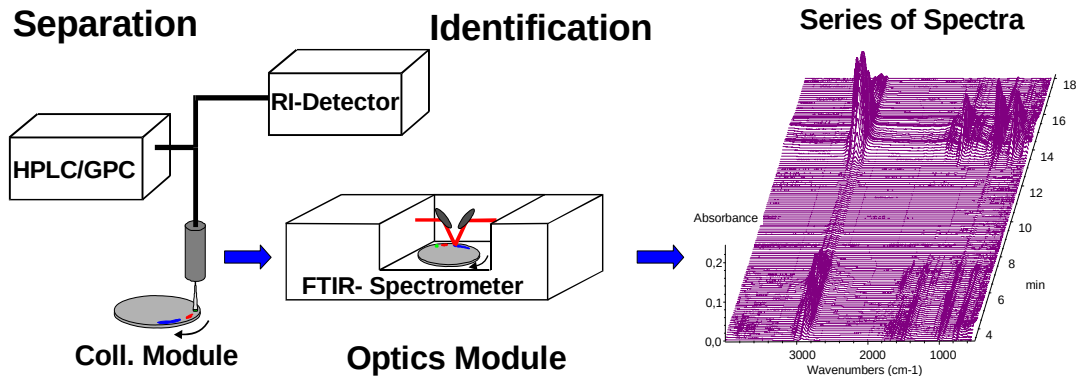

Figure 4: Setup for polymer analysis by SEC-FTIR.

The SEC-FTIR setup has been used for both high temperature [34-37, 40-43] and room temperature separations [30-34]. The SEC setup enables the determination of functional groups or chemical compositions as a function of molar mass.

4.5 Conclusions

Classical analytical techniques only provide average values for molar mass, melting properties, chemical compositions and branching of polyolefins. Several techniques have now been developed to study the chemical heterogeneity of polyolefin samples. TREF is the classical technique for studying the chemical composition distribution in a polyolefin sample. The technique is based on the slow controlled crystallisation of a sample, followed by the extraction of fractions at increasingly higher temperatures. TREF has been used successfully on polyethylene and polypropylene samples of different compositions. The technique is, however, very slow, limiting its applicability.

CRYSTAF is a relatively new technique for studying polymer crystallisability from solution. CRYSTAF eliminates the use of the controlled dissolution step. The polymer is dissolved at elevated temperatures and the concentration of the polymer in solution is followed. It is commonly used to study the chemical heterogeneity in polyolefin samples.
SEC-FTIR combines the separation efficiency of SEC with the spectral capability of FTIR. Two setups can be used: an on-line setup, where the SEC is connected to a flow cell inside the FTIR spectrophotometer, and an off-line setup, where the solution from the SEC is precipitated on a Germanium disc followed by off-line analysis in the FTIR spectrophotometer.

4.6 References

[1] Wild, L., *Advances in Polymer Science* **1990**, 98, 1-46
[2] Desreaux, V., Spiegels, M.C., *Bulletin of Society of Chemistry, Belgium* **1950** 476-489
[3] Holtrup, W., *Macromolecular Chemistry* **1977**, 178, 2335-
[4] Glöckner, G., *Journal of Applied Polymer Science* **1990**, 45, 1-24
[5] Mingozzi, I., Cecchin, G., Morine, G., *International Journal of Polymer Analysis* **1997**, 3, 293-317
[6] Monrabal, J., *Journal of Applied Polymer Science* **1994**, 52, 491-499
[7] Mirabella, F.M., *Journal of Polymer Science: Part B Polymer Physics* **2001**, 39, 2819-2832

[8] Starck, P., *Polymer International* **1996**, 40, 111-122

[9] Sarzotti, D.M., Soares, J.B.P., Simon, L.C., Britto, L.J.D., *Polymer* **2004**, 45, 4787-4799

[10] Pigeon, M.G., Rudin, A., *Journal of Applied Polymer Science* **1994**, 51, 303-311

[11] Neves, C.J., Monteiro, E., Habert, A.C., *Journal of Applied Polymer Science* **1993**, 50, 817-824

[12] Wilfong, D.L., *Journal of Polymer Science* **1990**, 28, 861-870

[13] Soares, J.B.P., Hamielec, A.E., *Polymer* **1995**, 36, 1639-1654

[14] Wang, C., Chu, M-C., Lin, T-L., Lai, S-M., Shih, S-S., Yang, J-C., *Polymer* **2001**, 42, 1733-1741

[15] Kulin, L.I., Meijerink, N.L., Starck, P., *Pure and Applied Chemistry* **1988**, 60, 1403-1415

[16] Xu, J., Feng, L., *European Polymer Journal* **2000**, 36, 867-878

[17] Collina, G., Noristi, L., Steward, C.A., *Journal of Molecular Catalysis* **1995**, 99, 161-165

[18] Mirabella, F., *Journal of Applied Polymer Science* **1992**, 51, 117-134

[19] Viville, P., Jonas, A.M., Nysten, B., Legras, R., Dupire, M., Michel, J., Debras, G., *Polymer* **2001**, 42, 1953-1967

[20] Feng, Y., Hay, J.N., *Polymer* **1998**, 39, 6723-6731

[21] Monrabal, B.; Blanco, J., Nieto, J.; Soares, J.B.P., *Journal of Polymer Science Part A: Polymer Chemistry* **1999**, 37, 89-93

[22] Monrabal, B., Presentation at the Waters GPC conference, 2000

[23] Monrabal, B.; *Macromolecular Symposia* **1996**, 110, 81-86

[24] Anantawaraskul, S., Soares, J.P.B., Wood-Adams, P.M., *Journal of Polymer Science Part B: Polymer Physics* **2003**, 41, 1762-1778

[25] Anantawaraskul, S., Soares, J.P.B., Wood-Adams, P.M., *Macromolecular Symposia* **2004**, 206, 57-68

[26] Britto, L.J.D., Soares, J.B.P., Penlidis, A., Monrabal, B., *Journal of Polymer Science Part B: Polymer Physics* **1999**, 37, 539-552

[27] Gabriel, C., Lilge, D., *Polymer* **2001** 42, 297-303

[28] Pasch, H., Brüll, R., Wahner, U.M., Monrabal, B., *Macromol. Mater. Eng.* **2000,** 279, 46-51

[29] Brüll, R., Grumel, V., Pasch, H., Raubenheimer, H. C., Sanderson, R., Wahner U.M., *Macromolecular Symposia* **2002**, 178, 81-91

[30] Kok, S.J., Wold, C.A., Hankemeier, T., Schoenmakers, P.J., *Journal of Chromatography A* **2003**, 1017, 83-96

[31] Kok, S.J., Arentsen, N.C., Cools, P.J.C.H., Hankemeier, T., Schoenmakers, P.J., *Journal of Chromatography A* **2002**, 948, 257-265

[32] van Zyl, A.J.P., Graef, S.M., Sanderson, R.D., Klumperman, B., Pasch, H., *Journal of Applied Polymer Science* **2003**, 88, 2539-2549

[33] Graef, S.M., Brüll, R., Pasch, H., Wahner, U.M*., e-Polymers* **2003** 005, 1-9

[34] Tso, C.C., DesLauriers, P.J., *Polymer* **2004**, 45, 2657-2663

[35] Faldi, A., Soares, J.B.P., *Polymer* **2001**, 3057-3066

[36] Verdurmen-Noël, L.; Baldo, L.; Bremmers, S., *Polymer* **2001**, 42, 5523-5529

[37] Willis, J.N., Dwyer, J.L., Liu, X, Dark, W., *ACS Symposium* **1999**, 226-231

[38] Willis, J.N., Dwyer, J.L., Liu, X., *International Journal of Polymer Analytical Characterisation* **1997**, 4, 21-29

[39] Ludlow, M., Louden, D., Handley, A., Taylor, S., Wright, B., Wilson, I.D., *Analytical Communications* **1999** 36, 85-87

[40] Cheung, P., Balke, S.T., *Polymer Materials Science and Engineering* **1993**, 69, 122-123

[41] Willis, J.N., Dwyer, J.L., Liu, X., *Polymer Materials Science and Engineering* **1997**, 77, 27

[42] Tackx, P., Bremmers, S., *Polymer Materials Science* **1998**, 78, 50

[43] Deslauriers, P.J., Rohlfing, D.C., Hsieh, E.T., *Polymer* **2002**, 43,159-170

[44] Monrabal, J., Ortin, A., Presentation at the Waters GPC Conference, 2000

Chapter Five

Monitoring the degradation of polypropylene by spectroscopic and fractionation techniques

5.1 Introduction

The development of fast and accurate detection methods for evaluating degradation and the products is an important challenge in the field of analytical polymer chemistry. The degradation of polymers has been a field of interest since the 1940's when Bolland and Gee carried out some preliminary investigations [1].

CRYSTAF is a relatively new analytical technique that utilises the crystallisability from solution to determine the chemical composition of semi-crystalline materials [2-6]. The crystallisation behaviour in solution can be correlated directly to the chemical composition distribution. The coupling of SEC with FTIR is also a relatively new technique that gives an insight into how certain chemical groups are distributed along the molar mass axis or what the chemical composition is as a function of the molar mass distribution [7-22]. CRYSTAF has been frequently used to study polymer composition, but to my knowledge, has not been used extensively in studying polymer degradation on a molecular level.

5.2 Objectives

The main objective of this section of the study was to investigate the use of fractionation (TREF and CRYSTAF) and hyphenated techniques (SEC-FTIR) to obtain more information on degradation in polyolefins. The focus was on method development and ensuring that the techniques were sensitive towards degradation. The classical analytical techniques (for example SEC and DSC) provide only limited information on the changes in chemical composition distribution during degradation. Furthermore, the classical techniques provide only average values for degradation products and it is not possible to predict what the effect of degradation will be on a certain fraction of the polymeric material during degradation. Normal high temperature-SEC (HT-SEC) can only provide information with regard to the distribution in the molar mass in a polyolefin sample. DSC on its own only provides information on the distribution of the crystallising units, but it is difficult to quantify the distribution of these units.

A second objective was to study the spatial heterogeneity of a thick degraded polypropylene sample. This was carried out by microtoming thin slices from the surface and analysing the fractions by FTIR and SEC. The fractions were also analysed by CRYSTAF to investigate the CCD differences.

5.3 Experimental

5.3.1.1 Sample preparation

For the present study, unstabilised samples of a Ziegler-Natta based polypropylene homopolymer were supplied by Sasol Polymers, Polypropylene Business, Secunda, South Africa. These were degraded in air at elevated temperatures (70 ºC, 110 ºC and 130 ºC respectively) and studied by FTIR, DSC, HT-SEC, SEC-FTIR, CRYSTAF and TREF. The Ziegler-Natta based sample was manufactured on a commercial Novolen Technology plant, using a Ziegler-Natta PTK catalyst system. A phosphite processing stabiliser (0,05% Irgafos P- EPQ, Ciba Speciality Chemicals, Switzerland see Appendix 1 for structure) was added to the sample to prevent degradation during extrusion and pressing. This processing stabiliser is extremely efficient during processing, but it normally does not influence the long-term stability of a polyolefin sample to a significant extent [23]. This is due to the kinetics of the conversion reaction of the phosphite to the phosphate, which takes place at temperatures above 150 ºC. An acid scavenger (DHT 4-A, Kyowa Chemical Industry Co. LTD, Japan) was also added to prevent acid build-up. It was assumed that the combination of the acid scavenger and the secondary anti-oxidant would not have a significant influence on the long-term stability experiments. The secondary anti-oxidant is only active at temperatures above 150 ºC.

The polypropylene powder, the stabiliser and the acid scavenger were subjected to dry blending, followed by melt-blending on a Brabender PL 2000-6 Plasticorder single-screw extruder (19-mm screw, with a length-to-diameter ratio of 25 and screw speeds of between 40 and 100 rpm). The extrudate was cooled and pelletised. Plaques were prepared using a Wabash Genesis press (Wabash, Indiana). Approximately 4,2 grams of pellets per plaque were weighed and placed between a stainless steel plate and polyethylene terephthalate (PET) film. All samples were compression moulded at 190 ºC, using a two phase compression cycle. Initial compression took place at 4 bar for 2 minutes, followed by a second compression step at 20 bar for three minutes. The plaques were cooled under pressure at a linear cooling rate of 15 ºC/min to 30 ºC.

5.3.1.2 Degradation conditions

Polypropylene plaques were degraded under different exposure conditions, specifically selected to represent different stages of degradation. The samples were thermally aged in a heat circulating oven (Scientific Engineering) at different temperatures. Samples were named according to carbonyl index (see Table 4 later in text). The identities of the four samples were as follows:

Sample A: Unstabilised PP (98/78) aged for four days at 70 ºC
Sample B: Unstabilised PP (98/78) aged for four days at 110 ºC
Sample C: Unstabilised PP (98/78) aged for 105 days at 70 ºC
Sample D: Unstabilised PP (98/78) aged for 1 day at 130 ºC

Although a totally undegraded virgin sample was not available for analysis, sample A was virtually undegraded and was used as a reference. The sample was still clear and no colour change was evident. Sample B and C were intermediate samples, and were visually more degraded than sample 1, but less than sample 4. Both samples were yellow on the surface. Sample D was totally degraded and yellow in colour.

5.3.2 Analyses

5.3.2.1 SEC analysis of the degraded PP samples

All high-temperature SEC analyses were performed on a high-temperature Waters Alliance 2000-SEC instrument. The instrument was equipped with five 300 mm x 7.8 mm Waters crosslinked divinylbenzene columns (Waters HT 2, 3, 4 and 5), enabling the separation of molar masses between 500 and 10 million g/mol. The system was calibrated using commercially available polystyrene standards, and relative calibration was performed. All molar mass values were reported relative to polystyrene.

Sample preparation for SEC analysis

Polymer samples were dissolved in 4 mL 1,2,4-trichlorobenzene. Approximately 12 mg of sample was added to a 4 mL glass vial and the dissolution period was 3 hours at a temperature of 150 ºC. BHT was added to prevent further degradation of the polymer in solution, and 0.1% Irganox 168 from Ciba Speciality Chemicals, Switzerland (see Appendix 1

for structure) was added to the solutions. Irganox 168 is a peroxide decomposer and will prevent further decomposition of the polymer under high-temperature conditions (instrument temperature set at 145 ºC).

All samples were cross-sectioned to obtain a representative sample. Later in the chapter the effect of the degradation profile in degraded samples will be discussed (Section 5.4.5).

Instrumental conditions

All SEC measurements were performed at a solvent flow rate of 1 mL/minute. The mobile phase was stabilised by adding 0,1% (w/v) BHT. The refractive index trace was used for all molar mass determinations. A set was analysed by first injecting a NBS control standard (National Bureau of Standards: NBS 1475). NBS 1475 was also injected at the end of the set to monitor system drift during a set of SEC samples. Each set was split into duplicates and each degraded sample was injected twice. No further degradation of the samples was noticed when comparing the first and the second analysis runs of the duplicate set.

5.3.2.2 FTIR analysis of the degraded PP samples

All samples were scanned on a Nicolet Fourier Transform (model Nexus) Infrared (FTIR) spectrometer. Spectra were recorded using Omnic software and 64 scans were acquired for each spectrum. The resolution was set at 2 cm^{-1}.

5.3.2.3 SEC-FTIR analysis of the degraded PP samples

A dedicated SEC-FTIR instrument, incorporating a Lab Connections LC 300 high-temperature interface, was used for all SEC-FTIR measurements. Samples were prepared by dissolving 12 mg of degraded sample in 4 mL 1,2,4-trichlorobenzene. BHT was added to prevent further degradation of the polymer samples. A peroxide decomposer (Irgafos 168, Ciba Chemicals) was also added to the degraded samples. A Waters 150 C HT-SEC instrument, equipped with Waters HT 2, 3, 4 and 5 columns, was modified to incorporate the LC-transform connection. The differential refractive index (DRI) detector was taken off-line during measurements and a flow rate of 1 mL/ min was employed during all experiments. To prevent precipitation of the polymer sample, the nozzle and stage temperatures were optimised separately. The following parameters can be set on the Lab Connections LC300 setup:

1. Vacuum
2. Temperature of the stage
3. Deposition rate: degrees per minute on the rotating Germanium disk

Careful optimisation of the instrument parameters was necessary to obtain a uniformly deposited film that could be analysed by off-line FTIR analysis. The control of the vacuum is of significance, as this will influence the removal of the solvent. A too high vacuum will result in a film with a bad surface finish (cannot be analysed by off-line FTIR), and a too low vacuum will result in a wet film, which can result in dispersion of the film. The transfer line was set at a fixed temperature, usually the same as the SEC column compartment temperature.

The stage temperature must be set correctly for each polymer analysed as this will also influence the film formation. The deposition rate was also of importance as this will influence the film thickness. A too thick or a too thin film will result in difficulties during the recording of the FTIR spectra. The film thickness and uniformity will also be influenced by the sample concentration and the injection volume. The following operating conditions were selected for the LC-transform setup (Table 1):

Table 1: LC-transform operating conditions for the analysis of degraded polypropylene homopolymer samples

Instrument Setting	Setpoint:
Transfer line temperature	126 °C
Stage temperature	160 °C
Vacuum	2 mTorr
Nozzle temperature	118 ºC

All samples were sprayed on a Germanium disk and analysed off-line on a Nicolet FTIR instrument. For this series of experiments the stage temperature was set at 160 ºC, and the nozzle temperature was set at 118 ºC. The injection volume had to be optimised, as the film on the Germanium disk needs to be sufficiently thin to obtain good FTIR spectra. The injection volume on the SEC instrument was set at 75 µL. The vacuum on the instrument was controlled accurately in order to remove all excess solvent. The films on the Germanium disks were conditioned by leaving the Germanium disks at room temperature for two hours before scanning on the FTIR spectrometer.

5.3.2.4 CRYSTAF analysis of the degraded PP samples

A Polymer Char CRYSTAF instrument (model 200) was used for all CRYSTAF measurements. The CRYSTAF instrument was operated on 1,2,4 trichlorobenzene as solvent. Approximately 20 mg of each sample was introduced into each of the CRYSTAF reactors. All samples were obtained as a cross section from the original degraded samples. The following standard CRYSTAF program was used for all PP measurements (Table 2):

Table 2: CRYSTAF operating conditions for the analysis of degraded polypropylene homopolymer samples

Condition	Set point
Dissolution temperature	160 ºC
Dissolution time	1 hour
Stabilisation time	40 minutes
Stabilisation temperature	100 ºC
Temperature gradient	0.1 ºC cooling per minute
Final temperature	30 ºC
Hold time at final set point	30 minutes

The soluble fraction was considered to be the polymeric material that does not crystallise after the precipitation period and 30 minutes at the final hold temperature.

5.3.2.5 TREF conditions

The TREF experiment was performed in a typical Holtrup TREF setup. The sample was dissolved in 400 mL xylene and refluxed for 20 minutes on a heating mantle. The hot solution was transferred to a heated oil bath and slowly cooled to room temperature. Crystallisation was carried out in the absence of any support material. This controlled crystallisation step was carried out at a cooling rate of 6 ºC per hour. Fractionations were carried out at 40 ºC, 80 ºC, 90 ºC, 94 ºC, 98 ºC 102 ºC and 107 ºC. Fractionations were attempted at 112 ºC, 117 ºC and 130 ºC, but the yields of these fractions were too low for further analysis (in total less than 1%).

5.4 Results

The purpose of this investigation was to determine the suitability of the hyphenated and fractionation techniques towards degradation, so although no undegraded sample was available for degradation, conclusions can still be made regarding the suitability of these techniques towards degradation. Sample A was aged for 4 days at 70 ºC. It was then hazy but visually indistinguishable from a normal undegraded sample. The sample showed no chalking and no loss of flexibility. No colour change was observed. Sample B was aged at 110 °C for a period of 4 days. The sample turned yellow (light yellow tone) but no embrittlement nor chalking was detected. Sample C was aged at 70 ºC for 105 days, and showed similar discolouration to sample B. Sample D was aged at 130 ºC for 1 day and became totally discoloured. The sample was yellow in appearance, and the smell of degraded plastic was detected. The sample was powdery and had no structural rigidity.

5.4.1 SEC results of the four degraded samples

As ß-scission is the predominant mechanism during polypropylene degradation, a definite effect on the molar mass averages was expected. In Table 3 the effect of the degradation process on the molar mass averages can be seen.

Table 3: Thermo-oxidative degradation and its effect on the molar mass averages of a polypropylene homopolymer sample

Sample ID	M_n (g/mol)	M_w (g/mol)	M_z (g/mol)	Polydispersity (M_w/M_n)
A	77,000	292,500	707,000	3.80
B	43,500	197,000	523,000	4.53
C	50,000	208,000	669,500	4.16
D	9,700	33,000	99,700	3.40

The effect can also be evaluated by visually inspecting an overlay of the SEC curves (Figure 1). The SEC results indicated that the molar mass averages of the degraded samples shifted to lower values when compared to the virtually undegraded material. The molar mass distribution curves for samples B and C were similar to the curve of the undegraded material, except for a low molar mass tail present in both samples (B and C). From the molar mass distribution curves it was evident that the amount of low molar mass material increased significantly.

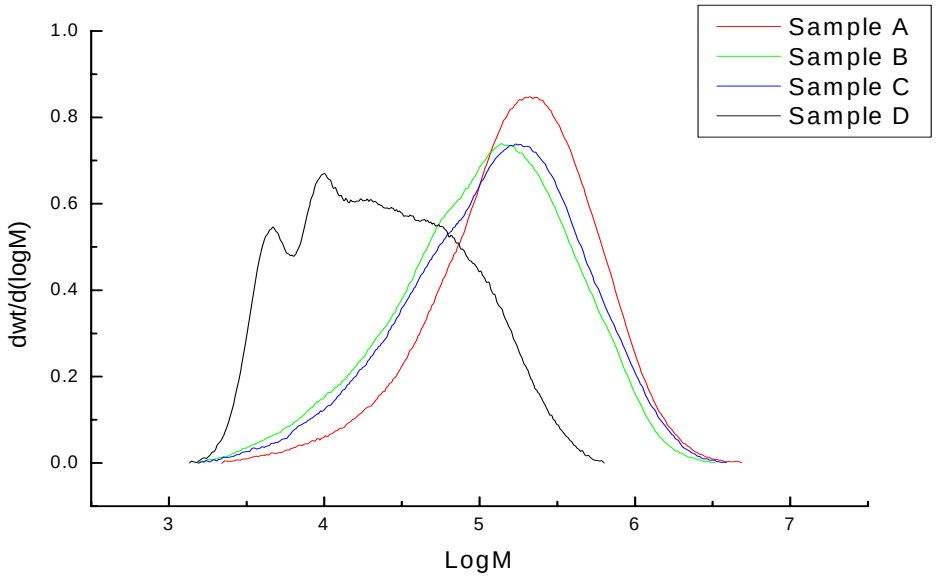

Figure 1: The decrease in molar mass in a polypropylene homopolymer sample introduced by the thermo-oxidative degradation process.

The molar mass distribution curve for sample D was very different to that of samples A, B and C. The curve was bimodal and the molar mass has shifted to significantly lower values. However, when using SEC alone, this decrease in the molar mass of the sample could not be correlated with the chemical changes in the sample. This effect will be studied later by SEC-FTIR (Section 5.4.3).

5.4.2 FTIR results of the four degraded PP samples

A typical FTIR spectrum of a polypropylene homopolymer shows the presence of several paraffinic peaks, including typical absorption peaks at 808 cm^{-1}, 841 cm^{-1}, 973 cm^{-1}, 997 cm^{-1} and 1375 cm^{-1} (methyl groups). During degradation, several carbonyl species may form [24-29]. These are detected in the infrared spectrum at around 1700 cm^{-1}. Hydroxyl groups also form during degradation, but unfortunately the hydroxyl absorption (above 3000 cm^{-1}) is not sharp, and it is difficult to use the FTIR determination for quantification of hydroxyl degradation products. The most important carbonyl peaks are detected at approximately 1714 cm^{-1} (ketones), 1740 cm^{-1} (peracids) and 1780 cm^{-1} (γ-lactones). The formation of the ketone groups is a direct consequence of β-scission (Scheme 1).

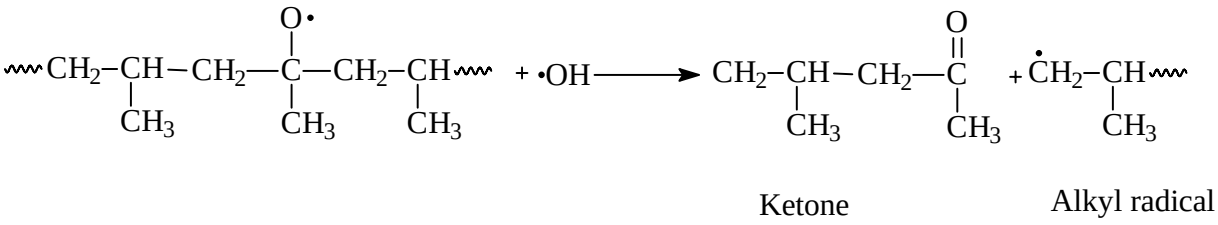

Scheme 1: β-scission of polypropylene

The FTIR spectrum of sample A shows very little degradation (Figure 2).

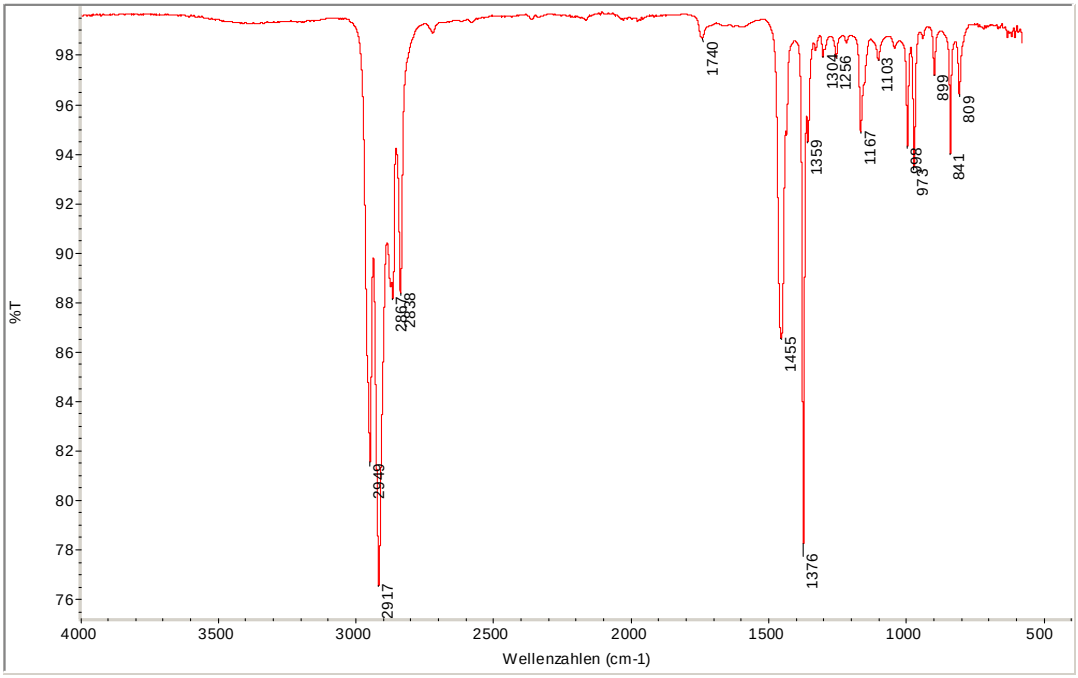

Figure 2: FTIR spectrum of polypropylene sample A (least degraded), showing a low level of carbonyl formation.

The infrared spectrum of sample D (Figure 3) shows the presence of a large carbonyl peak. The most significant carbonyl species was detected at 1716 cm^{-1}. This was due to the formation of ketone groups as the primary degradation products.

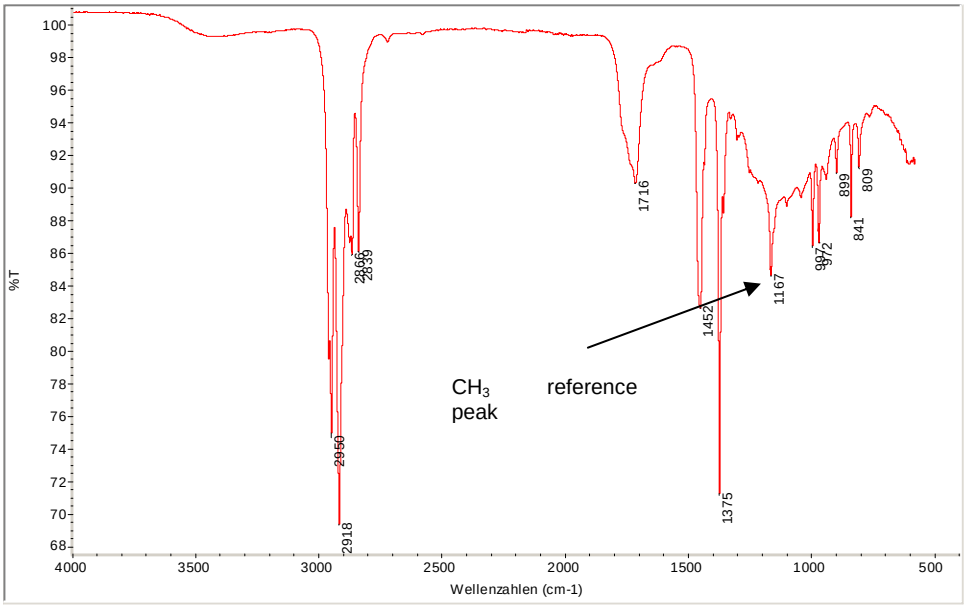

Figure 3: FTIR spectrum of polypropylene sample D (most degraded), showing a high level of carbonyl formation.

The carbonyl index was calculated by taking the height of the carbonyl peak at 1716 cm^{-1} and dividing it by the height of the FTIR peak at 1167 cm^{-1} which is a typical CH_3 rocking vibration peak [30] (Table 4). This peak is indicative of the CH_3 concentration in the polymer (indicated in Figure 3). However, due to the heterogeneous nature of degradation, reproducibility of the carbonyl analysis may be an issue. FTIR analyses on the plaques were performed in transmission mode, and, therefore, an average reading for the plaque was obtained (taking into account the degradation gradient in the sample).

Table 4: Carbonyl index of the four degraded PP homopolymer samples

Sample no	Carbonyl index (a.u.)
A	0.13
B	0.64
C	0.76
D	1.43

An overlay of all four samples is shown in Figure 4. It is evident that the four samples showed differences in the level of degradation. The degradation level of samples B and C appeared to be similar. There was also an increase in the OH area from sample A to D (between 3000 cm^{-1} and 3500 cm^{-1}), where the peroxides are detected.

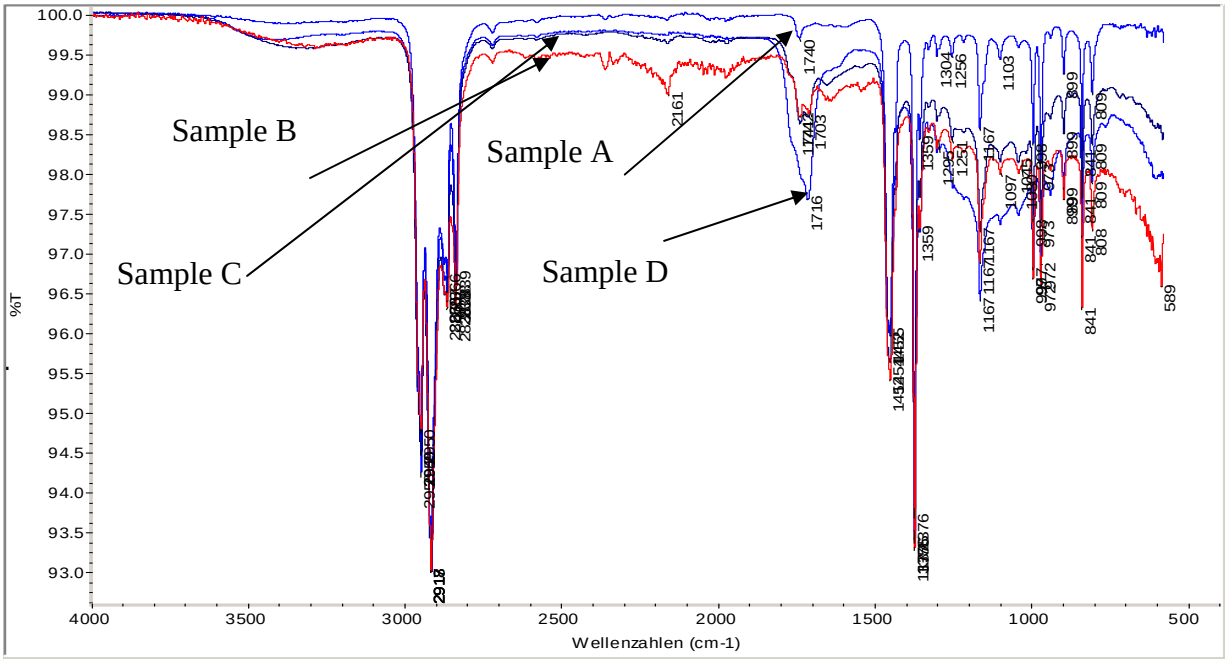

Figure 4: Overlay of the spectra of the four degraded PP homopolymer samples showing the differences in degradation level.

A closer investigation of the carbonyl area shows the presence of mainly three different types of carbonyl groups that form during polypropylene degradation. Ketones (the product of ß-scission) are detected at approximately 1716 cm^{-1} and are the main degradation products (highest concentration).

The more degraded samples show the presence of absorptions at 1740 cm^{-1} and 1780 cm^{-1}. The peak at 1740 cm^{-1} is due to the formation of peracids, and the peak at 1780 cm^{-1} is due to the formation of γ-lactones. Both these functionalities are secondary degradation products, formed during multiple degradation attack on a polymer molecule (Figure 5).

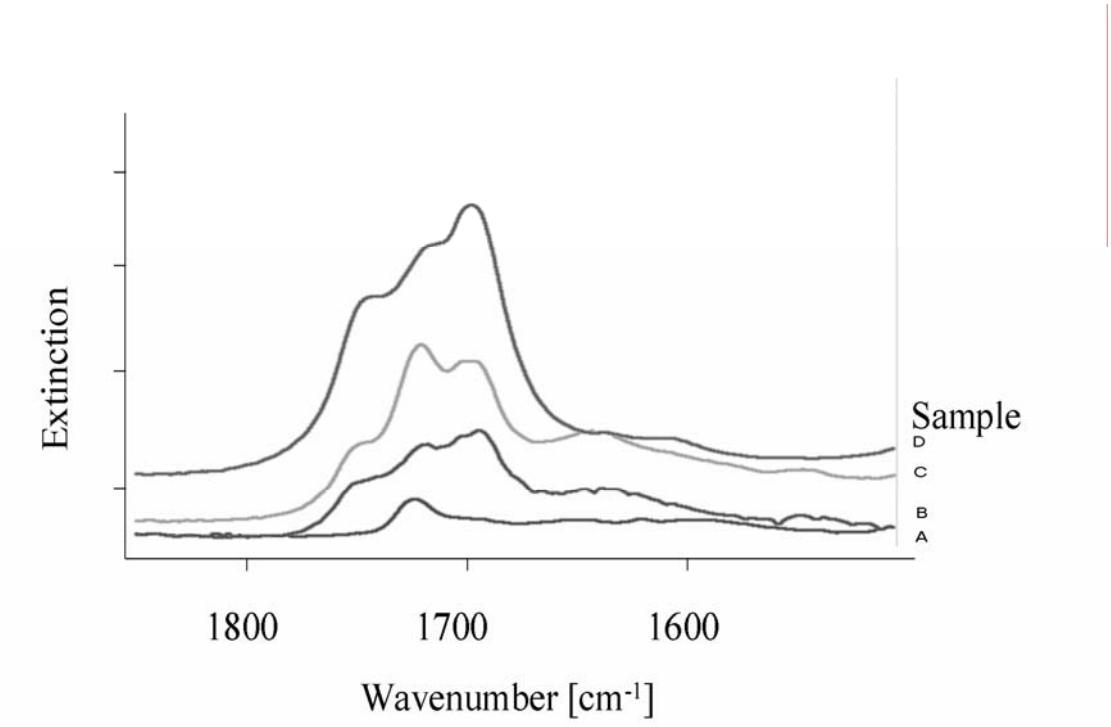

Figure 5: Overlay of the FTIR spectra of the four degraded PP homopolymer samples, focusing on the carbonyl area.

The four samples were, therefore, considered to be sufficiently different for studying by alternative techniques. The FTIR results are in good agreement with Marshall [23], who showed similar increases in carbonyl groups with an increase in degradation time.

5.4.3 SEC-FTIR results of the degraded PP samples

The four degraded samples were subjected to SEC-FTIR analysis. The SEC-FTIR technique enables the determination of infrared absorption intensity as a function of retention time. The result from an SEC-FTIR experiment will, therefore, differ slightly from a normal SEC result (recorded on a DRI detector or viscometer), although the shapes of the curves are usually comparable. A Gram-Schmidt curve can be defined as a graphical representation of the total IR absorption as a function of retention time. The retention time can be correlated with the molar mass distribution in the sample. Data manipulation is possible through a software package (Nicolet Omnic) and the infrared spectrum can be obtained at any point during the SEC-FTIR analysis. For all the analyses described in this chapter, the Gram-Schmidt wavelength range was set between 400 cm^{-1} and 4000 cm^{-1}.

A chemigram can be constructed from the FTIR data. A chemigram is the total infrared absorption of a specific group as a function of retention time. For example, for determining

the distribution of the degradation products (carbonyl groups), a chemigram can be constructed between 1600 cm^{-1} and 1800 cm^{-1}. The carbonyl chemigram will, therefore, be the sum of all absorptions between 1600 cm^{-1} and 1800 cm^{-1} as a function of retention time.

The SEC-FTIR data of sample B (Figure 6) show the distribution of the carbonyl absorption as a function of elution volume, which is equivalent to molar mass. For determining the carbonyl distribution, the carbonyl intensity was taken between 1600 and 1800 cm^{-1}. For the CH concentration (equivalent to the total concentration profile) the peak around 1167 cm^{-1} was used as a reference. The peak at 1167 cm^{-1} is due to the CH_3 rocking vibration [30]. The ratio of these two chemigrams provides information on the relative carbonyl concentration.

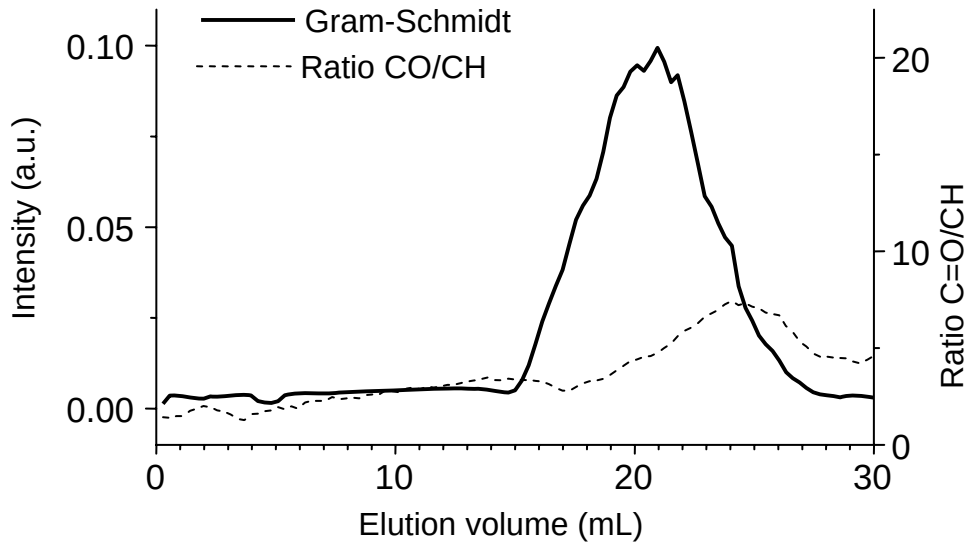

Figure 6: SEC-FTIR analysis of sample B (low level of degradation) showing the presence of a low concentration of carbonyl groups in the C=O chemigram.

Comparing the Gram-Schmidt plots of the four samples with the refractive index results, it was evident that the Gram-Schmidt plots are similar in shape to the refractive index SEC results. The retention times were also comparable to normal SEC results, as the column configurations and instrument settings were similar to those used for the HT-SEC measurements. Although these results were not converted to the normal average molar masses, the relative retention times could still be compared. A sample with a lower average molar mass will move to a higher retention time. The carbonyl concentration was relatively low in this sample, resulting in a weak intensity in the chemigram. A small increase in the carbonyl concentration at a lower molar mass was noted.

The LC-transform result of sample D with a high level of degradation is shown in Figure 7.

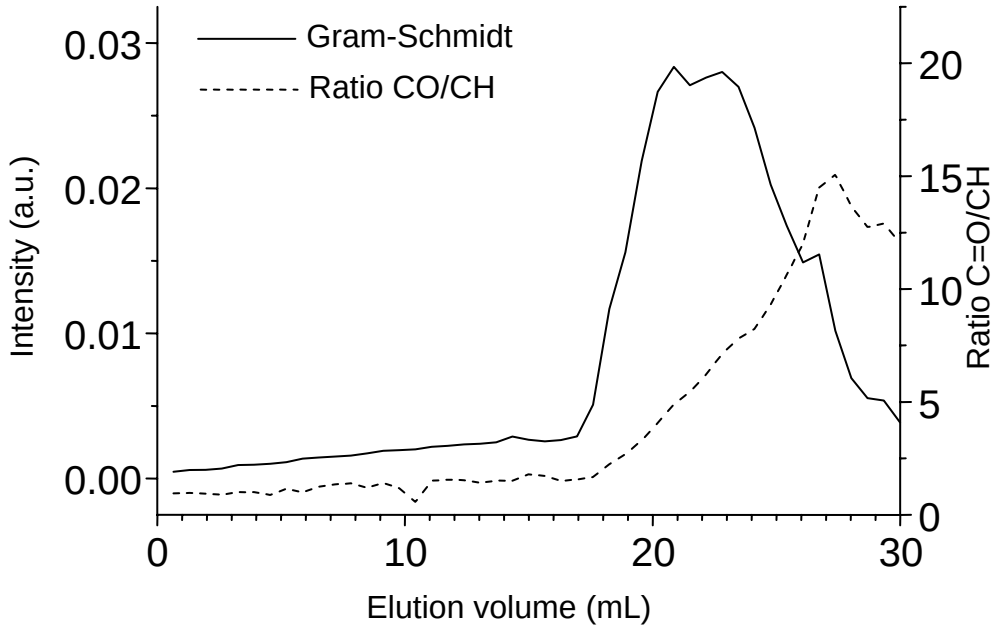

Figure 7: SEC-FTIR analysis of the polypropylene homopolymer sample D (the most degraded sample in this study), showing the presence of a high carbonyl concentration in the low molar mass region.

Comparing the SEC-FTIR results of the undegraded sample (sample A) and slightly degraded sample (sample B), several differences were seen in the Gram-Schmidt curves. The onset of the Gram-Schmidt curve of sample B had moved to higher retention times compared to sample A. This was in agreement with the results obtained by HT-SEC.

Comparing the results obtained by HT-SEC (with refractive index detection) and SEC-FTIR, it can be seen that the shape of the Gram-Schmidt curve of the most degraded sample (sample D) was slightly different from the curve obtained by HT-SEC. There may be several reasons for this: the longer pathlength of the LC-transform setup may result in band broadening and the high carbonyl concentration may change the total chemical absorption. The carbonyl groups were not distributed evenly across the molar mass region. There was a sharp increase in the carbonyl concentrations in the low molar mass area of the distribution. Degradation products were, therefore, mostly concentrated in the low molar mass region.

Using a hyphenated SEC-FTIR setup, the distribution of degradation products could be determined as a function of molar mass. This also confirmed the heterogeneity of the

degradation process, as the highest concentration of degraded species was found in the low molar mass region.

5.4.4 CRYSTAF results of the degraded PP samples

CRYSTAF has been used extensively to study the chemical composition distribution in polyolefins. However, no information exists on the changes in chemical composition distribution and crystallisability of a polyolefin sample degraded by thermo-oxidative degradation. Isotactic, syndiotactic and atactic material can easily be differentiated by CRYSTAF [6]. A highly isotactic polypropylene sample will yield a narrow, symmetrical CRYSTAF crystallisation curve, with a very low soluble fraction. The formation of several carbonyl containing functionalities during thermo-oxidative degradation will, however, influence the crystallisability of the fractions in the CRYSTAF. Theoretically, this should enable CRYSTAF to differentiate between samples with different levels of degradation.

The crystallisation curves of samples A and D, studied by CRYSTAF, show that CRYSTAF could be useful for determining degradation (Figures 8 and 9).

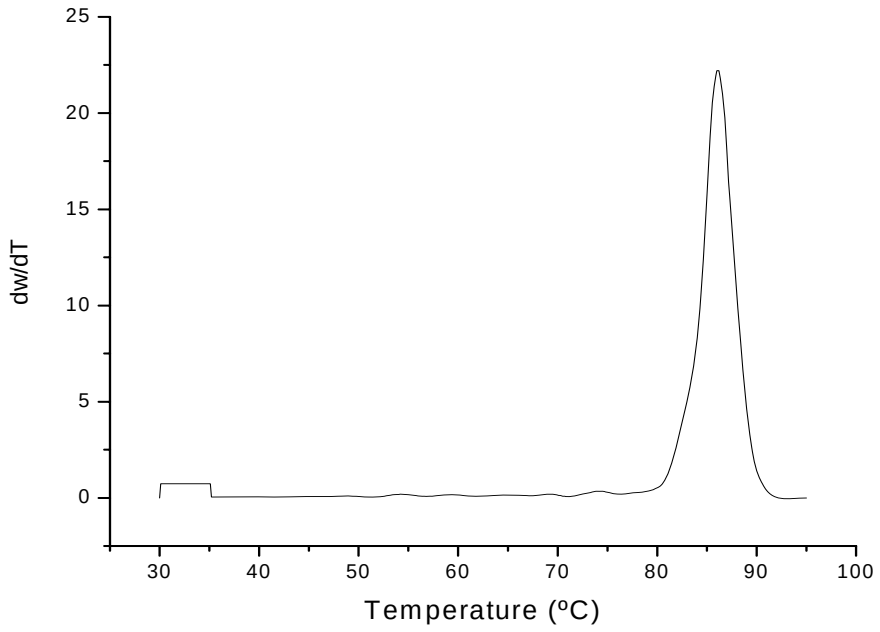

Figure 8: CRYSTAF curve for sample A (low degradation) showing a sharp crystallisation curve and a low soluble fraction, typical of isotactic PP.

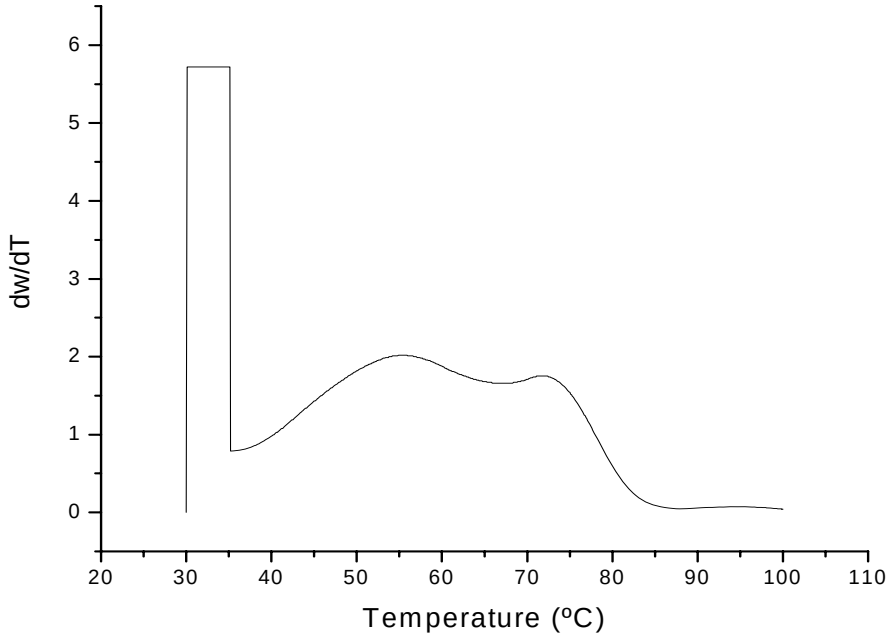

Figure 9: CRYSTAF curve for sample D (most degraded) showing a broad crystallisation peak and a high soluble fraction.

The two curves were significantly different. First, the CRYSTAF curve for the low degraded sample (sample A) was relatively sharp and a small soluble fraction was still in solution at 30 °C. Most of the polymer crystallises from solution above 70 ºC. This crystallisation curve was typical of the crystallisation of an isotactic polypropylene sample. In the degraded sample (sample D) the crystallisation curve was broad, with the broad chemical composition distribution of the degradation products clearly evident. The crystallisation commenced at a lower temperature, and there was a very significant soluble fraction present. No sharp crystallisation peak (typical of isotactic polypropylene) was detected in the CRYSTAF crystallisation curve of sample D, meaning that even the crystalline areas were degraded or melted during the aging at 130 ºC.

The broadening of the crystallisation curve can be attributed to the degradation process (increase in the chemical heterogeneity of the sample during degradation), and the effect of the introduction of carbonyl functionalities on the crystallisation behaviour. The soluble (non-crystallising) fraction may consist of highly oxidised non-crystallisable polypropylene chains.

In order to check the reproducibility of the technique on a degraded sample the following two parameters were considered:

1. The soluble fraction
2. The crystallisation temperature

It must, however, be taken in account that a degraded sample is heterogeneous (Section 4.6) and this will influence the reproducibility of the analyses.

In Table 5 it can be seen that the soluble fraction of the degraded sample is significantly higher than in the undegraded sample. It is also evident that the soluble fraction in the CRYSTAF curve is not totally reproducible (variation between 24% and 28,6% solubles) but this may be due to the non-homogeneity of the degradation process. However, this variation was smaller than the variation between the degraded and the undegraded samples.

Table 5: Variation in the soluble fraction in CRYSTAF analyses performed on the most degraded PP sample (sample D)

Analysis no	Soluble fraction (%)	Crystallisation temperature (ºC)
1	28,6	66.6
2	24.0	66.8
3	24.0	61.7

5.4.5 Evaluation of the spatial heterogeneity of the degradation process

Polyolefin degradation is heterogeneous on a molecular level due to the exclusion of oxygen from the crystalline regions. Polyolefin degradation in thicker samples may, however, also be heterogeneous due to the exclusion of oxygen from the inner part of the sample. Oxidative degradation in polyolefin plaques is limited by the availability of oxygen to the process. When studying a thin plaque, oxygen consumed during the degradation process may be rapidly replaced by oxygen diffusing through the amorphous phases. In a thicker plaque, diffusion of the oxygen will be limited by the thickness of the plaque. This may result in the development of an oxidation profile, as the areas closer to the surface will be more degraded than the internal areas, due to the slow diffusion of oxygen to the inner layers of the sample. In normal use this effect may not be as pronounced, as the degradation process may be slow enough to allow for the diffusion of oxygen to take place. However, in accelerated degradation (oven aging and multiple extrusions), oxygen availability may be limited.

Several authors studied the heterogeneous nature of degradation using FTIR analysis. The two approaches followed in literature to study the spatial heterogeneity of degradation are to microtome samples and obtain IR scans of microtomed slices [31-33], or to use the full potential of ATR to obtain spectra from different depths into the sample by a mathematical procedure [34].

ATR-FTIR analysis of the four PP samples showed that sample A was not degraded to a significant extent, and sample D was too brittle for further analysis. Therefore, sample B was selected for investigation of the alternative analytical approaches.

Microtoming was selected as a way of studying the degradation profile. The sample was mounted on a metal block and layers of 0,3 mm were microtomed from the sample. The profile that was to be obtained was therefore from the most degraded layers (surface and 0,3 mm into the sample) to the inside layer (1,2 mm into the sample). The latter would contain the least degraded material. The sample was roughly microtomed to the centre of the sample. The second half of the sample was thought to be a mirror image of the first half.

The FTIR results of the microtomed layers (Table 6) show a decrease in the carbonyl index from the outer layer (surface) to the inner layer (1,2 mm into the sample).

Table 6: Carbonyl indices of the abrased layers of PP sample B

Layer thickness (mm)	Area C=O (a.u.*)	Area CH_3 (a.u.*)	Carbonyl Index (a.u.*)
0,3	9,62	4,88	1,97
0,6	5,19	3,64	1,41
0,9	4,79	4,34	1,10
1,2	3,55	8,76	0,41

* a.u. is arbitrary units

The spatial heterogeneity of the degradation in a thick plaque could be seen from these results. The carbonyl index of the outer layer was significantly higher than that of the inner layer. The FTIR spectrum of the fraction taken at 0,3 mm abrasion depth showed that the layer was severely degraded, as is evident from the large carbonyl peak. In order to investigate the distribution of degradation products in these fractions, SEC-FTIR was used.

Again, there was a clear increase in the carbonyl level in the low molar mass end of the distribution, as seen in Figure 10.

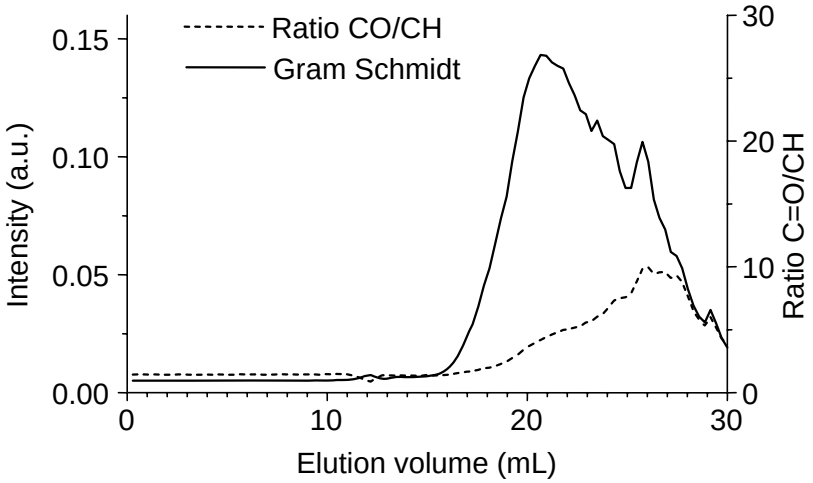

Figure 10: LC-transform result of the fraction obtained at 0,3 mm into the degraded PP sample B showing a non-symmetrical Gram-Schmidt curve.

The LC-transform result of the 1,2 mm fraction indicated that the molar mass was significantly higher than that of the 0,3 mm fraction (Figure 11). This was evident by the earlier onset of the Gram-Schmidt curve. It is, however, evident that a highly degraded fraction is present even in the layer at 1,2mm depth, showing that oxygen had access to this layer. This is also evident in the carbonyl index (CI = 0.41).

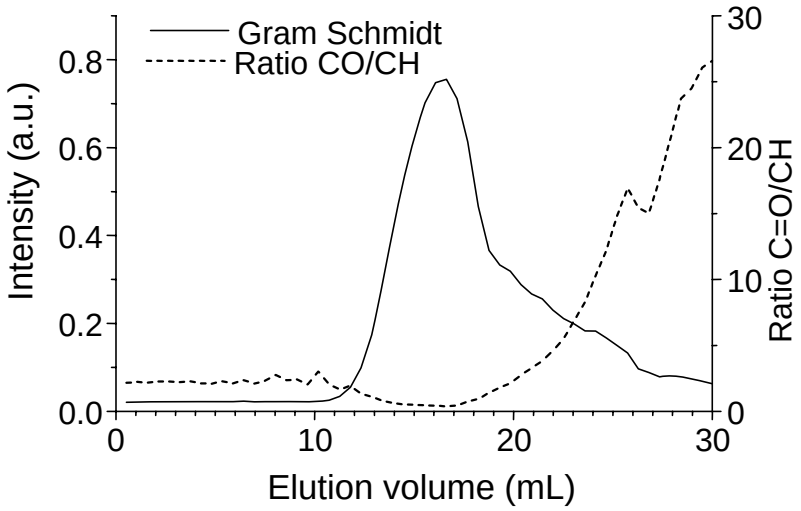

Figure 11: LC-transform result of the fraction obtained at 1,2 mm into the degraded PP sample B.

Although the carbonyl intensity in the SEC-FTIR analysis of the 1,2 mm sample appears to be high, it must be taken into account that the intensity of the chromatogram at 1,2mm depth

was significantly higher compared to the 0,3mm depth chromatogram. These results were in agreement with the HT-SEC results of the microtomed layers where an increase in molar mass was noticed, and the FTIR results where a decrease in carbonyl index was noted going from the surface of the sample to the inner layers of the sample.

CRYSTAF analysis was performed on the four PP fractions to determine if CRYSTAF could be useful in determining the level of degradation of the different layers. The results are given in Table 7. Similar to the results of the CRYSTAF analysis of the four unfractionated samples, it was expected that the higher level of degradation will result in a broader chemical composition distribution.

Table 7: CRYSTAF results of the fractions taken at different depths into PP sample B

Depth	Soluble fraction (%)	Crystallisation temperature (°C)
0.3 mm	44.3	66.0
0.6 mm	28.1	70.1
0.9 mm	5.8	76.5
1.2 mm	4.7	79.7

At 0,3 mm there was a very significant soluble fraction present (Figure 12). This decreased significantly to the inside of the sample. At 1,2 mm there was only a 4,7% soluble fraction present.

a) CRYSTAF plot at 0,3 mm b) CRYSTAF plot at 1,2 mm

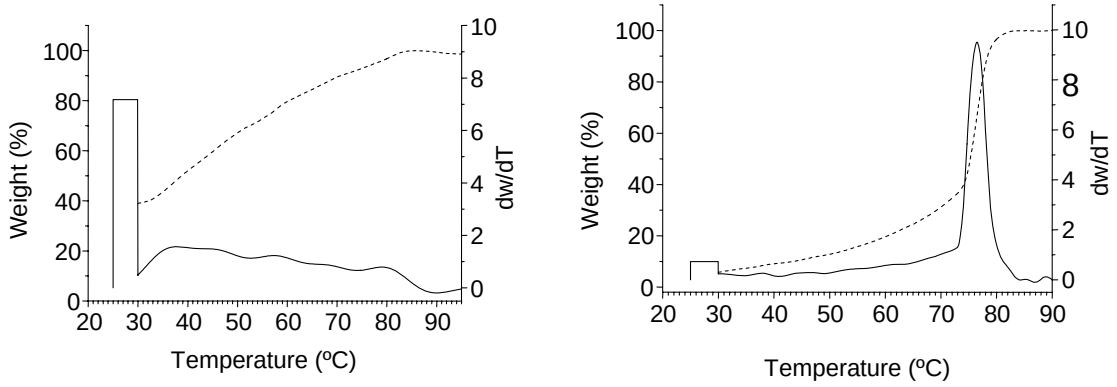

Figure 12: CRYSTAF plots showing the change in the degradation profile of PP sample B as a function of depth, with the sample taken at 0,3 mm into the sample showing a broad crystallisation curve and a high soluble fraction.

This was just slightly higher than the soluble fraction of the low degraded sample. The trend in the crystallisation temperatures was also significant, with a change from 79,7 ºC in the inner layer to 66 ºC in the outer layer.

This experiment proved that the CRYSTAF technique is extremely useful in determining the level of degradation of the sample. In the following chapters the use of CRYSTAF to determine the level of degradation as a function of exposure time at elevated temperatures will be discussed.

Virtually none of the original undegraded polymer was present in the 0,3-mm sample and the sample is very low in crystallinity. The CRYSTAF trace of the layer at 1,2 mm into the degraded samples showed the presence of the homopolymer crystallisation peak. Very little change in the crystallisation behaviour is noted, except for a slight change in the lower crystallinity end of the distribution.

5.5 Fractionation of a degraded polypropylene homopolymer sample by preparative TREF

In this chapter thus far, I have shown that SEC, DSC, CRYSTAF and LC-transform can provide more information on the degradation process. The next part of the experimental work in this chapter focuses on the use of TREF to study the degradation process. Preparative TREF is a fractionation technique that allows analytical quantities of a polymer to be obtained (see also Chapters 3 and 4). Prior to a prep-TREF experiment the sample is usually subjected to an analytical CRYSTAF or an analytical TREF analysis to obtain a suitable temperature range of fractionation. The polymer is separated according to crystallisability and the fractions obtained can be further analysed by DSC, FTIR, SEC and NMR. For example, a copolymer can be fractionated to determine the comonomer distribution.

Applying TREF to a degraded polyolefin sample may provide important information on the degradation process. First, information on the distribution of the degradation products as a function of crystallisability may be obtained. Second, the amount of undegraded material can also be investigated. Third, it can also provide information on the distribution of a comonomer as a function of crystallisability.

In this study, sample D (the most degraded sample) was selected for evaluating the usefulness of TREF for obtaining more information on the degradation process. This sample

was degraded at 130 °C for 1 day. It was assumed that this sample would contain a sufficient quantity of both degraded and undegraded species. Although a portion of the sample was lost as volatiles during degradation, the rest of the sample remained intact.

5.5.1 Analysis of the TREF fractions by SEC

The TREF fractions were analysed by SEC to investigate the molar mass dependence of the TREF separation. It is important to determine the molar mass of the fractions obtained by TREF, as this will give an indication of the correlation between chain length and crystallinity. All SEC analyses were carried out on a Waters 150 CV instrument. The results are given in Table 8. The TREF fractionation was carried out according to the method described in section 5.3.2.5.

Fraction 7 had the highest molar mass. Thereafter, the fractions were progressively of lower molar mass, except for fraction 1 that was not of decreasing molar mass. This is probably due to some of the original material of lower tacticity being part of this fraction. The molar masses of fractions 1, 3 and 4 were similar. Fraction 4 was bimodal, a similar effect was found by Mathot [35].

Table 8: Fractionation temperatures and properties of the fractions of the degraded PP sample (sample D)

Fraction no	Elution temperature (ºC)	Carbonyl index (a.u.)	M_w (g/mol)	PDI (M_w/M_n)	Weight %
1	40	0.33	21,000	4.67	4.5
2	80	0.53	10,500	3.23	27.5
3	90	0.26	20,500	2.19	21.3
4	94	0.19	21,800	4.78	16.1
5	98	0.07	39,300	2.01	9.3
6	102	0.04	62,200	2.12	12.4
7	107	n/a	98,500	2.21	8.3
8-10	<130	n/a	n/a	n/a	0.6

The molar mass of fraction 5 was similar to that of the undegraded material (39,300 g/mol vs 33,000 g/mol for the unfractionated sample). The molar mass of fraction 2 was, however, much lower than the starting material (Figure 13).

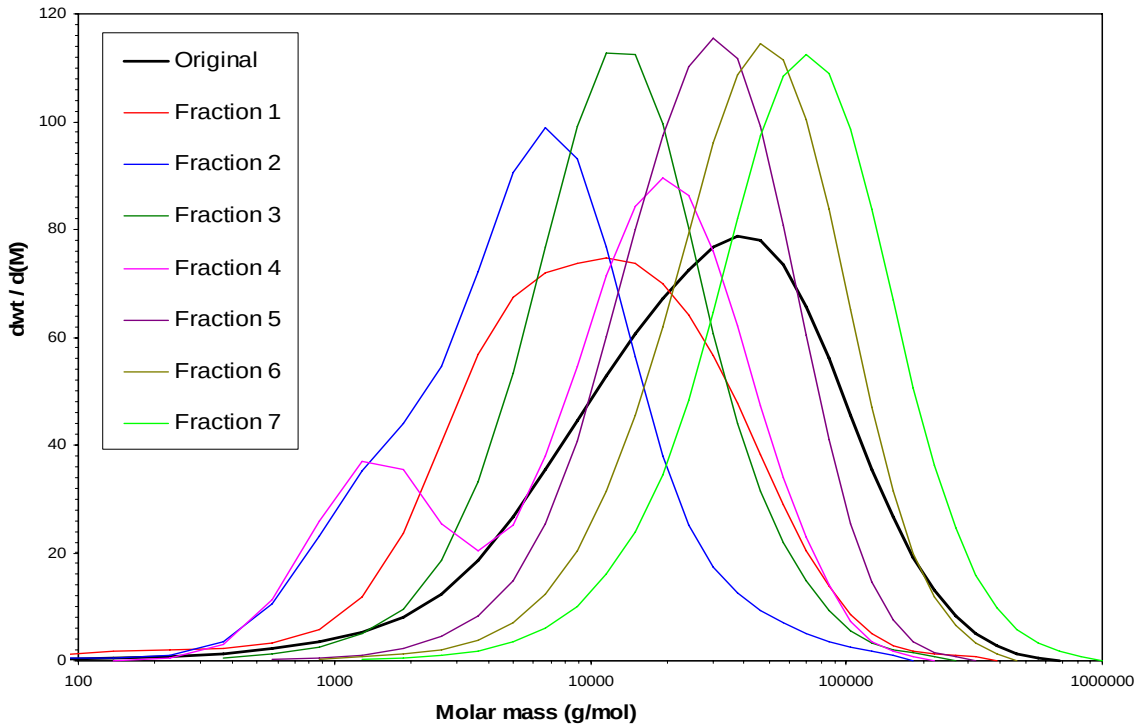

Figure 13: Molar mass distributions of the fractions of the PP homopolymer (sample D).

5.5.2 CRYSTAF results of the TREF fractions

The applicability of CRYSTAF to the analysis of degraded samples was shown earlier in this chapter. Generally CRYSTAF analysis is not molar mass dependent, except when the molar mass is lower than 15,000 g/mol [4]. The molar mass may, however, be as low as 1,000 g/mol for some polyolefin samples [4].

Approximately 20 mg of each TREF fraction was transferred to the CRYSTAF instrument. The results of this experiment on the fractions of sample D are given in Figure 14.

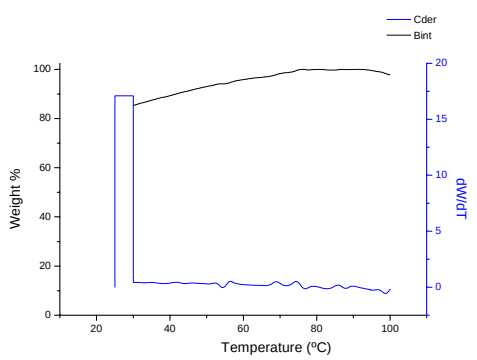

Fraction 1

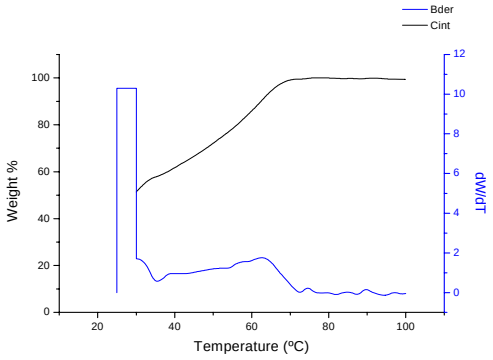

Fraction 2

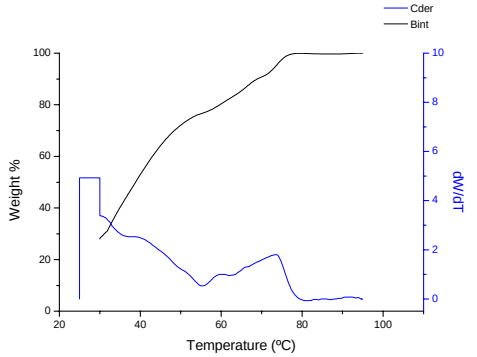

Fraction 3

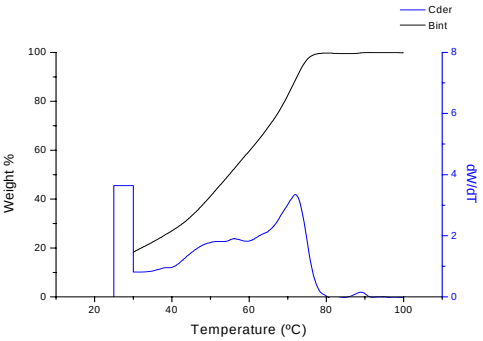

Fraction 4

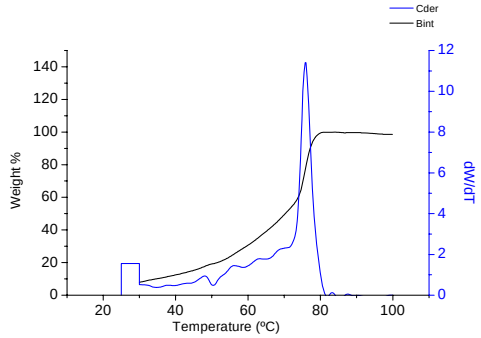

Fraction 5

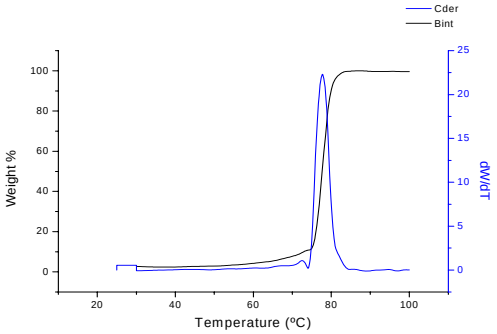

Fraction 6

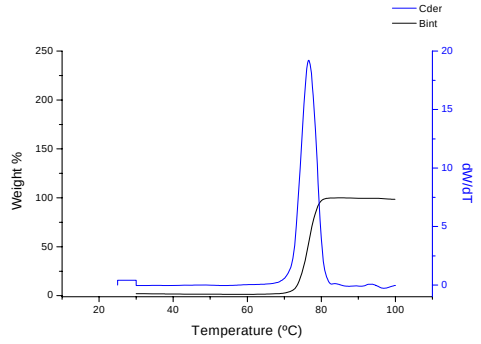

Fraction 7

<u>Figure 14:</u> CRYSTAF results of the individual TREF fractions, showing a significant difference between the CCDs of the different fractions.

The CRYSTAF results indicated significant differences between the seven TREF fractions. According to the SEC and FTIR results, fraction 1 consisted of low molar mass material, with a relatively high carbonyl index. In the CRYSTAF analysis, fraction 1 was basically non-crystallisable, indicating the virtual absence of any crystalline material. A very high soluble fraction was detected. Usually the soluble fraction in a CRYSTAF experiment can be ascribed to the presence of atactic or highly branched material [3]. However, according to the Flory-Huggins theory, non-crystallising comonomer units, diluents and polymer end groups may all contribute to the non-crystallisability in solution. For the degraded fraction, the incorporation of a high concentration of carbonyl groups, therefore, resulted in chain units that contribute to non-crystallisability in the CRYSTAF.

In fractions 2-4 there was a significant reduction in the soluble fractions, although the soluble fractions were still relatively high. A small crystallisation peak started forming at higher temperatures, indicating the presence of crystallisable material. There was a significant reduction in the carbonyl index with increasing fraction number, indicating the decreasing concentration of degradation products.

In fraction 5 a sharp crystallisation peak, typical of isotactic polypropylene, which shows a CRYSTAF crystallisation temperature of 75.9 ºC, can be seen. This fraction was, therefore, significantly higher in crystallisable material compared to the previous fractions. The soluble fraction was below 20% compared to Fraction 1, where the soluble fraction was more than 90%.
The CRYSTAF results for fractions 6 and 7 indicated the presence of highly crystalline material. A sharp crystallisation peak, typical of isotactic polypropylene, can be seen for both fractions 6 and 7. Very low amounts of soluble material were detected in these two samples.

In conclusion, TREF separated strictly according to crystallisability and longest crystallisable sequences. The results indicate that the fractions were generally different in chemical composition and molar mass. It is however difficult to make quantitative comments, as the CCD across the MMD is not known.

5.5.3 FTIR results of the recrystallised fractions

After the fractions were precipitated and dried, all the fractions were recrystallised to remove the anti-oxidant (added during the TREF experiment). The FTIR results indicated the presence of carbonyl functionalities in most of the degraded fractions. Although the spectra

were similar, all showing most of the characteristic bands of polypropylene, there was a significant difference in the carbonyl region. The carbonyl index decreased from Fraction 1 to Fraction 7. This is expected, as fraction 1 contained the least crystalline material. In Fraction 7, virtually no carbonyl groups were detected (Figure 15).

The trend can also be seen in the calculated carbonyl indices (Table 9).

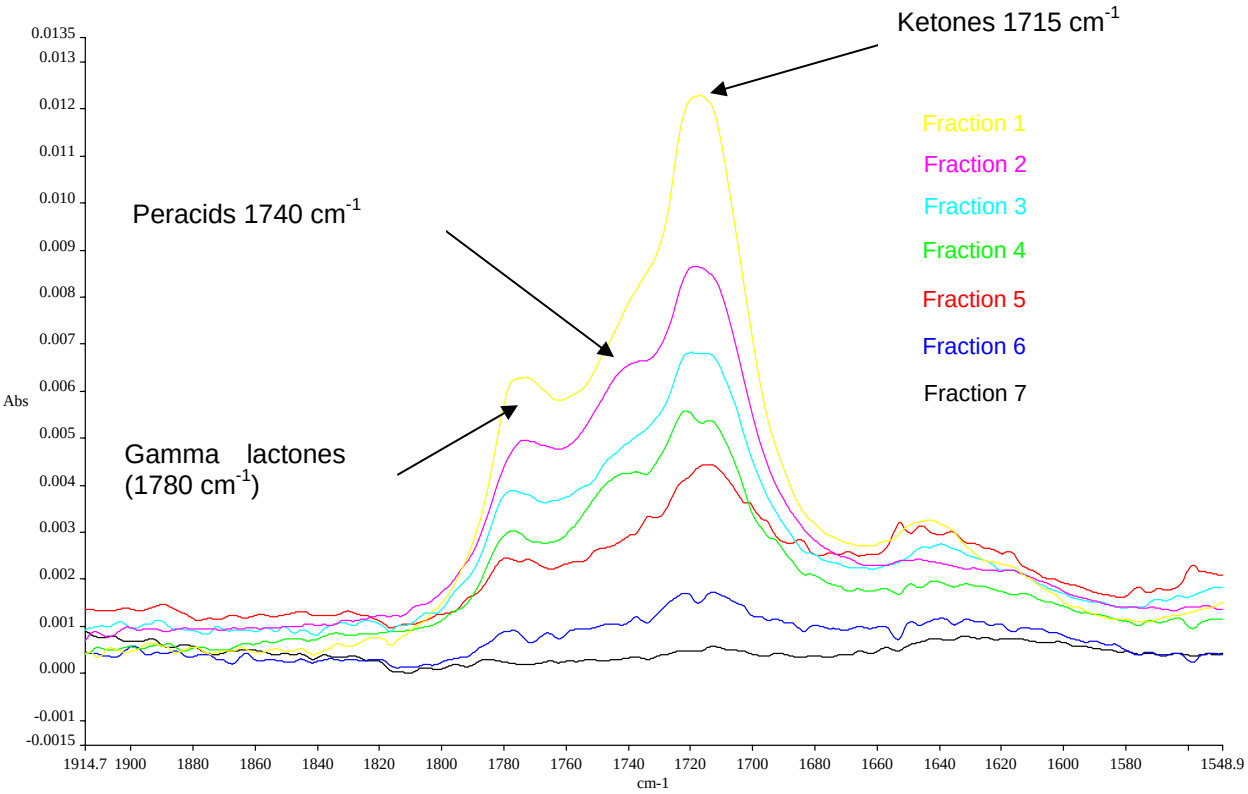

Figure 15: FTIR spectra of the fractions of the degraded PP sample, focusing on the carbonyl area.

Table 9: Carbonyl indices of the TREF fractions of the degraded PP sample

Fraction No.	Fractionation temp (ºC)	Area C=O (au)	Area CH_3 (au)	Carbonyl index (au)
1	40	1	3	0,33
2	80	0,75	1,43	0,53
3	90	0,55	2,11	0,26
4	94	0,46	2,47	0,19
5	98	0,2	2,72	0,07
6	102	0,07	1,99	0,04
7	107	-	-	-

The carbonyl index was plotted vs the fraction number. The curve in Figure 16 shows that the carbonyl index generally decreases with an increase in the fraction number (higher crystallisation temperature).

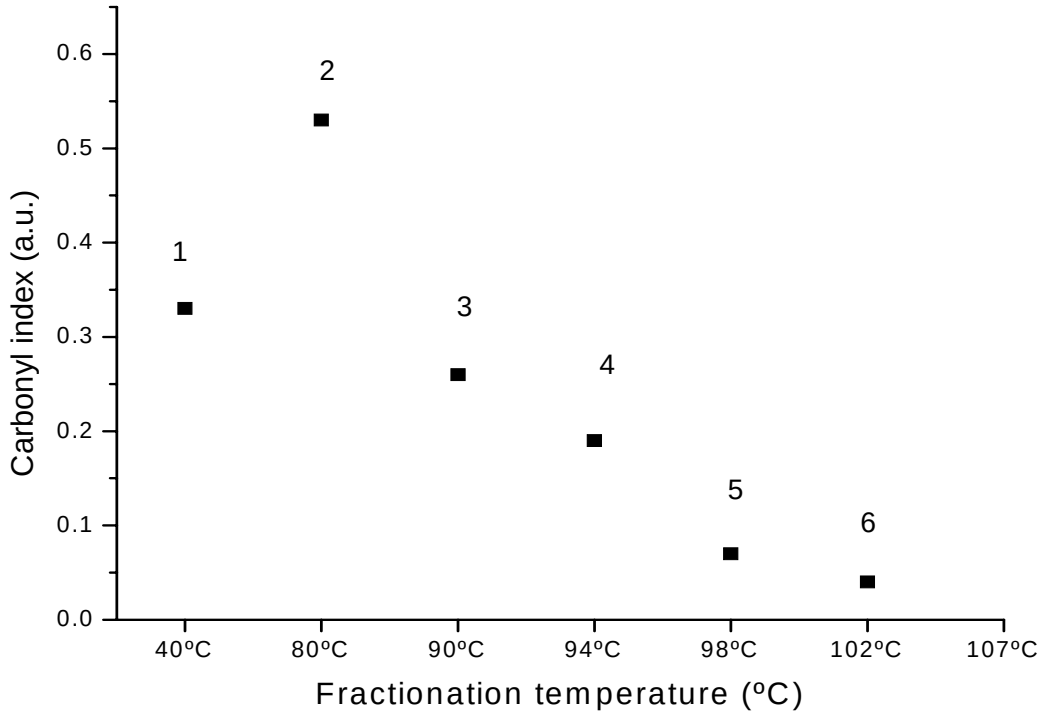

Figure 16: Carbonyl index as a function of fractionation temperature.

This indicated that the material crystallising in a certain fraction was dependent on the amount of degradation products. TREF was therefore useful in separating the degraded polymer into fractions of increasing levels of degradation. The lower crystallinity fraction had the highest carbonyl index and also the lowest molar masses. The highest crystallinity fraction had the highest molar mass and the lowest carbonyl index. The TREF crystallisation behaviour was, therefore, modified extensively by the incorporation of carbonyl groups. In Chapter 6 it will be shown that equipping the CRYSTAF with a carbonyl detector can provide information on the distribution of carbonyl groups as a function of the crystallisation behaviour.

These results show that the broadening of the CRYSTAF crystallisation curve can be related to the incorporation of carbonyl containing groups. Carbonyl groups can act as impurities which, according to the Flory-Huggins theory, will decrease the melting and crystallisation points [36, 37].

5.6 Conclusions

The main objective of this section of the study was to investigate the use of hyphenated techniques (SEC-FTIR) and fractionation (CRYSTAF and TREF) in studying polypropylene degradation. This information complimented the information obtained from the classical techniques (SEC, FTIR and DSC), yet provided a new approach to the problem of understanding polyolefin degradation.

For this investigation, oxidised polypropylene samples were prepared by the oven aging technique. Samples were suspended in a heat-circulating oven and degraded for different periods at different exposure temperatures. SEC results showed a significant decrease in the molar mass of the degraded polypropylene homopolymer samples, while FTIR spectroscopy investigations indicated a significant increase in the carbonyl group concentration. However, the hyphenated SEC-FTIR technique yielded even more information, as the FTIR spectra could be obtained at any time during the SEC curve. The hyphenated technique yielded SEC curves (Gram-Schmidt plots) similar to the normal RI traces, although this was distorted at higher levels of degradation, where the carbonyl functionalities can contribute to the Gram-Schmidt curve. It was shown that most of the degradation products were concentrated in the low molar mass region.

CRYSTAF results showed that the undegraded polypropylene sample yielded a sharp symmetrical crystallisation curve with a small soluble fraction. Degradation contributed to a broadening of the curve, with the formation of carbonyl containing functionalities. There was also a drop in crystallisation temperature and an increase in the soluble fraction with an increase in the level of degradation. The reproducibility of the CRYSTAF results was influenced by the level of degradation, as degradation is a process with spatial heterogeneity. This difference in reproducibility was, however, smaller than the difference in crystallisability between a degraded and an undegraded sample. CRYSTAF was, therefore, sensitive to the level of degradation in a polypropylene sample.

TREF and subsequent characterisation of the fractions obtained from TREF provided additional information on the degradation process. From the TREF results, the following could be concluded:

1. Similar to an undegraded polypropylene sample, a degraded sample was separated by TREF according to crystallisability. In this study, a degraded sample was

separated successfully into fractions of different carbonyl content. The incorporation of carbonyl groups resulted in a significant decrease in the crystallisation temperature and a high carbonyl concentration resulted in fractions that were non-crystallisable.

2. Some of the higher crystallinity fractions contained a low concentration of carbonyl groups and a very low soluble fraction was detected. These fractions of the sample were apparently mostly undegraded.

The second objective was to study the spatial heterogeneity of degradation in a thick polypropylene sample. Samples were microtomed into thin layers. FTIR results indicated that the carbonyl index decreased towards the middle of the degraded sample, while the SEC results indicated a molar mass increase towards the middle of the sample. CRYSTAF results showed a very significant difference between the chemical composition distributions of the samples taken at different depths in the degraded sample.

The present information will now be used to investigate the degradation of a series of propylene-pentene copolymers.

5.7 References

[1] Bolland, J.L., Gee, G*., Transactions of the Faraday Society* **1946**,42, 236-243

[2] Mendes, L.C., Rufino, E.S., de Paula, O.C., Torres, J.R., *Polymer Degradation and Stability* **2003**, 79, 371-383

[3] Monrabal, J., *Journal of Applied Polymer Science* **1994**, 52, 491-499

[4] Monrabal, B., Blanco, J., Nieto, J., Soares, J.B.P., *Journal of Polymer Science Part A: Polymer Chemistry* **1999**, 37, 89-93

[5] Monrabal, B., Presentation at the Waters SEC conference, Las Vegas, **2000**

[6] Monrabal, B.; *Macromolecular Symposia* **1996** 110, 81-86

[7] Britto, L.J.D., Soares, J.B.P., Penlidis, A., Monrabal, B., *Journal of Polymer Science: Part B Polymer Physics* **1999**, 37, 539-552

[8] Gabriel, C., Lilge, D., *Polymer* **2001** 42, 297-303

[9] Kok, S.J., Wold, C.A., Hankemeier, T., Schoenmakers, P.J., J*ournal of Chromatography A* **2003**, 1017, 83-96

[10] Kok, S.J., Arentsen, N.C., Cools, P.J.C.H., Hankemeier, T., Schoenmakers, P.J., *Journal of Chromatography A* **2002**, 948, 257-265

[11] van Zyl, A.J.P., Graef, S.M., Sanderson, R.D., Klumperman, B., Pasch, H., *Journal of Applied Polymer Science* **2003**, 88, 2539-2549

[12] Graef, S.M., Brüll, R., Pasch, H., Wahner, U.M*., e-Polymers* **2003** 005, 1-9

[13] Tso, C.C., DesLauriers, P.J., *Polymer* **2004**, 45, 2657-2663

[14] Faldi, A., Soares, J.B.P., *Polymer* **2001**, 3057-3066

[15] Verdurmen-Noël, L.; Baldo, L.; Bremmers, S., *Polymer* **2001**, 42, 5523-5529

[16] Willis, J.N., Dwyer, J.L., Liu, X., Dark, W., *ACS Symposium* **1999** 226-231

[17] Willis, J.N., Dwyer, J.L., Liu, X., *International Journal of Polymer Analytical Characterisation* **1997**, 4, 21-29

[18] Ludlow, M., Louden, D., Handley, A., Taylor, S., Wright, B., Wilson, I.D., *Analytical Communications* **1999** 36, 85-87

[19] Cheung, P., Balke, S.T., *Polymer Materials Science and Engineering* **1993**, 69, 122-123

[20] Willis, J.N., Dwyer, J.L., Liu, X., *Polymer Materials Science and Engineering* **1997**, 77, 27

[21] Tackx, P., Bremmers, S., *Polymer Material Science* **1998**, 78, 50

[22] Deslauriers, P.J., Rohlfing, D.C., Hsieh, E.T., *Polymer* **2002**, 43,159-170

[23] Marshall, N., PhD thesis, University of Sussex, **December 2001**

[24] Niki, E., Dekker, C., Mayo, F.R., *Journal of Polymer Science: Part A Polymer Chemistry* **1973**, 11, 2813-2845

[25] Adams, J.H., *Journal of Polymer Science: Part A-1 Polymer Chemistry* **1970**, 8, 1077-1090

[26] Adams, J.H., Goodrich, J.E., *Journal of Polymer Science: Part A-1 Polymer Chemistry* **1970**, 8, 1269-1277

[27] Lacoste, J., Vaillant, D., Carlsson, D.J., *Journal of Polymer Science: Part A Polymer Chemistry* **1993**, 31, 715

[28] Gijsman, P., Kroon, M., van Oorschot, M., *Polymer Degradation and Stability* **1996**, 51, 3-13

[29] Lacoste, J., Carlsson, D.J., *Journal of Polymer Science: Part A Polymer Chemistry* **1992**, 30, 493-500

[30] Pellerin, C., Frisk, S., Rabolt, J.F., Chase, D.B., *Applied Spectroscopy* **2004**, vol 50 no 7, 799-803

[31] Jouan, X., Gardette, J.L., *Polymer Communications* **1987**, 28, 239-241

[32] Adam, C., Lacoste J., Lemaire, J., *Polymer Degradation and Stability* **1989**, 24, 185-200

[33] Lacoste, J., Deslandes, Y., Black, P., Carlsson, D.J., *Polymer Degradation and Stability* **1995**, 49, 21-28

[34] Gulmine, J.V., Janissec, P.R., Heise, H.M., *Polymer Degradation and Stability* **2003**, 79, 385-397

[35] Mathot, V.B.F., *Calorimetry and Thermal Analysis of Polymers*, **1994**, ISBN: 1-56990-126-0 Hanser/Gardner Publications Incorporated, Cincinatti

[36] Brüll, R., Pasch, H., Raubenheimer, H.G., Sanderson, R., Van Reenen, A.J., Wahner, U.M., *Macromolecular Chemistry and Physics* **2001**, 202, 1281-1288

[37] Wild, L., *Advances in Polymer Science* **1990**, 98, 1-46

Chapter Six

Degradation behaviour of unstabilised commercial propylene-1-pentene copolymers

6.1 Introduction and background

The Sasol Synthol process, utilised for the conversion of synthesis gas to petrochemicals and gaseous hydrocarbon products, is the largest scale application of the high-temperature Fischer-Tropsch (HT-FT) process in the world [1]. In the decade up to 1999, Sasol employed sixteen Synthol CFB (continuous fluidised bed) reactors for this process, but these reactors were replaced in the late 1990's by the new generation Sasol Advanced Synthol (SAS) reactors. A SAS reactor is a conventional fluidised bed reactor, designed to operate at pressures between 20 and 40 bar and temperatures of around 340 ºC. Under these conditions, the Synthol product stream typically consists of the following (Table 1):

Table 1: Composition of a typical SAS reactor product stream

Product	(%)
Methane	7
C_2-C_4 olefins	24
C_2-C_4 paraffins	6
Gasoline	36
Middle distillates	12
Heavy cut and waxes	9
Oxygenates soluble in water	6

In addition to gasoline, nearly 24% of the Synthol stream consists of C_2-C_4 olefins. Of the heavier streams, nearly 70% of the C_5-C_{10} cut and 40% of the C_{11}-C_{14} cut consist of olefins. Therefore, the Fischer-Tropsch oil-from-coal process provides Sasol with a unique range of α-olefins that cannot be produced by any other commercial process. The Fischer-Tropsch process favours the production of the odd-numbered and branched α-olefins and this provides Sasol Polymers with a cost base that cannot be equalled by any other commercial process. Fischer-Tropsch olefins can be used in co-polymerisations and the incorporation of these olefins can provide unique polymer properties [2]. 1-Pentene is an example of a by-product of the Fischer-Tropsch process that can be utilised as a comonomer in polyolefin production [3-8].

A series of propylene-1-pentene copolymers was recently studied on a laboratory scale by Sasol Technology [3, 4, 5, 6] and subsequently patented and commercialised by Sasol Polymers. These commercial random propylene-1-pentene copolymers have several

advantages compared to ethylene-propylene copolymers, including superior hot melt strength, low haze, good gloss and good impact properties [3, 7, 8]. This range of copolymers is unique to Sasol Polymers and is not produced commercially by any other polyolefin manufacturer. Propylene-1-pentene copolymers have performed well in the marketplace, but concerns were raised regarding the yellowing of these copolymers during use. The yellowing of the pentene grades was thought to be related to either stabilisation or degradation during processing. During processing, several processes may be initiated that may result in radical formation and, subsequently, failure of the polymer. As discussed in Chapter 2, these processes generally proceed through initiation, propagation, branching and termination reactions [9, 10]. The process is known to be auto-accelerating [11] and each cycle produces a hydroperoxide and an alkyl radical that can participate in the next cycle. During the process, localised highly oxidised areas will be formed. From these highly oxidised areas degradation spreads to the rest of the matrix, through energy transfer, although migration of low molar mass radicals to other areas may also be possible [12].

A polymer can be characterised by its molar mass properties, chemical composition and chemical composition distribution. During degradation, changes are observed in all three of these parameters. While the changes in molar mass distribution and chemical composition during degradation have been investigated extensively there is no information in the open scientific literature about the influence of the chemical heterogeneity on polyolefin degradation and the changes in chemical heterogeneity that occurs during degradation.

The oxidation (transformation) products of hindered phenolic (stabiliser) degradation (known as quinoidal oxidation products) are also known to contribute to yellowing of polymers [13]. These products are formed during the reaction of the anti-oxidant with oxygen, heat and light. Several of these transformation products, including conjugated and unconjugated quinoidal compounds, have been identified in hindered phenol stabilised systems. Especially stilbenequinone has been shown to contribute significantly to the yellowness index and even at 5 ppm it can contribute to the yellowness index [13].

The base polypropylene polymer may, however, also contribute to yellowing by the formation of conjugated double bond structures during degradation. The stability of the base polymer influences the stabiliser requirements to maintain its performance during processing and end use.

6.2 An overview of stability studies performed on propylene-1-pentene copolymers

The physical properties of the propylene-1-pentene copolymers differ in several regards from the polypropylene homopolymers [3, 7]. This is reflected by differences in several physical and mechanical properties. For example, the melting points, crystallinities and T_g values of the propylene-1-pentene copolymers are significantly lower than the polypropylene homopolymers. Mechanical properties are also significantly different, especially the modulus and impact strength [14].

Several authors performed detailed studies on the thermo-oxidative stability of stabilised propylene-1-pentene copolymers [3, 7]. These studies were, however, all performed on samples stabilised with primary and/or secondary stabilisers. There are several factors that may influence the stability of propylene-1-pentene copolymers. These factors include the presence of impurities in the polymer, for example, catalysts and catalyst residues (discussed in Chapter 2, Section 2.5.2). The stability of these copolymers may, however, also be influenced by several morphological properties. Differences in crystallinity and crystal structure may also have a significant influence on the degradation behaviour. Any differences in the soluble fractions (low molar mass species) may have a significant influence on the degradation behaviour.

Joubert [15] investigated the stability of several stabilised propylene-1-pentene samples, containing 0.3%, 1.2%, 1.8%, 2.4% and 6% pentene. The stabilised samples were pressed into thin films of 200-micron thickness and degraded at 110 ºC. Carbonyl formation and embrittlement was followed as a function of degradation time. The stability of these polymers was influenced significantly by the incorporation of pentene. The sample containing 6% pentene degraded significantly faster than the samples containing less pentene (Figure 1*). Oxygen and carbon dioxide uptake values increased significantly in copolymer samples containing more than 3% pentene.

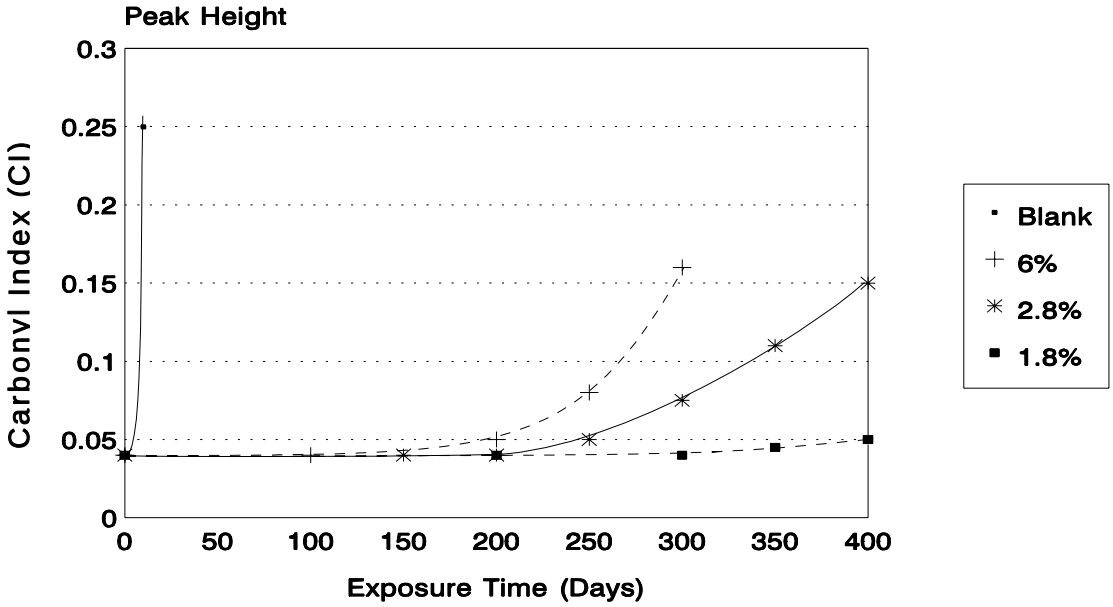

Figure 1: Effect of pentene content on the carbonyl index and long term thermal stability (LTTS) of stabilised propylene-1-pentene copolymers with different pentene contents.

* With permission, Dr D Joubert, Sastech Polymer group

Oven aging is considered to be the standard method for the assessment of polymer thermo-oxidative stability. The method has several drawbacks, however, including volatilisation of low molar mass additives in stabilised sample testing, volatilisation of transformation products in the oven and the effect of some volatile degradation products (volatile carbonyl containing compounds) [16], but it is still the most convenient method to obtain more information on the thermal stability of a non-stabilised or stabilised polymer. Traditionally, samples degraded by thermo-oxidative degradation have been studied by tensile properties (elongation at break, stress at break, tensile impact strength) [16], impact strength and time to embrittlement. Alternatively, yellowing index, haze and loss of gloss have been used to study the progress of degradation [16]. Other properties like crack formation, weight loss, surface roughness and electrical properties have also been used as a measure of the extent of degradation [16]. In the study performed by Marshall [7], polypropylene samples were aged at 70 ºC, 90 ºC, 110 ºC and 130 ºC and analysed for OIt (oxidation induction time), OIT (oxidation induction temperature), SEC and crystallinity measurements. The samples aged at 110 ºC and 130 ºC failed rapidly and were not considered for further analysis.

Marshall [7] evaluated the thermal stability of several pilot plant scale polypropylene homopolymers, ethylene-propylene random copolymers (containing 2% and 3% ethylene) and propylene-1-pentene copolymers (containing 1,5%, 3.5% and 5% pentene, respectively).

He found that the stabilised propylene-1-pentene copolymers had significantly shorter lifetimes compared to the homopolymer samples, especially when the pentene content was higher than 3%. Marshall also investigated several stabilised commercial propylene-1-pentene copolymer samples, containing 1%, 3%, and 5% pentene. The degradation behaviour of these samples was compared to polypropylene homopolymer samples. In these evaluations, samples were aged at 130 ºC in a heat circulating oven and the carbonyl and yellowness indices were measured daily. Samples were also removed for chemiluminescence and molar mass distribution determinations. The long term thermal stability of a stabilised propylene-1-pentene sample (containing 5% pentene) was about a third of that of a polypropylene homopolymer sample, containing half the level of Irganox 1010. In Figure 2** the normalised stability results (normalised to similar stabiliser levels) are given. The incorporation of pentene resulted in a decrease in the stability of the polymer compared to the homopolymer. Even at 1% pentene incorporation there was a significant reduction in the stability of the copolymer. Although it seemed as if the 3% pentene-containing sample was more stable than the 1% sample, it must be kept in mind that these stabilities were normalised results, with the results adjusted according to the relative quantities of stabilisers in these samples.

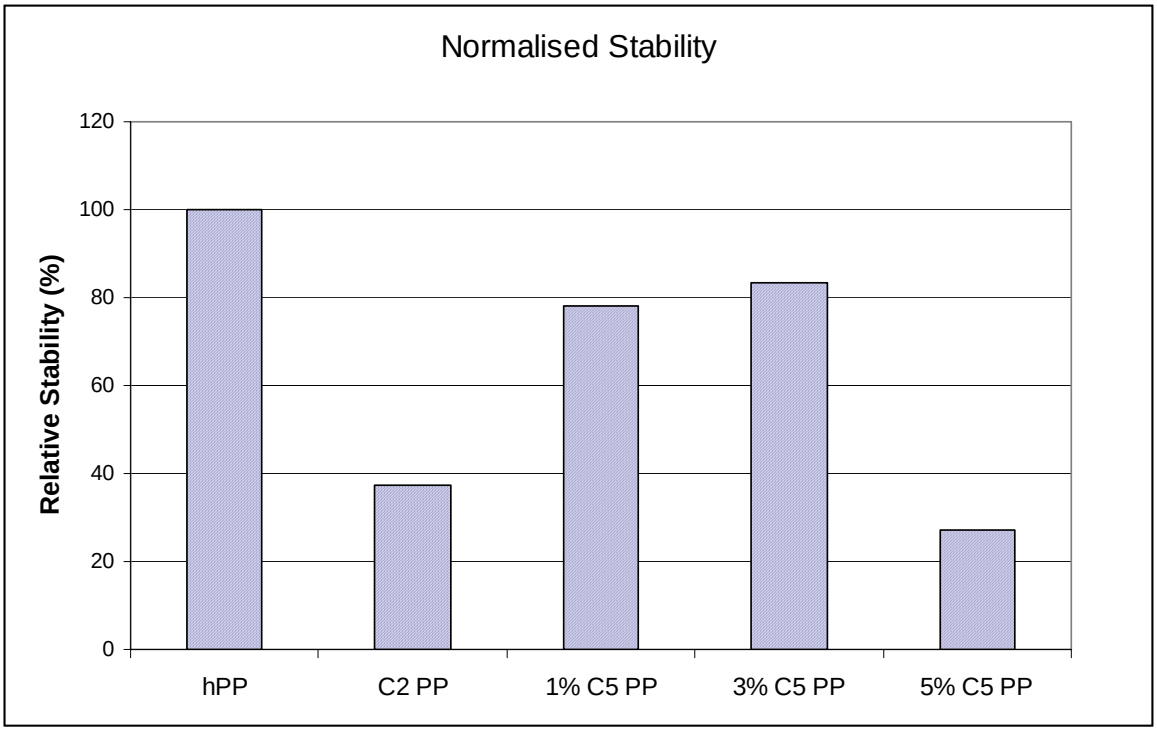

Figure 2: Effect of pentene content on the normalised stability of three propylene-1-pentene copolymers, a propylene homopolymer and a propylene-ethylene copolymer.

** With permission, Dr N Marshall, Sasol Wax, South Africa

This dramatic drop in stability of the stabilised propylene-1-pentene samples was attributed to the reduction in crystallinity in the copolymer samples, which could result in a higher oxygen permeability and oxygen solubility. At higher pentene content, the pentene distribution between copolymer molecules may have a dramatic effect on the stability, with the heterogeneity showing preferred incorporation in the amorphous and crystalline phases. Thus there may be clustering, resulting in the pentene not being statistically distributed through the sample.

These studies confirmed that the stabilised propylene-1-pentene samples were less stable than the polypropylene homopolymer samples studied. All these studies were, however, performed on stabilised samples and therefore the question arose: how would the unstabilised samples perform under thermo-oxidative degradation conditions?

6.3 Objectives

The overall objective of this section of the study was to investigate the degradation behaviour of commercial unstabilised Sasol Polymers propylene-1-pentene copolymers by various analytical techniques and to compare the degradation behaviour of the propylene-1-pentene copolymers with that of Sasol Polymers polypropylene homopolymer. Although the degradation behaviour of stabilised propylene-1-pentene copolymers was studied by the classical techniques, including SEC, FTIR and DSC-OIT, and newer techniques, including CL-OIT (chemiluminescence oxidation induction temperature) [7], the degradation behaviour of unstabilised propylene-1-pentene copolymers had not been studied. Secondly, during the previous studies, no information was obtained on the change in chemical composition distribution with the degradation of the propylene-1-pentene copolymers [7]. The physical changes (tensile strength, impact properties etc) will not be studied as part of this investigation.

A further objective of the current section was to investigate the effect of pentene incorporation on the polymer microstructure. This can provide more information on the fundamental stability of the propylene-1-pentene copolymers and may provide information that could be utilised to determine optimum stabilisers and stabiliser concentrations. It may also provide information on how the polymer may be tailored to limit degradation during exposure and heat.

In the previous chapter (Chapter 5), novel methodologies for studying polyolefin degradation were established. In this chapter, additional to the classical techniques used for studying polymer degradation, the changes in chemical composition distribution with degradation were studied by SEC-FTIR and CRYSTAF. SEC-FTIR will be used to study the change in chemical composition as a function of molar mass and CRYSTAF will be used to investigate the change in crystallisability from solution with an increase in the level of degradation.

Furthermore, there was no information available in literature on the changes in chemical composition distribution during the degradation of unstabilised polypropylene. Information on the changes in chemical composition distribution could provide information on the effect of the molecular structure of the propylene-1-pentene copolymers on the degradation mechanism.

6.4 Experimental

6.4.1 Samples used in this study

Two commercial unstabilised propylene-1-pentene samples were obtained from the Sasol Polymers polypropylene production plant in Secunda, South Africa and used to study the degradation behaviour of the commercial propylene-1-pentene copolymers. A homopolymer sample of polypropylene was supplied as a reference. The Sasol Polymers PP plant employs commercial Novolen Ziegler-Natta gas-phase technology. Unstabilised, production campaign reactor powder samples were used for all evaluations. Traces of Irgafos 168 (processing stabiliser, Ciba Speciality Chemicals, Switzerland) were added to all samples to prevent the onset of degradation during compression moulding (see Appendix 1). No other stabilisers were added. The samples were compounded on a Brabender twin screw extruder.

The following three polymers were used for this investigation (Table 2):

1. A PP homopolymer (M_w of 356,000). This polymer sample was unstabilised and obtained from a production campaign (Code PP).
2. A polypropylene-1-pentene copolymer (M_w of 339,870 g/mol) containing 1,7% pentene (determined by FTIR). This polymer sample was unstabilised and obtained from a production campaign (Code P1).

3. A polypropylene-1-pentene copolymer (M_w of 272,460 g/mol) containing 2.9% pentene (determined by FTIR). This copolymer also contained no stabiliser (Code P2).

Table 2: Properties of the three polymers used in this investigation (samples PP, P1 and P2)

Formulation	% Pentene comonomer (weight% FTIR)	MFI (g/10 min)	Density (g/cm^3)
Sample PP	0	4	0.910
Sample P1	1.7	14	0.908
Sample P2	2.9	17	0.904

6.4.2 Preparation of samples for thermal degradation

Plaques of the three samples were compression moulded individually on a Wabash press (Wabash, Indiana), using a final melting temperature of 190 ºC. The samples were compressed in a two-step process whereby the sample is pre-compressed in the first phase to 5 tons and then compressed at 25 tons for 5 minutes. Samples were cooled down at a controlled rate of 15 ºC/minute. Approximately 4 grams of polymer per plaque were used and plaques with a thickness of approximately 1 mm were obtained. After compression moulding, samples were kept in a fridge to prevent further oxidation before the oven aging experiments [16].

6.4.3 Degradation conditions

As the samples used in the current study were non-stabilised, only thermo-oxidative degradation at 70 ºC and 90 ºC was considered. The samples were heat-aged in air in a heat circulating laboratory oven (Scientific Engineering) at two temperatures, 70 ºC and 90 ºC, to investigate the temperature dependence of the degradation process. Light was excluded from all experiments, so experiments were limited to studying thermo-oxidative degradation and excluding any photo-oxidation effects. Thin strips were cut to enable easy sampling at the predetermined sampling interval. Samples were evaluated daily for physical changes and small samples for analysis by DSC, FTIR and SEC were taken daily for the first 5 days and then regularly after the onset of degradation. FTIR scans were performed twice daily for the first 5 days, followed by once daily until failure of the samples.

In the current study, the degradation study was repeated at 90 ºC to evaluate the effect of temperature on the degradation mechanism in propylene-1-pentene copolymers. The same three samples were subjected to oven aging at 90 ºC in a heat circulating oven. Samples were again compression moulded and pre-cut into small strips and removed every three hours on the first day and then every morning and afternoon in the subsequent days to follow the degradation process.

Samples were visually evaluated daily for signs of discolouration and embrittlement. Although an embrittlement test is not as accurate as, for example, molar mass determinations and carbonyl index measurements, it is still a good indication of the actual performance of the polymer in end-use applications [16]. In assessing embrittlement, the polymer is bent through a certain angle (approximately 90 º was used in this study). If the polymer sample breaks, this will be seen as failure.

6.4.4 NMR analysis of the undegraded samples

NMR analysis was carried out according to a novel sample preparation method. Samples were measured quantitatively using a 5-mm probe. The polymer (±60 mg) was dissolved in 0.6 mL deuterated tetrachloroethane (*d*-TCE) (6 wt%), stabilised with di-tertiary butyl para-cresol (DtBpC). The solvent was purged with nitrogen for a period of 2 hours prior to preparing the sample for analysis. Approximately 0.3 mL of the stabilised solvent was added to 60 mg of the polymer. The polymer was melted in the NMR tube in the presence of the solvent by carefully heating the tube with a heat-gun. The rest of the solvent was added and the tube sealed with Teflon® tape. The sample was placed in a ventilated oven to homogenise at 140 °C for approximately 2 hours. Quantitative ^{13}C NMR experiments were performed at 125 MHz on a 5 mm PFG switchable/broadband probe (^{1}H -^{19}F, ^{15}N - ^{31}P) on a Varian ^{UNITY}*INOVA* 600 MHz spectrometer at 130°C. 90° pulse widths of approximately 6 μs and delay times between pulses of 15 s were used, with an acquisition time of 1.8 s. The number of scans was set to 5120, but a signal-to-noise parameter was set to 2000. Thus, either 2400 scans were acquired or the acquisition was stopped after the required signal-to-noise was reached. The analysis time, therefore, ranged from 3 -10 h. Chemical shifts were referenced internally to the PP methyl peak at 19.68 ppm.

6.4.5 SEC analysis

The molar mass distributions for the degradation and undegraded samples (samples degraded at 70 ºC) were determined on a Polymer Laboratories PL 220 instrument (Polymer Laboratories, Shropshire, UK), using ultra-pure 1,2,4-trichlorobenzene (TCB) as the mobile phase. The TCB was distilled and filtered before use. The mobile phase was stabilised with trace amounts of BHT to prevent compositional changes to the solvent. The column temperature was set at 145 ºC. A combination of Waters Styragel high-temperature, crosslinked divinylbenzene SEC columns was used for SEC determinations (Waters HT 2-6). A relative calibration was performed using a set of Polymer Labs Easical™ polystyrene calibration standards. An instrument flow rate of 1mL/min was used for all SEC determinations.

All samples were prepared by weighing approximately 3 mg of polymer into a 4 mL glass vial. Approximately 4 mL of TCB was added to all samples. Sample dissolution was carried out at 150 ºC in a heat-circulating laboratory oven. Irgafos 168 was added to prevent further degradation during the analysis run.

All molar mass averages for the 90 ºC study were determined on a Waters 2000 Alliance SEC (Waters, Milford, Massachusetts) instrument. A PL 220 instrument was used for the study at 70 ºC and values should not be compared due to different standards and instrument conditions being used. TCB, stabilised with 0.26% BHT, was used as mobile phase for all experiments. The mobile phase was filtered twice to remove any impurities. The instrument was equipped with Waters HT 3, 4, 5 and 6 columns. Sample preparation was similar to the 70 ºC experiments.

6.4.6 FTIR analysis

Spectra were acquired on a Perkin Elmer Spectrum 2000 instrument (Perkin Elmer Corporation, Norwalk, Connecticut). All spectra were determined in transmission mode and 64 scans were acquired per spectrum. The resolution was set at 2 cm^{-1}.

The pentene content was determined by monitoring the peak height at 737 cm^{-1} in the FTIR spectrum. The peak at 737 cm^{-1} is due to the CH_2-rocking vibration of the 1-pentene comonomer and can be used for the quantification of the comonomer content [26]. Although the absolute content was not determined, the relative pentene content was calculated by

determining the FTIR peak height t 737 cm^{-1}. The 1167 cm^{-1} peak was used as an internal reference. The pentene content (determined at 737cm^{-1}) was corrected by using the ratio of the 1167 cm^{-1} peak intensity at the specific day, divided by the 1167 cm^{-1} peak of the day 1 sample (for samples P1 and P2 respectively).

6.4.7 DSC analysis conditions

DSC analyses were carried out on the initial and the degraded samples using a Mettler DSC 822 instrument (Mettler Toledo, Switzerland). In order to ensure identical thermal histories, samples were first heated at 10 ºC/min to 220 ºC, followed by controlled cooling to 30 ºC. The subsequent heating cycle (from 30 ºC to 190 ºC) was used for all thermal analysis calculations.

6.4.8 CRYSTAF analysis conditions

A CRYSTAF model 200 instrument (Polymer Char, Valencia, Spain) was used for all analysis. CRYSTAF analyses of the homopolymer and copolymer samples were performed on the initial and degraded samples of each set. Samples were dissolved for 120 minutes at 160 ºC. The samples were then stabilised for 45 minutes at 95 ºC. A linear temperature gradient was followed at 0.1ºC/ min until a temperature of 29 ºC was reached. During this time, 22 points were taken between 95 and 60 ºC, followed by 18 points down to 29 ºC.

6.4.9 SEC-FTIR analysis

A dedicated SEC-FTIR instrument, incorporating a Lab Connections LC 300 high-temperature interface was used for all SEC-FTIR measurements. Samples were prepared by dissolving 12 mg of degraded sample in 4 mL TCB. BHT was added to prevent further degradation of the polymer samples. A peroxide decomposer (Irgafos 168, Ciba Chemicals) was also added to the degraded samples. A Waters 150 C HT-SEC instrument, equipped with Waters HT 2, 3, 4 and 5 columns, was modified to incorporate the LC-transform connection. The differential refractive index (DRI) detector was taken off-line during measurements and a flow rate of 1 mL/ min was employed during all experiments. To prevent precipitation of the polymer sample, the nozzle and stage temperatures were optimised separately. All samples were sprayed on a Germanium disk and analysed off-line on a Nicolet FTIR instrument. For this series of experiments the stage temperature was set at 160 ºC, and the nozzle temperature was set at 118 ºC. The injection volume had to be optimised,

as the film on the Germanium disk needs to be sufficiently thin to obtain good FTIR spectra. The vacuum on the instrument was controlled accurately to remove all excess solvent.

The films on the Germanium disks were conditioned by leaving the Germanium disks at room temperature for two hours before scanning on the FTIR spectrometer.

6.5. Results of the degradation study at 70 ºC and 90 ºC

During thermal exposure at 70 ºC, sample P2 showed the first signs of degradation; fine cracks appeared on the plaque surface. The sample showed signs of embrittlement after 10 days. Sample P1 was the next to show degradation after approximately 15 days at 70 ºC. The homopolymer sample only showed signs of degradation after approximately 35 days. It was noticed that the homopolymer showed a slower colour change (yellowing) compared to the copolymer samples. In stabilised samples the colour change in the samples may be due to transformation reactions in the phenolic anti-oxidants [13]. In unstabilised samples the origin of the colour change is associated with the formation of chromophores during the degradation process [7]. The failure point for this study was taken as the time at 70 ºC until embrittlement of the samples (Table 3).

Table 3: Days-to-failure (embrittlement) of the three samples under investigation (samples PP, P1 and P2)

Sample	Days to failure at 70 ºC
Homopolymer	35
P1	15
P2	10

6.5.1 Effect of catalyst residues and annealing on thermal degradation

The effect of catalyst residues on the degradation behaviour of polyolefins has been discussed earlier (Section 2.5.2). Catalyst residues may accelerate the degradation process and, therefore, any significant differences in the catalyst residues may contribute to differences in the degradation rate. In the current, commercial Ziegler-Natta LLDPE and PP grades, the levels of metal residues are generally low [12]. Titanium and aluminium residues are generally considered to be poor pro-oxidative agents, and their influence on the degradation behaviour of polyolefins is temperature dependent. Alkylaluminium usually is

totally deactivated by the end of polymer synthesis due to its reaction with oxygen. It may, if still active, result in a depletion of the phosphate stabilisers in stabilised products. In comparison, chromium residues are very active pro-oxidation agents [12]. Copper and iron residues are also strong pro-oxidation agents. Goss [17] used chemiluminescence to study the effect of titanium residues and temperature on the degradation behaviour of polypropylene. He showed that the chemiluminescence intensity increased with a higher level of titanium residues. He also found that the time needed to obtain maximum chemiluminescence was less at a higher titanium concentration. These two observations confirmed the classical theories that titanium can catalyse the decomposition reaction of the hydroperoxides in the polymer matrix, the higher the concentration of titanium, the higher the rate of peroxide decomposition [18]. The effect of catalyst residues on the mechanism of degradation can be seen in Scheme 1.

Effect of Ti residues on the initiation and branching steps:

$$POOH + Ti^{3+} \longrightarrow PO\cdot + {}^{-}OH + Ti^{4+} \quad (6.1)$$

$$POOH + Ti^{4+} \longrightarrow PO_2\cdot + H\cdot + Ti^{3+} \quad (6.2)$$

Scheme 1: Effect of catalyst residues on the kinetics of degradation of polyolefins

Most of the peroxides formed in PP are associated peroxides, so most of the reactions stated above will convert associated peroxides to degradation products.

The catalyst residues in the three samples were evaluated (Table 4). For this determination, 5g of sample was ashed and analysed by inductively coupled plasma (ICP) analysis. The titanium concentration was not evaluated, as this is typically only 5% of the Al concentration (around 2 ppm) in these commercial polymers and is not thought to have an influence on the degradation behaviour.

Table 4: Catalyst residues in the samples (samples PP, P1 and P2) analysed by ICP

Sample	Mg (ppm)	Al (ppm)
Sample PP	10.7	39
Sample P1	10.3	40
Sample P2	11.1	40

The levels of aluminium and magnesium residues in the three samples were not significantly different. They are therefore not expected to influence the degradation behaviour to a significant extent. Annealing can occur when polypropylene is exposed to elevated temperatures [16]. This involves the re-organisation of chain segments and, as a result of this, an increase in crystallinity will occur. Although annealing is significant at temperatures above 100 ºC, it may already commence at temperatures just above room temperature, although the process will be extremely slow. For a non-nucleated sample, the initial morphology depends on the cooling history [7]. When a sample is cooled at more that 80 °C s^{-1} the sample is mesomorphic, while at slower cooling rates the α-monoclinic form dominates. The annealing of polypropylene will result in morphological changes, including the formation of more perfect crystals and lamellar thickening.

Annealing of polypropylene above 100 ºC results in a decrease in the amorphous content and an increase in the amorphous-crystalline interface. The crystallinity, density and apparent crystal size have been found to increase significantly even after annealing times as short as 5 minutes. At 70 ºC annealing is not considered to be significant, but at 90 ºC it may be.

Hawkins et al. [19] compared the thermal stability of linear and branched polyethylene samples below and above their melting points. Below the melting point, the branched polyethylene degraded significantly faster than the linear polyethylene, while at temperatures above the melting point, both polymers were completely amorphous, resulting in higher oxygen uptakes and similar degradation rates for the two polymers.

6.5.2 NMR results

The three undegraded polypropylene samples were analysed by ^{13}C NMR spectroscopy to evaluate their composition and tacticities. The ^{13}C NMR spectra are given in Figure 3. It can be seen that the branching can be clearly detected clearly in the propylene-1-pentene spectra (between 10 and 50 ppm). The allocation of these branching peaks can be seen in Chapter 7.

These spectra were used to determine the pentene content of the two propylene-1-pentene copolymer samples. The tacticities and stereo-errors were also determined. The determination of the pentene content by NMR is described in Chapter 7 (Section 7.4.3).

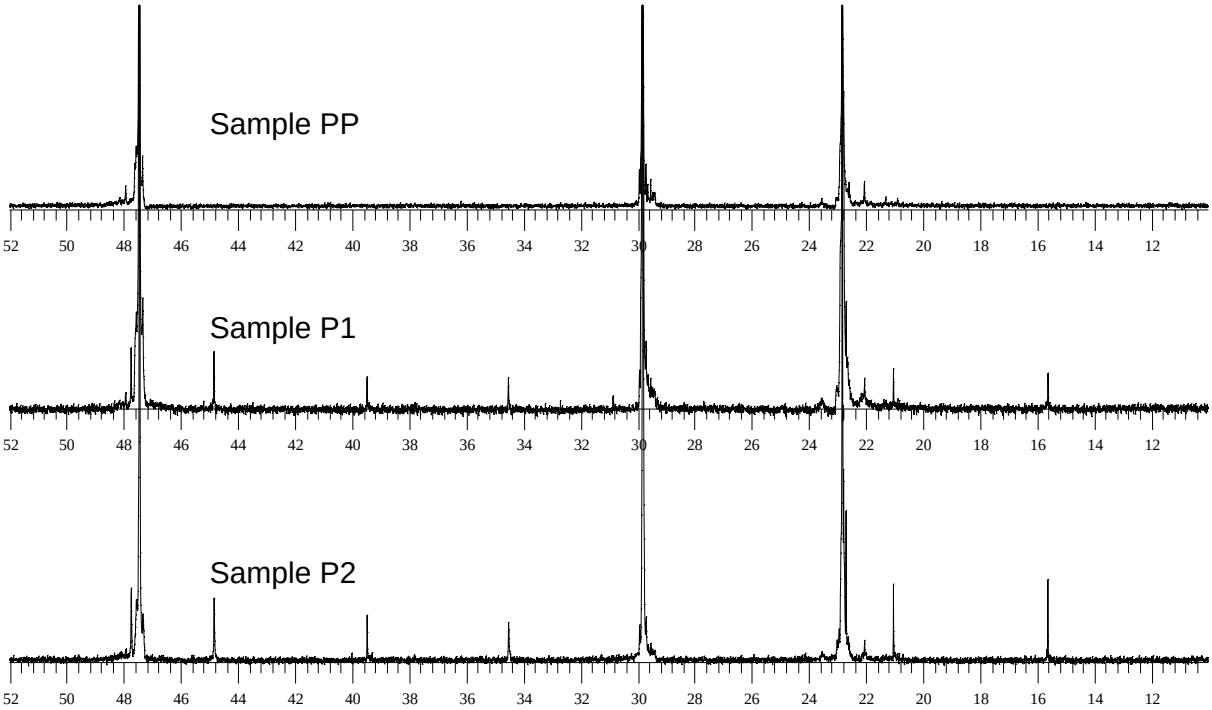

Figure 3: ^{13}C NMR spectra of the three polypropylene samples, dissolved in deuterated tetrachloroethane.

The two copolymers, samples P1 and P2, show the presence of several branching peaks. The tacticities of the three samples were similar, as seen in Table 5. Sample P1 contained approximately 1.07 mol% pentene, and sample P2 contained approximately 2.24 mol%. The mmmr and mmrr insertions were the highest in the homopolymer, followed by P1. P2 had the lowest level of these stereo-errors.

Table 5: ^{13}C NMR results of the three undegraded polypropylene samples PP, P1 and P2

Sample no	Isotacticity index (%)	Pentene content (mol%)	mmmm	mmmr + mmrr	mrrm
Sample PP	94.06	0	94.01	5.37	0.57
Sample P1	94.59	1.07	93.94	4.8	0.57
Sample P2	94.7	2.24	93.46	4.27	0.96

6.5.3 Changes in molar mass of samples PP, P1 and P2 during degradation

6.5.3.1 Effect of degradation at 70 ºC

In Figure 4 the molar mass curves of P2, measured at days 0, 12, 15, 20 and 26, are shown. With progressing degradation (longer exposure times at 70 ºC), there was a significant shift

in the molar mass distribution curves to lower molar masses. The shape of the molar mass distribution curves does not change significantly during the initial stages of degradation, it only shifted to longer retention times (lower molar mass). During the later stages of degradation, a shoulder developed on the low molar mass side of the degradation curve, and it increases as degradation progresses.

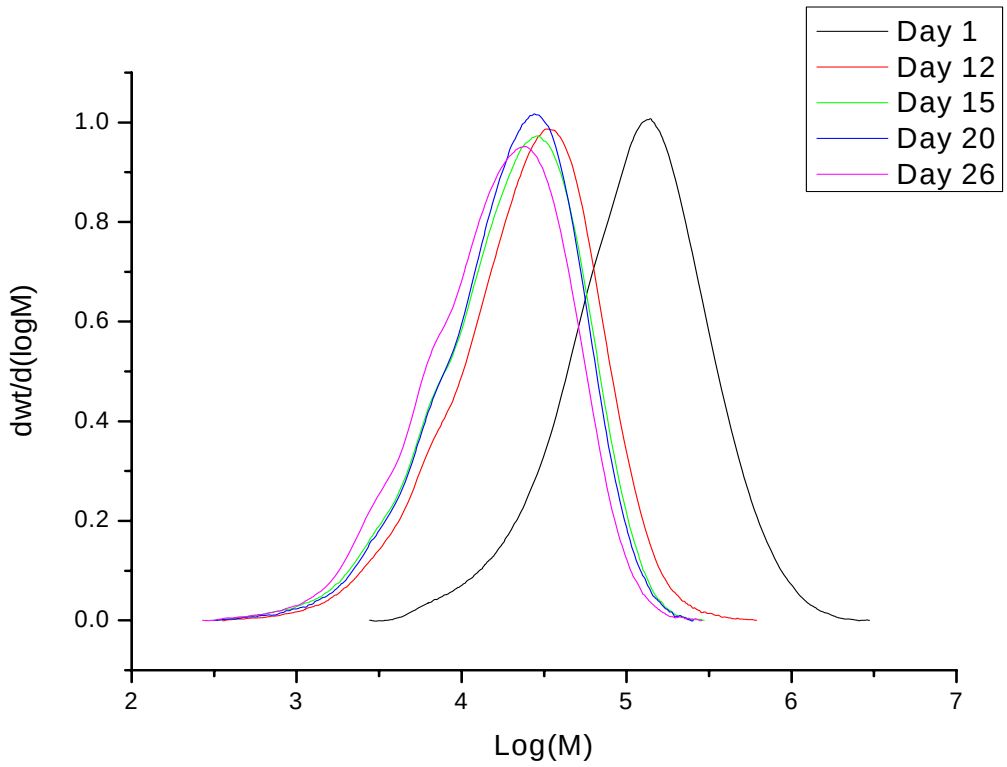

Figure 4: Change in the molar mass distribution curves and the reduction in molar mass during the degradation of sample P2 at 70 ºC.

In order to determine the rate of decrease in the molecular weight averages, the molecular weight averages were converted to log values. All log molar mass averages were exported to Microcal® Origin for data manipulation. The following molar mass averages were considered: M_n, M_w and polydispersity values. Figure 5 shows the effect of degradation on the M_w averages of the three copolymers. The homopolymer showed a slower decrease in molar mass during thermo-oxidative degradation than the two copolymer samples. The M_w of the homopolymer sample before exposure was approximately 356,000 g/mol. This value remained constant until approximately day 28, whereafter there was a significant decrease in the molar mass. The molar mass of the 1,5% pentene containing copolymer (P1) started decreasing at day 3. By day 5 the molar mass had decreased from an initial 339,870 g/mol to approximately 296,000 g/mol. The molar mass of the P2 sample decreased from 272,000

g/mol to 224,000 g/mol by day 4. The molar mass of the two copolymer samples initially decreased at similar rates. The slopes of the M_w decrease for samples P1 and P2 were comparable (-0.041 compared to -0.038). This could possibly be due to the incorporation pattern of the pentene in the polymer backbone, resulting in the decrease in the stability of the polymer.

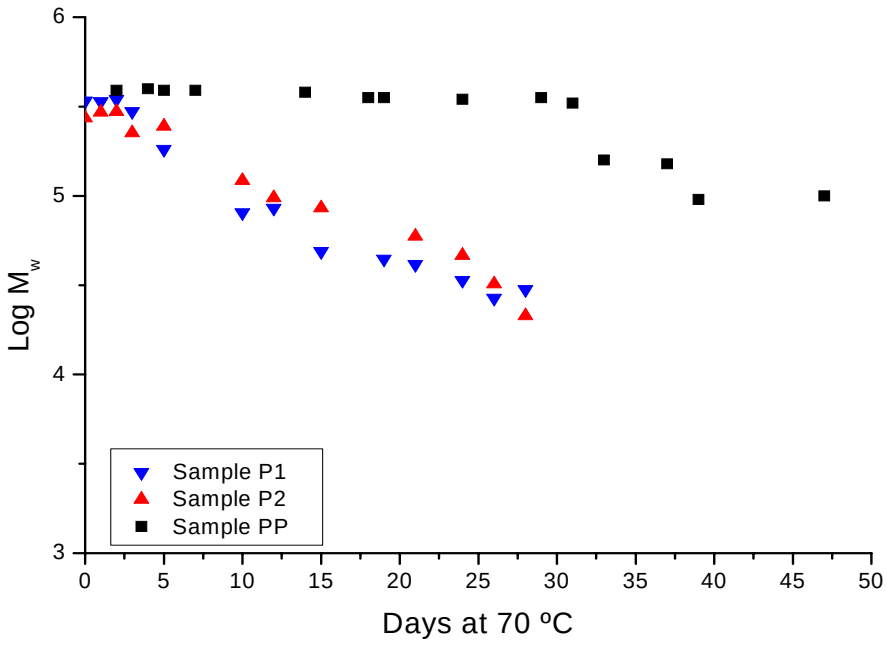

Figure 5: Change in the M_w values of the two copolymer samples and the homopolymer sample with degradation.

The homopolymer sample showed a slower change in molar mass compared to the two copolymer samples.

The M_n values have been used in literature to determine the amount of bond scissions per mol of polymer molecules [20]. Similar equations were also developed by Canevarolo to describe the degradation process in polyolefins (Section 2.3.3). The number of bonds cleaved per mol of polymer was defined by:

$$\frac{\text{Number of bonds cleaved}}{\text{Mol of starting polymer}} = \left\{ \frac{M_n \text{ (initial)}}{M_n \text{ (final)}} \right\} - 1 \qquad (6.3)$$

therefore:

$$\text{Number of bonds cleaved} = \text{Mol of starting polymer} \times \frac{M_n \text{ (initial)}}{M_n \text{ (final)}} - 1 \qquad (6.4)$$

where: M_n *(initial)* is the number average molar mass before degradation
and M_n *(final)* is the number average molar mass after degradation

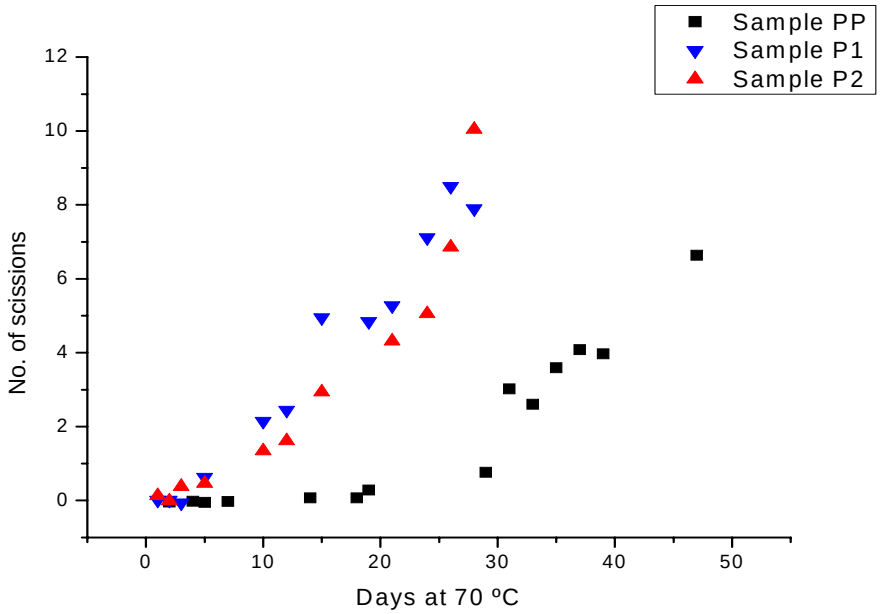

Figure 6: Change in the number of scissions of the two copolymer samples and the homopolymer sample with degradation.

The rate of increase in the number of scissions of the two copolymer samples was similar. This is also evident from the gradient of the two M_n curves (not shown in the text: -0.037 for P1 compared to -0.036 for P2). The homopolymer had a slower gradient of M_n decrease as well as number of scissions. The same trends are seen in the number of scissions (Figure 6).

The changes in the polydispersity of the samples during degradation were evaluated (Figure 7). It is evident that the polydispersity broadened significantly during the degradation of the polypropylene homopolymer sample. There was only a slight narrowing in the polydispersity values of the two copolymer samples.

From these results it can be concluded that scission was the dominant mechanism in the degradation of the polypropylene homopolymer and that crosslinking only plays a minor role (if any). The slight narrowing of the molar mass distributions in the two propylene-1-pentene

copolymers is due to preferential scission of the longer chains, which, from a statistical viewpoint, will be more prone to scission. The polydispersity is expected to broaden when approaching total breakdown of the samples.

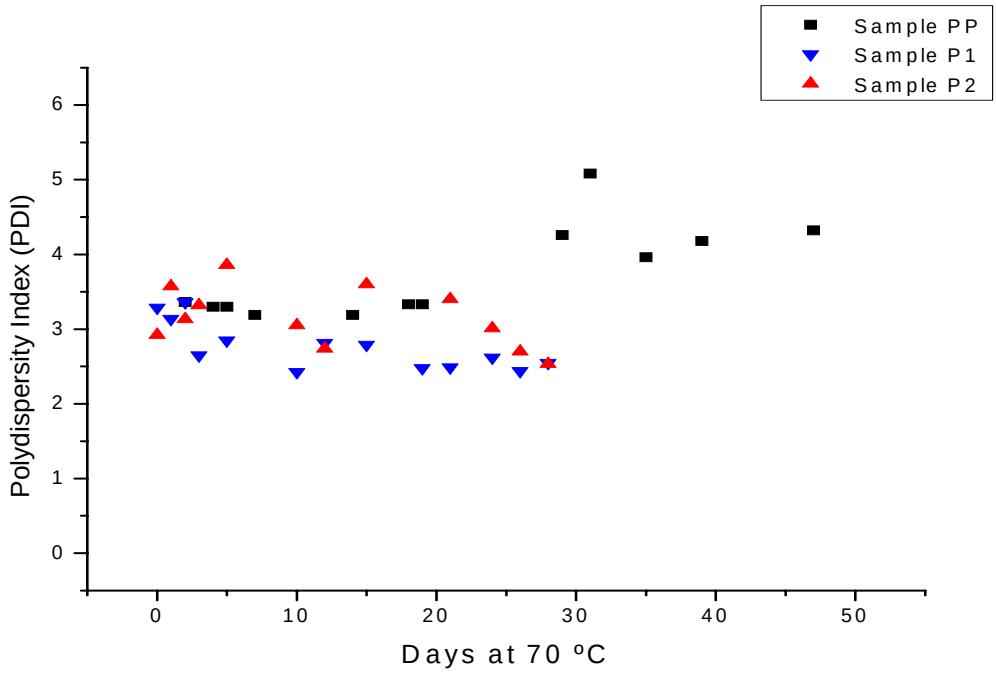

Figure 7: Change in the polydispersity index of the two copolymer samples and the homopolymer sample with degradation.

6.5.3.2 Effect of degradation at 90 ºC

The two copolymer samples showed a decrease in the molar mass values after only 6 hours of exposure (Figure 8) with no change in the molar mass of the homopolymer sample. On day 3, the molar mass of P1 had decreased from 240,000 g/mol to approximately 43,000 g/mol, and the molar mass of P2 had decreased from 150,000 g/mol to approximately 50,000 g/mol. The homopolymer, however, only showed a significant decrease in molar mass after day 3. This was similar to results of the study performed at 70 ºC, where the stability of the homopolymer was also higher than the stability of the copolymers.

The M_n values showed a similar trend to the M_w values (Figure 9). At day three the M_n value of the homopolymer is unchanged, while P1 shows a decrease from 87,000 g/mol to 21,000 g/mol (Figure 9). The molar mass of P2 decreased from 62,500 g/mol to 23,000 g/mol in the same time. This is similar to the results obtained at 70 ºC, although the kinetics at 70 ºC was

significantly slower. Embrittlement of sample P1 occurred at day 15 at 70 ºC, while at 90 ºC embrittlement occurred at day 3.

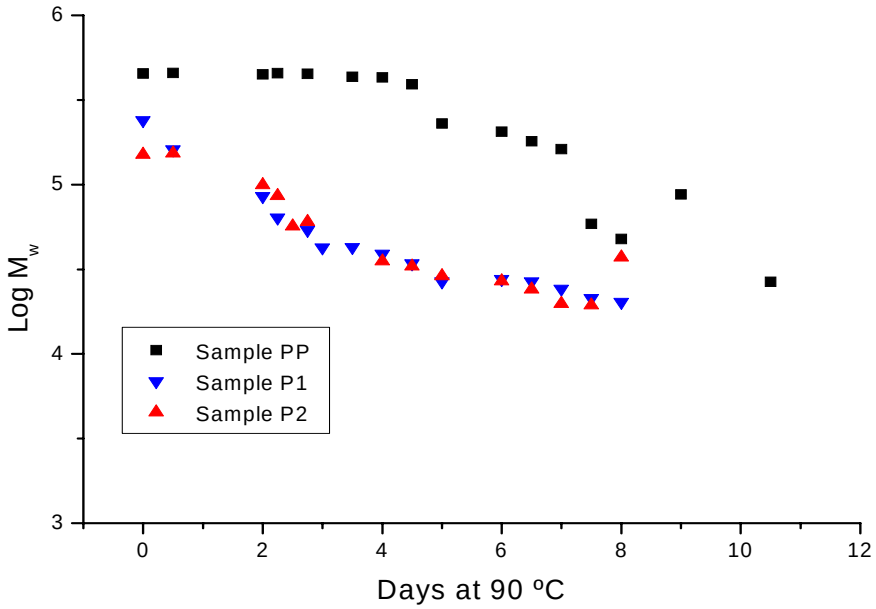

Figure 8: Change in the log M_w values of the two copolymer samples and the homopolymer sample with degradation at 90 ºC.

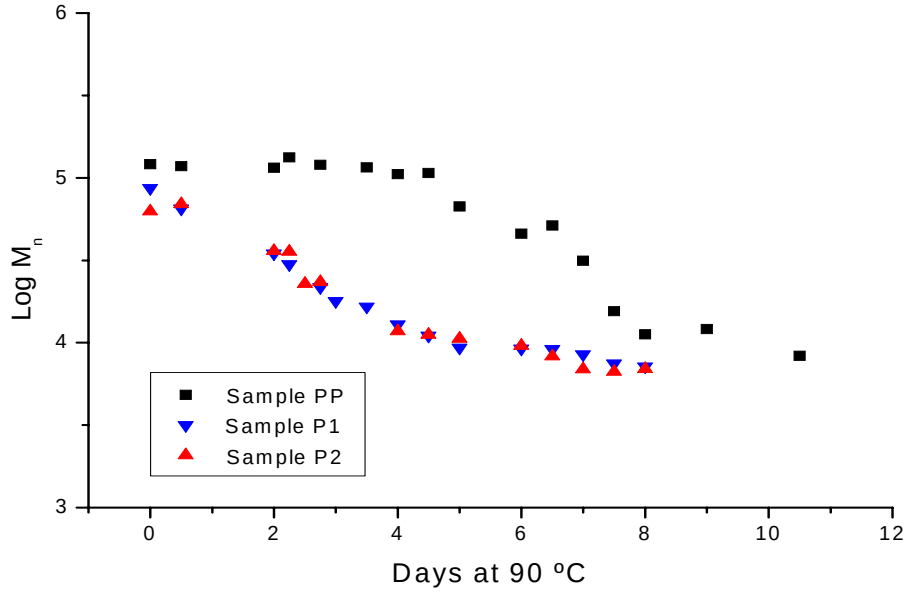

Figure 9: Change in the log M_n *values of the two copolymer samples and the homopolymer sample with degradation at 90 ºC.*

Polydispersity values were evaluated for the 90 ºC data and it appears as if there is a slight narrowing in the PDI values of the two copolymer samples, before the onset of an increase in the polydispersity values.

6.5.4 Changes in the carbonyl content of samples PP, P1 and P2

6.5.4.1 Degradation at 70 ºC

Several authors, including Mendes et al. [21], Gulmine et al. [22] and Jansson et al. [23] found an increase in the carbonyl concentration (as determined by the FTIR) with progressing thermo-oxidative and radiation-induced [24] degradation. A range of volatile carbonyl-containing products was also produced during degradation, including acetone, acetaldehyde and acetic acid [25]. Although these studies were performed on polyethylene, similar principles apply to polypropylene. The level of carbonyl formation is directly related to the extent of degradation, and the FTIR is sensitive to increases in the carbonyl concentration. The FTIR spectra of sample P2, with progressing degradation, can be seen in Figure 10. Three main differences can be detected with the increasing level of degradation: an increase in the carbonyl and peroxide concentration and a decrease in the pentene content (detected at 737 cm^{-1}).

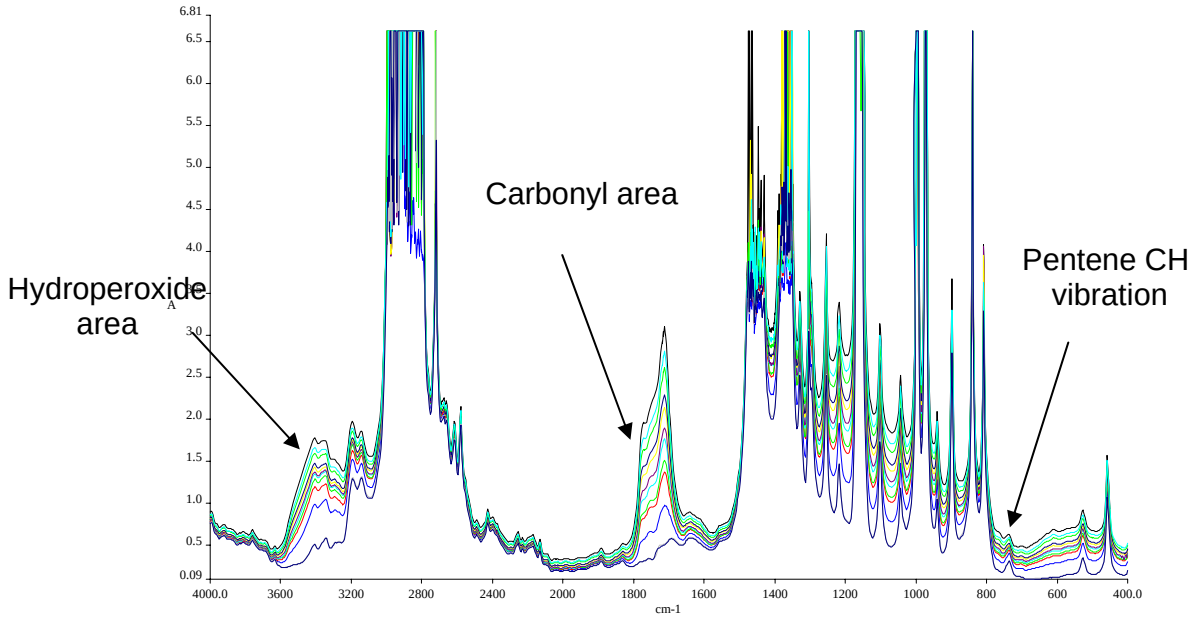

<u>Figure 10:</u> FTIR spectra of the P2 sample degraded at 70 ºC, showing increases in the carbonyl and hydroperoxide concentrations.

In Figure 11 the effect of degradation on carbonyl formation in sample P2 can be seen. The samples taken at the onset of degradation show the presence of ketone groups at 1716 cm^{-1} only. Further absorptions can be observed with progressing degradation at ca. 1740 cm^{-1} and 1780 cm^{-1}, corresponding to the carbonyl absorption bands of peracids and γ-lactones respectively, which are secondary oxidation products.

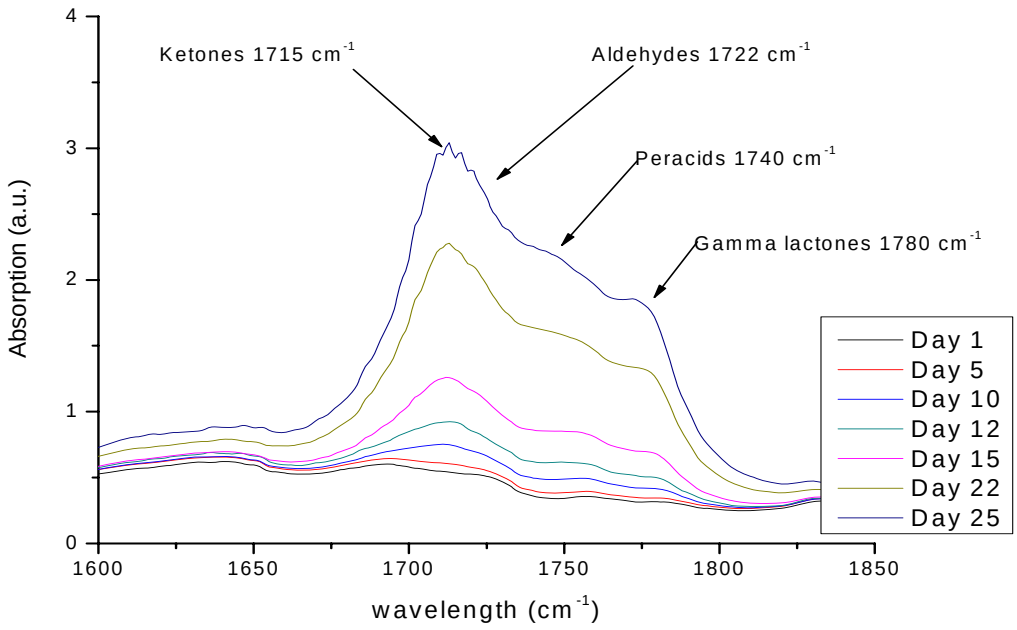

Figure 11: Increase in the carbonyl absorption (as measured by FTIR) of sample P2 with degradation time.

The two pentene copolymer samples showed an early increase in carbonyl concentration, while the homopolymer only showed an increase after 30 days of exposure. This correlates well with the SEC results (Figure 5). Of particular interest was the fact that the carbonyl indices in the two pentene-propylene copolymers increased at similar rates (Figure 12).

This exponential increase in the carbonyl content after an induction period is in line with the results obtained by Marshall [7] for stabilised propylene-1-pentene samples, where the propylene-1-pentene samples degraded significantly faster than the polypropylene homopolymer samples. Although the samples studied by Marshall were stabilised, oxidative degradation leads to a depletion of the antioxidant. After the stabiliser is fully depleted, the polymers showed an exponential increase in the carbonyl index. This is due to the auto-accelerating nature of polyolefin degradation.

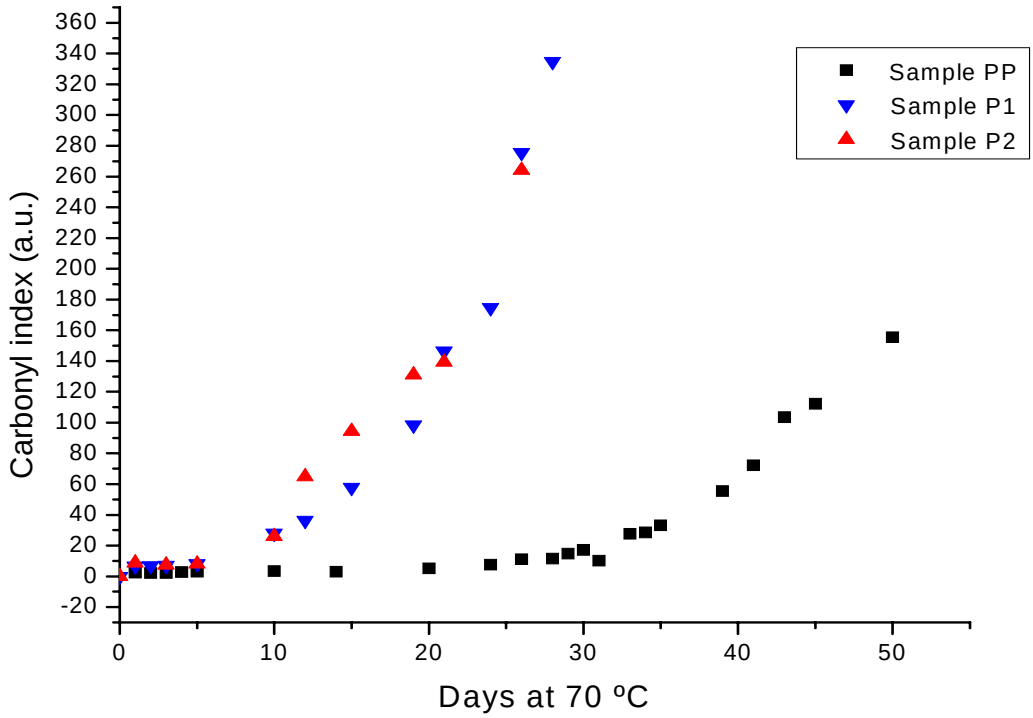

Figure 12: Increase in the carbonyl index with increase in the level of degradation at 70 ºC.

6.5.4.2 Degradation at 90 ºC

Typically, higher exposure temperatures will result in faster degradation of a semi-crystalline polymer. An alternative way of accelerating polymer degradation is by increasing the oxygen pressure during the degradation experiment [16]. This, however, results in the penetration of the oxygen into the deeper layers, altering the degradation profile typically obtained by normal oven aging.

The trends in the carbonyl indices obtained at 90 ºC (Figure 13) were similar to the results obtained at 70 ºC. The carbonyl index in sample P2 showed the fastest onset at around 12 h of exposure at 90 ºC (shortest induction period). This was followed by sample P1, which showed an increase in the carbonyl index after 24 h. The degradation process was significantly faster than at 70 ºC. These results were similar to the trends obtained at 70 ºC; the two copolymer samples degraded significantly faster than the homopolymer sample.

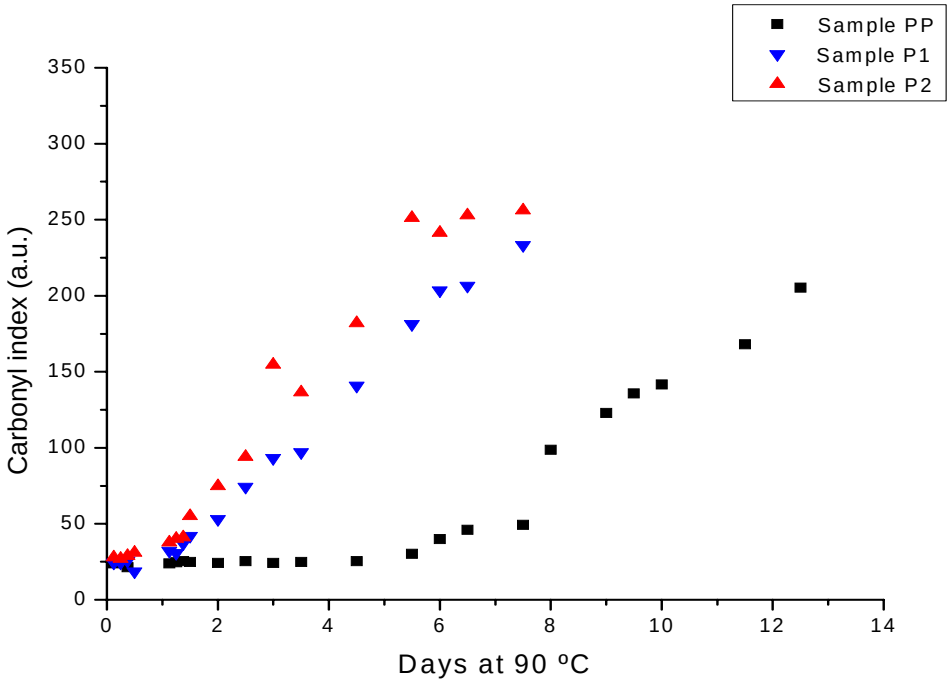

Figure 13: Increase in the carbonyl index with increase in the level of degradation at 90 ºC.

6.5.5 Changes in the relative pentene contents of samples P1 and P2

In Figure 14 it is evident that the relative pentene level decreased with an increase in the degradation level in both pentene copolymer samples. It would appear as if the pentene level only starts decreasing after an induction period, therefore trendlines were not fitted to the data. This decrease in pentene content during degradation could possibly be due to one of the following:

1. A loss of pentene from the pentene copolymer sample during degradation.
2. A rearrangement of the pentene units upon degradation.

Marshall [7] suggested that, in theory, the pentene comonomer should be no less stable than the tertiary carbon atom in a polypropylene chain (same number of tertiary carbons in the main chain). There are, however, two factors that may activate the branching position towards oxidative attack:

1. The higher inductive effect of a propyl side branch compared to a methyl side branch in polypropylene homopolymer. The inductive effect will stabilise the formation of a radical.

2. The incorporation of pentene will result in a lower crystallinity (density) and will, therefore, promote oxygen permeability into the polymer matrix compared to the polypropylene homopolymer.

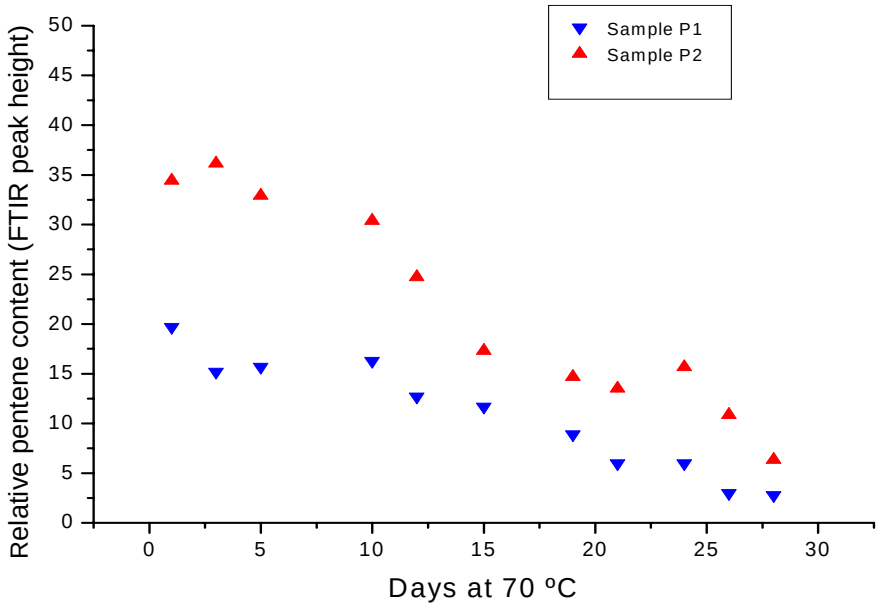

Figure 14: The decrease in relative pentene content (determined by FTIR) with degradation at 70 ºC in samples P1 and P2.

The relative pentene content of the two copolymer samples, degraded at 90 ºC, is plotted in Figure 15. Again it appears as if the pentene content only starts decreasing after an induction period. The pentene contents in both copolymer samples decreased linearly after this induction period. These results are also in agreement with the results obtained at 70 ºC.

6.5.6 Changes in the hydroperoxide content of the samples with increased degradation

FTIR can be used to quantify the hydroperoxide degradation products in polyethylene [27] and polypropylene samples [28]. An alternative technique for the detection of hydroperoxides is iodometry [29, 30]. In iodometry, the hydroperoxide reacts with iodine. Acetic acid is used as a catalyst. Peracids will, however, also be detected by iodometry [30].

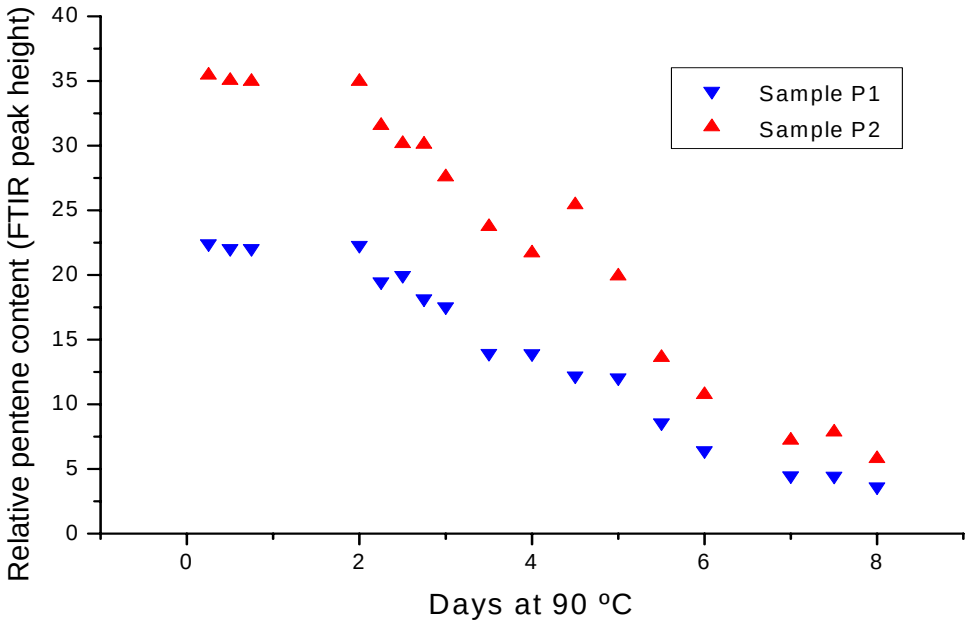

Figure 15: Decrease in the pentene content of samples P1 and P2 during degradation at 90 ºC.

Hydroperoxides are generally stable at room temperature, but will decompose rapidly at elevated temperatures [31]. The decomposition of these peroxides can be followed quite accurately by the chemiluminescence (weak energy) emitted from degraded samples [32]. Konar and Ghosh [27] monitored the formation of free hydroperoxides at 3600 cm^{-1}, and the hydrogen-bonded hydroperoxides at 3360 cm^{-1}. Several other authors, however, monitored the free and associated hydroperoxides in polyethylene at 3550 cm^{-1} and 3410 cm^{-1} respectively. The concentration of the associated hydroperoxides, formed during the thermo-oxidative degradation at 70 ºC, was monitored as a function of degradation time (Figure 16).

The concentration of the hydroperoxides was monitored by the FTIR absorption band at 3410 cm^{-1}, using a baseline between 3391 cm^{-1} and 3494 cm^{-1} (Figure 16). The hydroperoxide concentration in all three samples increased after an induction period, and it was evident that the hydroperoxide concentration in the P1 and P2 samples increased at similar rates. Similar to the carbonyl index increase, the intensity of the hydroperoxide group increased significantly faster for the two pentene copolymer samples than in the polypropylene homopolymer sample. No detectable increase was found in the free hydroperoxides. It was evident that the hydroperoxides increase in concentration before any increase in carbonyls is discernible.

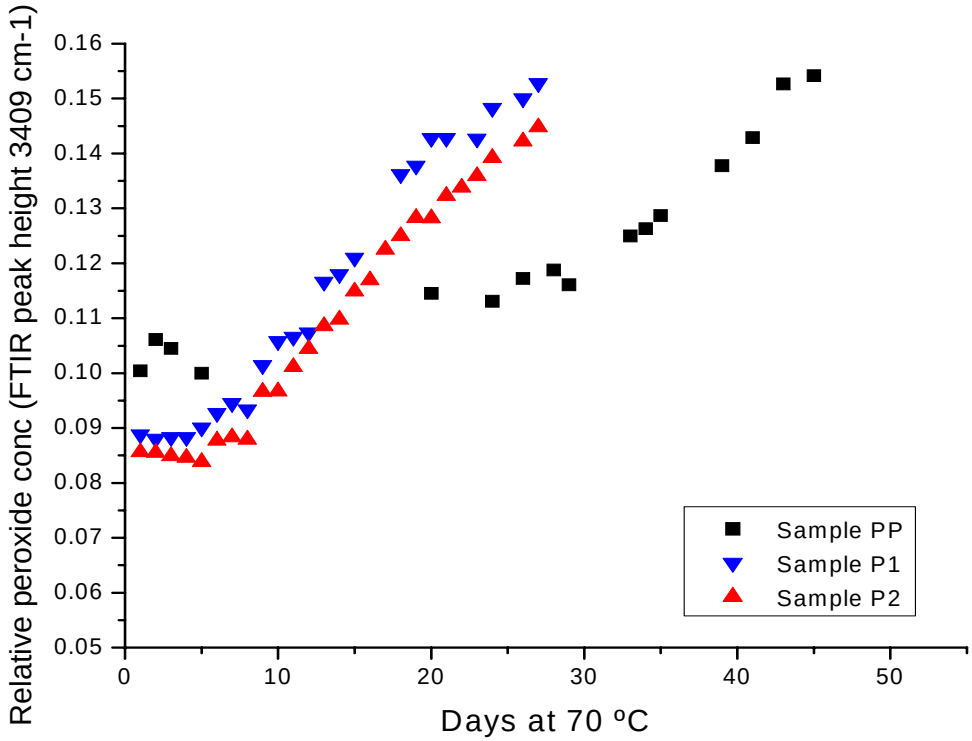

Figure 16: Increase in the associated hydroperoxides with an increase in the exposure at 70 ºC.

6.5.7 Change in the crystallinity of the samples during degradation at 70 ºC

There are several analytical techniques that can be employed for studying the crystallinity of a polymeric sample. Wide angle X-ray scattering (WAXS), small angle X-ray scattering (SAXS) and X-ray diffraction are commonly used to study crystallinity in semi-crystalline polymers. Density measurements, DSC and FTIR are also used as an estimation of the crystallinity in polyethylene and polypropylene. In this chapter FTIR (ATR) and DSC (melt enthalpy) were used to study crystallinity changes during degradation. DSC is also commonly used to study the performance of stabilised samples.

In polyethylene, the ratio of the infrared peaks at 720 cm^{-1} and 730 cm^{-1} is used to determine the relative crystallinity of a sample [33]. The peak at 730 cm^{-1} is due to the CH_2 groups in the crystalline phase, while the peak at 720 cm^{-1} is due to the CH_2 groups in the amorphous phase, with a small contribution of the crystalline phase. In polypropylene, the ratio of the peaks at 973 cm^{-1} and 997 cm^{-1} can be used to determine the relative crystallinity of a sample. The surface crystallinity of the degraded samples was evaluated by ATR (attenuated

total reflectance) FTIR. The ratio of the 997 cm^{-1} to the 973 cm^{-1} absorption band was used as an indication of the change in surface crystallinity during degradation.

Figure 17 shows the increase in crystallinity in samples PP, P1 and P2 during degradation. The initial crystallinity of sample P1 was higher than sample P2, while sample PP had the highest initial density. Gulmine et al. [22] found an increase in apparent density during the degradation of polyethylene. This was attributed to increases in crystallinity and crosslinking reactions, leading to an increase in density. In polypropylene, the crosslinking reaction is not expected to be significant. However, ß-scission will result in shorter chains that could re-organise easily and, therefore, will result in an increase in crystallinity and thus in density. It was also found that the lower the initial crystallinity, the higher the increase in crystallinity.

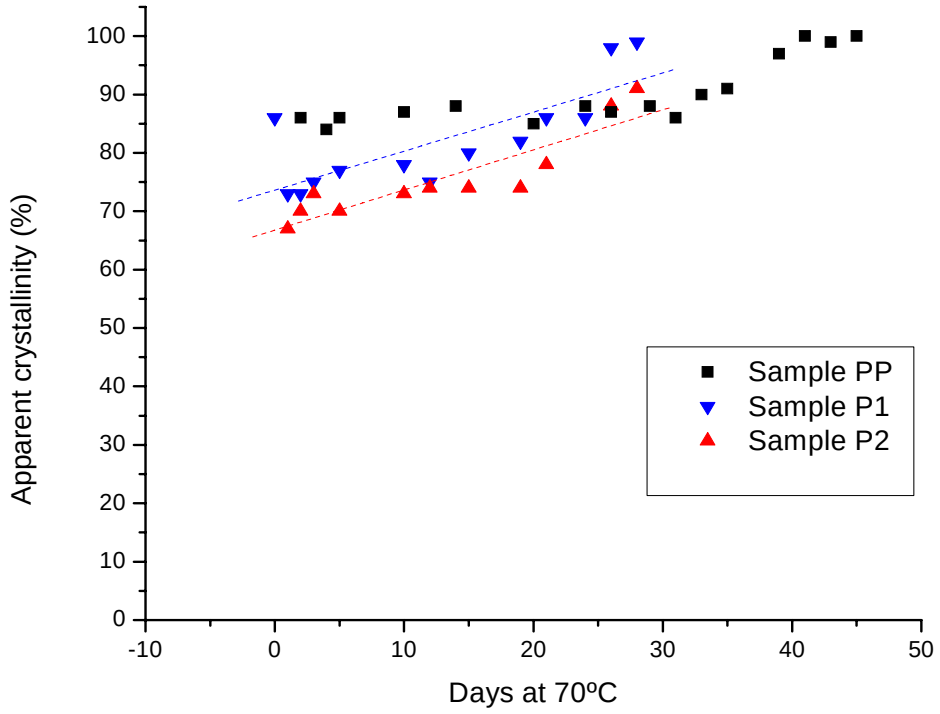

Figure 17: Increase in the apparent crystallinity of the two propylene-1-pentene samples during degradation.

In a propylene-1-pentene copolymer sample with a low pentene content, the macromolecular chain length and the pentene content are both factors that could influence the polymer morphology and, thus, melting and crystallisation properties. From the theory of Flory, the propylene units may be considered as crystallisable units. The pentene comonomer will result in a disruption in this structure and will be excluded from the polypropylene crystal lattice. This can be explained in theoretical terms using Flory's theory (see Section 4.2.2).

According to the theory, there are two possible species that could result in low melting point material: highly branched material (high comonomer content or branching) and very low molar mass material.

The crystallinity of a polypropylene sample can be defined as the ratio of the experimentally measured enthalpy of fusion (ΔH_f) to the enthalpy of fusion of a theoretical 100% crystalline sample of the same polymer (ΔH_f^0).

$$\textit{Crystallinity}\ (\%) = (\Delta H_f)/\ (\Delta H_f^0)\ x100\% \qquad (6.5)$$

These calculations were performed automatically by the Mettler software, using a ΔH_f^0 value of 209 joule/g for pure polypropylene [35]. The initial crystallinity of the homopolymer sample was the highest (51.59%), followed by P1 (44,5%) and P2 (40,76%) (lowest). This is in line with the Flory-Huggins theory, that indicates that addition of a comonomer will disrupt the crystalline structure and lead to a decrease in crystallinity [36]. DSC analysis showed an increase in the crystallinity of the pentene-containing samples during degradation. Secondly, degradation will preferentially attack the amorphous phase, leading to a destruction of the tie molecules. Both these effects will result in a decrease in the mechanical properties of the polymer, resulting in the polymer being more brittle. The two copolymer samples showed a sharper increase in crystallinity during degradation compared with the homopolymer sample (Figure 18). The homopolymer showed virtually no increase in crystallinity. This could possibly be related to the lower amorphous fraction present in the homopolymer, resulting in a lower amount of material that could participate in chemi-crystallisation. Looking at Figures 17 and 18, one can see that the trends observed by FTIR (Figure 17) and DSC (Figure 18) for the two copolymer samples are very similar.

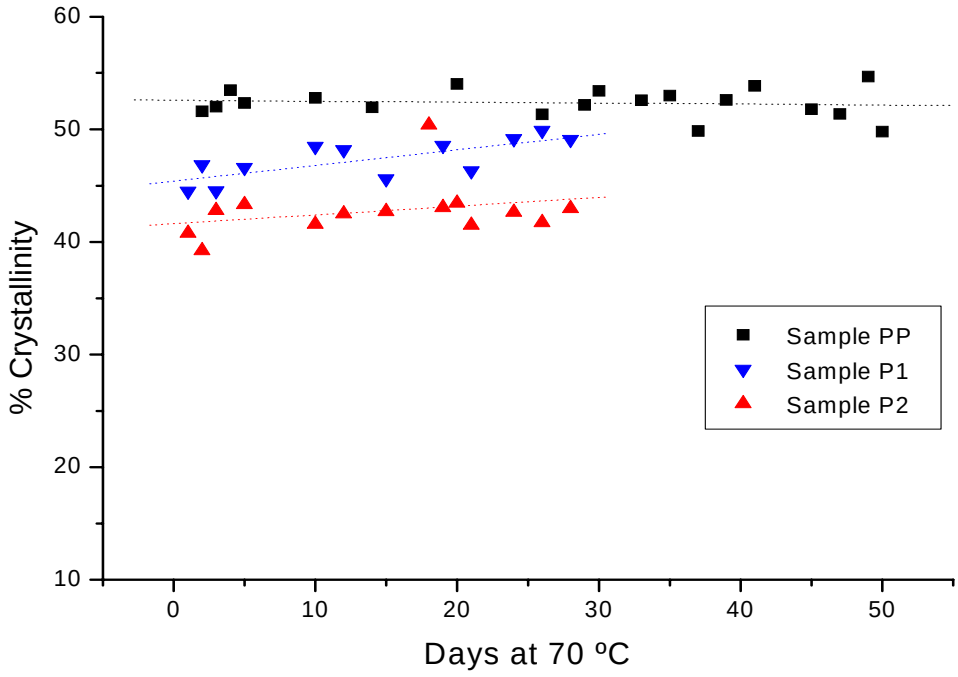

Figure 18: Changes in the crystallinity (DSC) during degradation at 70ºC with slight increases in the crystallinity of the two copolymer samples.

Thermal properties of a polymer sample depend on the molecular size and the chemical composition. In the previous sections it was shown that thermo-oxidation resulted in a decrease in the molar mass and an increase in the carbonyl and the hydroperoxide concentrations. These modifications to the molecular structure could have a significant effect on the polymer crystallisation and melting properties. Some authors detected a decrease in the crystallinity of semi-crystalline polymers. Others, however, found an increase in the polymer crystallinity with degradation. This was thought to be due to the scission of chains in the amorphous phase and the subsequent increase in the mobility of chains previously involved in chain entanglements and tie molecules [37]. Degradation may, however, also take place at the lamella fold surface [38]. Free chains and chain segments can then rearrange in a crystalline phase. This effect is known as chemi-crystallisation. Chemi-crystallisation will ultimately result in the formation of surface cracks, which will lead to a reduction in the polymer‘s mechanical properties.

Rabello and White [37, 39] studied the crystallinity in photo-oxidised samples by using both X-ray diffraction and DSC analysis. The X-ray diffraction studies indicated that during the photo-degradation process, no change was detected in the shape or the position of peaks in the X-ray diffractogram. A reduction was however detected in the intensity of the amorphous

phase, indicating an increase in the polymer crystallinity. DSC melting studies confirmed this increase in the crystallinity with increasing levels of degradation.

Rabello and White [37, 39] and Elvira et al. [40] both found a reduction in the melting point and a linear reduction in the crystallisation temperature with an increase in the degradation time.

Elvira et al. [40] found that, in the degraded samples, metastable crystals are present. From this it can be concluded that the degradation process results in the formation of unstable crystals with a lower T_m at the expense of the higher T_m crystals with, as a result, a drop in the melting temperature. Similar results were found in this study, with decreases in the melting points of the homopolymer and copolymer samples (Figure 20).

6.5.8 Mechanism of chemi-crystallisation during degradation

The mechanism of chemi-crystallisation in degraded samples has been extensively reviewed by Rabello and White [37]. When a non-degraded semi-crystalline polymer crystallises from the melt, a considerable number of entanglements will form. The polymer will also contain a considerable number of tie molecules, linking separate crystalline regions together. These entanglements and tie molecules will, however, be excluded from the crystalline phase. Under degradation, which will predominantly take place in the amorphous phase, the chain scissions will result in an increase in the mobility of these chains by scissioning into segments with higher mobility (not constrained by entanglements and tie molecules). This will result in an increase in the % crystallinitiy in a degraded sample. Opposing this process, however, is the formation of functional groups like carbonyls and hydroperoxides, which could theoretically result in a reduction in the crystallinity by decreasing the molecular order (increase in chemical heterogeneity). The formation of the functional groups is thought to be responsible for a broadening in the melting curve.

Three possible mechanisms were suggested for this increase in crystallinity:

1. The incorporation of the released segments into existing crystals.
2. The formation of new crystals by the free segments.
3. The loss of volatile products from the amorphous phase resulting in an increase in crystallinity.

The third mechanism is not considered to be likely, while the first mechanism may be more likely. This is due to the known capability of polypropylene to self-nucleate. The interphase between totally crystalline material (spherulites) and the totally random molecules (true amorphous phase) is considered to be important in this increase in crystallinity with degradation. This interphase has been shown to constitute approximately 12-30% of the polymer. Theoretically, if scissions occur within or close to the crystalline phase, it will be easier to incorporate into existing structures, compared to the increase in crystallinity by scission in the middle of the amorphous phase.

This was attributed to the lower molar mass and the chemical irregularities in the polymer chain. Shorter chains crystallise faster but at lower T_c. They have a lower T_m and higher crystallinity. In Figure 19 the slight decrease in DSC crystallisation temperature with degradation of all three samples can be seen.

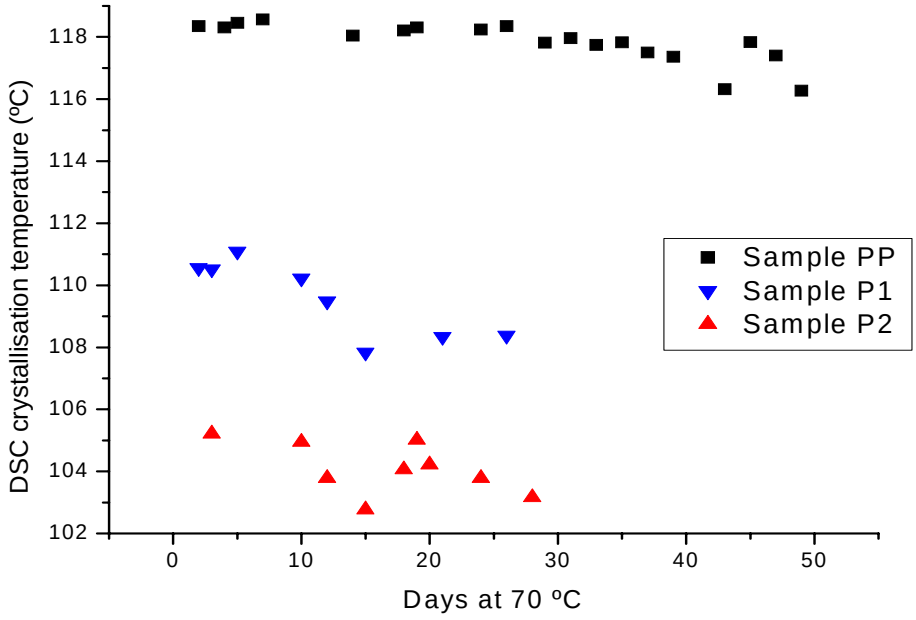

Figure 19: Decrease in DSC crystallisation temperature with an increase in level of degradation at 70 ºC for all three polypropylene samples (PP, P1 and P2).

Looking at the DSC crystallisation curves of sample P1 (Figure 20), this decrease in the crystalllisation temperature with increasing level of degradation. The shape of the melting curves is similar. Generally, slight increases were found in the crystallinity (as determined by the DSC crystallisation runs).

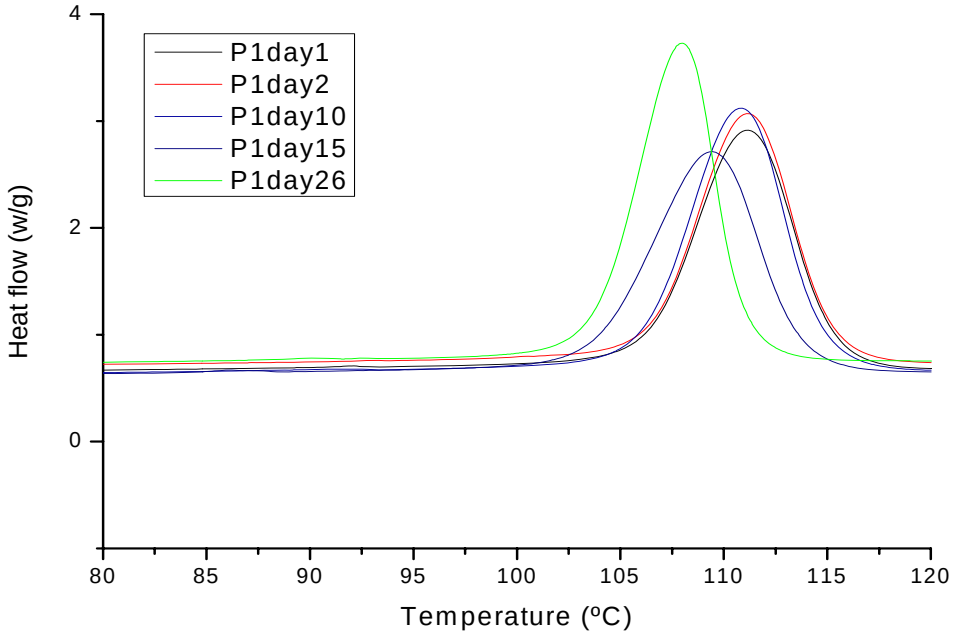

Figure 20: DSC crystallisation corves of sample P1 showing a decrease in the crystallisation temperatures.

The melting curve of sample P2 was relatively broad (Figure 21), indicating a wide distribution of lamellae thicknesses. At 10 days of degradation the melting peak split into two peaks, one higher than the original melting peak and one lower. The peak at higher temperatures increased in intensity with continuing exposure. The peak melting temperature of the main melting peak, however, showed a significant decrease. In the P1 sample this peak splitting occurred later, at around 15 days. The homopolymer did not show double peaks during the period of degradation. According to Rabello and White [37], this double peaking phenomenon could be due to two possible reasons:

1. The melting of crystals of different melting points.
2. Re-crystallisation or re-organisation during melting.

Experiments performed by Rabello and White [37] suggest that the double peaks are due to the recrystallisation or re-organising taking place during melting. According to this theory, the degraded material forms relatively unstable crystals during cooling. During subsequent melting, the material first melts, recrystallises into a more stable phase and then melts again.

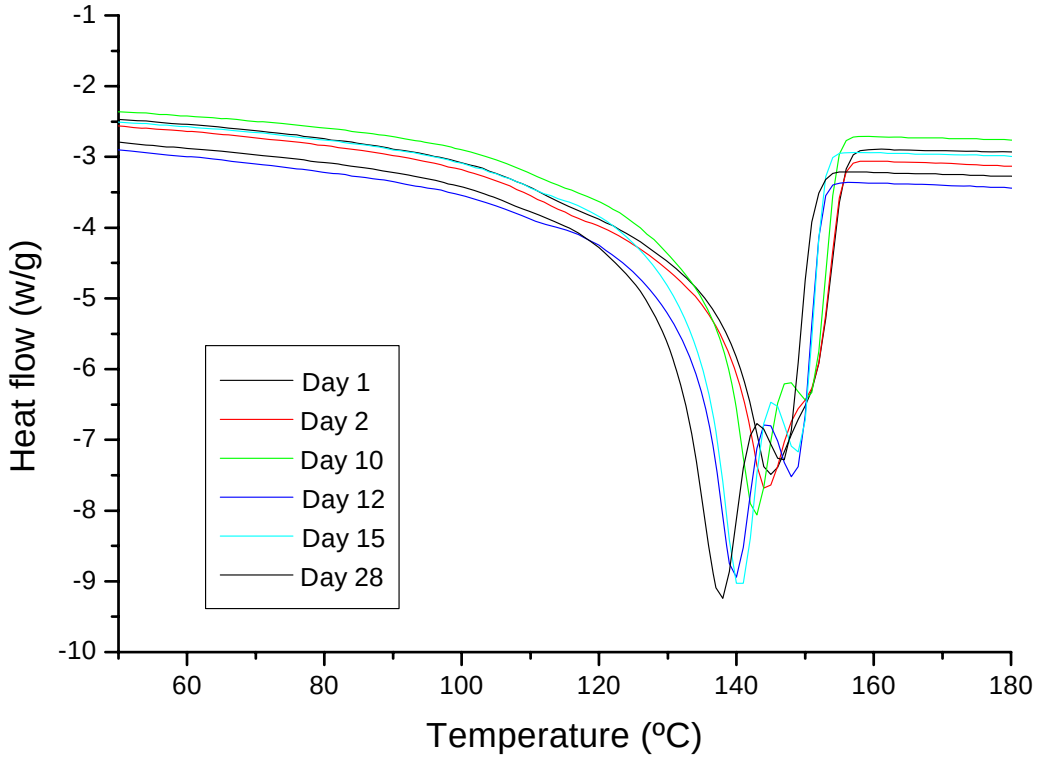

Figure 21: Melting curve for P2 at different exposure times showing a broadening in the crystallisation curves and a decrease in melting temperatures.

They also detected a decrease in the DSC crystallisation temperature during cooling. In general, a decrease in crystallisation temperature could be due to the incorporation of a comonomer, a change in tacticity or the incorporation of impurities (functional groups) in a polymer. In this case, it is possible that the formation of functional groups during degradation may be responsible for a decrease in the crystallisation temperature. They initially detected an increase in the crystallinity as a result of decreasing molecular size, followed by a decrease in crystallinity at higher degradation levels.

6.6 Analysis of the degraded samples by chemical composition analysis and fractionation techniques

The degradation experiments, performed at 70 ºC and 90 ºC, respectively, indicated similar trends for the SEC data (faster reduction in molar mass for the two pentene-containing samples) and FTIR data (faster increase in carbonyl indices of the two pentene samples compared to the homopolymer sample). Therefore, although fractionation and chemical composition distribution experiments were performed at both 70 ºC and 90 ºC, only the

fractionation data and chemical composition data, generated at 70 ºC, will be discussed in the next sections.

6.6.1 CRYSTAF analysis of the degraded samples (degraded at 70 ºC)

In the previous chapters and several articles [41-44] it has been shown that CRYSTAF provides useful information on the chemical composition distribution in polyolefins. From the CRYSTAF crystallisation curve, information can be obtained regarding the compositional heterogeneity of a sample [44]. The chemical compositional heterogeneity is related directly to the distribution of crystallising units. In the previous chapter it was concluded that CRYSTAF is sensitive to polymer degradation, with a decrease in the crystallisation temperature, an increase in the soluble fraction and a widening of the crystallisation curve. Monitoring of these three parameters was performed on all three samples. In Figure 22 the effect of degradation of sample P1 on the CRYSTAF crystallisation curves can be seen.

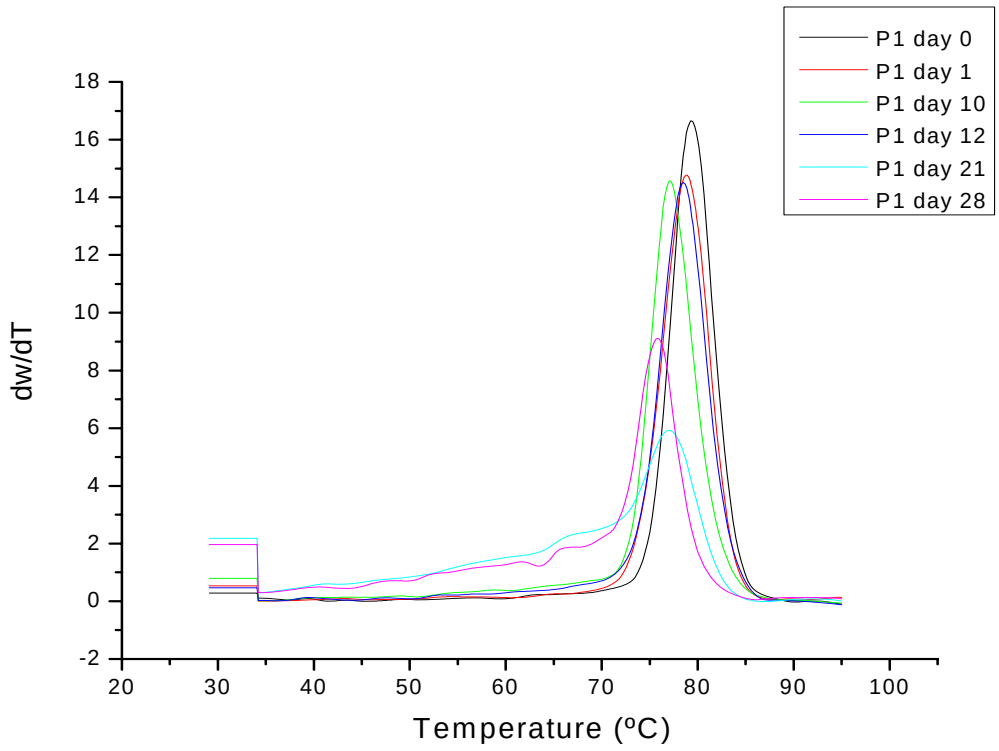

Figure 22: Influence of degradation on the crystallisability of sample P1 in the CRYSTAF with a broadening of the crystallisation curve and an increase in the soluble fraction.

During degradation of P1, there was a significant increase in the soluble fraction of the sample. The maximum intensity of the crystallisation curve decreased and there was a

broadening of the crystallisation curve, as discussed in the previous chapter. The CRYSTAF curves of sample P2 after different degradation periods were also overlaid and a similar trend was evident (Figure 23). There was, however, a significant difference between the soluble fractions of sample P1 and P2; sample P2 generally showed higher soluble fractions with degradation.

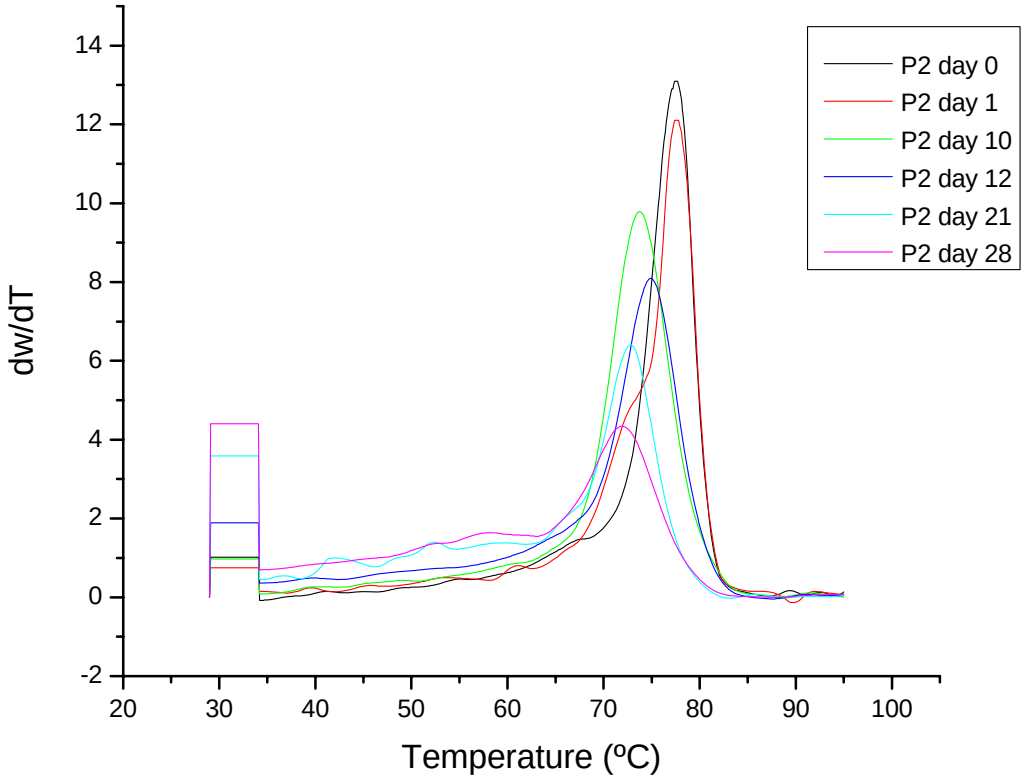

Figure 23: Influence of degradation on the crystallisability of sample P2 in the CRYSTAF.

The homopolymer sample showed a smaller increase in the soluble fraction compared to the two copolymer samples, although there was a significant decrease in the crystallisation temperature with degradation (Figure 24). The lower soluble fraction in the homopolymer, formed during the degradation process, is due to the higher crystallinity of the homopolymer (and consequently, smaller amorphous phase). As oxygen is excluded from the crystalline regions, the amorphous fraction and lower crystallinity material will preferentially degrade. This fraction was smaller in the homopolymer than the propylene-1-pentene copolymers, therefore resulting in a smaller fraction that will degrade.

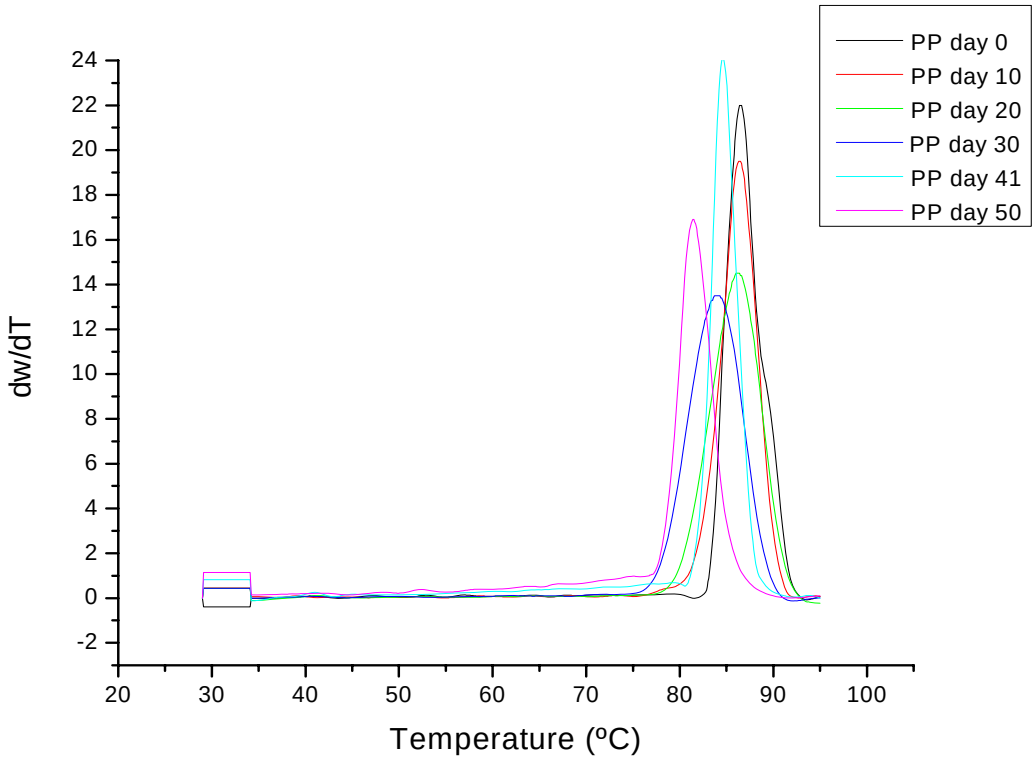

Figure 24: Influence of degradation on the crystallisability of the homopolymer sample (PP) in the CRYSTAF.

The CRYSTAF crystallisation curves of samples PP, P1 and P2 were compared after 28 days (30 days for the homopolymer) of degradation (Figure 25). Although the molar mass averages of the two copolymer samples decreased at similar rates, there was a significant difference in the CRYSTAF behaviour at similar degradation times. The soluble fraction of P2 was higher, the crystallisation temperature was lower and the curve was less sharp than the P1 curve. The homopolymer showed no change after 30 days.

The soluble fraction of P2 increased the fastest and from an initial soluble fraction of 3,7% increased to 22%. The soluble fraction in the P1 sample increased from 2,7 to 13%, while the homopolymer soluble fraction increased from 1.1% to 5,7%. From this it was evident that the degradation processes are different in the three polymer samples, with the degradation in P2 resulting in more material that cannot crystallise out of solution at this temperature (Figure 26). It is however possible, using a better cooling system (cryogenic cooling) and a different solvent (lower freezing point) that more material could precipitate out of solution. Correlating the soluble fraction with the carbonyl index results showed that P2 had the highest carbonyl

index at a given time, and this will, therefore, result in chains with relatively higher carbonyl content.

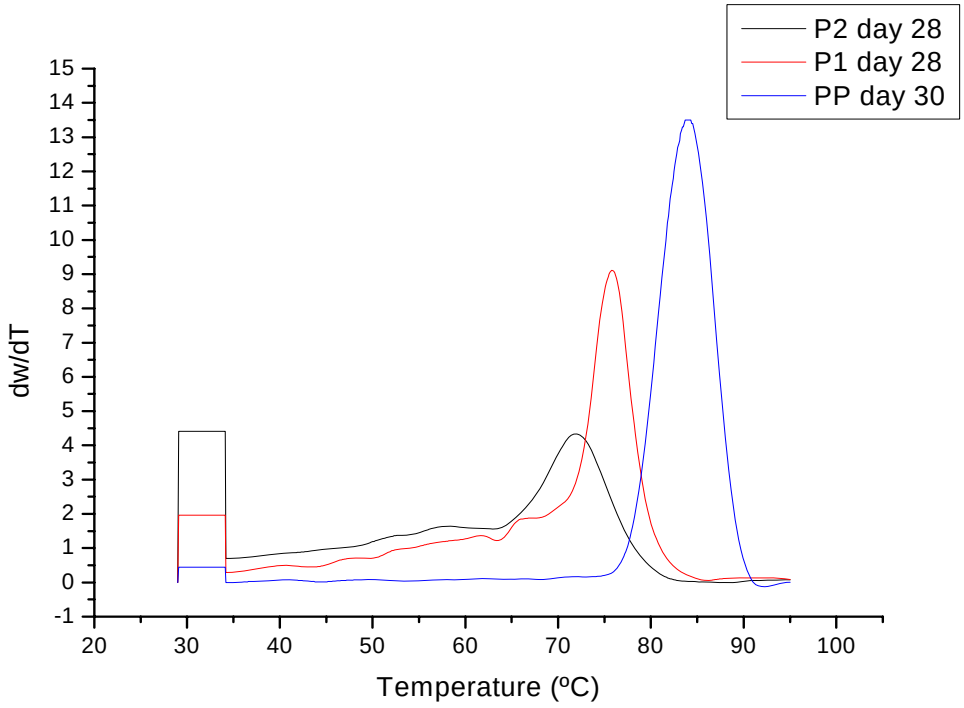

Figure 25: Differences between the CRYSTAF behaviour of PP, P1 and P2 after 28 days at 70 ºC.

The lower crystallinity of the pentene copolymer samples resulted in a higher fraction of the polymer being present in the amorphous fraction. From the relative pentene contents it was evident that the pentene group is preferentially attacked and, therefore, the P2 sample will be attacked to a more significant extent. This will result in a higher amount of oxygen containing groups, increasing the amount of material in the soluble fraction.

The change in the CRYSTAF crystallisation temperature was also monitored as a function of degradation. From Figure 27 it is evident that the rate of decrease in the crystallisation temperature of P2 is steeper than of P1 and the homopolymer. The degradation process and the incorporation of the carbonyl functionality will, therefore, influence the temperature at which the polymer will crystallise out of solution.

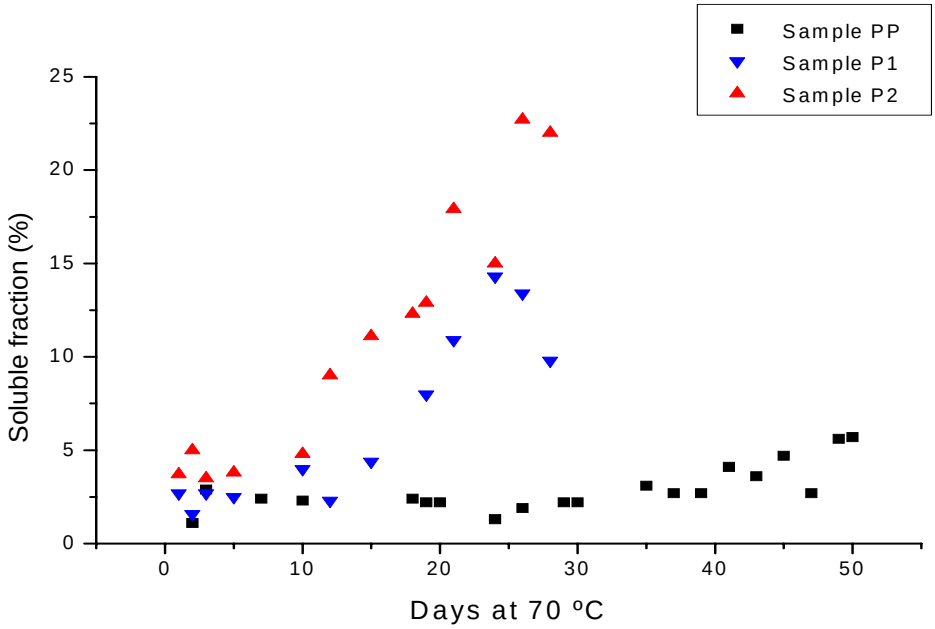

Figure 26: Effect of degradation on the soluble fraction of PP, P1 and P2 as detected by CRYSTAF.

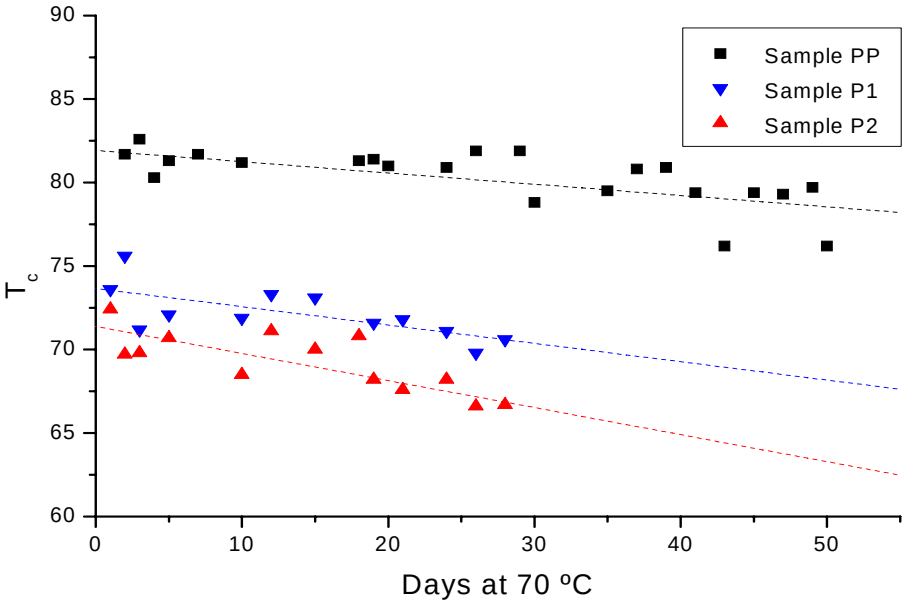

Figure 27: Decrease in the CRYSTAF crystallisation temperature with increased degradation in PP, P1 and P2.

The crystallisation temperatures, obtained by CRYSTAF, are approximately 36 ºC lower than in the DSC (for the PP homopolymer and copolymer samples). This is due to the influence of the diluent on the CRYSTAF experiment.

6.6.2 Comparison of the crystallinity results obtained by DSC, FTIR and CRYSTAF

The results obtained from DSC and FTIR indicate that there was an increase in the crystallinity of the polypropylene copolymer samples during degradation. The CRYSTAF results indicated, however, that the crystallisable fraction (crystallising above 30ºC in TCB) decreased during degradation. This may however be different in a system with a different solvent (for example O-DCB) and sub-ambient cooling. These seemingly conflicting results must be interpreted taking into account the fundamentals of the instruments. Classical techniques like XRD also showed the increase in crystallinity with degradation [37-39].

There are several fundamental differences between the DSC and CRYSTAF techniques. According to Sarzotti et al. [45], CRYSTAF can virtually be seen as a solution DSC experiment. Sarzotti et al. [45] found a very good correlation between CRYSTAF experiments and solution DSC experiments with several metallocene ethylene/1-hexene copolymers. Fundamentally, it is known that when a polymer is dissolved in a low molecular weight, non-crystallisable diluent, the melting and crystallisation temperatures will decrease. The magnitude of this decrease will be related to the concentration of the polymer in solution. The crystallisation temperature, obtained from CRYSTAF, will therefore be lower than the melting and crystallisation temperatures obtained from DSC. Due to several limitations, the concentration of the polymer used for CRYSTAF analysis must be within a narrow range. The concentration needed for solution DSC measurements are within a broader range, but typically much higher than in a CRYSTAF experiment.

As discussed earlier, the reason for an increase in DSC crystallinity during degradation is due to the scission of long entangled chains (including tie molecules) and the free ends being able to assume a low-energy crystalline form on the edges of crystals. The aging temperatures are well above the T_g (T_g of polypropylene is around 0 ºC) and so the molecules have sufficient energy to move as long as they are not sterically bound. At the elevated temperatures used for accelerated aging there is a certain amount of secondary crystallisation occurring even without degradation.

CRYSTAF measures temperature-dependent solubility, where the temperature dependence of the solubility is primarily determined by crystallinity. Although the shorter chains can crystallise more easily in bulk, in solution the crystallisation behaviour is influenced significantly by the carbonyl functionalities incorporated into the main polymer chain during degradation. These carbonyl functionalities will disturb the crystallisation and will result in

material that will be detected in the soluble fraction (confirmed by CRYSTAF results incorporating a carbonyl sensor).

Considering that the T_c (measured by CRYSTAF) is approximately 36-40 ºC lower than the T_c (measured by DSC), one would expect that a soluble fraction in the CRYSTAF (below 30 ºC) will correspond to DSC crystallisation occurring below 70 ºC. None of the polymers studied here had significant amounts of crystallisation in the DSC thermograms below 70 º C, but it may be that due to the different mechanisms of CRYSTAF and DSC, that some of the CRYSTAF soluble fractions may be crystallisable below 30 ºC should a lower analysis temperature be possible.

CRYSTAF analysis is, therefore, more sensitive to degradation than DSC and, therefore, more useful for studying the degradation process. The presence of oxygen-containing functionalised groups is the main reason for the decreased % crystallinity, but small chains (even if they do not contain functionalised groups) will also be more soluble, even if they are able to crystallise, at relatively lower temperatures.

Both techniques, however, showed a decrease in the crystallisation temperature of melting of the polypropylene samples, indicating that the degradation process results in incorporation of groups in the crystal that will decrease the melting and crystallisation temperatures.

6.6.3 SEC-FTIR analysis of the propylene-1-pentene copolymers and the degraded polypropylene samples

The analyses and techniques discussed so far focused on the analysis of bulk samples. The SEC curve and the FTIR spectra, for example, focused on the properties of a sample (usually a few milligrams) and could not distinguish between different fractions that may be present in the sample. In a degraded polyolefin sample there may, for example, be areas that are highly oxidised and areas that may be totally un-oxidised. In Chapter 5, fractionation techniques have been shown to provide more information on degraded samples. There are several techniques available that can provide more information on the chemical composition and chemical composition distribution in a polyolefin sample, including CRYSTAF, TREF and SEC-FTIR. SEC-FTIR was developed to provide information on the change in the chemical composition as a function of molar mass. Although this technique has been used for several polyolefin-related applications, it has not been used as an analytical tool for studying degradation of polyolefin samples. SEC-FTIR can be used to study the FTIR spectra of

fractions of a polyolefin sample and can subsequently provide information on the distribution of degradation products as a function of molar mass.

6.6.3.1 SEC-FTIR analysis of the undegraded polypropylene homopolymer and P2 sample

In Figure 28 the Gram-Schmidt curve for the undegraded polypropylene homopolymer is shown. The Gram-Schmidt plot obtained from the SEC-FTIR experiment is a sum over all absorptions corresponding to the concentration of the sample in the eluate [46].

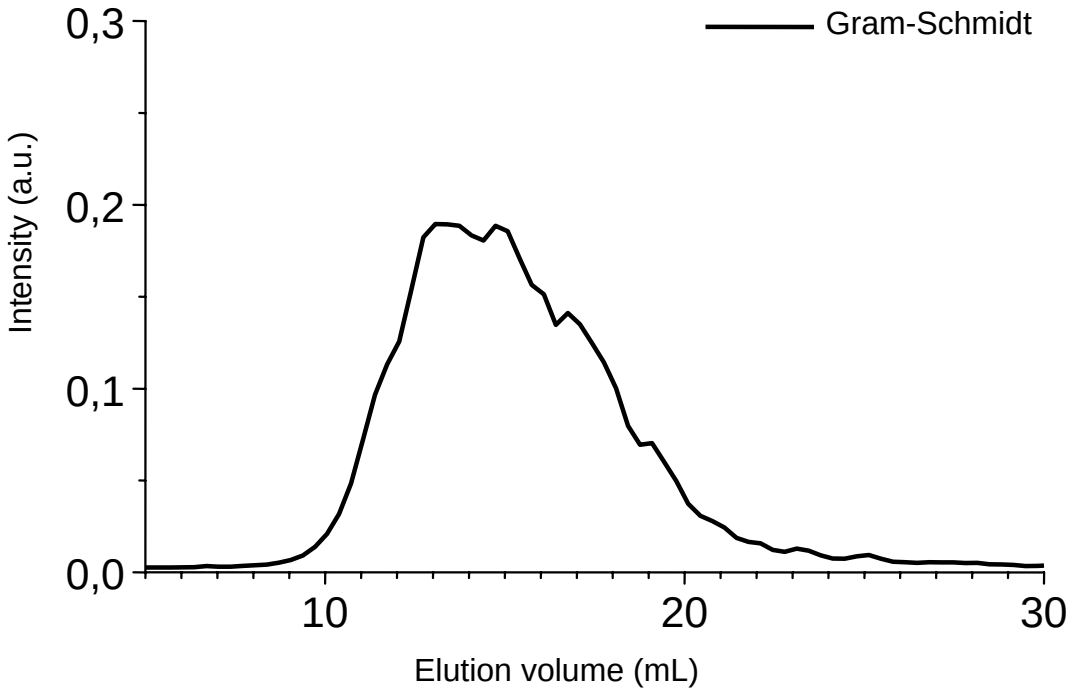

Figure 28: Gram-Schmidt curve of the undegraded polypropylene homopolymer sample.

Chemigrams can then be generated to investigate the intensity of a particular absorption along the elution volume axis. A chemigram was constructed for sample P2 to investigate the distribution of the pentene comonomer over the molar mass profile. The chemigram based on the CH_2-rocking vibration of the 1-pentene comonomer at 737 cm^{-1} (Figure 29) revealed a higher pentene content in the low molar mass fractions, which is typical for Ziegler-Natta based materials.

The sample, therefore, contained a large number of long chains with low comonomer content. These chains are similar to polypropylene homopolymer. There was, however, a

small fraction containing a high amount of comonomer. Oxygen diffusibility will be higher through the highly-branched chains. The chains could also be more susceptible to degradation due to the presence of several propylene side branches which could stabilise the formation of stable radicals during degradation through a positive inductive effect. The high pentene in the short chains also suggests that most of the pentene is in the interlamellae and interspherulite boundary amorphous zones (least crystalline components have short length and most copolymer structure).

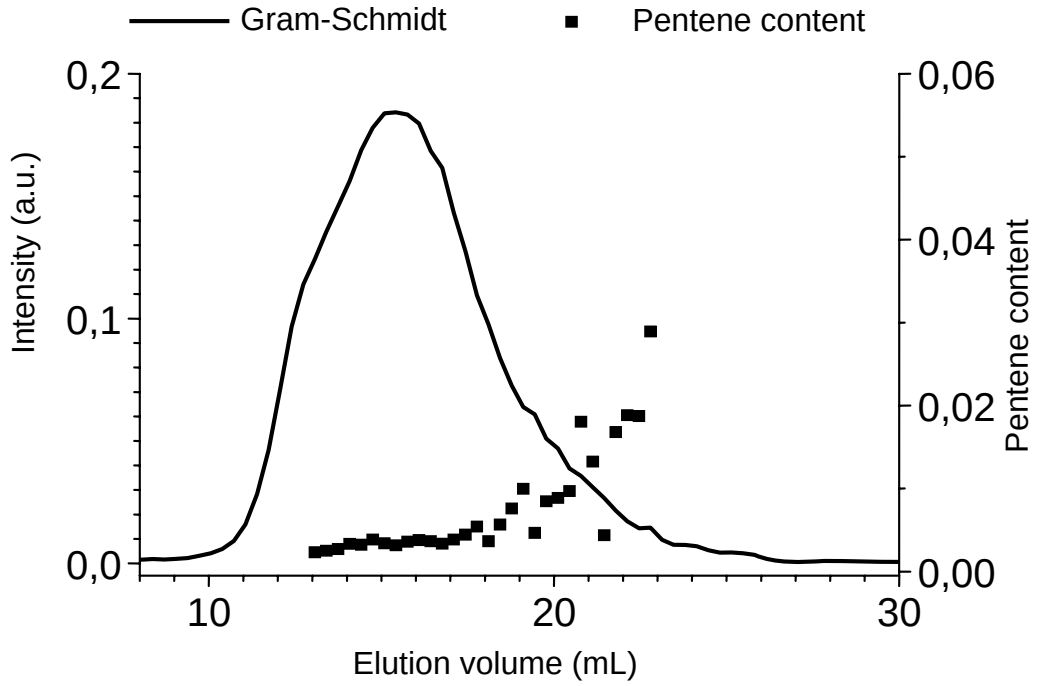

Figure 29: Distribution of the pentene content over the molar mass distribution for sample P2.

6.6.3.2 SEC-FTIR analysis of the degraded samples

In order to determine the concentration of the carbonyl groups, chemigrams were taken in the carbonyl region (1600-1800 cm^{-1}). For the overall CH-concentration, the chemigram based on the vibration around 1167 cm^{-1} was drawn. The ratio of these absorption bands (carbonyl/1167 cm^{-1}) then reflects the relative concentration of degraded species. Overlaying the ratio of these chemigrams with the Gram-Schmidt plot showed that for both samples the degraded fraction was mainly found in the low molar mass end while parts of the high molar mass end were virtually undegraded (Figure 30). The distribution of individual carbonyl species was also determined as a function of molar mass (Figure 31).

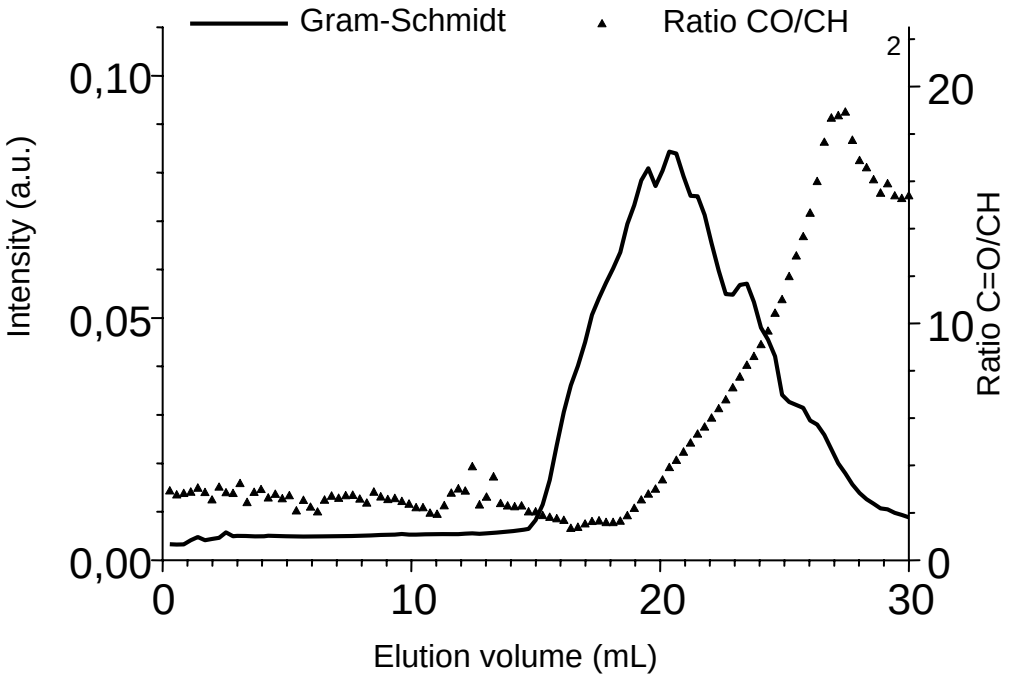

<u>Figure 30:</u> Distribution of the carbonyl index as a function of molar mass of sample P2 (day 28).

From Figure 31 it can be seen that the carbonyl index distribution has a steeper slope compared to the lactone concentration (determined at 1780 cm^{-1}). This was possibly due to the higher probability for ketone formation compared to the lactone formation. The ketones were present in the highest concentration in the degradation products and would, therefore, significantly influence the total carbonyl content. The pentene content was still predominantly present in the low molar mass fraction, while the carbonyl containing functionalities were also predominantly present in the low molar mass fraction.

A similar study was carried out for P1. For the degraded samples, the study on sample P1 yielded similar results for the carbonyl concentration as a function of molar mass (high concentration of the carbonyl species in the low molar mass region).

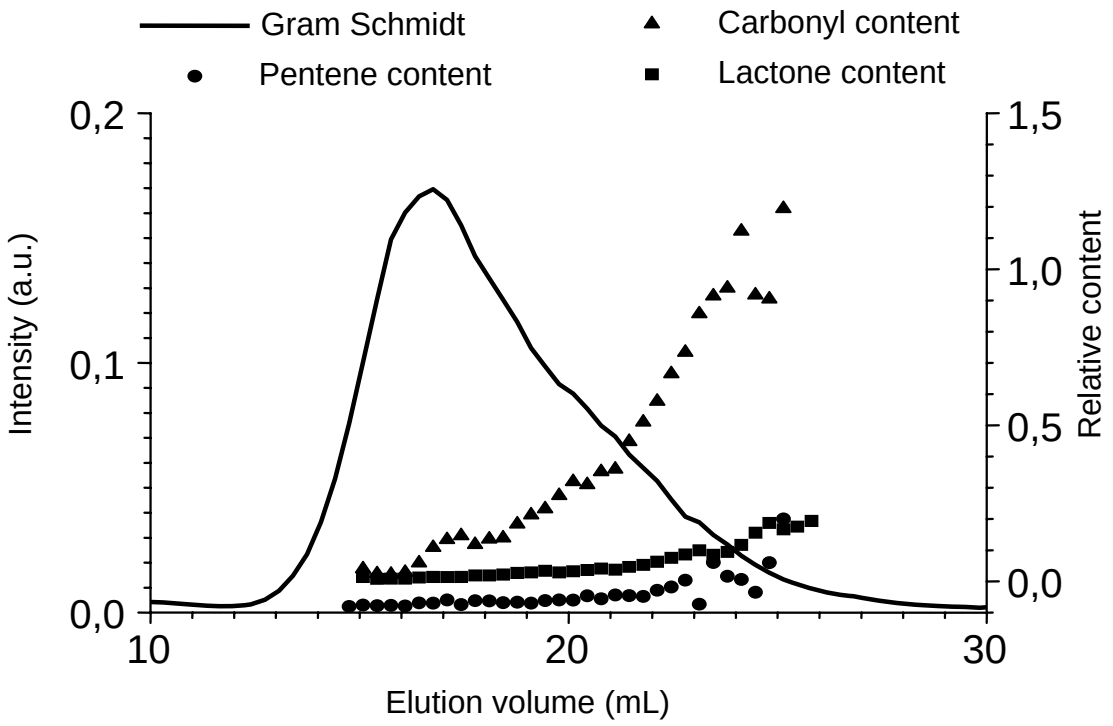

Figure 31: Increase in the lactone concentration of sample P2 due to degradation as a function of molar mass.

6.7 Comparison of the sensitivity of the various analytical techniques towards the detection of degradation in the samples

The sensitivity of the different techniques towards degradation is of importance. The results of the various analytical techniques are tabulated in Table 6. The initial stages of degradation are difficult to detect and, therefore, the sensitivities of the analytical techniques were compared using the analytical data for sample P1. The % change in a certain property from the initial value was calculated for the 70 ºC degradation data and then compared, to determine the relative sensitivity of the property towards the determination of degradation.

The change in molar masses was very sensitive to the degradation process. By day 3, in sample P1, there was already an approximately 13% decrease in the molar mass. At the same time the carbonyl index has increased significantly (by 8%). These findings are in line with the findings of Guisandez et al. [35], who also saw a decrease in the molar mass averages before an increase in the carbonyl index. They excluded the sensitivity of the FTIR spectrophotometer as the reason for this phenomenon, and attributed this to scission taking place before carbonyl formation occurs. The pentene content determination (determined by FTIR), T_c (determined by CRYSTAF) and polydispersity are less sensitive to degradation.

Similar trends were found for sample PP. The soluble fraction (measured by CRYSTAF) is, however, very sensitive to the degradation process. For sample P2, the soluble fraction increase was more sensitive than the molar mass decrease.

6.8 Studying the spatial heterogeneity of the degradation process

In Chapters 2 and 4 it was discussed that the degradation of a polyolefin sample is a heterogeneous process. This was mainly due to the presence of areas of higher crystallinity (crystalline areas) and areas of lower crystallinity (amorphous areas), with the crystalline areas suspended in the amorphous matrix. The first studies performed on the heterogeneous nature of polymer degradation were performed using SO_2 staining and microscopy. A more recent assessment of the heterogeneity of degradation around a catalyst particle was carried out using Raman spectroscopy [17]. An important factor that influences the degradation heterogeneity is the sample thickness. In a thick sample (100 microns or more), oxidation will be oxygen diffusion limited (rate of oxygen consumption is higher than rate of diffusion), resulting in highly degraded areas or layers close to the surface and less degraded areas towards the middle of the samples. A concentration gradient will, therefore, develop in a thick sample. This will result in depth-varying concentrations of oxidation products such as carbonyl species, hydroperoxides and double bonds. Shyichuk et al. [47] used a molecular weight distribution computer analysis (MWDCA) to determine chain scission and crosslink concentrations at a certain depth into a photodegraded polypropylene sample. In a thick sample, the inner parts of the polymer may be able to support surface cracks for a long time during the degradation process [16]. In polyethylene, samples may, for example, show both crosslinking and scission. In an irradiated sample, the surfaces were shown to predominantly degrade via scission, while the inner layers degraded via crosslinking [24].

For this study, plaques of 3-mm thickness were aged for 9 days at 90 ºC. The effect of sample heterogeneity on the degradation of propylene-1-pentene samples is of importance, as propylene-1-pentene copolymers are used in several thick-wall applications, where the surface may be exposed to degradation.

Table 6: Comparison of the sensitivity of the analytical techniques towards the detection of degradation (Sample P1)

Day	CO Index	% change	Relative pentene content	% change	Relative crystallinity	% change	T_c	% change	Soluble fraction	% change	M_n	% change	M_w	% change	PDI	% change
0	6.7	100.00	19.74	100.00	86	100	75.5	100	0.18	100	103,390	100.00	339,870	100.00	3.29	100.00
1	6.7	100.00	19.74	100.00	73	84.88	74.7	98.94	0.9	500	107,650	104.12	337,740	99.37	3.14	95.44
2	7	104.48	19.86	100.61	73	84.88	74.3	98.41	0.7	388.89	103,410	100.02	347,780	102.33	3.36	102.13
3	7.1	105.97	21.38	108.31	75	87.21	74.1	98.15	0.7	388.89	112,090	108.41	296,770	87.32	2.65	80.55
5	8.124	121.25	21.95	111.20	77	89.53	73.6	97.48	1.3	722.22	64,027	61.93	182,160	53.60	2.85	86.63
10	28.2	420.90	16.3	82.57	78	90.70	73.6	97.48	2.7	1500.00	33,69	32.08	80,530	23.69	2.43	73.86
12	36.4	543.28	14.12	71.53	75	87.21	74.2	98.28	2.8	1555.56	30,274	29.28	85,500	25.16	2.82	85.71
15	57.8	862.69	11.64	58.97	80	93.02	72.8	96.42	5.1	2833.33	17,555	16.98	48,958	14.40	2.79	84.80
19	98.4	1468.66	8.4	42.55	82	95.35	73.3	97.09	6	3333.33	17,863	17.28	44,289	13.03	2.48	75.38
21	146.6	2188.06	5.91	29.94	86	100	72.8	96.42	8.5	4722.22	16,633	16.09	41,414	12.19	2.49	75.68
24	174.8	2608.96	5.74	29.08	86	100	71.5	94.70	11.5	6388.89	12,871	12.45	33,660	9.90	2.62	79.64
26	275.7	4114.93	3.72	18.84	98	113.95	71.9	95.23	9.9	5500.00	10,984	10.62	26,825	7.89	2.44	74.16
28	334.9	4998.51	3.18	16.11	99	115.12	71.6	94.83	11.4	6333.33	11,727	11.34	29,903	8.80	2.55	77.51

CO Index: Determined as the area of the carbonyl group divided by the 1167 cm^{-1} reference peak

Relative pentene content: Defined as the peak height at 737 cm^{-1} divided by the 1167 cm^{-1} reference peak

Relative crystallinity: calculated as the peak height at 997 cm^{-1} divided by the peak height at 973 cm^{-1}

T_c is the CRYSTAF crystallisation temperature

Soluble fraction is the integrated area in the CRYSTAF curve of the hydrocarbons left in solution at 30 ºC

M_n is the number average molar mass as determined by SEC

M_w is the weight average molar mass as determined by SEC

PDI is the polydispersity index as determined by SEC (M_W/M_n)

This will provide information on the distribution of degradation products through a thick compression-moulded article.

As discussed in Chapter 2, there are several techniques for studying the degradation profile in thick degraded samples. These include FTIR analysis of microtomed fractions [24, 47, 48], as well as FTIR microscopy, ATR and photoacoustic spectroscopy [49] analyses of degraded samples. Papet et al. [24] performed DSC analyses on the microtomed layers and found a significant decrease in the melting points of degraded fractions. The homopolymer sample was also degraded as a reference for the CRYSTAF analyses. The degradation profile in the two pentene-propylene copolymers was studied by abrading layers from the samples. Abrasion depths of 0.05 cm were used for this study. In Figure 32 the degradation profiles of the two samples can be seen. From the carbonyl index values it can be concluded that the highest level of degradation is close to the surfaces of the samples. The carbonyl index decreases towards the inside of the samples and it can be seen that this decrease is quite rapid. The inside of the samples are, therefore, virtually undegraded (degradation limited by oxygen availability).

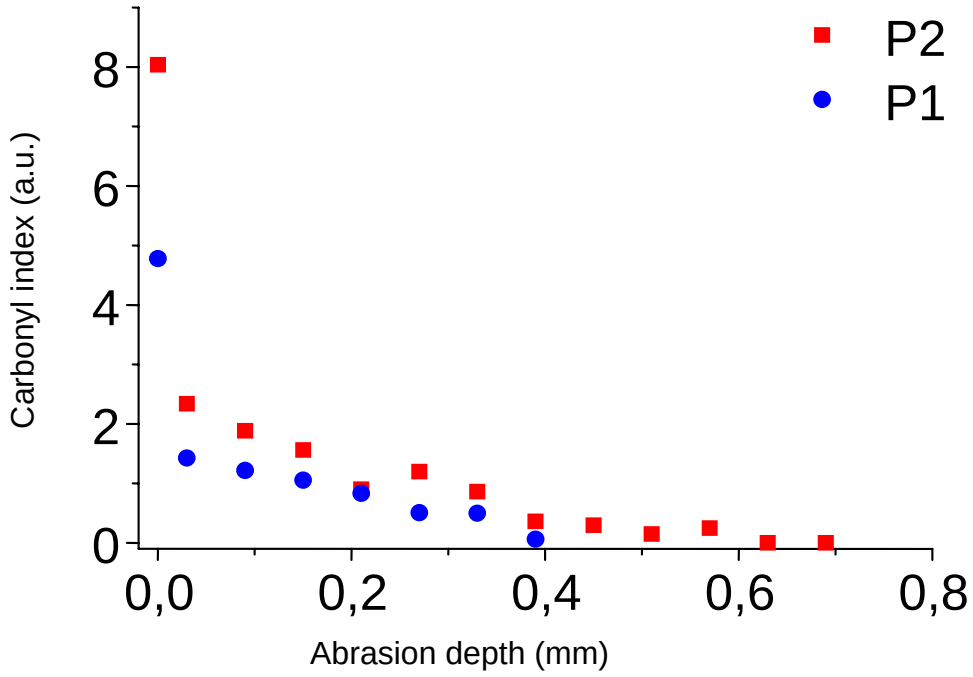

Figure 32: Carbonyl index determined at different abrasion depths, showing a higher carbonyl index close to the surface.

For samples P1 and P2, the weight average molar masses of the different layers were also determined (Figure 33). The molar mass determined on a fraction close to the surface

showed a significant decrease compared to the sample taken at 1 mm into the degraded sample. Although the FTIR result indicated the formation of carbonyl groups to be virtually at 0 at 0,4 mm into the sample, the molar mass determinations showed that even at 0,7 mm into the sample, the weight average molar mass was still lower than the original value. This is due to the relatively higher sensitivity of molar mass determinations towards the degradation process as well as scission taking place before carbonyl formation occur. Therefore, there are areas where the molar mass has decreased significantly without the formation of measurable carbonyl functionalities.

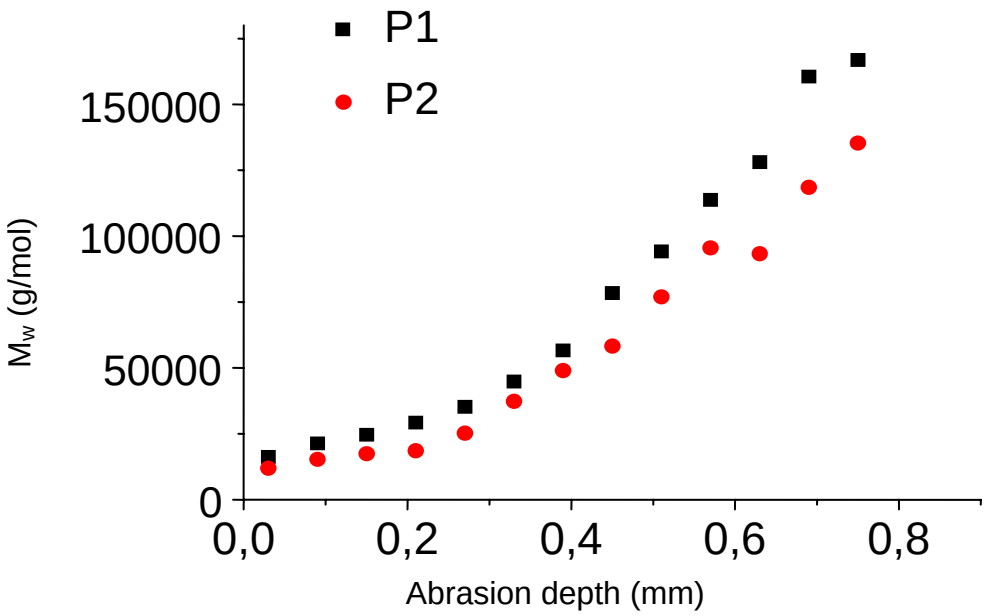

Figure 33: Weight average molar mass (M_w) values determined at different abrasion depths for sample P1 and P2

6.8.1 Comparison of the CRYSTAF crystallisation curves of the homopolymer and P2 at different depths into the samples

The CRYSTAF behaviour of the abraded layers of the homopolymer and P2, taken at 0.15 mm, 0.45 mm and 1.5 mm, was evaluated. The molar mass and carbonyl index values of these layers are given in Table 7.

Table 7: Molar mass and carbonyl index properties of the abrased layers of samples PP and P2

	PP		P2	
Abrasion depth (mm)	Carbonyl index (a.u)	Weight average molar mass M_w (g/mol)	Carbonyl index (a.u)	Weight average molar mass M_w (g/mol)
0.15	0,9	181,800	2.56	9,800
0.45	--	464,000	0.86	27,000
1.5	--	443,000	--	243,00

The molar mass and carbonyl index gradients in the P2 sample were steeper than in the homopolymer sample. This is consistent with the higher level of degradation in the copolymer sample at a given degradation period. The CRYSTAF behaviour of sample PP at 0.15 mm and 1.5 mm into the samples are compared in Figure 34.

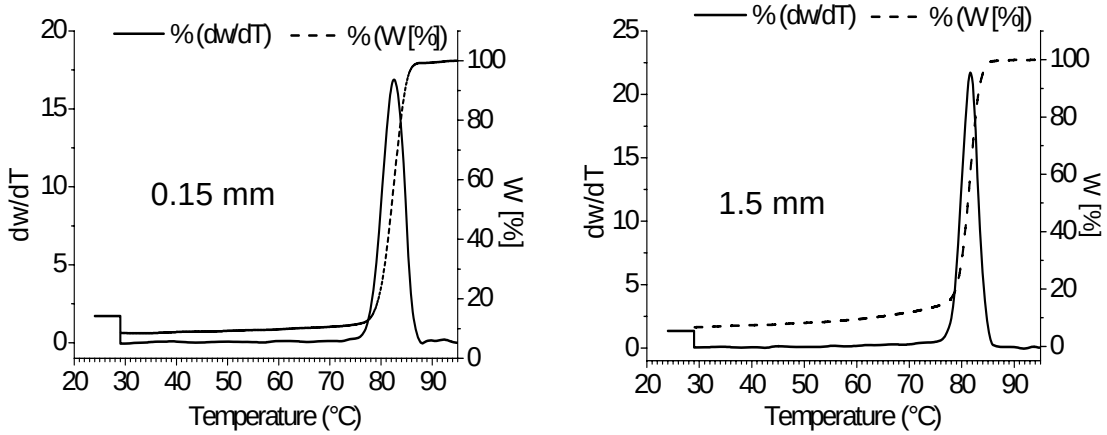

Figure 34a: CRYSTAF behaviour of the homopolymer fractions at 0.15 and 1.5 mm into the sample.

In the homopolymer, there is very little difference in the CRYSTAF crystallisation between the layer at 0.15 mm and the layer at 1,5 mm (Figure 34a). In the copolymer sample, however, the surface layer is highly degraded, with a high soluble fraction and a broad crystallisation curve compared to the curve taken at 1.5 mm into the sample (Figure 34b).

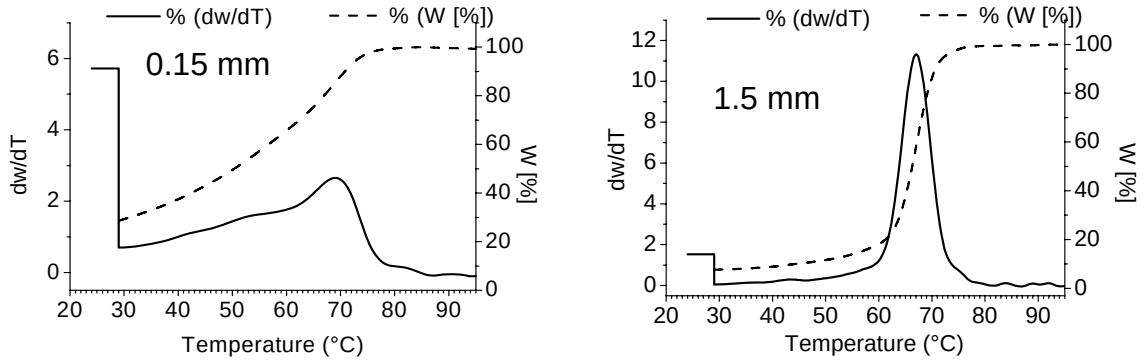

Figure 34b: CRYSTAF behaviour of the propylene-1-pentene fractions at 0.15 and 1.5 mm into sample P2.

The CRYSTAF results, therefore, confirmed the differences found in molar masses and carbonyl indices at the different abrasion depths. The homopolymer sample was less affected by the degradation process than the propylene-1-pentene copolymer sample.

6.9 TREF fractionation of the P2 (undegraded) and P2 (degraded) samples

A prep-TREF analysis can potentially provide information on the degradation process, especially the shift in chemical composition distribution during the degradation process. The CRYSTAF results of sample P2 indicated a broadening of the chemical composition distribution with an increasing level of degradation in the sample. Prep-TREF would, in theory, be able to study the broadening of the chemical composition curve by providing analytical quantities of the fractions of the sample. The chemical composition distribution of the undegraded sample may provide information on sites that may be more susceptible to oxidative degradation. Performing a prep-TREF analysis on a partially degraded sample can provide more in-depth information on changes in the chemical composition of the sample with thermo-oxidative degradation. Similar to the CRYSTAF results, the soluble fraction will increase with degradation. However, there will also be chemical changes in the different fractions with degradation.

The incorporation of a comonomer can have a drastic effect on polymer morphology. The polypropylene molecular structure is very dependent on the tacticity and the comonomer content [50]. Comonomers can theoretically be considered as defects in the polymer chain, so a clear effect of the comonomer on the fractions of a comonomer sample is expected. The compositional analysis of block copolymers of ethylene and propylene has received much attention in literature [50]. The random copolymers of propylene, however, have not been

investigated to a similar extent. Similarly, very little information is available on the compositional analysis of propylene-1-pentene copolymers.

6.9.1 TREF fractionation of the undegraded P2 sample

The undegraded P2 sample was fractionated into 12 fractions to obtain information on the chemical composition distribution in the sample. Approximately 5 g of sample was refluxed in xylene (Merck, Darmstadt, Germany) and the solution was slowly cooled to room temperature at 0.1 ºC per minute in the absence of any support material. The fractions were precipitated in acetone (non-solvent). Extractions were performed between 33 and 130 ºC. The fractions crystallising below 76 ºC are relatively small, typically less than 5% per fraction (17% in total). The largest fraction (31% of all crystallised material) was taken at 91 ºC. Significant fractions were also taken at 81, 86, 96 and 104 ºC (Figure 35).

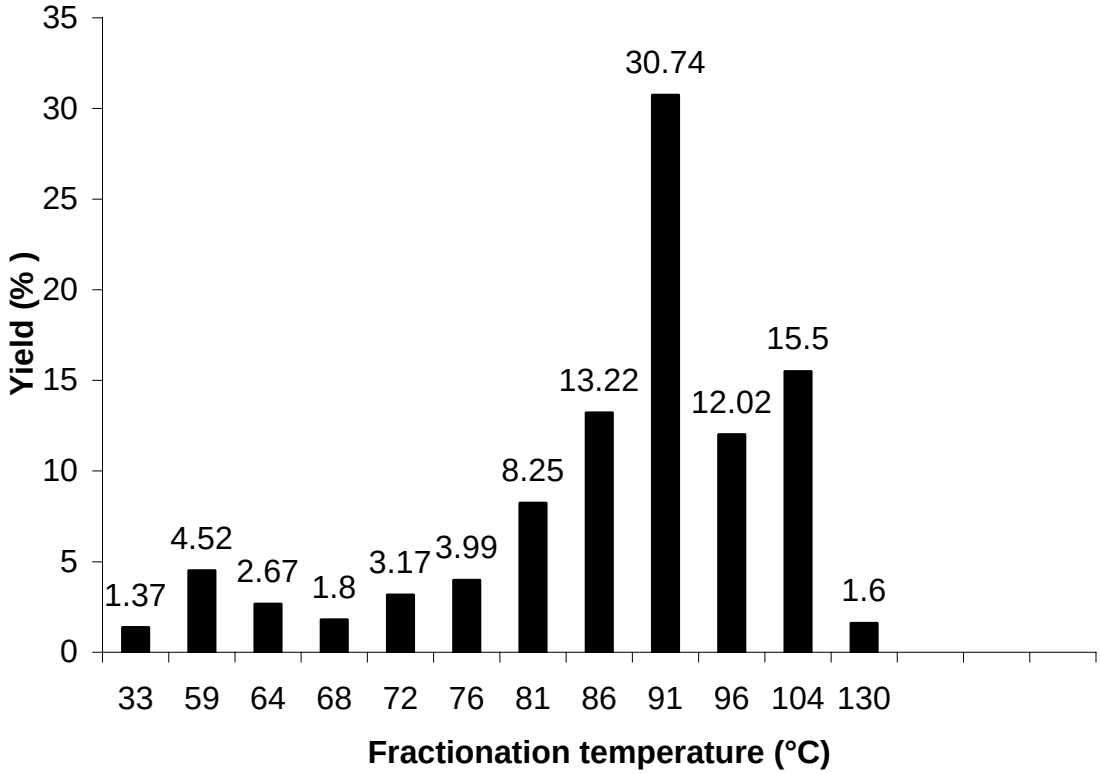

Figure 35: Fractionation temperatures and % of the polymer extracted at each temperature of the undegraded P2 sample.

6.9.1.1 Molar mass and molar mass distributions of the fractions of the undegraded P2 sample

The molar mass and molar mass distribution values for the twelve fractions were determined using a Waters 150 GPC. The molar mass distribution curves are given in Figure 36. The molar mass properties of the fractions are given in Table 8.

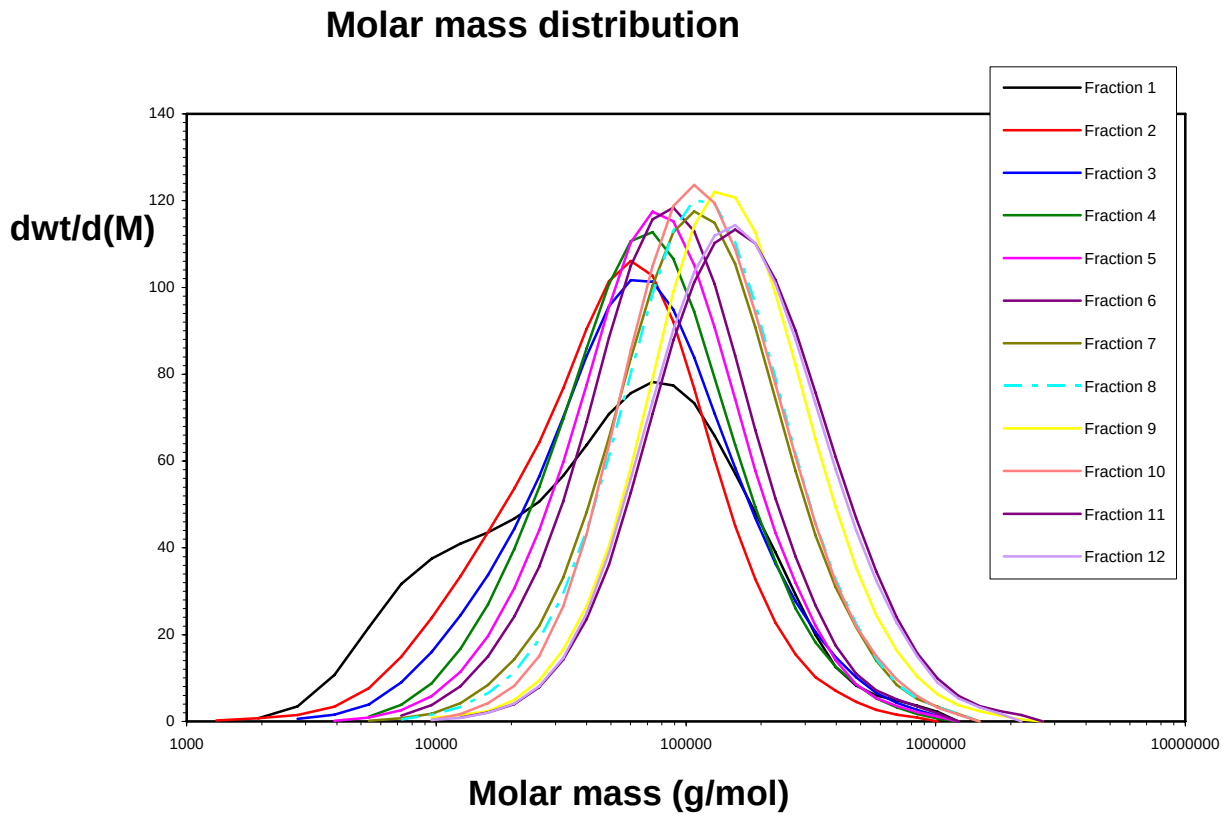

Figure 36: Molar mass distribution curves of the fractions of the undegraded P2 sample.

The molar mass distribution of the first fraction was relatively broad and consisted of highly branched material (PDI = 3.71). The rest of the fractions are relatively narrow (Table 8). All fractions from 2-12 were monomodal in nature. From fraction 5 to 12 the fractions were all relatively narrow in polydispersity (PDI<2).

Table 8: Molar mass properties of the fractions of the undegraded P2 sample

Fraction no.	Fractionation temp.	M_n	M_w	Yield (%)	PDI
1	33	27,100	100,500	1.37	3.71
2	59	34,200	82,300	4.52	2.40
3	64	43,900	106,900	2.67	2.44
4	68	52,500	106,500	1.80	2.03
5	72	59,900	116,800	3.17	1.95
6	76	68,100	130,700	3.99	1.92
7	81	86,600	167,100	8.25	1.93
8	86	92,400	172,400	13.22	1.87
9	91	119,000	220,800	30.74	1.85
10	96	97,600	173,300	12.02	1.78
11	104	131,300	255,700	15.50	1.95
12	130	128,000	254,400	1.60	1.91

6.9.1.2 Determination of the pentene content of the different fractions

The pentene contents of the individual fractions were determined using an in-house calibration curve. Pentene standards were analysed by NMR and the results were correlated with FTIR peak heights at 737 cm^{-1} (Table 9).

Table 9: Distribution of pentene in the propylene-1-pentene copolymer (sample P2)

Fractionation temperature (ºC)	% Pentene
33	2.5
59	7.5
64	6.3
68	4.3
72	5.5
76	4.1
81	3.9
86	3.3
91	2.1
96	1.8
104	1.5
130	1.4

The polymer was produced using a Ziegler-Natta catalyst. The Flory-Huggins theory predicts that the melting point will decrease with the incorporation of a comonomer into the chain, with the resultant drop in the crystallinity. This will be even more severe for a more bulky side group. It is evident that all fractions contain pentene. Fraction 1 contained significantly lower pentene levels compared to the next fraction. This is interesting and here the decrease in the crystallisation temperature is not related to the incorporation of the pentene in the polymer.

6.9.1.3 NMR study of the propylene-1-pentene copolymer fractions

Several of the fractions were analysed by NMR to verify the pentene content of the fractions as well as to determine the tacticity of the fractions (Table 10). The tacticity was defined as the % of mmmm pentads, present in the ^{13}C NMR spectrum.

Table 10: NMR analysis of fractions from the TREF analysis

Fraction number	Pentene content (NMR)	Pentene content (FTIR)	Tacticity
3	4.68	6.3	90.32
5	3.62	5.5	92.41
7	2.01	3.9	97.84
9	0.60	2.1	96.48
10	1.89	1.8	94.09
11	1.30	1.5	94.28

Generally there was a good correlation between the FTIR results and the NMR results, except for the lower pentene region. It was still evident that pentene was present in all the fractions, with the highest crystallinity fraction still containing 1.5 mol% pentene. The tacticity of the 3rd fraction was approximately 90.3%, followed by the fractions of higher tacticity.

Correlation of the molar mass of the fractions with the pentene content

From Figure 37 it can be seen that the polymer consists of fractions of highly branched (high pentene content) low molar mass material containing more than 7% of pentene and lowly branched high molar mass material (molar mass approximately 250,000 g/mol, containing 1.4 % pentene). The low molar mass material was, therefore, high in pentene content, and the

tacticity of these fractions is generally lower than that of the high molar mass material. The low molar mass material will, therefore, contain more atactic material.

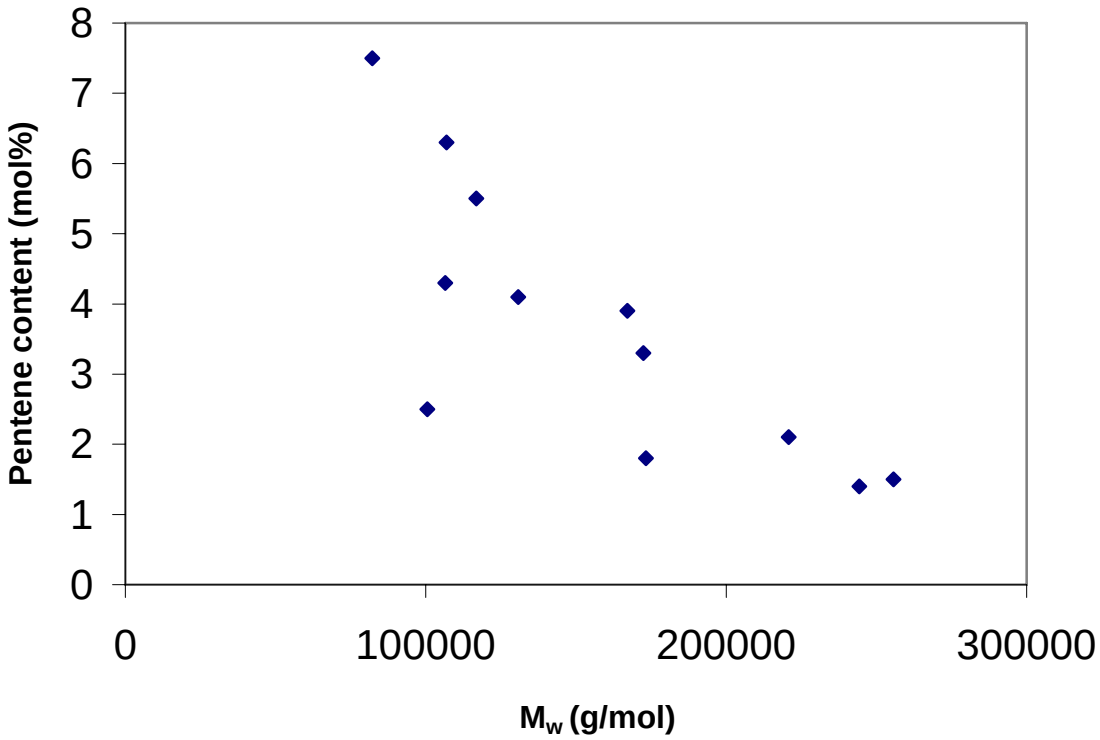

Figure 37: Pentene content as a function of weight average molar mass (M_w) of the undegraded sample (sample P2).

6.9.2 Investigation of the shift in chemical composition distribution during the degradation of sample P2

In the previous section the chemical composition distribution of the undegraded P2 sample was investigated by fractionating the sample into 12 fractions. This provided information on the pentene distribution as a function of the crystallinity of the polymer. The degradation process will, however, result in a significant shift in the chemical composition distribution, which was already detected in the CRYSTAF results, discussed earlier in this chapter. Due to the low yield of some of the fractions (Fractions 1, 2, 3, 4, 5, 6 and 12), it was decided to perform the comparison of the chemical composition distribution before and after degradation by only fractionating the polymer into 9 fractions. Similar to the fractionations performed in Chapter 8, fractionation was carried out at 60 ºC, 70 ºC, 76 ºC, 81 ºC, 86 ºC, 91 ºC, 96 ºC, 105 ºC and 125 ºC. This will provide information on the comparison of the material crystallising at a certain temperature in both the degraded and undegraded polymer. Sample

P2 (undegraded) and P2 (degraded for 15 days at 70 ºC) were fractionated in this study. In Figure 38, the shift in the yields of the fractions can be seen.

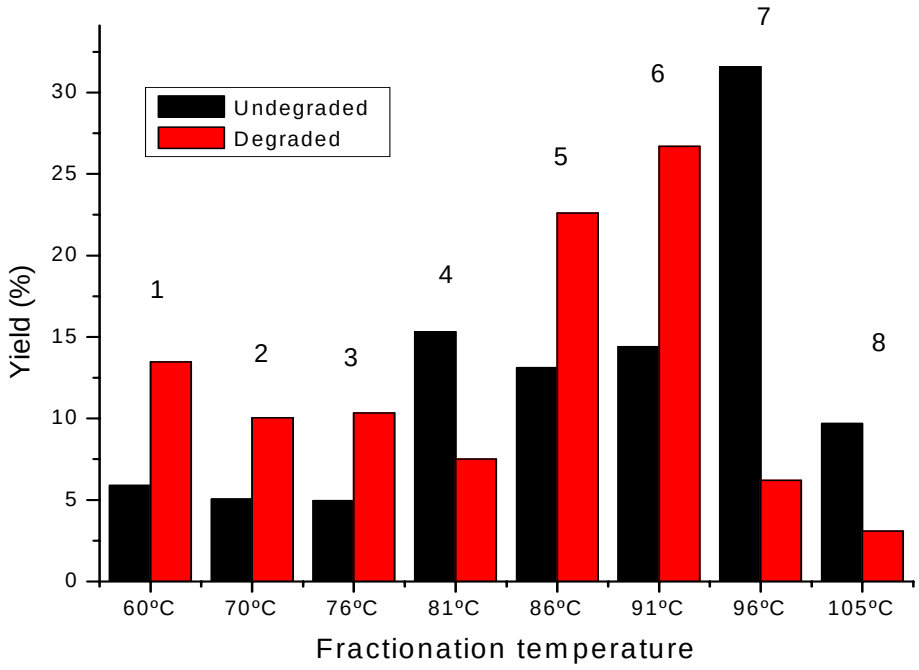

Figure 38: Effect of thermo-oxidative degradation on the yield of the TREF fractions of sample P2.

The total yield (in weight %) of the fractionation was 95% for the undegraded sample and 89% for the degraded sample. Sufficient material was, therefore, recovered from both samples to give a good indication of the CCD in both samples. No polymer was detected in the highest crystallinity fraction (125 ºC) of both the undegraded and the degraded samples. It is evident from Figure 37 that there was a significant shift in the yields of most fractions with degradation. The yield of the 96 ºC fraction (fraction 7) was significantly reduced in the degraded sample, while the yields of fractions 1, 2, 3, 5 and 6 increased significantly. This indicates the destruction of higher molar mass chains into shorter functionalised chains. This shift in the yields of the fractions is in line with the broadening of the crystallisation curve as detected by CRYSTAF. To investigate the possible reasons for this broadening in the CRYSTAF curve, DSC, FTIR, GPC and CRYSTAF analyses were performed on the individual fractions of the undegraded and degraded samples. Too little material was recovered from Fraction 8 of the degraded sample, so comparison of the fractions was performed on fractions 1-7.

6.9.2.1 Comparison of the molar masses of the fractions of P2 (degraded) and P2 (undegraded)

The M_w and M_z values of the fractions of the degraded and the undegraded samples were compared. In Figure 39 (a) and (b) it can be seen that these molar mass averages were significantly lower for the degraded fractions compared to the undegraded samples. One must, however, keep in mind that the thermo-oxidative degradation results in a drop in the yield of some fractions (and a shift in crystallinity): certain polymer chains may be modified to be included in fractions of lower crystallinities.

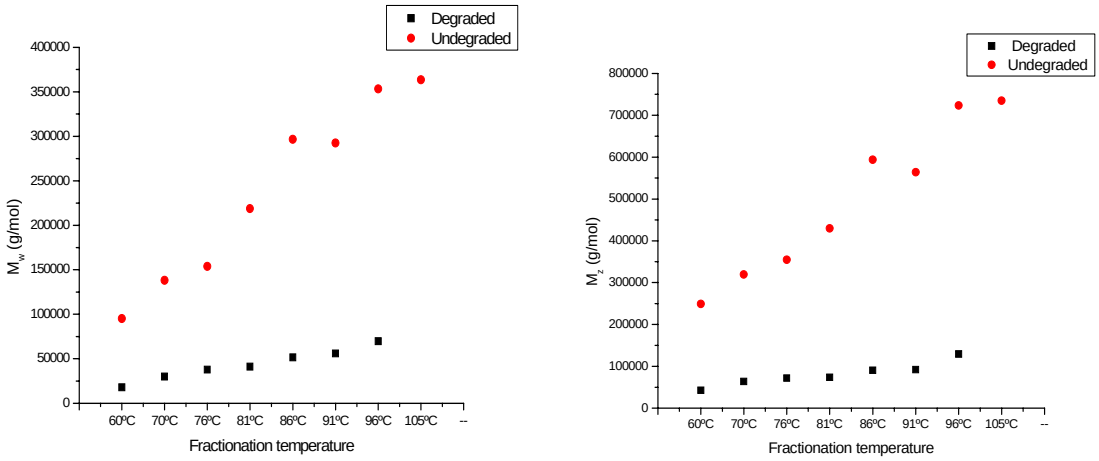

Figure 39 a and b: Comparison of (a) the M_w values and (b) M_z values obtained from the degraded and undegraded samples.

6.9.2.2 Comparison of the thermal properties of the fractions of P2 (degraded) and P2 (undegraded)

The thermal properties of the fractions of the undegraded and degraded samples were compared. The melting points of the first three fractions were significantly different: they were higher for the degraded sample compared with the undegraded sample (Figure 40a). The crystallinities of the fractions of the two samples were significantly different: generally most of the fractions of the degraded samples were of higher crystallinity compared to the undegraded sample (Figure 40b). In the undegraded sample, the separation was according to crystallinity, while in the degraded sample, the first fractions (fractions 1-6) were separated according to crystallinity while the crystallinity of fraction 7 was less (but of higher melting point) compared to fraction 6.

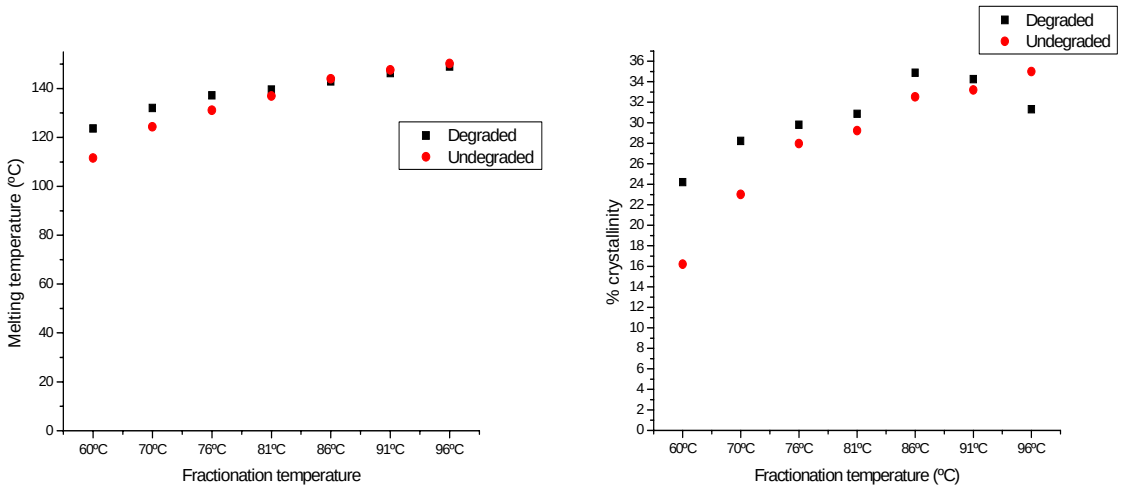

Figure 40 a and b: Comparison of (a) the melting points and (b) % crystallinities obtained from the degraded and undegraded samples.

6.9.2.3 Comparison of the carbonyl indices of the fractions of P2 (degraded) and P2 (undegraded)

In Figure 41 the carbonyl indices of the fractions can be seen. Carbonyl indices were determined as the peak height at 1714 cm^{-1} divided by the peak height at 899 cm^{-1}. It is evident that the highest carbonyl content was found in the lowest crystallinity (also lowest molar mass) fraction. The two fractions with the highest crystallinity showed very small differences in degraded product content. The carbonyl indices of all the fractions of the undegraded polymer were significantly lower than the degraded polymer.

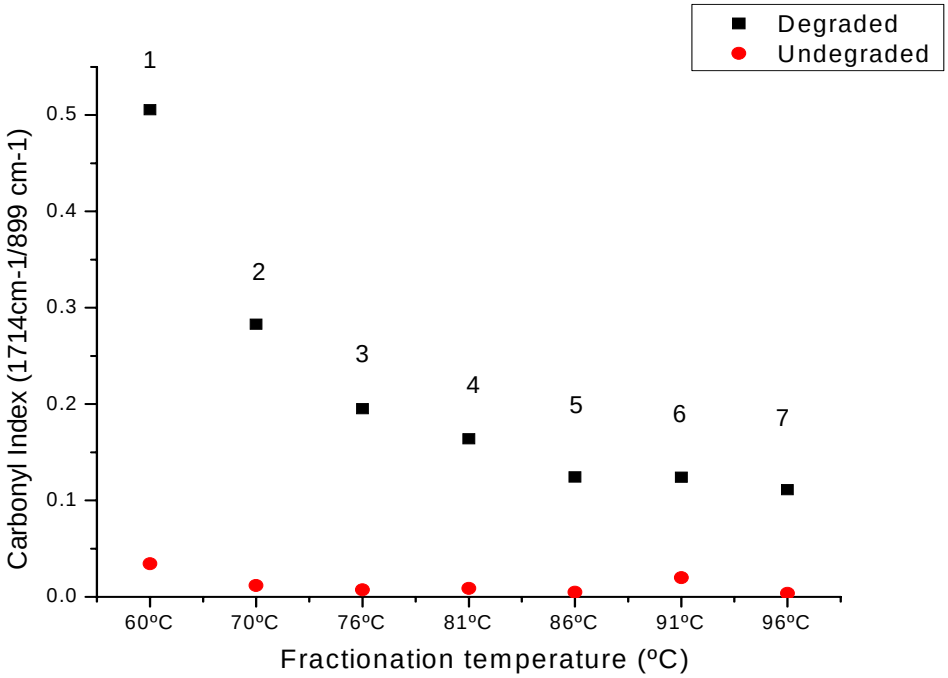

Figure 41: Carbonyl indices of the fractions of the degraded and undegraded P2 samples.

6.9.2.4 Comparison of the CRYSTAF behaviour of the fractions of P2 (degraded) and P2 (undegraded)

The CRYSTAF behaviour of the fractions of the undegraded and the degraded samples were compared. In the undegraded sample, fraction 1 consisted of a high percentage of material that does not crystallise in TCB. The soluble fraction was relatively high at 50%. Fraction 2 contained a significantly lower soluble fraction, and a crystallisation peak could be detected at 50 ºC. The crystallisation peaks of fractions 4-7 were relatively sharp. These fractions were characterised by small soluble fractions (<1%). The crystallisation temperatures of the fractions generally increased with an increase in fractionation temperature, except for fraction 7 that had a lower crystallisation temperature compared with fraction 6 (Figure 42).

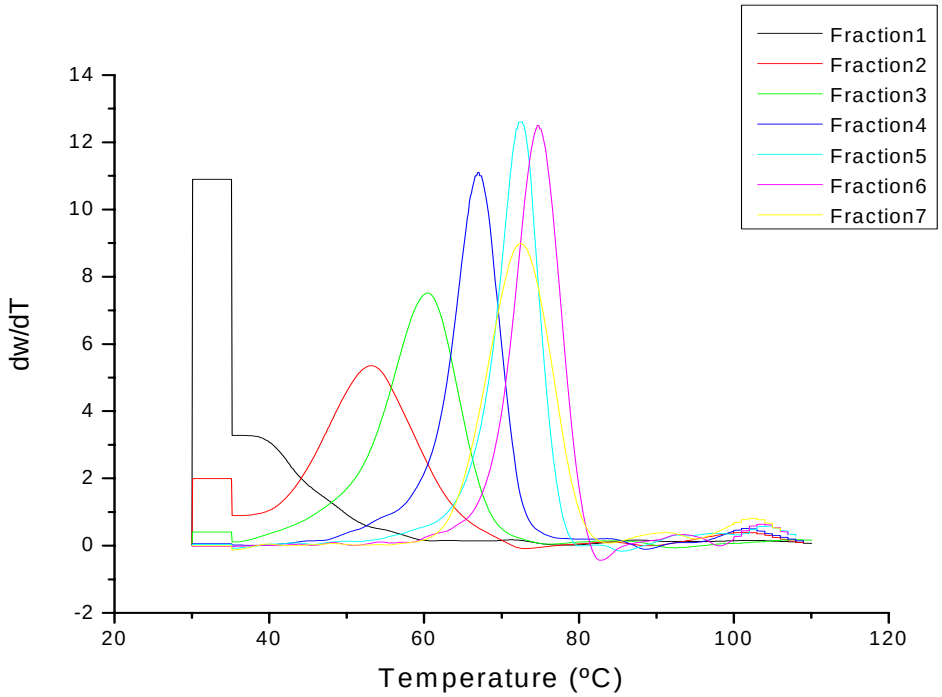

Figure 42: CRYSTAF behaviour of the fractions of sample P2 (undegraded).

The fractions of the degraded sample were significantly different in composition (Figure 43). Fraction 1 contained a high soluble fraction (in TCB) (similar to the undegraded sample, >50%), but in the degraded sample, the amount of sample recovered in fraction 1 was significantly higher compared to the undegraded sample (14% compared to 6% in the undegraded sample). Fraction 2 of the degraded sample was also significantly different compared to the fraction in the undegraded sample, with a high soluble fraction compared to the undegraded sample. In fraction 2 of the undegraded sample, a crystallisation peak was visible, while it was absent in the degraded sample. The carbonyl index values (as determined by FTIR) indicated that fractions 1 and 2 contained high levels of carbonyl groups. From fractions 3-6 the chemical composition distributions of the fractions of the degraded sample were typically broader compared to the fractions of the undegraded sample. The soluble fractions of the degraded samples were also typically higher than in the undegraded sample.

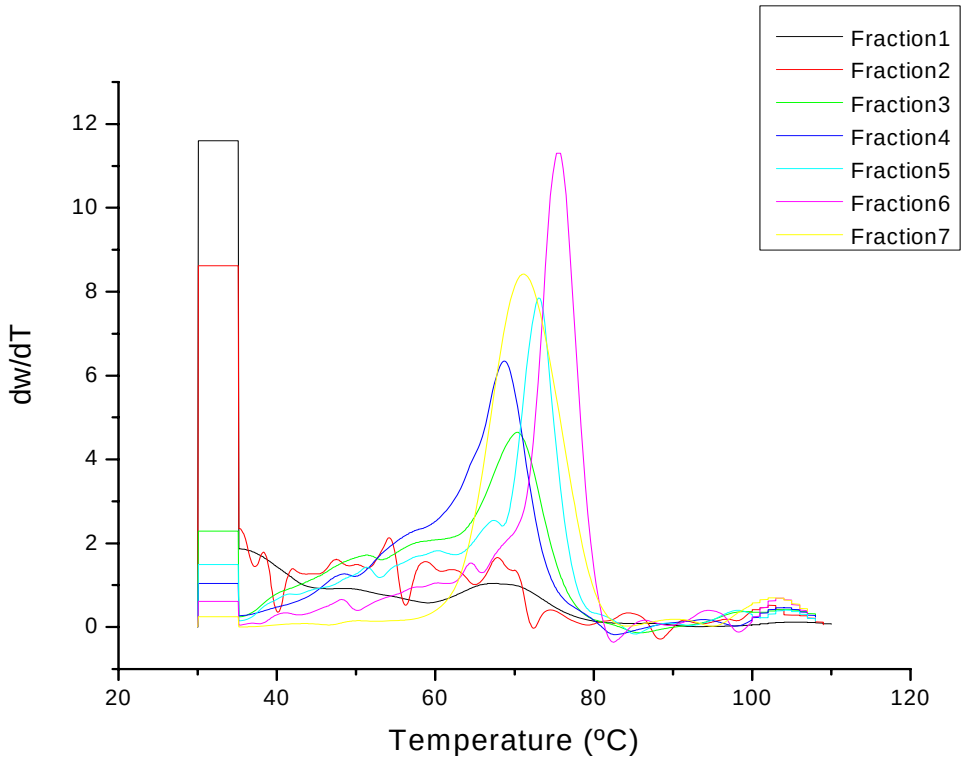

Figure 43: CRYSTAF behaviour of the fractions of sample P2 (degraded).

The broadening of the CRYSTAF crystallisation peaks with degradation was, therefore, due to a significant broadening in the chemical composition. As seen in the fractions of the undegraded sample, most of the fractions were narrow in CCD. In the degraded sample, the chemical composition was modified by the incorporation of carbonyl groups into the chains. Although the DSC analysis indicated that the first three fractions of the degraded sample had higher crystallinities and melting points compared to the fractions of the undegraded sample, the CRYSTAF indicated that these fractions typically have higher soluble fractions (soluble below 30 ºC in TCB) compared to the undegraded sample, and were therefore less able to crystallise in the CRYSTAF. This may, however, be different if a different solvent/cooling combination is used.

6.10 Theories on the possible faster degradation of propylene-1-pentene copolymer compared to polypropylene homopolymers

A major contributing factor to the lower stability of the propylene-1-pentene copolymers is the reduction in density by the incorporation of a bulky side group. As seen from the SEC-FTIR results, the pentene will mostly be present in the amorphous areas. Oxygen will diffuse freely through these amorphous regions. It may also be possible that the positive inductive effect on the tertiary carbon at a pentene group may contribute to the stability of the tertiary radical. Clustering effects may also play a role in the acceleration of the degradation in propylene-1-pentene copolymers (pentene clustering).

In order to better understand the effect of degradation on the chemical composition, NMR analysis was carried out on the undegraded and degraded Sample P2. In Figure 44 the effect of thermo-oxidative degradation on the NMR spectrum of the propylene-1-pentene sample can be seen.

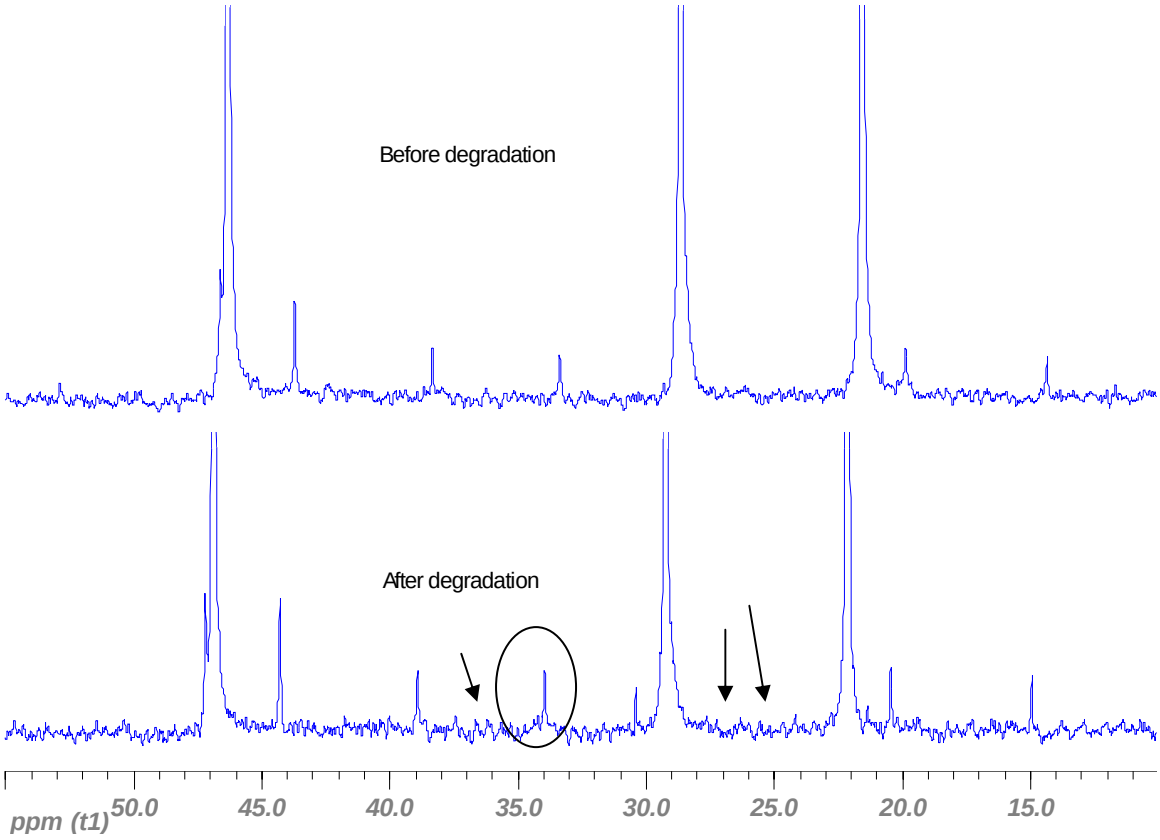

Figure 44: Effect of degradation on the 13C NMR spectrum of sample P2.

The major differences between the two spectra (undegraded vs degraded) are indicated by the black circle and arrows. This new peak appearing in the spectrum may be due to the formation of $CH_2CH_2CH_2$ sequences. This is probably due to the side-chain scission of 1-pentene units (n-propyl groups).

The circled peak is due to the propylene unit either side of the above CH_2-sequence. Small peaks are also visible around 24 – 26 ppm, as well as 36 – 38 ppm. These are typical of the above type of sequence. The fact that there appears to be more than one small peak in the above area seems to indicate that these types of “scission reactions” could very well be taking place where more than one pentene unit is found next to one another in the chain (clustering).

In theory the above could also be ascribed to end groups being formed after scission at a pentene unit, but this is unlikely, as more peaks in the 14 – 16 ppm region should be visible as well.

6.11 Conclusions

The overall objective of this chapter was to study the degradation behaviour of unstabilised commercial Sasol Polymers propylene-1-pentene copolymers and contrast that with the degradation behaviour of a Sasol Polymers polypropylene homopolymer sample. The degradation process in polyolefins has a significant influence on the molar mass, chemical composition and the chemical composition distribution of the polymer.

In this chapter, the degradation behaviour of two unstabilised commercial propylene-1-pentene copolymers were contrasted with a polypropylene sample produced under similar conditions. NMR indicated that the tacticities of the propylene-1-pentene samples were similar to the homopolymer sample. DSC indicated a broadening of the melting curve and decreases in the melting points and crystallinity with the incorporation of higher levels of pentene. The soluble fractions (as measured by CRYSTAF) were higher for the copolymer samples compared to the homopolymer. It was also found that the incorporation of pentene resulted in a significant decrease in the crystallinity of a propylene-1-pentene sample. The samples were found to contain similar levels of catalyst residues.

Classical analytical techniques like SEC and FTIR were able to distinguish differences in degradation behaviour. The propylene-1-pentene samples degraded significantly faster than

the polypropylene homopolymer sample (faster decrease in molar mass and faster increase in carbonyl index). DSC analysis indicated a slight decrease in melting point and an increase in crystallinity with progressing degradation. These theories are in line with the observations by Rabello and White [37-39]. Using SEC-FTIR analysis, it was possible to determine the relative pentene distribution in a propylene-1-pentene copolymer. It was also possible to confirm the observations in Chapter 5, namely that the degradation products are concentrated in the low molar mass regions. The ketone concentration was found to increase significantly faster than the lactone concentration. This is expected as ketone formation will be the primary product of scission. Lactones are secondary oxidation products, formed during the further oxidation of aldehydes. CRYSTAF analysis showed a significant increase in the soluble fractions of the samples with progressing degradation, and a decrease in crystallisation temperature was also found. The crystallisation curves were influenced to a different extent during the degradation process, with a smaller decrease in crystallisation and smaller increase in soluble fraction with degradation compared to the copolymer samples and comparable carbonyl index values. This was thought to be related to the differences in crystallinity between the three samples. With TREF fractionation it was possible to obtain a significant amount of information on the undegraded sample. It was found that the fractions differed with regard to the pentene content and that pentene was detected in all fractions. The pentene contents of the lower crystallinity fractions were, however, higher than in the higher crystallinity fractions. TREF fractionation of the degraded sample indicated that the increase in the width of the crystallisation curve can be attributed to the increase in carbonyl content of all fractions. A decrease in the yield of the higher crystallinity fractions was found, while the yield of some of the lower crystallinity fractions increased significantly. CRYSTAF analysis was performed on all fractions and it can be seen that all fractions in the degraded and the undegraded samples were significantly different.

6.12 References

[1] Steynberg, A.P., Espinoza, R.L., Jager, B., Vosloo, A.C., *Applied Catalysis A: General* **1999**, 186, 41-54

[2] Tincul, I., Joubert, D.J., Smith, J., Van Zyl, P., *Polymeric Materials: Science and Engineering* **2001**, 84, 121-122

[3] Tincul, I., Joubert, D.J., conference abstract, www.zae-bayern.de/ectp/abstracts/tincul1.html

[4] Tincul, I., Potgieter, I.H., Joubert, D.J., Potgieter, A.H., International patent number WO 99/01485, publication date 14/01/1999

[5] Joubert, D.J., Potgieter, A.H., Potgieter, I.H., Tincul, I., International patent number WO 96/24623, publication date 15/08/1996

[6] Tincul, I., Joubert, D.J., Wahner, U.M., Smith, S.P.J., van Zyl, P.W., United States patent number US 2003/0225224 A1, publication date 04/12/2003

[7] Marshall, N., PhD thesis, University of Sussex, **December 2001**

[8] Smith, M., Sasol internal report, *Propylene/1-pentene random copolymers,* **March 2005**

[9] Bolland, J.L., Gee, G., *Transactions of the Faraday Society* **1946** 42, 236-243

[10] Bolland, J.L., Gee, G., *Transactions of the Faraday Society* **1946** 44, 669-677

[11] Billingham, N.C., Walker, T.J., *Journal of Polymer Science: Polymer Chemistry Edition* **1975** 13, 1209-1222

[12] Pospisil, J., Horak, Z., Krulis, Z., Nespurec, S*., Macromolecular Symposia* **1998**, 135, 247-263

[13] Klemchuck, P.P., Horng, P-L., *Polymer Degradation and Stability* **1991**, 34, 333-346

[14] Marshall N., Presentation at Sasol Polymers: The thermo-oxidative stability of poly(propylene-co-1-pentene), **May 2004**

[15] Joubert, D.J., Sasol Internal report 005/93

[16] Pospisil, J., Horak, Z., Pilar, J., Billingham, N.C., Zweifel, H., Nespurec, S., *Polymer Degradation and Stability* **2003**, 82, 145-162

[17] Goss, B.J.S., Nakatani, H., George, G.A., Terano, M., *Polymer Degradation and Stability* **2003**, 82, 119-126

[18] Gugumus, F., *Polymer Degradation and Stability* **1999**, 63, 41-52

[19] Hawkins, W.L., Matreyek, W., Winslow, F.H., *Journal of Polymer Science* **1959**, 1-11

[20] van Sicle, D.E., *Macromolecules* **1977**, 10, 474-476

[21] Mendes, L.C., Rufino, E.S., de Paula, O.C., Torres, J.R., *Polymer Degradation and Stability* 2003, 79, 371-383

[22] Gulmine, J.V., Janissec, P.R., Heise, H.M., *Polymer Degradation and Stability* **2003**, 79, 385-397

[23] Jansson, A., Moeller, K., Gevert, T., *Polymer Degradation and Stability **2003**,* 82, 37-46

[24] Papet, G., Jiracova-Audouin, L., Verdu, J., *Radiation Physics and Chemistry* **1987**, 29, 65-69

[25] Kato, Y., Carlsson, D.J., Wiles, D.M., *Journal of Applied Polymer Science* **1969**, 1447-1458

[26] De Goede, S., Brüll, R., Pasch, H., Marshall, N., *e-polymers* **2004**, 12, 1-9

[27] Konar, J., Ghosh, R., *Polymer Degradation and Stability* **1988**, 21, 263-275

[28] Castejon, M.J., Tiemblo, P., Gomez-Elvira J-M., *Polymer Degradation and Stability* **2000**, 70, 357-364

[29] Jansson, A., Moeller, K., Hjertberg, T., *Polymer Degradation and Stability* ***2004****, 84, 227-232*

[30] Lacoste, J., Deslandes, Y., Black, P., Carlsson, D.J., *Polymer Degradation and Stability* ***1995****, 21-28*

[31] Dulog, L., Radlmann, E., Kern, W., *Macromoleculare Chemie* **1963**, 60, 1-17

[32] Billingham, N.C., Then, E.T.H., Kron, A., *Polymer Degradation and Stability* **1997**, 55, 339-346

[33] Luongo, J.P., *Journal of Polymer Science* **1963**, 141-143

[34] Brüll, R., Pasch, H., Raubenheimer, H.G., Sanderson, R., Van Reenen, A.J., Wahner, U.M., *Macromolecular Chemistry and Physics* **2001**, 202, 1281-1288

[35] Guisandez, J., Tiemblo, P., Gomez-Elvira, J.M., *Polymer Degradation and Stability* ***2005****, 87, 543-553*

[36] Monrabal, B., *Journal of Applied Polymer Science* **1994**, 52, 491-499

[37] Rabello, M.S., White, J.R., *Polymer* **1997**, 38, 6379-6387

[38] Rabello, M.S., White, J.R., *Polymer Degradation and Stability* **1997**, 56, 55-73

[39] Rabello, M.S., White, J.R., *Polymer* **1997**, 38, 6389-6399

[40] Elvira, M., Tiemblo, P., Gomez-Elvira, J.M., *Polymer Degradation and Stability* **2004**, 509-518

[41] Gabriel, C., Lilge, D., *Polymer* **2001**, 42, 297-303

[42] Monrabal, B., Journal of *Applied Polymer Science* **1994**, 52, 491-499

[43] Monrabal, B., in “New Trends in Polyolefin Science and Technology”, Hosoda, S., editor; Research Signpost 1996.

[44] Simon, L.C., de Souza, R.F., Soares, J.B.P., Mauler, R.S., *Polymer* **2001**, 42, 4885-4892

[45] Sarzotti, D.M., Soares, J.B.P., Simon, L.C., Britto, L.J.D., *Polymer* **2004**, 45, 4787-4799

[46] Willis, J.N., Dwyer, J.L., Liu, X., Dark, W., *ACS Symposium* **1999**, 226-231

[47] Shyichuck, A.V., White, J.R., Craig, I.H., Syrotynska, I.D., *Polymer Degradation and Stability* **2005**, 88, 415-419

[48] Nagai, N., Matsunobe, T., Imai, T., *Polymer Degradation and Stability* **2005**, 224-233

[49] Gardette, J.L., *Die Angewandte Makromolekulare Chemie* **1995**, 232, 85-105

[50] Zhang, Y-D., Wu, C-J., Zhu, S-N., *Polymer Journal* **2002**, vol 34 no 9, 700-708

Chapter Seven

Degradation behaviour of unstabilised laboratory-synthesised propylene-1-pentene copolymers

7.1 Introduction and background

In the previous chapter (Chapter 6) it was shown that two commercial propylene-1-pentene samples, with different pentene contents, degraded faster than a sample of homopolymer polypropylene produced by the same process. The incorporation of low levels of pentene comonomer (< 3% pentene) resulted in a significant decrease in the crystallinity and melting point of a commercial propylene-1-pentene copolymer sample. Pentene incorporation also resulted in a slight broadening of the DSC melting curve. NMR and FTIR analyses of TREF fractions and SEC-FTIR analysis proved that most of the pentene comonomer was incorporated in the low molar mass region. Furthermore, pentene comonomer was detected in all fractions, even in the highest crystallinity fractions. From the NMR analyses it was evident that the incorporation of low levels of pentene did not influence the isotacticity of the samples to a significant extent.

La Mantia [1] and others found an increased resistance to photo-oxidative degradation of polyolefin samples with an increase in crystallinity. Oxygen diffuses through the amorphous regions and is mostly excluded from the crystalline regions. Differences in crystallinity may influence the oxygen uptake and, therefore, the kinetics of degradation. Synthesising and degrading a series of samples containing pentene in various concentrations, and prepared under similar conditions, could therefore be used to study the effect of comonomer incorporation on the degradation behaviour.

7.2 Objectives

The objective of this section of the work was to determine to what extent the incorporation of higher levels of pentene (up to 8 mol%) into a propylene-1-pentene sample will influence the stability of the copolymer. A second objective was to fully characterise the structure of these laboratory-synthesised propylene-1-pentene copolymers. The two commercial propylene-1-pentene copolymers, studied in the previous chapter, contained only low percentages of comonomer (2,24 mol%) and the question arises as to whether this decrease in thermo-oxidative stability (determined by oven aging) will be linear with an increase in pentene content. The influence of higher levels of pentene incorporation (up to 8 mol%) on the polymer structure was also investigated. Samples were investigated for morphology and the relationship between crystallinity and degradation behaviour was also investigated. These samples were fully characterised by FTIR, DSC, NMR and SEC.

7.3 Experimental

7.3.1 Synthesis of the polypropylene homopolymer and propylene-1-pentene copolymer samples

Samples were prepared using a similar reactor setup to those used for the synthesis of the metallocene propylene-1-pentene samples as described in references 2 and 3. Several propylene-1-pentene copolymer samples were synthesised in the laboratory and thermally degraded at 70 ºC. The same Ziegler-Natta catalyst system and reactor conditions were used for all syntheses. Propylene (synthesis grade) was obtained from Afrox (SA). The 1-pentene (polymerisation grade) was obtained from Sasol, Monomers Business, Sasolburg, South Africa. A pure Sasol C7/C8 cut was used as a solvent for all polymerisations. Polymerisation reactions were carried out in a 1-litre stirred autoclave reactor. All samples were prepared by dissolving 0.1 g of catalyst in 10 ml xylene. Exactly 1 ml of silane and 4 ml of a 10% triethyl aluminium solution was added to the reactor and 20 mg of hydrogen was added to all reactions. A proprietary Ziegler-Natta catalyst system was used. Reaction conditions were kept constant during all polymerisations. The ratio of pentene to propylene was varied. The following comonomer ratios were used (Table 1):

Table 1: Quantity and type of comonomer added as well as the yield of each reaction for the polypropylene homopolymer and propylene-1-pentene samples studied in this section

Sample ID	Propylene (g)	Comonomer added (ml)	Comonomer	Ratio of propylene to pentene (molar ratio)	Polymer yield (g)
S137	100	0	0	n.a.	71.2
S143	100	26	Pentene	0.1	74.5
S139	100	52.1	Pentene	0.2	64.3
S157	100	66.7	Pentene	0.4	72.4
S150	100	133.3	Pentene	0.8	86.2

7.3.2 Sample preparation and degradation of the samples

All samples used in this study were unstabilised. The samples were pressed into films with a constant thickness of 0,2 mm, using a Wabash (Wabash, Indiana) controlled heated press, set at an initial temperature of 190 ºC. Samples were pre-compressed at 5 tons, followed by a high pressure compression at 25 tons pressure. Samples were kept isothermally for 5

minutes, followed by cooling at a linear rate of 15 ºC, to room temperature. The plaques were removed and stored in a fridge until the degradation experiments were performed.
Samples were thermally degraded at 70 ºC in a Scientific Engineering heat circulating oven. The FTIR spectra were recorded daily. Small strips were removed from the oven for further analysis by SEC, DSC and SEC-FTIR.

7.3.3 SEC analysis of the undegraded samples

The molar mass distributions of the samples were determined on a Polymer Labs PL 220 high temperature SEC instrument, equipped with Waters HT 3,4,5 and 6 crosslinked divinylbenzene columns. Samples were dissolved in 1,2,4-trichlorobenzene, stabilised with 0,1% BHT. The dissolution time was 3 hours at 150 ºC in a heated aluminium block. The instrument flow rate was set at 1 ml/min. Calibration was performed relative to PL Easical™ polystyrene standards.

7.3.4 DSC analysis of the undegraded samples

To investigate the initial crystallinity of all samples, DSC analyses were carried out. The melting properties of the samples were determined on a Mettler model DSC 822 instrument. Samples were heated to 220 ºC to remove the thermal history, cooled down to 30 ºC, and the subsequent heating and cooling cycles were measured. Heating and cooling rates of 10 ºC were used.

7.3.5 NMR analysis of the undegraded polypropylene homopolymer and propylene-1-pentene samples

Several NMR studies of metallocene-based propylene-1-pentene copolymers have been published in literature [2, 3]. In these studies the microstructures of propylene-1-pentene copolymers, synthesised with two different metallocene catalyst systems, were compared. To my knowledge, NMR studies of Ziegler-Natta synthesised propylene-1-pentene samples have not yet been described in literature. NMR analysis of the polypropylene homopolymer sample and the propylene-1-pentene samples was carried out using a novel sample preparation method developed by Assumption [4]. Samples were measured quantitatively, using a 5-mm probe. The polymer (±60 mg) was dissolved in 0.6 ml deuterated tetrachloroethane (*d*-TCE) (6 wt%), stabilized with di-tertiary butyl para-cresol (DtBpC). The solvent was first purged with nitrogen for a period of 2 hours prior to using it to prepare the

sample for analysis. Approximately 0.3 ml of the stabilized solvent was added to 60 mg of the polymer. The polymer was melted in the NMR tube in the presence of the solvent by carefully heating the tube with a heat-gun. The rest of the solvent was added and the tube sealed with Teflon® tape. The sample was then placed in a ventilated oven to homogenise at 140 °C for approximately 2 hours.

Quantitative ^{13}C NMR experiments were performed at 125 MHz on a 5-mm PFG switchable/broadband probe (^{1}H -^{19}F, ^{15}N - ^{31}P) on a Varian ^{UNITY}*INOVA* 600 MHz spectrometer at 130°C. 90° pulse widths of approximately 6 μs and delay times between pulses of 15 s were used with an acquisition time of 1.8 s. The number of scans was set to 5120, but the signal-to-noise parameter was set to 2000. Thus, either 2400 scans were acquired or the acquisition was stopped after the required signal-to-noise was reached. The analysis time, therefore, ranged from 3-10 h. Chemical shifts were referenced internally to the PP methyl peak at 19.68 ppm.

7.3.6 FTIR analysis of the degraded and undegraded polypropylene homopolymer and propylene-1-pentene copolymers

FTIR scans were carried out on a Perkin Elmer 2000 FTIR spectrophotometer. A total of 64 scans were carried out per analysis. The spectrum and background ranges were set between 400 cm^{-1} and 4000 cm^{-1}.

7.3.7 CRYSTAF analysis of the degraded and undegraded polypropylene homopolymer and propylene-1-pentene copolymers

A CRYSTAF model 200 instrument (Polymer Char, Valencia, Spain) was used for all analysis. CRYSTAF analysis of the homopolymer and copolymer samples was performed on the initial and degraded samples of each set. Samples were dissolved for 120 minutes at 160 ºC. The samples were then stabilised for 45 minutes at 95 ºC. A linear temperature gradient was followed at 0.1ºC/ min until a temperature of 29 ºC was reached. During this time, 22 points were taken between 95 and 60 ºC, followed by 18 points down to 29ºC.

7.3.8 SEC-FTIR analysis

All SEC-FTIR determinations were carried out on a Lab Connections LC 300 high-temperature LC transform setup. The LC transform setup was connected to a Waters 150 C

HT-SEC instrument equipped with Waters HT 3, 4, 5 and 6 crosslinked divinylbenzene columns. Approximately 12 mg of sample was dissolved in TCB. The transfer line was set at 126 ºC, the stage temperature at 160 ºC and the vacuum at around 2 mTorr. The nozzle temperature was set at 118 ºC. The injection volume was 70 microliters. The samples were deposited on a rotating Germanium disk and scanned offline on a Nicolet model Nexus spectrophotometer. The wavelength range was set between 400 and 4000 cm^{-1}.

7.4 Results

7.4.1 SEC analysis of the undegraded polypropylene samples

The weight average molar masses and polydispersity indices of the propylene-1-pentene copolymers and the polypropylene homopolymer sample are given in Figure 1 and Table 2. It is evident that samples S137, S139 and S150 had similar molar masses (Table 2). The molar mass of S143 was slightly lower, and the molar mass of sample S157 was the lowest.

Table 2: Weight average molar mass and molar mass distribution data of the polypropylene homopolymer and propylene-1-pentene samples synthesised in this section

Sample ID	Feed ratio of pentene to propylene	Feed volume Pentene (ml)	Weight average molar mass (SEC)	Polydispersity M_w/M_n (SEC)
S137	0	0	93,600	4.8
S143	0.1	26	80,800	6.4
S139	0.2	52.1	92,800	6.2
S157	0.4	66.7	68,200	4.5
S150	0.8	133.3	95,800	5.6

The molar mass distributions were monomodal and similar in shape (Figure 1). The polydispersities of all the samples were relatively high with a broad molar mass distribution, characteristic of Ziegler-Natta polymers.

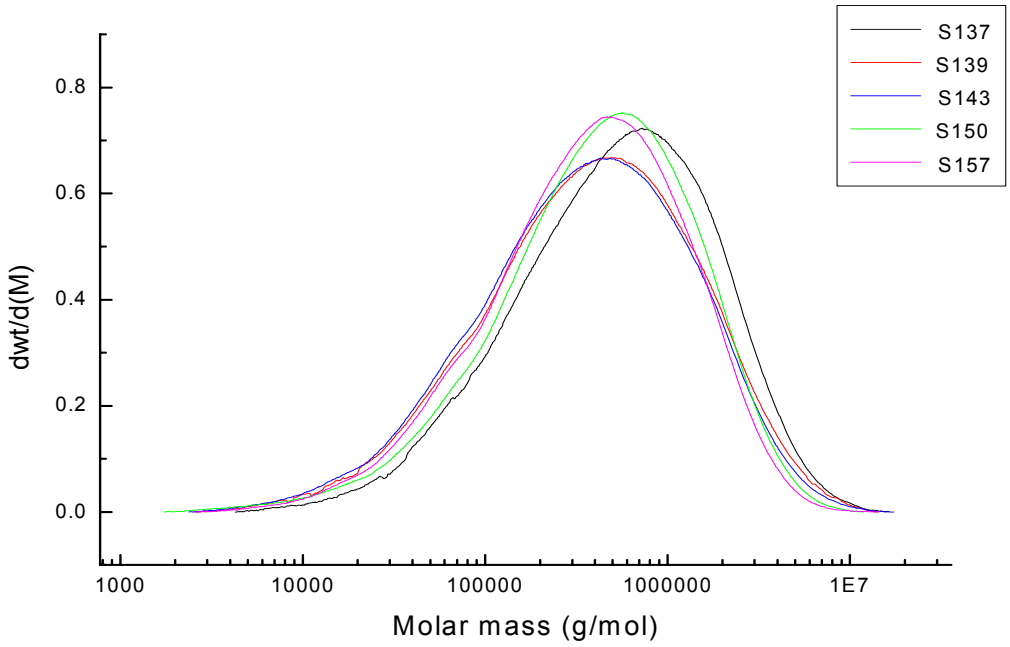

Figure 1: Molar mass distributions of the five polypropylene samples analysed in this study.

7.4.2 DSC analysis of the undegraded polypropylene samples

The crystallinities of the polypropylene homopolymer and the copolymer samples were determined. The results are summarised in Table 3.

Table 3: Crystallinities of the homopolymer and propylene-1-pentene copolymer samples determined by DSC

Sample ID.	% Crystallinity (DSC)
S137	48.78
S143	34.85
S139	32.83
S157	22.73
S150	20.22

From Table 3 it can be seen that the homopolymer sample (S137) had the highest crystallinity, while sample S150 had less than half the crystallinity (48% compared with 20%). There was virtually a linear decrease in the crystallinity with an increase in the pentene content. Samples S143 and S139 had similar crystallinities, while sample S157 was only 24.73% crystalline. These results were confirmed by FTIR analyses; the ratio of the 973 cm^{-1}

to 997 cm^{-1} peaks, representative of the crystalline and amorphous phases respectively, decreased with an increase in the pentene content. The crystallinity in polypropylene is primarily influenced by the tacticity. The effect of pentene incorporation on the tacticity of the copolymer samples will be investigated further by NMR (Section 7.4.3). Figure 2 also shows that the melting point decreased with increasing pentene content.

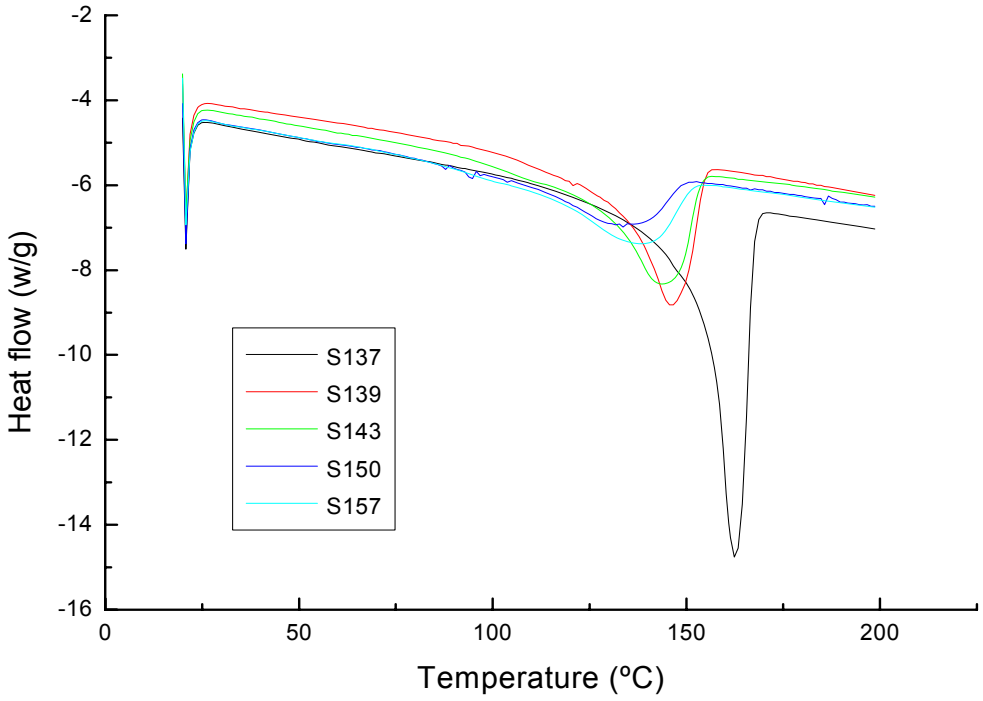

Figure 2: The melting properties of the polypropylene homopolymer (S137) and propylene-1-pentene copolymer samples with different pentene contents.

Graef [5] studied the effect of the incorporation of higher α-olefins into syndiotactic polypropylene. He found a significant, almost linear decrease in the melting points (determined by DSC) of a range of copolymer samples, in line with the Flory-Huggins theory. He correlated the melting points (as determined by DSC) and the crystallisation temperatures (as determined by CRYSTAF) and found a good correlation between this decrease in melting point and the decrease in CRYSTAF crystallisation temperature. A correlation of the T_c (determined by CRYSTAF) and the T_c (determined by DSC) would have provided even more information on the copolymers studied.

7.4.3 ^{13}C NMR analysis of the undegraded polypropylene samples

NMR analysis of the undegraded polypropylene samples was performed to establish the comonomer incorporation and the effect of the comonomer incorporation on the tacticity of the samples.

7.4.3.1 Allocation of the chemical shifts of the individual peaks in the ^{13}C NMR spectrum of a propylene-1-pentene copolymer

The peak allocation in the NMR spectra of the propylene-1-pentene copolymers was performed based on the work by Wahner et al. [2, 3]. Stereoerrors were assigned according to Busico et al. [6, 7]. In Figure 3, the allocation of the different peaks in sample S139 is shown. Peaks A and B are due to main chain CH_2 groups. A peak corresponding to C was not detected. Peaks F and G are due to the CH and the CH_3 of an original propylene monomer unit. Peak I is due to the CH_3 group in the propyl side chain, while D and H are due to the two CH_2 groups in the propyl side chains.

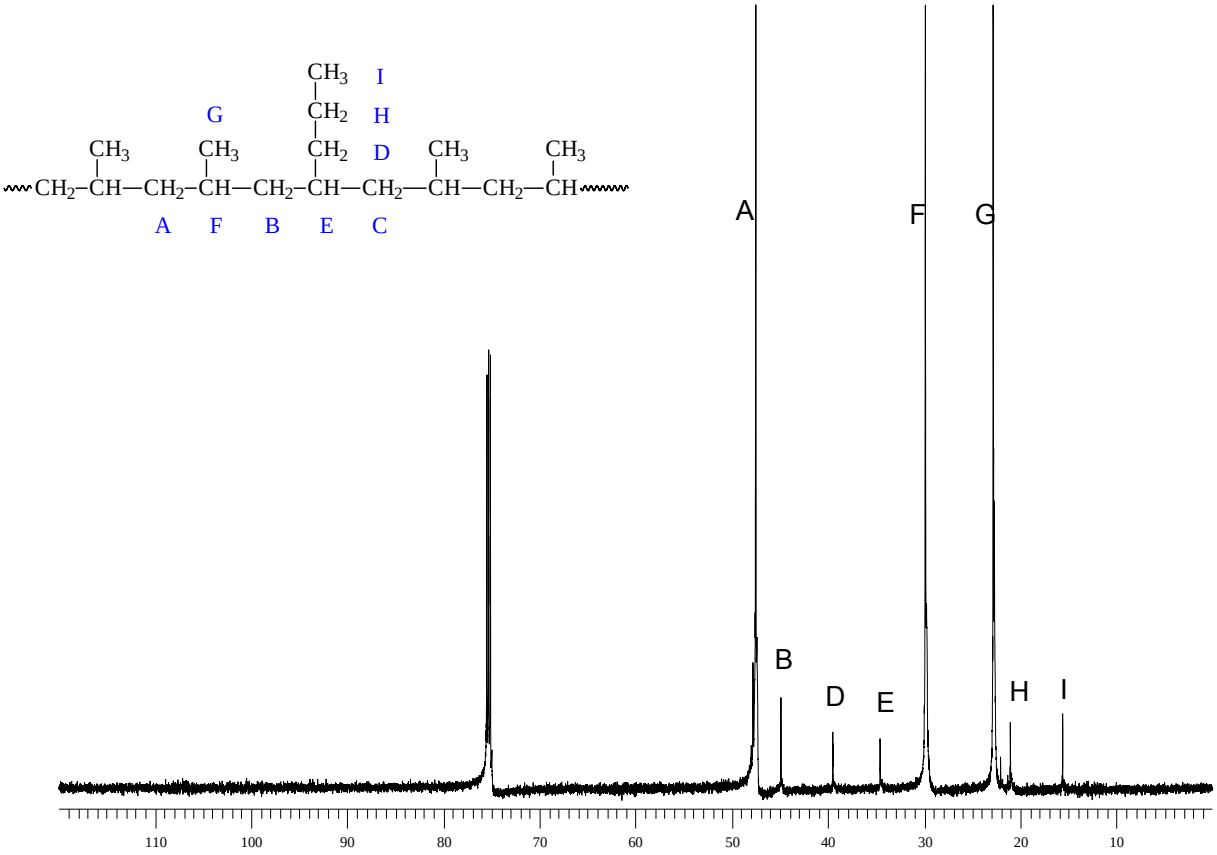

Figure 3: ^{13}C NMR spectrum of the propylene-1-pentene sample (S139), dissolved in deuterated tetrachloroethane showing the allocation of all spectrum peaks.

A summary of the chemical shifts of the peaks are given in Table 4.

Table 4: ^{13}C NMR shifts of the peak identified in Figure 3

Peak	Chemical shift (ppm)
A	44.583
A	44.407
A	44.298
A	44.175
B	41.683
D	36.320
E	31.365
F	26.775
F	26.665
F	26.540
G	19.785
G	19.675
G	19.543
H	17.882
I	12.473

Areas under the different peaks were integrated for the calculation of the pentene content. The pentene content was determined using the following formula:

$$\% \text{ pentene} = \frac{2\int \text{Branched carbons}}{\sum \int \text{Backbone Carbons}} \quad (7.1)$$

therefore:

$$\% \text{ pentene} = \frac{2\int \text{Peak E}}{\sum \int \text{Peak A+B+C+E+F}} \quad (7.2)$$

Stereo-errors may occur during the polymerisation process. These stereo-errors may be due to misinsertions of the monomer unit. The methyl-centered pentad distributions in the homopolymer and the copolymers were determined. In addition to the mmmm pentad, mmmr, mmrr and mrrm pentads were detected (Figure 4)in the propylene methyl region (region G in Figure 3). These pentads are characteristic of misinsertions taking place in the polymer. The stereorerrors appear to increase with increasing levels of comonomer. The ^{13}C NMR results are given in Table 5.

At low pentene incorporation, the tacticity of the copolymer was only slightly lower than the homopolymer. In the two commercial propylene-1-pentene copolymers studied in the previous chapter (low pentene contents), the tacticity was virtually unaffected by the incorporation of pentene.

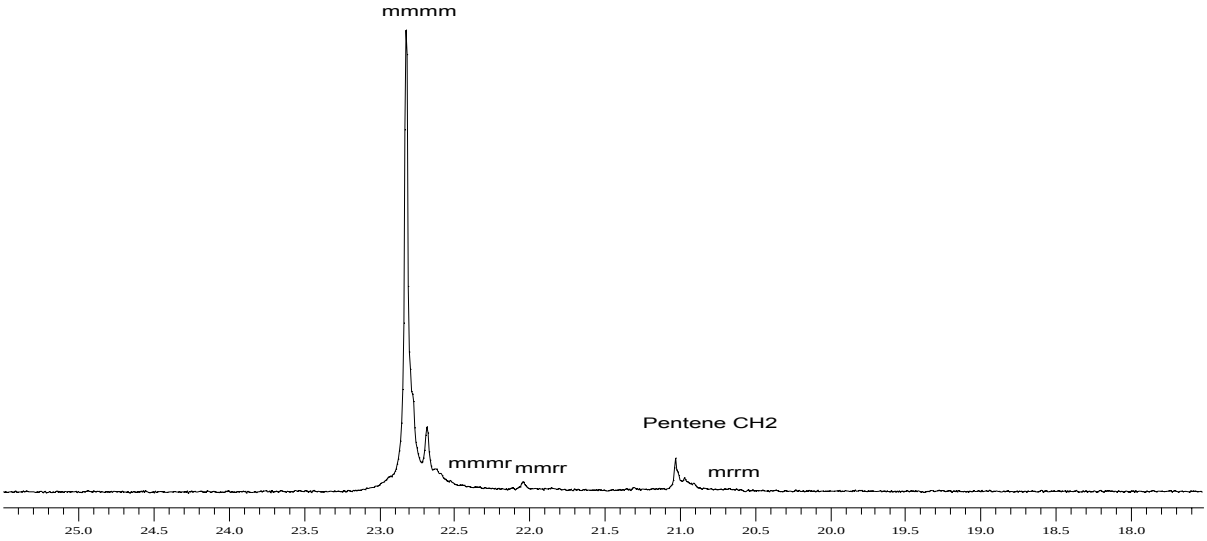

Figure 4: Stereo-errors present in the ^{13}C NMR spectrum of sample S139.

In sample S143, with a similar pentene content to sample P2, the tacticity was also comparable to the homopolymer sample (sample S137). In this study, the isotacticity is given as molar fractions of the isotactic pentads [mmmm]. The concentration of the mmmm, mmmr, mmrr and mrrm groups are reported relative to the propylene methyl region (region G in Figure 3). At higher pentene contents, the tacticity decreased significantly. This was due to an increase in the amount of stereoerrors in the samples.

Table 5: Pentene incorporated, tacticities and stereo-error data for the polypropylene homopolymer and propylene-1-pentene polymers evaluated in this study

Sample ID	Pentene incorporated (^{13}C NMR, mol%)	Isotacticity index (^{13}C NMR)	mmmm	mmmr + mmrr	mrrm
S137	0	94.73	94.70	4.62	0.65
S143	1.99	93.50	92.39	5.30	1.12
S139	2.93	91.06	90.14	7.02	1.83
S157	6.91	88.61	86.76	6.87	4.28
S150	7.82	84.92	82.87	10.84	3.88

Figure 5 shows the effect of the quantity of pentene in the feed vs pentene incorporated, as determined by ^{13}C NMR.

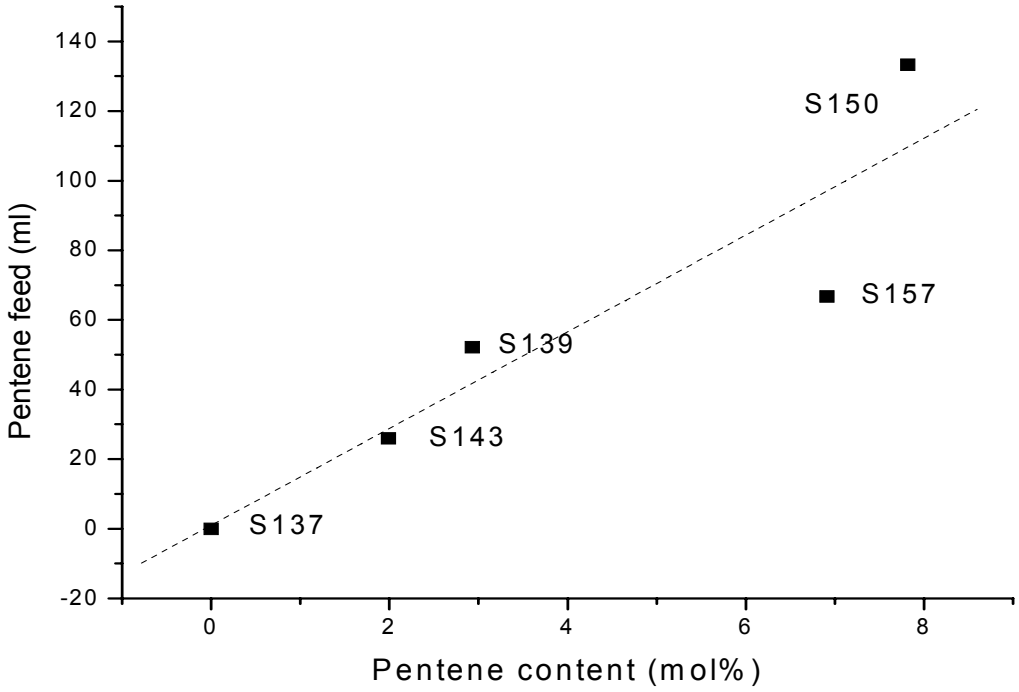

Figure 5: Quantity of pentene incorporated into the propylene-1-pentene copolymers at different pentene feed volumes.

There was a good correlation between the increase in the pentene content in the copolymers and the increase in the pentene feed. In Figure 6 the effect of pentene incorporation on the isotacticity can be seen. A linear decrease was found in the tacticity with an increase in the pentene content.

There was a significant increase in the stereo-errors with an increase in the pentene content. The presence of a bulkier comonomer, therefore, resulted in more stereo-errors in the final product.

7.4.4 FTIR analysis of the undegraded polypropylene samples

The molecular structure of the polypropylene homopolymer and the propylene-1-pentene copolymers was also quantified by FTIR analysis. The FTIR spectra of the samples are shown in Figure 7 and the increase in the 737 cm^{-1} peak, representative of the CH_2-rocking vibration of the 1-pentene-comonomer, is shown.

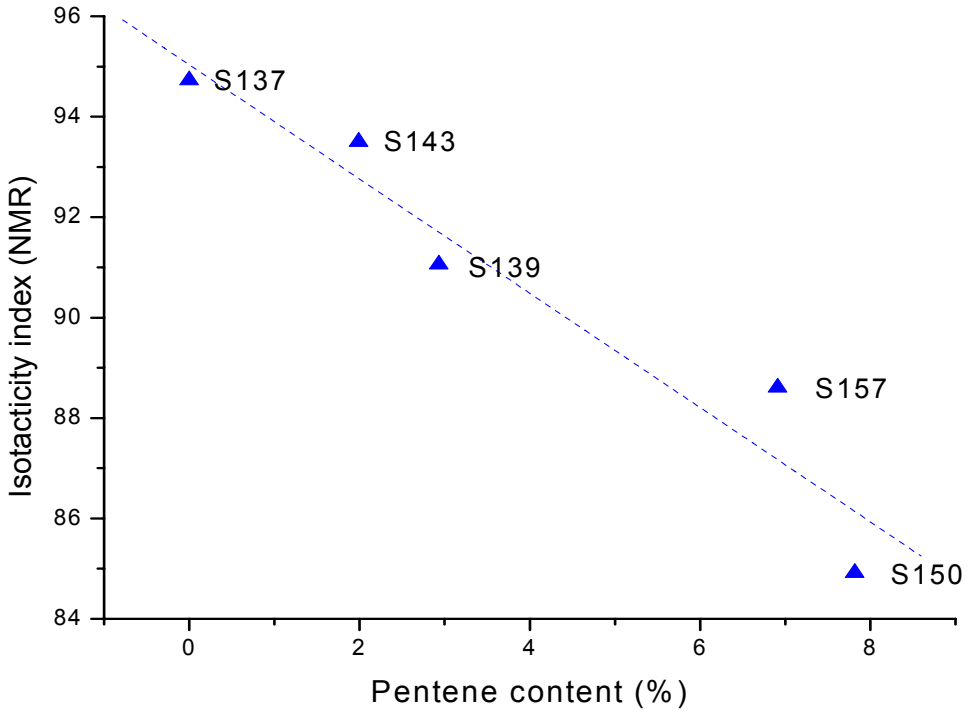

Figure 6: Effect of increasing pentene content on the isotacticity of several propylene-1-pentene samples

It was also already discussed that the ratio of the 973 cm^{-1} to the 997 cm^{-1} decreased with an increase in pentene content.

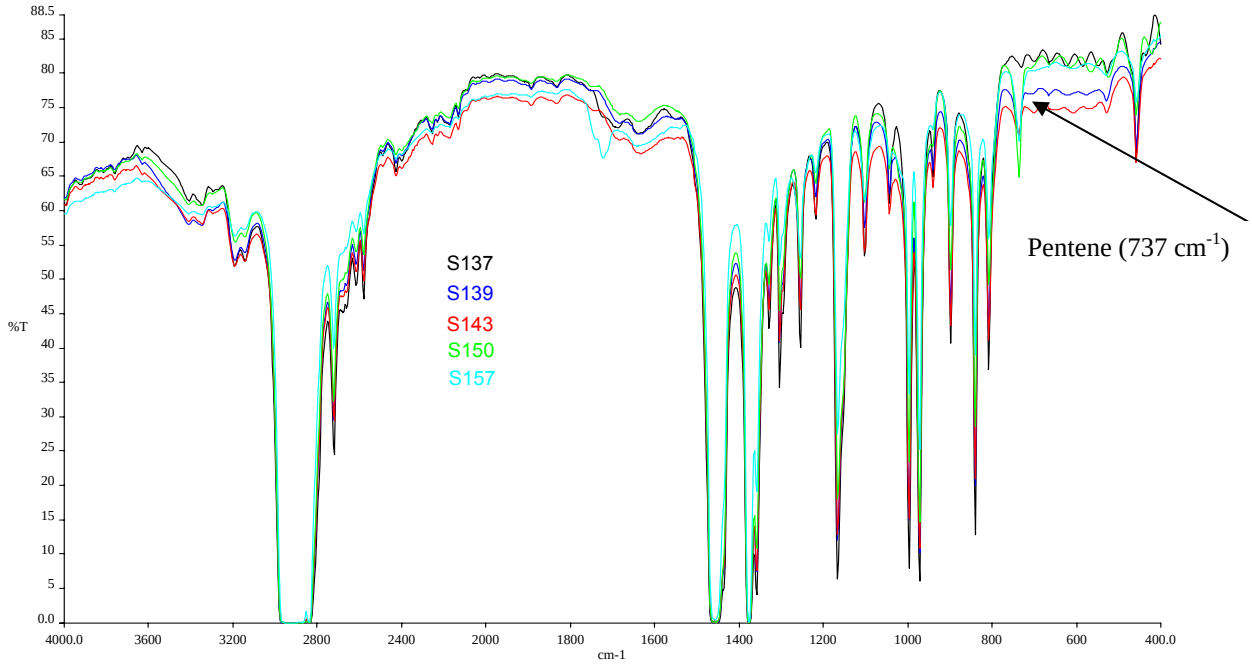

Figure 7: Transmission FTIR spectra of the PP homopolymer and propylene-1-pentene samples prepared with the same catalyst system.

7.4.5 CRYSTAF analysis of the undegraded polypropylene samples

The five undegraded samples, S137, S139, S143, S150 and S157, were analysed by CRYSTAF. In Figure 8 the CRYSTAF curves are shown.

The CRYSTAF curves provided complimentary information to the DSC curves: the homopolymer sample (S137) had the highest crystallisation temperature, the narrowest chemical composition distribution and the lowest soluble fraction. With an increase in the pentene content, there was a significant decrease in the crystallisation temperature. There was also a significant broadening of the crystallisation curves with an increase in comonomer content (<3%) and an increase in the soluble (non-crystallisable) fraction. At low pentene contents, this increase in soluble fraction was relatively small, but at higher pentene contents (>7%) the soluble fraction increased significantly. This may be indicative of the formation of highly branched polypentene sequences forming during the polymerisation process. These sequences will be unable to crystallise at room temperature.

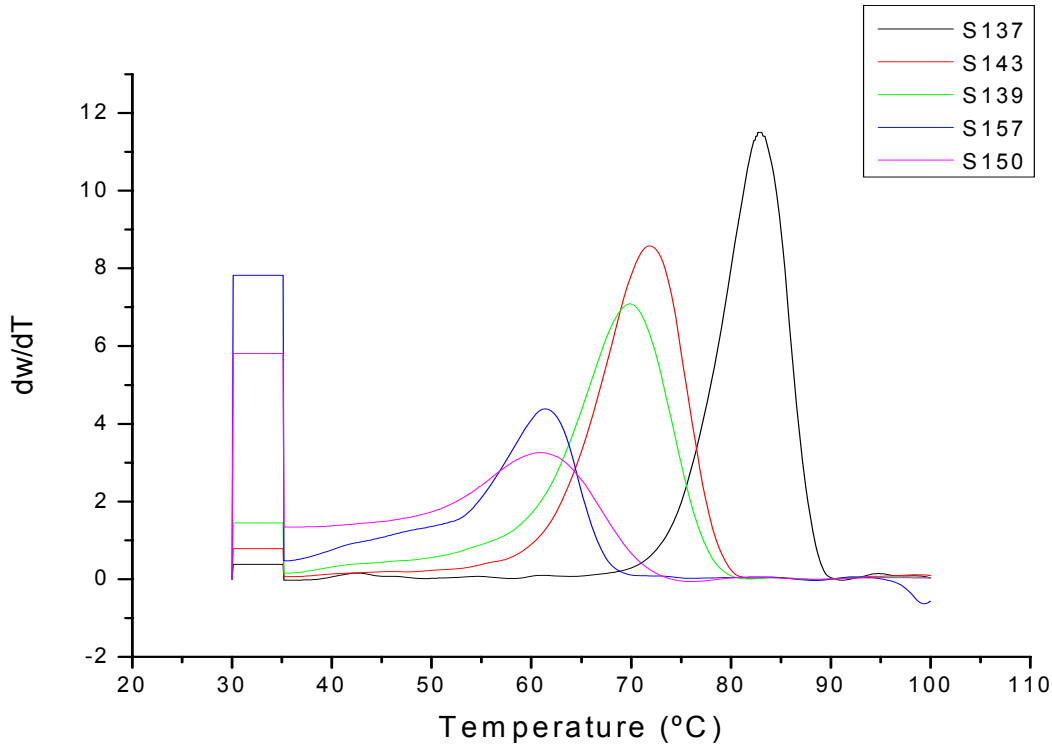

Figure 8: CRYSTAF crystallisation curves of the polypropylene homopolymer and propylene-1-pentene samples.

In Figure 9 it can be seen that there is a non-linear dependence of the soluble fraction on the pentene content. At low pentene content (<3%) the polymer chains were still be able to crystallise from solution. At higher pentene contents (>3%), the branching frequency will be such that it results in chains that are unable to crystallise.

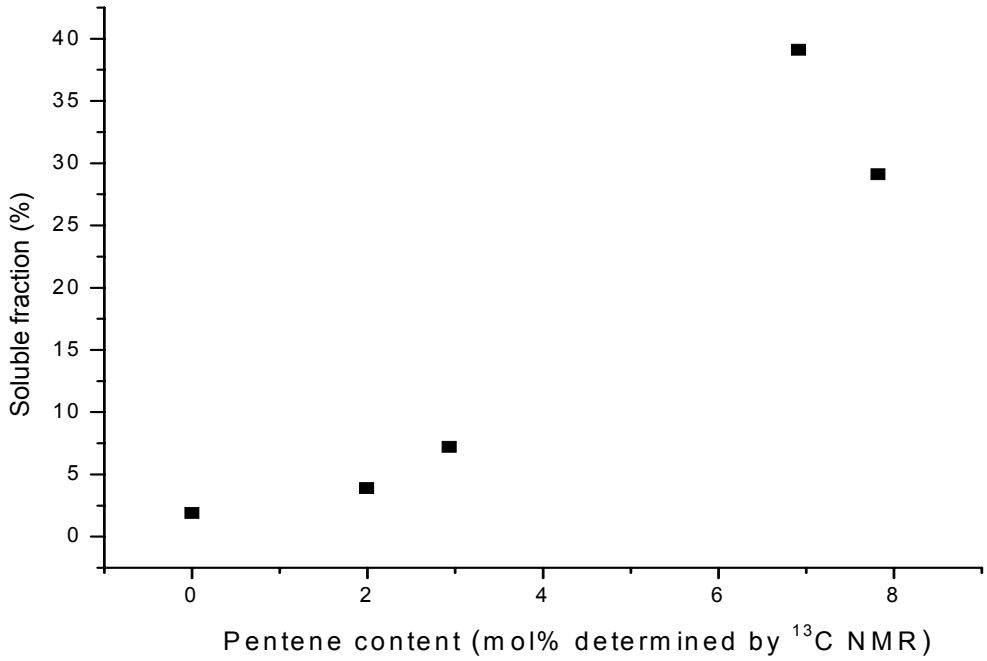

Figure 9: Increase in the soluble fraction of the propylene-1-pentene copolymer samples with an increase in pentene content.

7.5 Thermo-oxidative degradation of the samples

7.5.1 FTIR analysis of the degraded samples

FTIR scans were performed on a Perkin Elmer Spectrum 2000 spectrophotometer. In Figure 10 the increase in the carbonyl content of the samples with progressing thermo-oxidative degradation is shown.

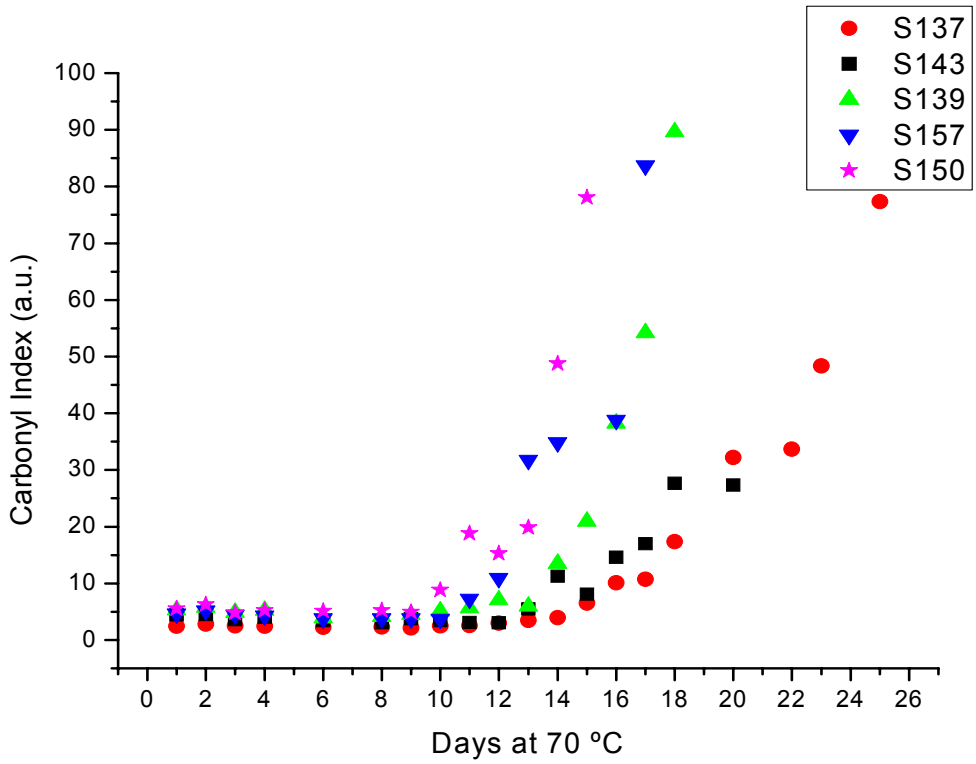

Figure 10: Increase in carbonyl index of the samples with increasing degradation time at 70 ºC.

Figure 10 shows that the samples degraded according to pentene content. Sample S150 (highest pentene content) degraded significantly faster than the samples with lower pentene content. Sample S137 (polypropylene homopolymer) degraded the slowest, and samples S143, S139 and S157 degrading according to pentene content.

The crystallinity appeared to correlate with a 50% increase in carbonyl index, with an R^2 value of more than 88% (Figure 11). This confirms findings by Marshall [8], namely that the rate of carbonyl index increase can be correlated with the initial crystallinity.

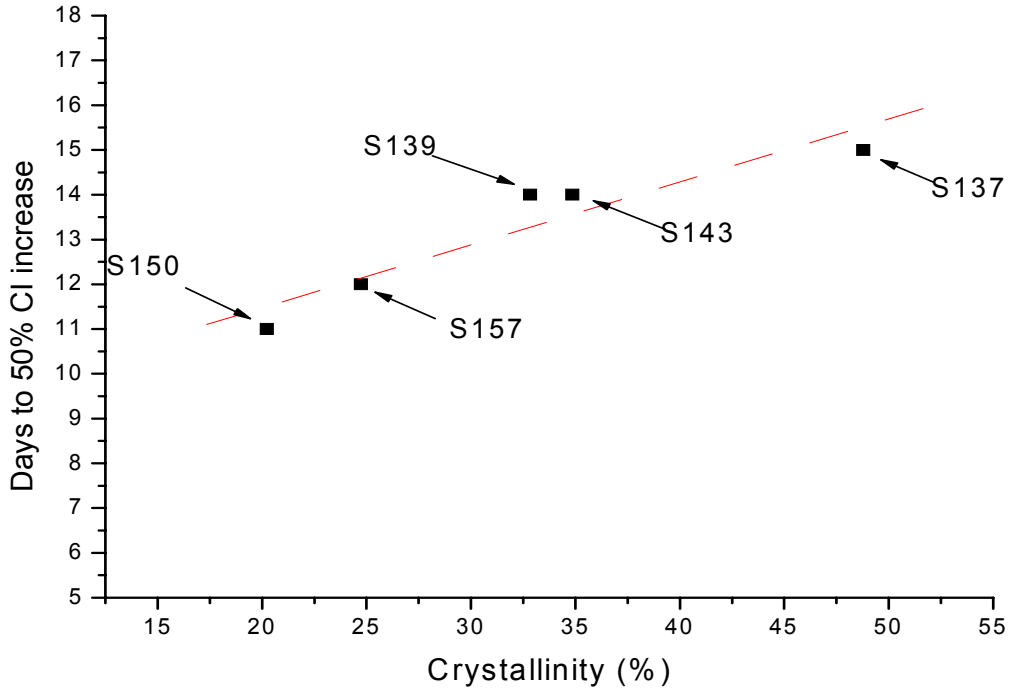

Figure 11: Effect of crystallinity on the 50% carbonyl index increase.

Another variable that was investigated was the influence of the initial molecular weight on the degradation behaviour of the samples. Several investigations have shown that degradation behaviour is independent of the molecular weight [8]. In the current study it was found that the sample with the highest molecular weight (S150) degraded the fastest. The molecular weight of the homopolymer was comparable to that of sample S150 (93,600 g/mol), but the homopolymer had significantly higher stability than sample S150. A linear correlation factor (R^2 value) of less than 10% was found. The degradation behaviour of the set of propylene-1-pentene samples was, therefore, virtually independent of molecular weight (Figure 12).

7.5.2 Molar mass determinations of the degraded samples

The effect of degradation on the number of scissions (calculated by the method described in section 6.5.3.1) is given in Figure 13. Sample S137 (pp homopolymer) showed the slowest increase in the number of scissions (slowest degradation) followed by S143 (lowest pentene content). Sample S150 degraded the fastest, followed by S157. There was a reasonable correlation between the sequence of degradation and the chemical composition as determined by FTIR and by SEC.

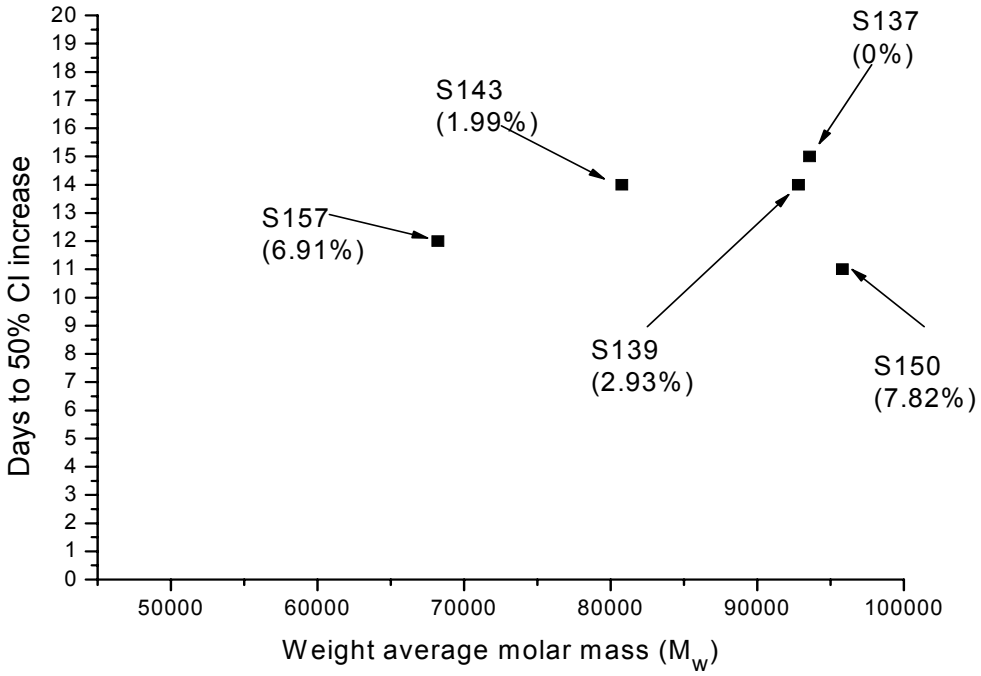

Figure 12: Effect of molar mass on the time to 50% increase in carbonyl index.

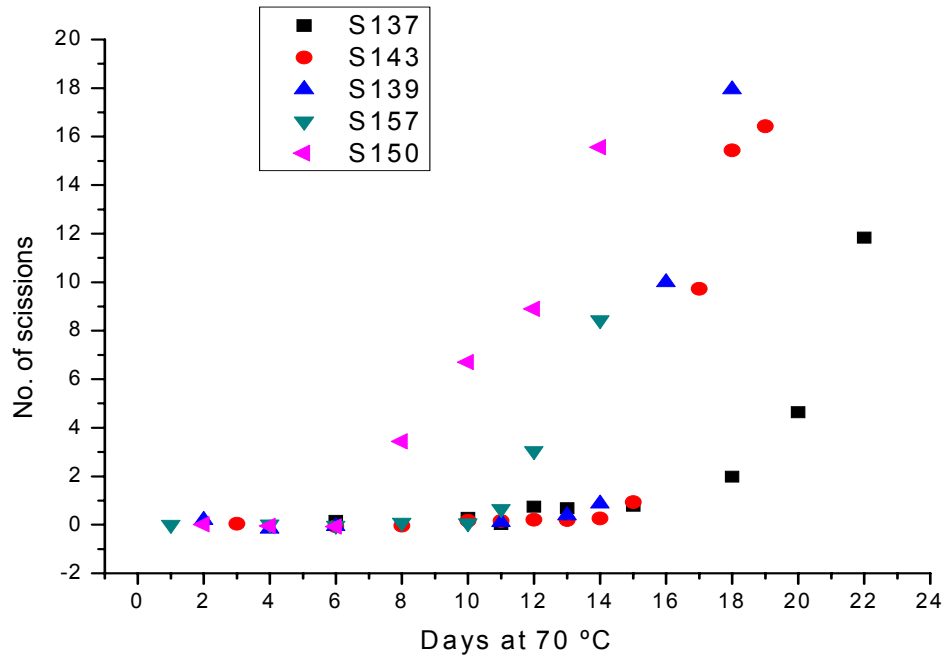

Figure 13: Effect of degradation on the number of scissions of the polypropylene homopolymer (S137) and the propylene-1-pentene copolymer samples (S139, S143, S150 and S157).

Molar mass averages decreased to a minimum of around 2000 g/mol, after which no further decrease in molar mass was noted. The final molar mass consisted of a combination of undegraded crystalline material and highly degraded amorphous material.

7.5.3 SEC-FTIR behaviour of the degraded samples

The SEC-FTIR behaviour of the degraded samples was studied under the standard conditions described in Chapter 6 (Section 6.4.9) to determine whether there was any difference in the degraded samples with regard to carbonyl distribution as a function of molecular weight. In Figure 14 the SEC-FTIR curve for S143 (low pentene contents) after 18 days of degradation at 70 ºC is given.

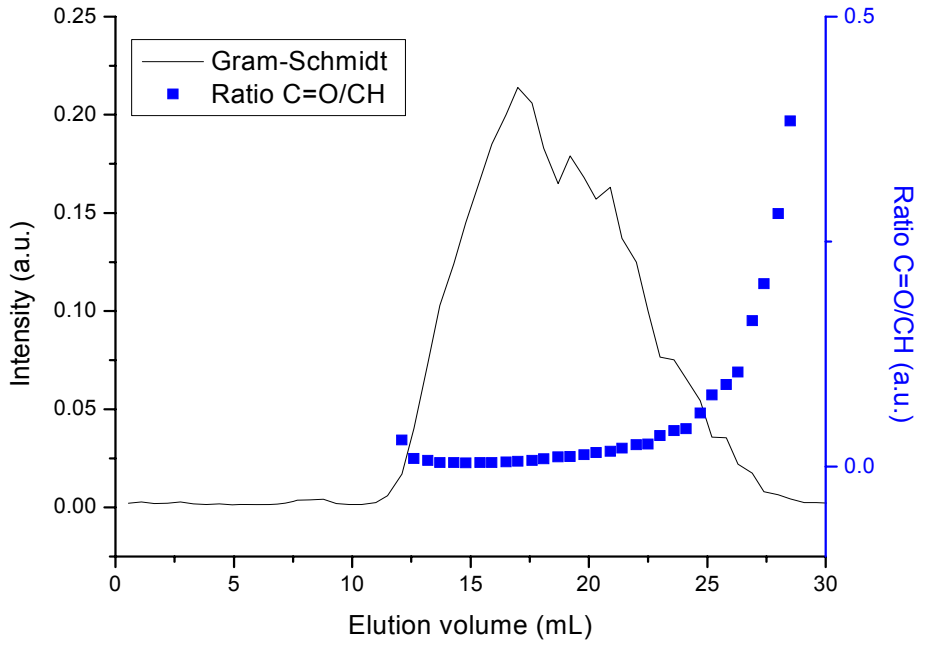

Figure 14: Carbonyl concentration as a function of molar mass in sample S143, degraded for 18 days at 70 ºC, showing a high concentration of carbonyl groups in the low molar mass region.

The highest carbonyl concentration was detected in the low molar mass region. Figure 15 shows the molar mass distribution and carbonyl concentration of sample S157 containing 6.9% pentene (relatively high pentene content) after degradation for 18 days at 70 ºC. Again, the highest carbonyl concentration was present in the low molar mass region of the sample.

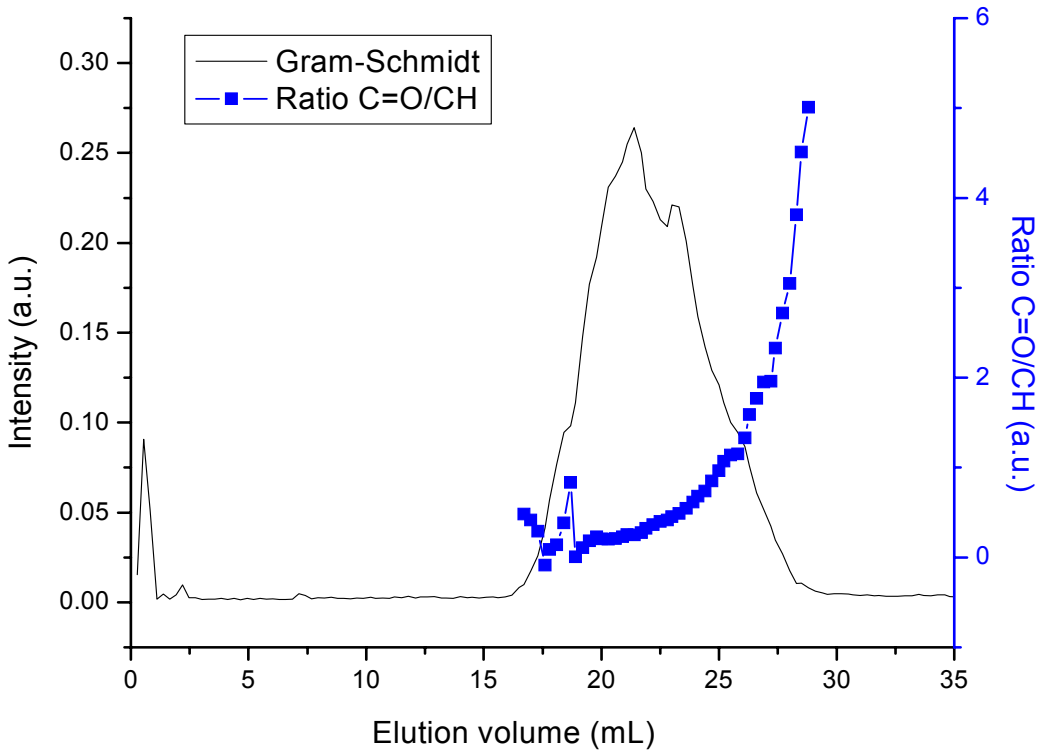

Figure 15: Carbonyl concentration as a function of molar mass in sample S157 degraded for 16 days at 70 ºC, showing a high concentration of carbonyl groups in the low molar mass region.

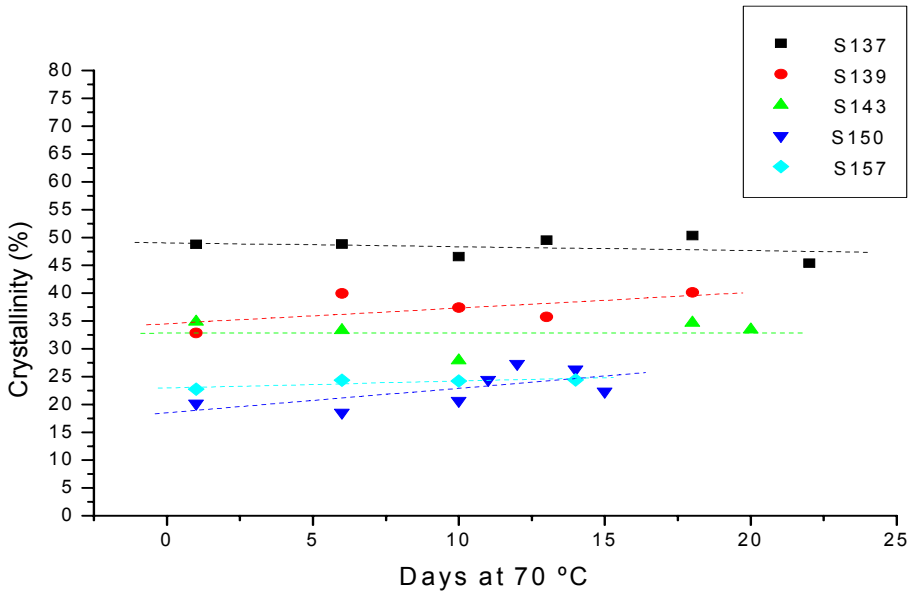

Figure 16: Percent crystallinity of the polypropylene homopolymer and the propylene-1-pentene copolymer samples, determined as a function of degradation time.

7.5.4 DSC behaviour of the degraded samples

DSC analysis was performed on the undegraded and degraded samples. The results are shown in Figure 16. Similar to the results in Chapter 6 (Section 6.5.7), the increasing degradation time resulted in no change, except for a small increase in crystallinity of the copolymer samples.

7.6 Conclusions

The main objective of this section was to study the effect of the incorporation of higher levels of pentene incorporation on the structure and copolymer stability. A propylene homopolymer and a series of propylene-1-pentene copolymers were synthesised using similar reaction conditions and the same Ziegler-Natta catalyst system. Molar masses of the samples were similar, with only small differences in the weight average molar masses. Polydispersity indices were generally around 4, typical of Ziegler-Natta catalysed systems. With an increase in the pentene content, a significant decrease was noted in the crystallinity (measured by DSC), decreasing from 48% for the homopolymer to 20% for a propylene-1-pentene copolymer containing 7.82% pentene. CRYSTAF analysis generally indicated a decrease in the crystallisation temperature, a broadening of the chemical composition distribution and an increase in the soluble fraction with an increase in pentene content. NMR analysis showed similar tacticities for the homopolymer sample and samples at low pentene addition, but at higher pentene contents (>3%) a significant reduction in the isotacticity was found. Stereo-errors also generally increased with an increase in the pentene content. FTIR analysis indicated that the samples degraded according to pentene content, with the sample containing the highest pentene content degrading at the fastest rate. The polypropylene homopolymer showed the longest induction period and degraded last. The thermo-oxidative degradation process was shown to be highly dependent on the crystallinity and independent of the molar mass. The SEC results indicated similar trends.

7.7 References

[1] La Mantia, F.P., *Polymer Degradation and Stability* **1985**, 13, 297-304

[2] Sacchi, M.C., Forlini, F., Losio, S., Tritto, I., Wahner, U.M., Tincul, I., Joubert, D. J., Sadiku, E. R., *Macromol. Chem. Phys*. **2003**, 204, 1643-1652

[3] Wahner, U.M., Tincul, I., Joubert, D.J., Sadiku, E.R., Forlini, F., Losio, S., Tritto, I., Sacchi, M.C., *Macromol. Chem. Phys.* **2003**, 204, 1738-1746

[4] Assumption, H.J., PhD thesis, University of Southern Mississippi, **December 2003**

[5] Graef, S.M., PhD thesis, University of Stellenbosch, **December 2002**

[6] Busico, V., Cipullo, R., *Progress in Polymer Science* **2001**, 443-533

[7] Busico, V., Cipullo, R., Monaco, G., Segre, A.L., *Macromolecules* **1997**, 30, 6251

[8] Marshall, N., PhD thesis, University of Sussex, **December 2001**

Chapter Eight

Effect of processing on propylene-1-pentene copolymer stability

8.1 Introduction

8.1.1 Factors affecting the extrusion process

In the oven-aging studies of the commercial propylene-1-pentene copolymers and polypropylene homopolymers it was shown that the unstabilised propylene-1-pentene copolymers were more prone to thermo-oxidative degradation at elevated temperatures compared to polypropylene homopolymers (Chapters 6, 7). The oxygen availability under oven-aging conditions is relatively high and the question arises as to whether the propylene-1-pentene copolymers will have lower stability under oxygen-deficient conditions compared to a polypropylene homopolymer. During extrusion of a polymer, the polymer is subjected to thermal and mechanical stress (thermo-mechanical degradation). These factors may promote chemical changes that could lead to degradation [1]. Several factors do influence the extrusion process, making the studying of the changes to a polymer during extrusion a very complex subject. Factors that do play a role include: initial molar mass of the polymer, polymer viscosity, temperature of extrusion, shear stress, extruder and die geometry, screw type and screw velocity. Canevarolo and Babetto [2] showed that the screw profile aggressiveness (compression ratio of the screw) will have a significant influence on polymer chain scission during extrusion. They found that the degradation of polypropylene during multiple extrusions resulted in a narrowing of the molar mass distribution curves and a shift towards lower molar masses. This shift in molar mass distributions and molar mass averages could be used to calculate the chain-scission distribution function during these multiple extrusions [3].

In an extruder the oxygen concentration is usually very low; the only oxygen present will be introduced in the hopper or dissolved in the polymer. The tacticity of the polymer also plays a role in oxygen absorption. Shlyapnikov et al. [4] modelled the absorption of oxygen in isotactic and atactic polypropylene. He showed that the oxygen solubility was significantly higher in the atactic polypropylene compared to the isotactic polypropylene.

Moss and Zweifel [5] evaluated the effect of oxygen during multiple extrusions. In the evaluations performed, the polymer powder was purged with nitrogen and all extrusions were performed under a nitrogen atmosphere. For an unstabilised HDPE sample, nitrogen had a positive effect on the stability of the virgin polymer, while the nitrogen had no effect on the stability of a stabilised sample. It was, however, shown that the consumption of the phosphite stabiliser was higher in the stabilised sample extruded in air compared to the sample

extruded under a nitrogen atmosphere. These studies show that oxygen has virtually no access to the melt and that air dissolved in the polymer or adsorbed on the surface is the only source of oxygen during the extrusion process. As the oxygen supply is limited, it decreases quickly as the polymer melt progresses through the extruder. The polymer is usually protected during the extrusion process by the addition of a phosphite stabiliser. In combination with phenols, the phosphite stabiliser provides excellent protection to the polymer against degradation during extrusion.

Hinsken et al. [6] postulated that during the multiple extrusions of polypropylene, the molar mass decrease could be attributed to ß-scission, the breakdown of peroxy radicals and shear. The relative importance of these three factors obviously depends on the extrusion conditions: higher temperatures will favour ß-scission while decreasing the importance of shear (the polymer viscosity decreases at higher temperatures). It is known that the solubility of oxygen in a polyolefin is comparable to that of a hydrocarbon liquid [6], so especially powders do have a significant amount of dissolved oxygen present. It was also shown that a Phillips HDPE sample showed an increase in molar mass due to crosslinking [5]. The shear in the extruder will, however, have an influence on polymer stability, especially in polypropylene that can easily degrade by β-scission.

Tochácek and Sedlar [7] monitored the consumption of phosphite stabilisers during multiple extrusions of stabilised formulations. In a comparison of the efficiency of four commercially-available phosphite stabilisers, he showed that the most efficient phosphite stabiliser is consumed faster than the less effective phosphites. The phosphite stabiliser, therefore, needs to be converted to an active species to participate in the stabilisation reaction. If the phosphite stabiliser is too stable, it will not participate in stabilisation (peroxide decomposition).

Marshall [8] studied the multiple extrusion behaviour of several stabilised, co-stabilised (primary and secondary stabiliser) and unstabilised polypropylene homopolymer samples. He found that the multiple extrusions of unstabilised polypropylene samples resulted in a significant decrease in the molar mass averages, while the stabilised polypropylene homopolymer samples showed little change, even after up to 17 multiple extrusions at 230 ºC or more than 5 extrusions at 260 ºC. In a stabilised sample the stability of the base polymer will be maintained as long as there is active anti-oxidant present in the polymer to protect the polymer.

8.1.2 Mechanisms during multiple extrusions

The shear forces, together with the high processing temperatures experienced during the extrusion processes, result in mechanical scission of the polymer chain. This results in the formation of highly reactive alkyl radicals. In the presence of oxygen, these alkyl radicals (R·) will be converted to peroxy radicals (ROO·). Hinsken et al. [6] postulated that several possible reactions could take place (Scheme 1). During extrusion (oxygen deficient conditions) only a small quantity of alkyl (R·) radicals are converted to ROO· radicals. Reaction 3 will result in the formation of the peroxy radical in the normal degradation route during oxidative degradation.

Reactions 1 (termination) and 2 (crosslinking) will result in an increase in molar mass. Reaction 2 will result in gel formation. These two reactions can occur during polyethylene degradation, but in polypropylene these two reactions are not favoured. Due to energetic reasons, reaction 5 is not likely at normal processing temperatures. Reaction 4 will lead to a reduction in the molar mass by forming a shorter polymer molecule and a terminal vinyl group.

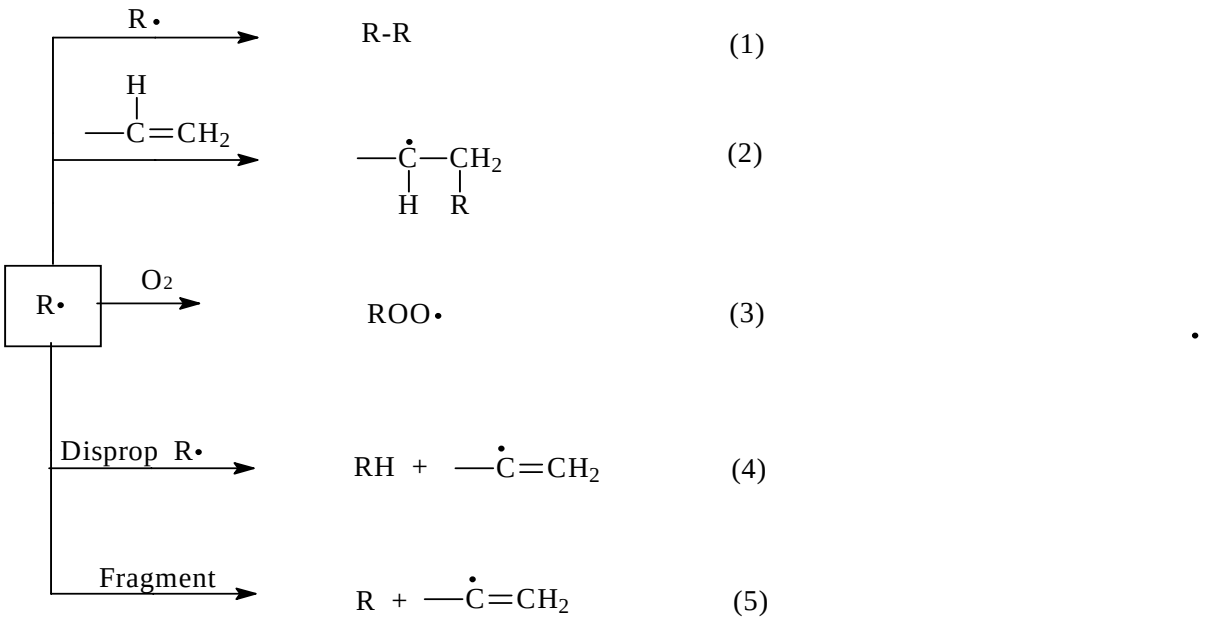

Scheme 1: Possible reactions during thermo-mechanical degradation of polyolefins including crosslinking, disproportionation and fragmentation reactions

Rheology characterisation can be useful in the evaluation of multiply-extruded samples. Several authors noted that rheology characterisation may provide useful information on the multiple extrusion process [8, 9]. A molten polymer behaves like a Newtonian fluid at low shear rates, but at higher shear rates there is a non-linear relationship between shear stress

and shear rate. The power law is used to describe the viscosity of a polymer under normal extrusion conditions [9].

$$\eta = m^{n-1} \qquad (8.1)$$

The coefficient *m* is a measure of the viscous nature of the polymer, while n, the power law index, is the measure of the shear thinning behaviour. The closer n is to 1, the more Newtonian a fluid is. The rheological behaviour of a polymer is directly related to the molar mass characteristics of a polymer. The length of a molecule is directly related to the viscosity (higher chain length will result in higher viscosity) and the wider the molar mass distribution curve, the higher the tendency to shear thin.

Polymers are visco-elastic, and rheology can be used to distinguish between the viscous and the elastic properties.

One can define the time dependent stress relaxation modulus G(*t*) as:

$$G(t) = \tau/\gamma \qquad (8.2)$$

where τ is the applied shear stress and γ is the shear strain.

With the application of a sinusoidal rotational shear strain, (like on a parallel plate rheometer) G will be a function of the applied rotational speed (ω) and can be written as:

$$G(\omega) = G'(\omega) + iG''(\omega) \qquad (8.3)$$

where G'(ω) is the elastic or storage modulus and G"(ω) is the loss modulus or the viscous component of the elasticity. The visco-elastic properties can be related to the molecular properties [9]. The crossover point between the loss and storage modulus can be related to the molar mass distribution.

8.2 Objectives

The overall objective of this section was to investigate the processing stability and degradation (effect of multiple extrusions) on an unstabilised polypropylene homopolymer and one propylene-1-pentene copolymer sample using FTIR, SEC and DSC. Fractionation,

rheology and CRYSTAF analyses were used to obtain more information on the degradation process. A second objective was to study the TREF fractions of an unextruded copolymer sample and compare that with the fractions of a polymer extruded five times. A mathematical model, recently developed by Prof S Canevarolo [2, 3], will be used to determine the amount of chain scissions as a function of molar mass. The oxidative degradation behaviour of extruded samples of the polypropylene homopolymer and the propylene-1-pentene copolymer was also investigated.

8.3 Experimental

8.3.1 Sample preparation

Two commercial, unstabilised polypropylene samples were obtained from the Sasol Polymers polypropylene plant in Secunda:

1. A polypropylene homopolymer (M_w = 415,000 g/mol)
2. A propylene-1-pentene copolymer (containing approximately 2% pentene) produced under similar reactor conditions to the above homopolymer (M_w = 519,000 g/mol)

The initial samples were received as powders and introduced into the Brabender PL 2000-6 Plasticorder single-screw extruder (19-mm screw, with a length-to-diameter ratio of 25 and screw speed set at 40 rpm), with all zone temperatures set at 220 °C. Subsequent extrusions were performed on the pelletised products of the previous extrusions. The product from each extrusion was re-introduced into the extruder hopper for further extrusions after removing a small sample for further analysis. Both samples were extruded five times.

All samples were characterised by SEC, FTIR, DSC and CRYSTAF analysis. Samples were also analysed by rheology measurements.

Multiple extruded samples were pressed into thin plaques and aged at 70 ºC in a heat circulating oven (Scientific Engineering).

8.3.2 SEC analysis of the PP homopolymer and propylene-1-pentene samples

Molar mass determinations were carried out on a Waters Alliance 2000 SEC instrument. Samples were prepared by dissolving 4 mg of sample in 4 mL of 1,2,4-trichlorobenzene. A

combination of Waters HT 3, 4, 5 and 6 columns were utilised for all SEC determinations. Calibration was performed using PL Easical™ standards.
Samples were analysed in duplicate and data manipulation was performed using Waters Millenium® software. All values are quoted relative to polystyrene standards and no universal calibration was carried out.

8.3.3 Rheology determinations of the PP homopolymer and propylene-1-pentene samples

Rheological evaluations were performed on a model SR500 Rheometric Scientific Dynamic Stress Rheometer. The temperature was set at 190 ºC and a gap of 1 mm was used. The experiments were run using parallel plate geometry, with a plate diameter of 25 mm. The frequency range from 490 – 0.03 rad/second was scanned.

8.3.4 FTIR analysis of the PP homopolymer and propylene-1-pentene samples

All FTIR analyses were carried out on a Perkin Elmer 2000 FTIR spectrophotometer. A total of 64 scans were acquired per spectrum and the resolution was set at 2 cm^{-1}. Integrations were performed using Perkin Elmer Spectrum™ software.

8.3.5 DSC characterisation of the PP homopolymer and propylene-1-pentene samples

All DSC characterisations were carried out on a TA Instruments DSC. Approximately 4 mg of sample were weighed accurately. All analyses were carried out by first heating the sample to 190 ºC to remove the thermal history. The sample was then cooled at 10 ºC/min to 30 ºC, followed by a linear heating step to 180 ºC.

8.3.6 CRYSTAF analysis of the PP homopolymer and propylene-1-pentene samples

CRYSTAF analyses were carried out on a Polymer Char model 200 CRYSTAF instrument. The instrument was equipped with five reactors. Approximately 20 mg of sample was used per analysis. All analyses were carried out in 1,2,4-trichlorobenzene. The dissolution time was 120 minutes at 160 ºC. This was followed by cooling to 95 ºC and stabilisation at 95 ºC for 45 minutes. A linear cooling profile was followed (0.1 ºC/ min) to 29 ºC.

8.3.7 TREF fractionation

The Holtrup TREF procedure used in this chapter involved the dissolution of 5 g of the polymer in 400 ml boiling xylene. Agitation was created using boiling beads of a magnetic stirrer. The polymer was precipitated by cooling the solution to 25 °C, at a cooling rate of 6 °C/h, using a programmable thermostat and no support material.

8.3.7.1 The first fractionation step: A suspension of polymer crystals was introduced into the fractionation vessel and heated to the first elution temperature (for example 60 °C). The polymer crystals were agitated by the vibromixer for 20 minutes. Then the polymer in solution was discharged through the lower drainage valve, whereas the remaining undissolved polymer crystals remained in the fractionation vessel. The hot solution was discharged into 800 mL of refrigerated, cold acetone (temperature < 0 °C) and the eluted polymer was precipitated. The precipitate was filtered through Büchner-funnels (glas frit No.3) and washed with refrigerated acetone (temperature < 0°C). The isolated polymer fractions were then dried for about 24 hours at 60°C in vacuum, and weighed.

8.3.7.2 The second and subsequent steps: The temperature of the fractionation vessel was increased to the next desired temperature and 400 ml of xylene of the same temperature was introduced into the fractionation vessel. The remaining polymer crystals in the apparatus were then agitated by the vibromixer for 20 minutes. The polymer solution was again discharged, the dissolved polymer precipitated and filtered, and the isolated polymer dried as described in the first step.

Nine fractions were obtained at the following fractionation temperatures: 60, 70, 76, 81, 86, 91, 96, 105 and 125 ºC. This step was repeated at the subsequent temperatures, until approximately 125 °C, the boiling point of the solvent. At this temperature all the crystallised material was extracted.

8.4 Results

8.4.1 SEC results of the extruded polypropylene samples

Several authors found that melt flow index measurements can be used to study the effect of multiple extrusions on polyolefins [1, 5-8, 10-12. Multiple extrusions result in an increase (typically for polypropylene) or a decrease (typical for some polyethylene samples, for

example chromium-catalysed HDPE) in the MFI. MFI measurements, however, only give one data point. The melt flow index is the mass of polymer going through a small die in 10 minutes. MFI measurements cannot provide information on the change in the molar mass averages and the polydispersity indices. SEC results can provide this information. The effect of multiple extrusions on the molar mass distribution curves of the polypropylene homopolymer and propylene-1-pentene copolymer are shown in Figures 1 and 2 respectively.

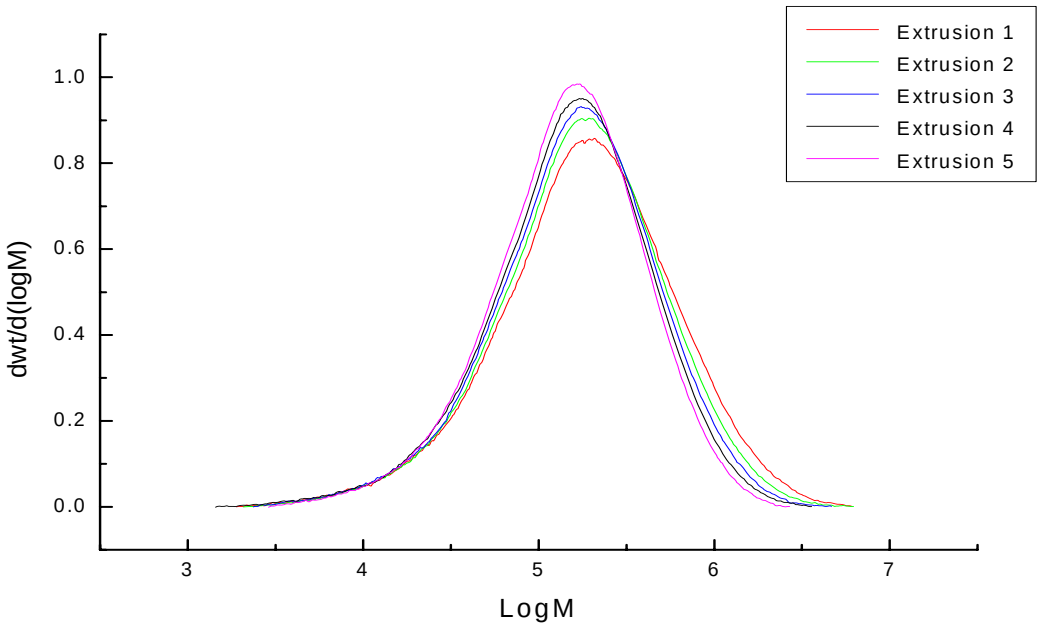

<u>Figure 1:</u> Effect of multiple extrusions on the molar mass distribution curves of a polypropylene homopolymer showing a significant reduction on the M_z side of the molar mass distribution.

The molar mass distribution curves show that there was an overall shift in the molar mass distribution curves of both the homopolymer and the copolymer during multiple extrusions. This stepwise decrease in molar mass is typical for a sample where scission of the polyolefin sample is the dominant mechanism (no crosslinking). It can also be seen that the high molar mass side (M_z) decreased more than the M_n side of the molar mass distribution curves.

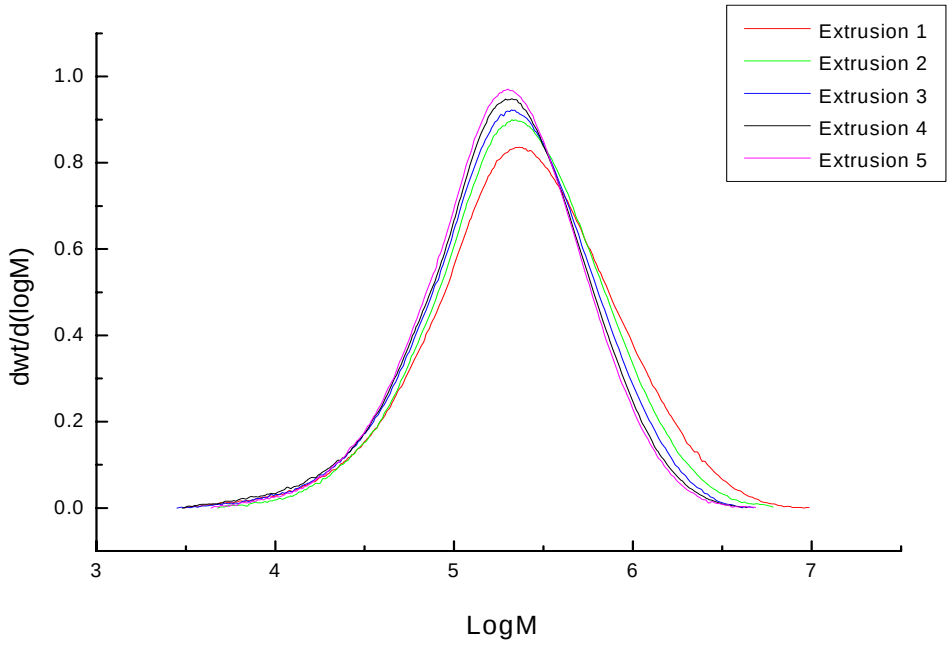

Figure 2: Effect of multiple extrusions on the molar mass distribution curves of a propylene-1-pentene copolymer showing a significant reduction on the M_z side of the molar mass distribution.

The individual molar mass averages were compared to investigate whether the various molar mass averages were affected to different degrees by the multiple extrusions. The changes in molar mass averages and polydispersity index values are given in Table 1.

Table 1: Effect of multiple extrusions on the molar mass averages and PDIs of the polypropylene homopolymer and the propylene-1-pentene samples

	Propylene-1-pentene copolymer				Polypropylene homopolymer			
Extr no	M_n	M_w	M_z	PDI	M_n	M_w	M_z	PDI
0	113,600	519,300	1,616,900	4.58	87,100	415,300	1,214,900	4.77
1	115,100	448,100	1,290,000	3.89	86,800	339,300	924,100	3.91
2	123,800	381,800	970,000	3.09	88,100	299,900	765,800	3.40
3	105,800	331,900	762,400	3.14	83,400	270,100	635,400	3.24
4	102,600	309,000	697,500	3.02	74,300	245,900	558,800	3.31
5	109,200	297,700	665,300	2.73	80,800	225,000	468,900	2.78

The effect of multiple extrusions on the individual molar mass averages M_z, M_w, M_n and polydispersity values are plotted in Figures 3-6.

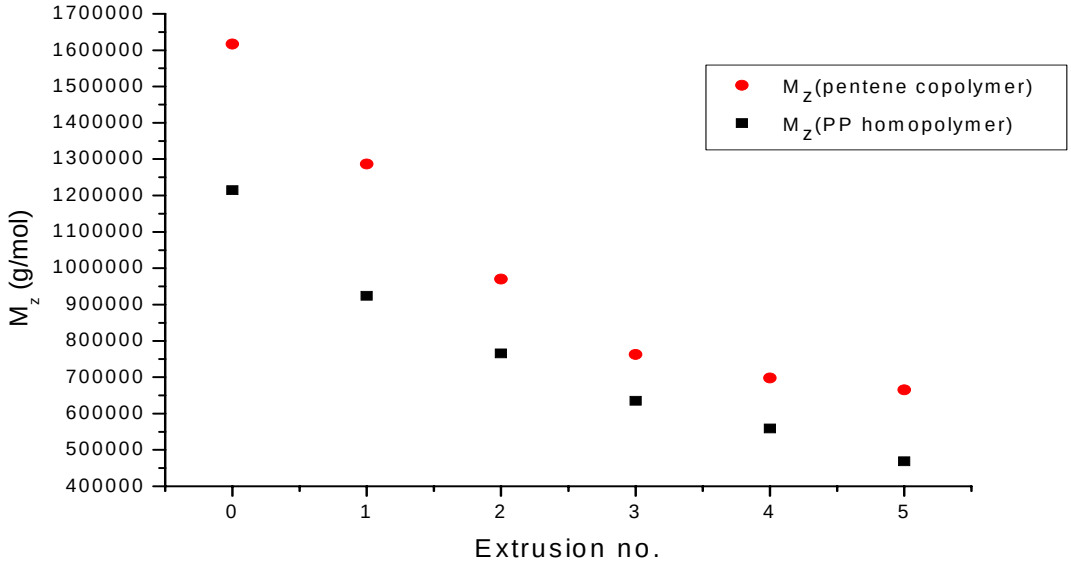

Figure 3: Effect of multiple extrusions on the M_z values with reductions in M_z values of both the homopolymer and the propylene-1-pentene with increasing number of extrusions.

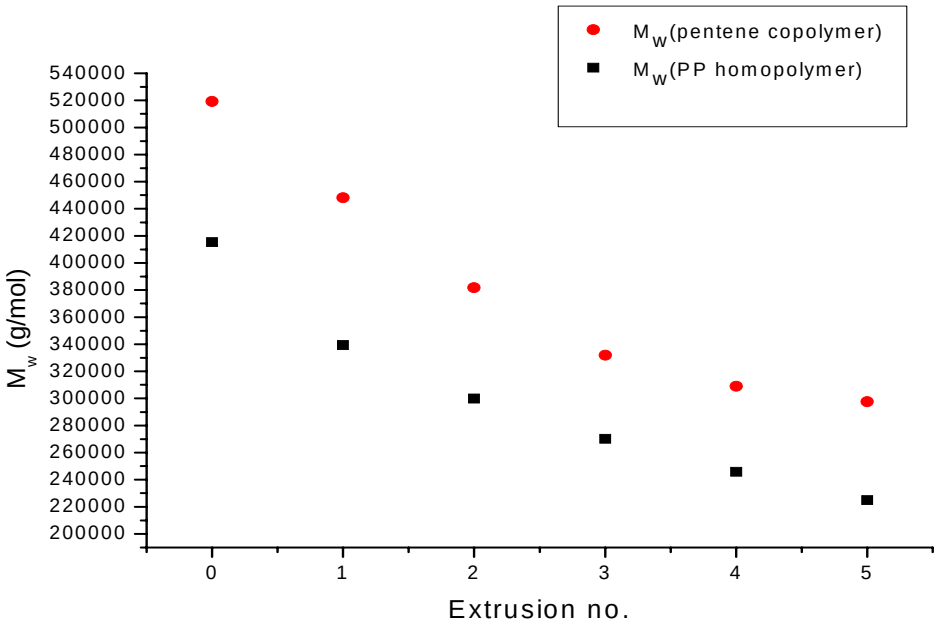

Figure 4: Effect of multiple extrusions on the M_w values with reductions in M_w values of both the homopolymer and the propylene-1-pentene with increasing number of extrusions.

The M_z and M_w averages decreased significantly and it was evident that the molar mass averages were affected to a different extent. The M_z value of the pentene copolymer decreased by 59% after five extrusions, similar to the homopolymer which decreased by 61% after five extrusions. After five extrusions the M_w value of the polypropylene homopolymer and the propylene-1-pentene copolymer both only decreased by about 43%. This was also

evident from the polydispersity values, showing a narrowing in the polydispersity values with each following extrusion. Comparing the different molar mass averages for a given polymer, it was evident that the M_z values decreased faster than the other molar mass averages. The longer chains were, therefore, attacked preferentially during the extrusion process. This is to be expected as the longer chains are more flexible and will be more entangled (higher entanglement density). During extrusion, the longer chains will have the highest viscosity and will, therefore, experience the highest shear. Mead [13] attributed this to the higher probability of a long chain to be subjected to random scission, which is higher than the probability that a shorter chain will be subjected to random scission (more sites for attack). Bueche [14] also showed that the probability of chain scissions was higher for the longer chains. Scission of a long polymer chain would yield smaller molecules, of about half the original size. According to Bueche [14], the chain scission occurs due to tensions concentrating close to the centre of the chain. He attributed these tensions to three factors: chain entanglements, viscosity (η) and shear rate (γ). The molar mass between entanglements is given by M_e. His work showed that the entanglements in a chain are very important in concentrating the tension in the centre of the chain. A longer chain will also be subjected to higher shear than a shorter chain (higher viscosity in the melt). A shorter chain can also have lubricating properties during the extrusion process.

The M_n values of both polymers only showed a small decrease during the multiple extrusions (Figure 5). These findings were in line with the findings by Gonzales-Gonzales et al. [15], who also showed a small linear decrease in the number average molar mass with an increase in extrusion number. They showed that this linearity was valid for multiple extrusions performed at 240 ºC, but showed that at higher temperatures the reduction in M_n was only linear up to 8 cycles with a rapid non-linear change up to 16 extrusions.

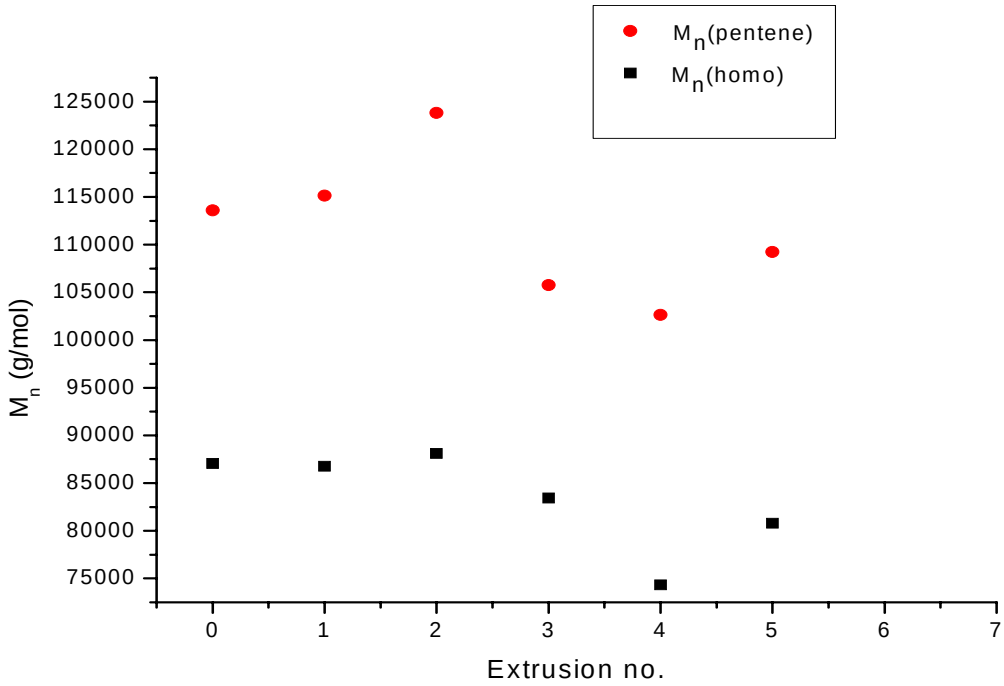

Figure 5: Effect of multiple extrusions on the M_n values.

The effect of the multiple extrusions on the polydispersity indices of both the polypropylene homopolymer and propylene-1-pentene copolymers is shown in Figure 6. The polydispersity indices decreased with each subsequent extrusion, leading to a further reduction in polydispersity. This can be directly correlated to the reduction in the concentration of the longer chains (reflected in the M_w and M_z values).

Gonzales-Gonzales et al. [15] showed that this reduction in PDI is not linear over a large number of extrusions (they used 19 extrusions) and it levels out after the initial linear decrease.

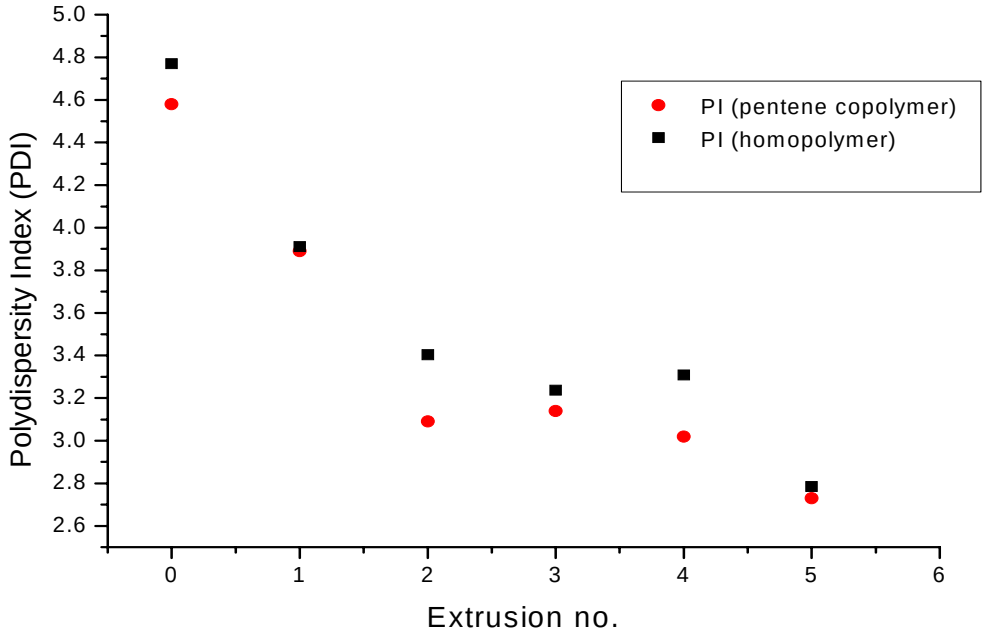

Figure 6: Effect of multiple extrusions on the PDI values showing that the polydispersity values generally decrease with an increase in the number of extrusions.

From the SEC results it would appear as if the stability of the propylene-1-pentene copolymer studied was similar to the polypropylene homopolymer, with similar reductions in the molar mass averages.

8.4.2 Rheology results of the extruded polypropylene samples

The zero shear viscosity of the propylene-1-pentene copolymer after one extrusion was higher than that of the polypropylene homopolymer. This is because of the significantly higher molar mass of the propylene-1-pentene sample after the first extrusion (448,000 g/mol vs 339,000 g/mol of the polypropylene homopolymer). The complex viscosity curves of the polypropylene homopolymer (Figure 7) and propylene-1-pentene copolymer (Figure 8) showed a decrease in the complex viscosity of both polymers with increasing extrusion number. In both cases, there was a linear decrease in the zero shear viscosity for the first 3 extrusions, followed by an area of less steep slope from extrusions 4 to 5.

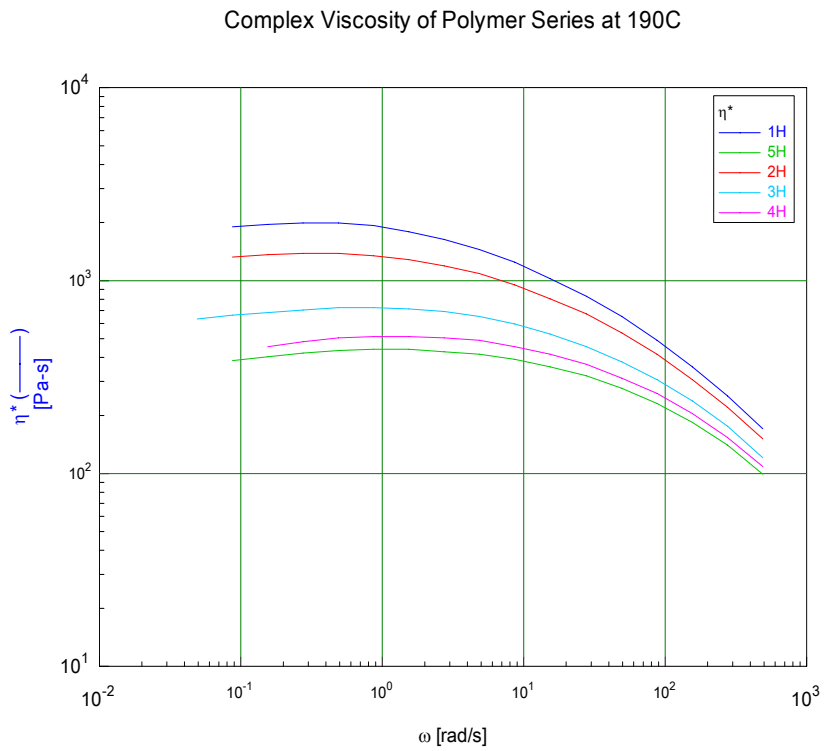

Figure 7: Complex viscosity measurements of the polypropylene homopolymer samples (extruded 1x, 2x, 3x, 4x and 5x) showing a reduction in the zero shear viscosity with an increase in the number of extrusions.

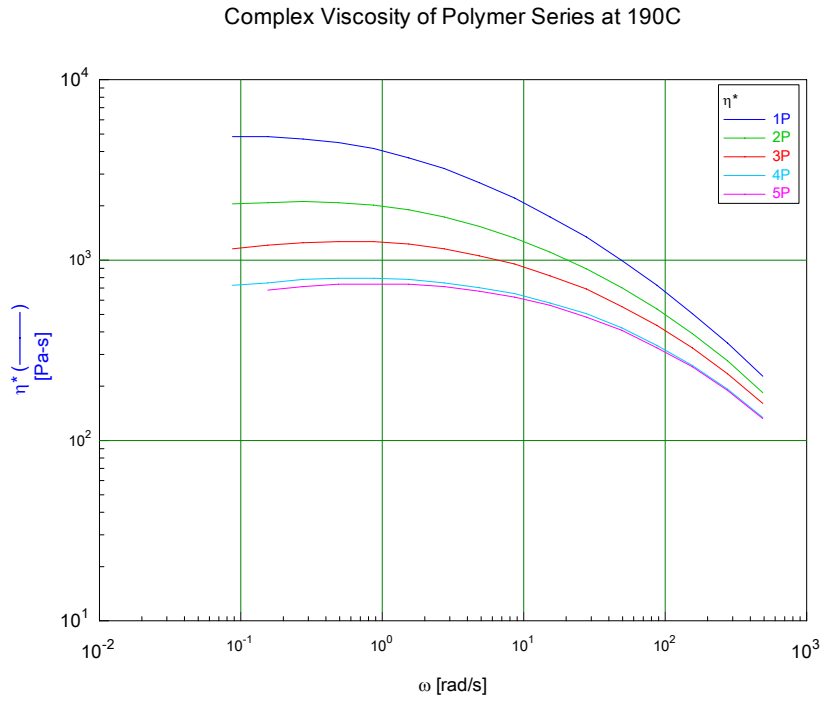

Figure 8: Complex viscosity measurements of the propylene-1-pentene copolymer samples (extruded 1x, 2x, 3x, 4x and 5x) showing a reduction in the zero shear viscosity with an increase in the number of extrusions.

As the molar mass is related to the zero shear viscosity, the zero shear viscosities were plotted against M_w. Initially the decrease in molar mass correlated well with the decrease in zero shear viscosity (linear decrease), followed by an area of non-linearity at low molar masses (Figure 9). This was due to a smaller decrease in the molar mass with a more significant decrease in zero shear viscosity.

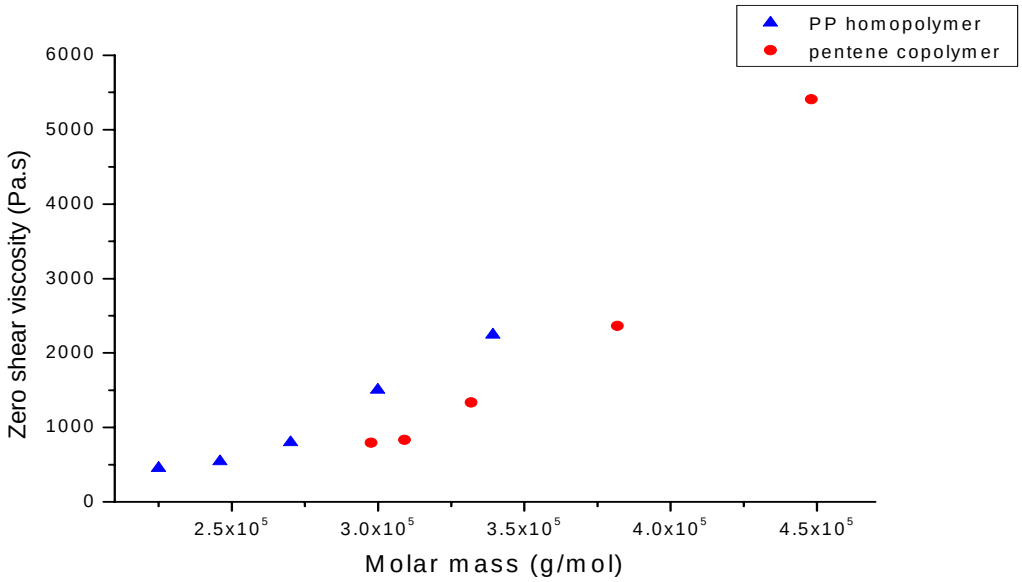

Figure 9: Correlation of the zero shear viscosity with the decrease in molar mass for the homopolymer and copolymer samples.

Although there was a deviation between the molar mass averages, as determined by SEC and rheology, both indicated a significant reduction in molar mass with increasing number of extrusions. The fundamentals of the two techniques are, however, vastly different and must be considered when comparing the values.

8.4.3 FTIR results of the multiply-extruded polypropylene samples

8.4.3.1 Carbonyl index

The FTIR spectra of the multiply-extruded polypropylene homopolymer sample and the propylene-1-pentene sample showed no significant change in either of the samples after the multiple extrusions (Figures 10 and 11). Focussing on the carbonyl area showed no increase in the carbonyl index with higher extrusion number. This is in line with the findings of Marshall [8] and others [15].

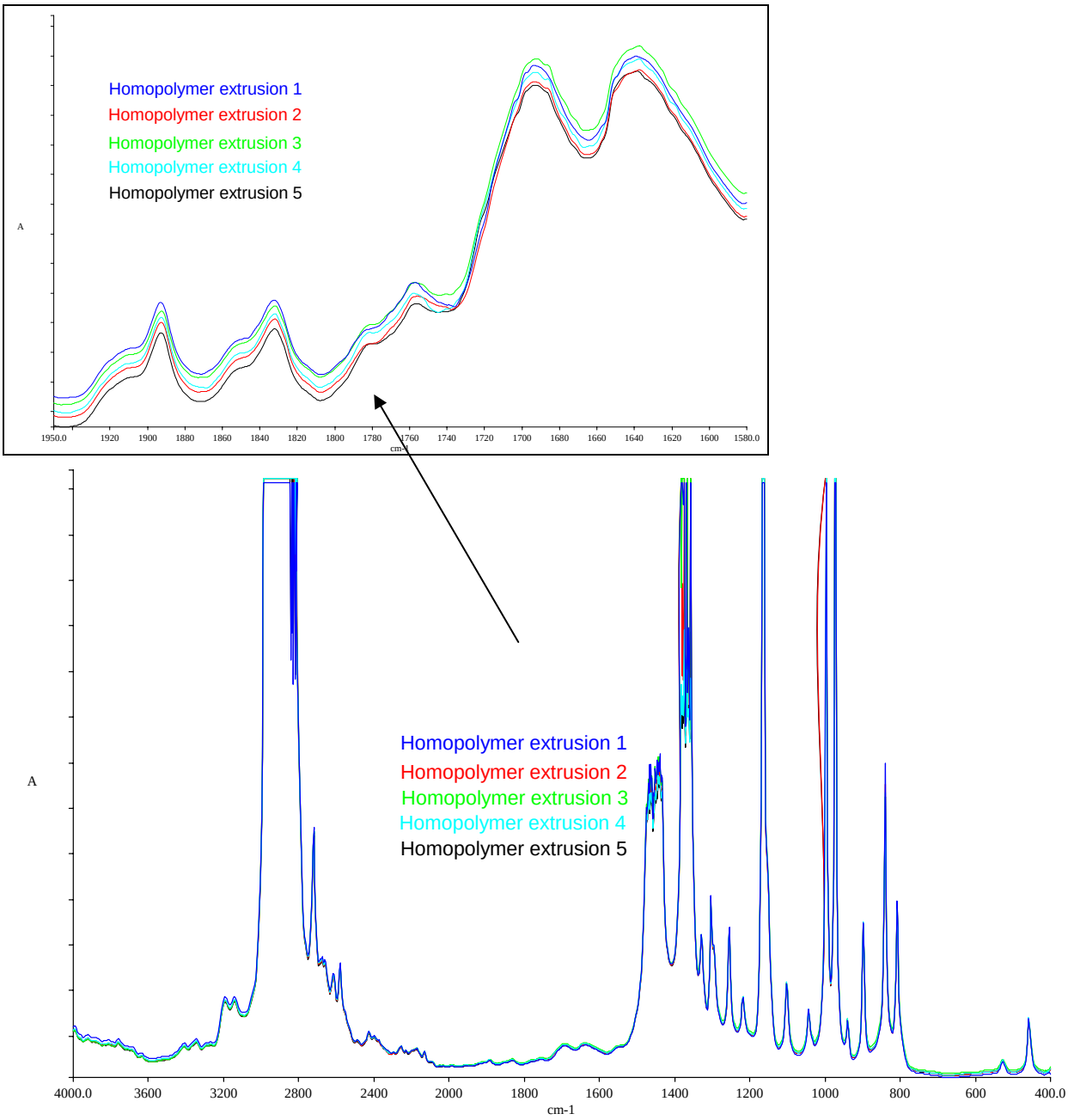

Figure 10: FTIR spectra of the multiply-extruded polypropylene homopolymer.

Gonzales-Gonzales et al. [15] and others showed similar findings for a commercial polypropylene sample. They showed that after up to 19 extrusions of a stabilised polypropylene homopolymer sample there was no significant increase in the carbonyl concentrations. It was attributed to the fact that almost no oxidative reactions took place during the extrusions. This finding was confirmed by Marshall [8].

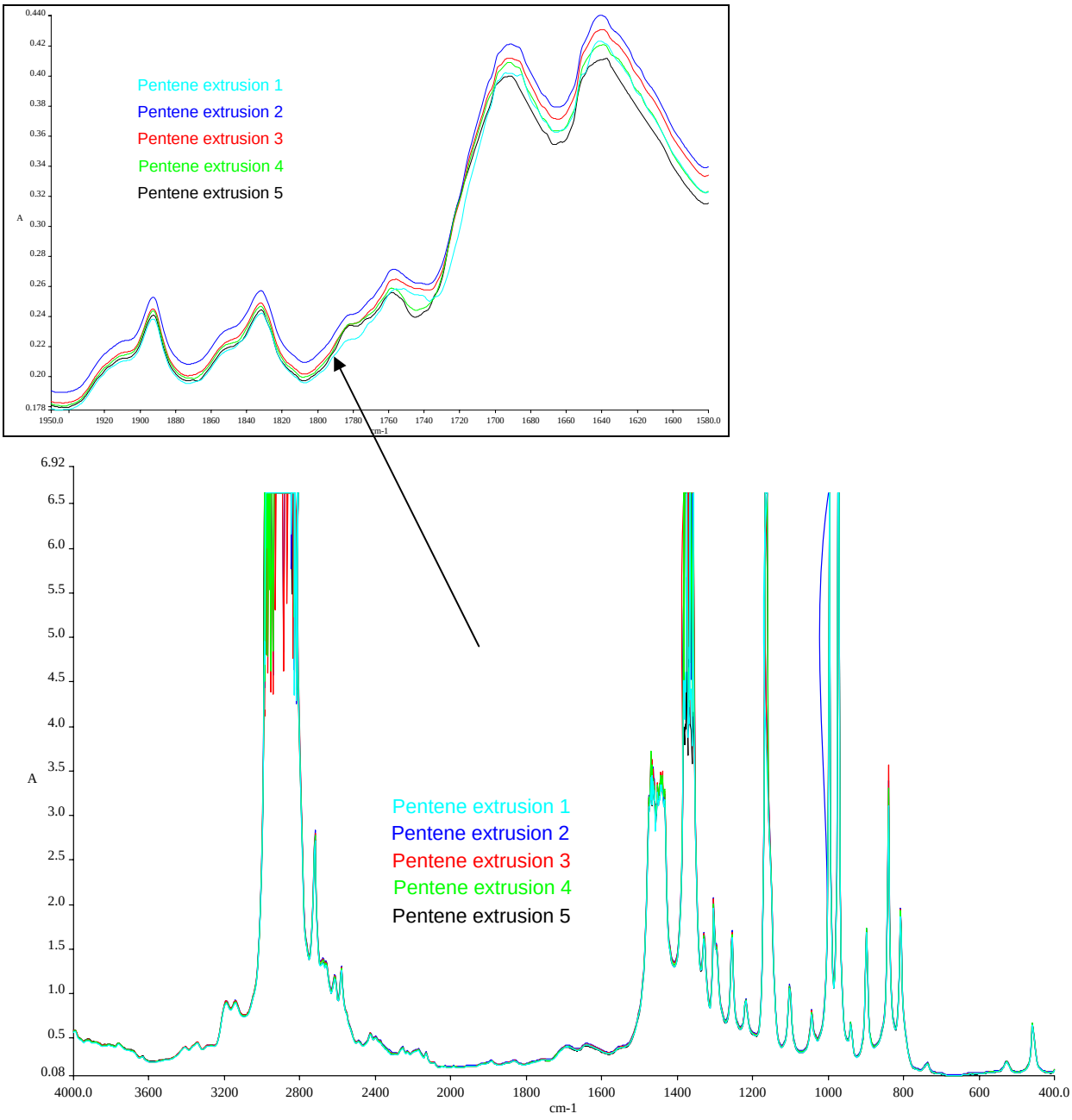

Figure 11: FTIR spectra of the multiply-extruded propylene-1-pentene sample.

Marshall showed that with the addition of a phosphite stabiliser, no increase will be found in the carbonyl index until the stabiliser is totally exhausted [8]. Hinsken et al. [6], however, showed an increase in both the carbonyl functionalities and the C=C double bond concentration (detected at 1650 cm^{-1}) during multiple extrusions. Polyethylene samples showed thermo-oxidative degradation in combination with the mechanical degradation. Canevarolo and Babetto [2] also showed a small increase in vinyl functionalities and carbonyl groups during multiple extrusions of polypropylene samples.

8.4.3.2 Pentene content

The relative pentene content of the propylene-1-pentene samples (unextruded and extruded 1, 2, 3, 4 and 5X) was measured by FTIR. When looking at the peak height at 737 cm^{-1} no difference was noted in the pentene concentration with an increasing number of extrusions. The thermo-mechanical behaviour was, therefore, non-specific to the pentene group. This is different from the case of thermo-oxidative degradation, where a decrease was noted in the pentene content. This indicates scission of the longer chains but without a preference for the pentene group.

8.4.3.3 Relative crystallinity

The relative crystallinity of the polypropylene homopolymer and the propylene-1-pentene copolymer samples (as calculated by the ratio of the FTIR absorption bands at 973 cm^{-1} and 993 cm^{-1}) was recorded at 1, 3 and 5 extrusions to investigate the effect of multiple extrusions on the crystallinity. The absorption band at 997 cm^{-1} corresponds to the crystalline phase [17]. The crystallinity can be measured directly by DSC and X-ray diffraction but FTIR data can also provide a good indication on relative changes. The baselines for the peak height determinations were set at 950 cm^{-1} and 1029 cm^{-1} respectively.

No difference was found in the relative crystallinity of both samples after multiple extrusions, the homopolymer had about 90% apparent crystallinity and the copolymer about 83% crystallinity.

During the thermo-oxidative degradation of the two commercial propylene-1-pentene samples (P1 and P2) in Chapter 6, a significant increase was found in the apparent crystallinity (Section 6.5.7). It can therefore be concluded that the thermal degradation and the mechanical degradation will have different effects on the apparent crystallinity. This is related to the mechanism of degradation: thermo-oxidative degradation will selectively target the tertiary carbon in the side chains in the amorphous phase and preferentially spread through the amorphous phase (low crystallinity region) with the formation of carbonyl containing groups. Thermo-mechanical degradation will preferentially attack the longer chains (high crystallinity chains) and is not inhibited by the discrepancy between the crystalline and amorphous fractions.

8.4.4 DSC analysis of the multiply-extruded polypropylene samples

The melting and crystallisation properties of the multiply-extruded homopolymer and propylene-1-pentene copolymer samples were studied. In Figure 12 an overlay of the melting curves of the homopolymer can be seen.

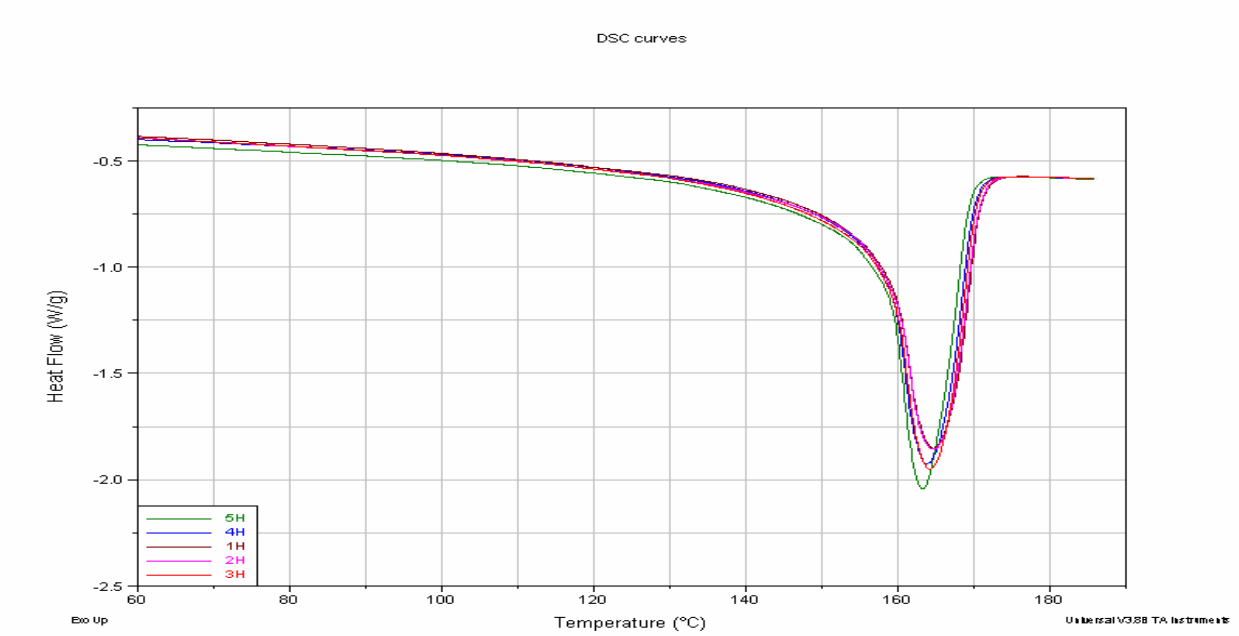

Figure 12: Overlay of the melting curves of the propylene homopolymer multiply-extruded samples showing no significant change in the melting behaviour.

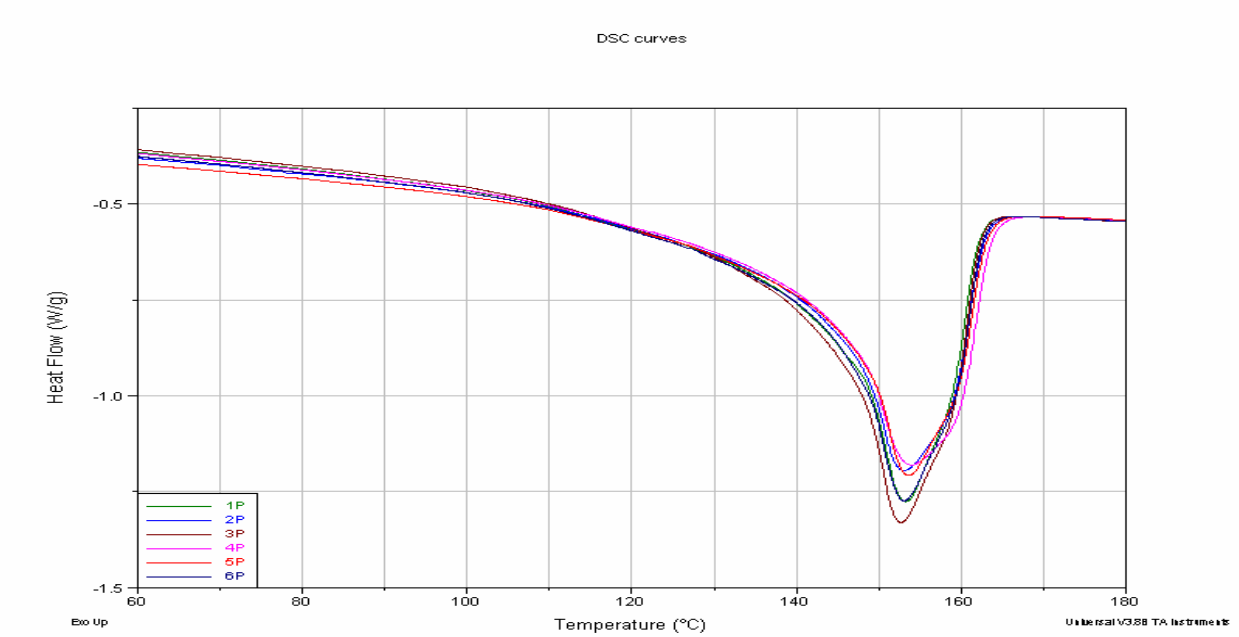

Figure 13: Overlay of the melting curves of the propylene-1-pentene multiply-extruded samples showing no significant change in the melting behaviour.

The DSC melting curves of the multiply-extruded propylene-1-pentene copolymers are shown in Figure 13.

The homopolymer had a significantly narrower melting peak compared to the propylene-1-pentene copolymer. Both samples showed very little change in the melting temperature and relative crystallinity (Tables 2 and 3) with an increasing number of extrusions.

The initial crystallinity of the propylene-1-pentene copolymer was significantly lower than that of the propylene homopolymer (42% compared to 28%). The presence of a comonomer did not influence the thermo-mechanical degradation behaviour to a significant extent. Multiple extrusions resulted in an insignificant change in the polymer crystallinity, as determined by DSC. As the longer chains are preferentially broken during multiple extrusions, shorter chains are formed that are still able to crystallise in the unit crystal. The multiple extrusions had no effect on the supercooling (difference between melting temperature and crystallisation temperature was constant).

Table 2: Melting and crystallisation properties of the propylene-1-pentene copolymer

	Sample: propylene-1-pentene				
Melting properties	**1x extruded**	**2x extruded**	**3x extruded**	**4x extruded**	**5x extruded**
Final temperature of melting T_m (ºC)	162.27	162.90	162.41	163.71	163.20
Peak temperature(s) (ºC)	153.51; 158.81	153.41; 158.85	152.83; 158.80	154.30; 159.46	153.85; 159.51
Onset temperature of melting (ºC)	145.39	144.99	145.24	144.94	145.87
Heat of melting (J/g)	60.12	56.60	65.43	57.45	57.15
% Crystallinity	28.76*	27.08*	31.31*	27.49*	27.34*
Crystallisation properties					
Starting temperature T_c (ºC)	113.01	112.61	113.01	112.94	113.17
Peak temperature(s) (ºC)	109.81	109.60	110.24	108.42	110.22
Final temperature (ºC)	105.05	104.59	105.77	102.90	105.86
Heat of crystallisation (J/g)	80.76	76.73	87.78	79.12	75.20
% Crystallinity	38.64*	36.71*	42.00*	37.85*	35.98*
Supercooling (T_m-T_c) (ºC)	49.26	50.29	49.40	50.77	50.03

**Based on the theoretical value of 209J/g for 100% crystalline polypropylene*

Table 3: Melting and crystallisation properties of the polypropylene homopolymer

	Sample: polypropylene homopolymer				
Melting properties	**1x extruded**	**2x extruded**	**3x extruded**	**4x extruded**	**5x extruded**
Final temperature of melting T_m (ºC)	171.02	170.93	170.42	170.24	169.56
Peak temperature(s) (ºC)	164.73	164.77	164.33	163.85	163.37
Onset temperature of melting (ºC)	158.05	158.18	158.13	157.92	157.89
Heat of melting (J/g)	85.98	86.67	87.43	88.50	88.32
% Crystallinity	41.14*	41.47*	41.83*	42.34*	42.26*
Crystallisation properties					
Starting temperature T_c (ºC)	118.59	120.60	120.46	120.80	121.00
Peak temperature(s) (ºC)	113.93	116.06	116.02	116.58	117.05
Final temperature (ºC)	109.36	110.98	111.35	111.83	112.73
Heat of crystallisation (J/g)	95.17	97.07	99.94	98.90	100.3
% Crystallinity	45.54*	46.45*	47.82*	47.32*	47.99*
Supercooling (T_m-T_c) (ºC)	52.43	50.33	49.96	49.44	48.56

**Based on the theoretical value of 209J/g for 100% crystalline polypropylene*

8.4.5 CRYSTAF results of the degraded samples

CRYSTAF analyses were performed on the multiply-extruded samples to establish if any change could be detected in the chemical composition distribution of the samples. In the thermo-oxidative degradation, a decrease in the CRYSTAF crystallisation temperature and a broadening of the crystallisation curve were detected (broadening of the chemical composition distribution) with increasing levels of degradation. In Table 4 the effect of multiple extrusions on the crystallisation temperatures and soluble fractions can be seen.

Table 4: Crystallisation temperatures and soluble fractions of the extruded polypropylene homopolymer and propylene-1-pentene samples

Sample no.	T_c	Soluble fraction (%)
Homo extrusion 1	80.1	0.9
Homo extrusion 2	79.8	1.1
Homo extrusion 3	78.2	1.2
Homo extrusion 4	77.8	1.7
Homo extrusion 5	77.6	1.6
Pentene extrusion 1	75.2	0.8
Pentene extrusion 2	74.6	0.3
Pentene extrusion 3	75.4	0.5
Pentene extrusion 4	72.1	0.9
Pentene extrusion 5	70.8	1.5

From extrusions 1-5, the crystallisation temperatures and soluble fractions were influenced to a small extent, with a slight increase in the soluble fractions and a slight reduction in the crystallisation temperatures. This indicates that during the multiple extrusions the scission of the chains influenced the CRYSTAF crystallisation behaviour; there was a decrease in the crystallisation temperature and a slight increase in the soluble fraction. One does not expect a significant change in the crystallisation behaviour with multiple extrusions if the mechanism is based purely on scission (CRYSTAF is molar mass independent). However, it is possible that some modification takes place to the chemical composition distribution or the crystallisability of the shorter chains, which, from a kinetic viewpoint, may be able to crystallise more easily than the longer chains from which they were formed. This modification in chemical composition was seen from the CRYSTAF behaviour. Figure 14 shows that there is a shift to slightly lower crystallisation temperatures. This was also evident from the results of the TREF experiment, where the yields of the highest crystallinity fraction decreased, resulting in an increase in the yield of some of the lower crystallinity fractions.

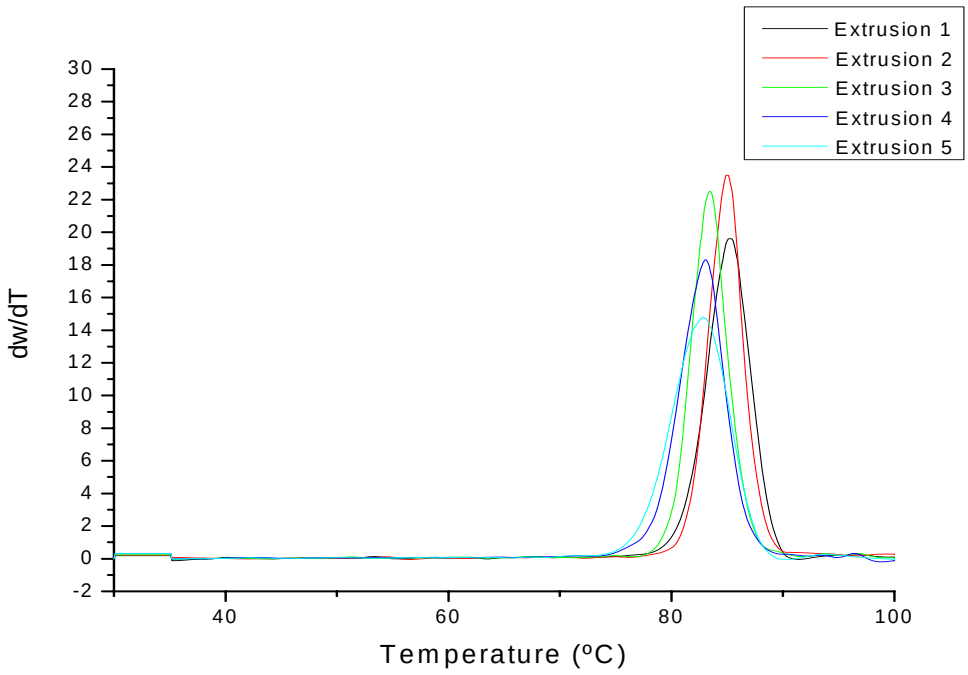

Figure 14: Effect of multiple extrusions on the crystallisation behaviour of the homopolymer as measured by CRYSTAF.

8.5 Calculation of the number of chain scissions during the multiple extrusions

The following equation can be used to calculate the average number of chain scissions:

$$N_S = (M_{n0}/M_{nt})-1 \qquad (8.4)$$

where: n_S is the number of chain scissions

M_{nt} is the molar mass of the polymer after t extrusions

M_{n0} the molar mass of the original polymer

The calculated number of chain scission can be seen in Figure 15.

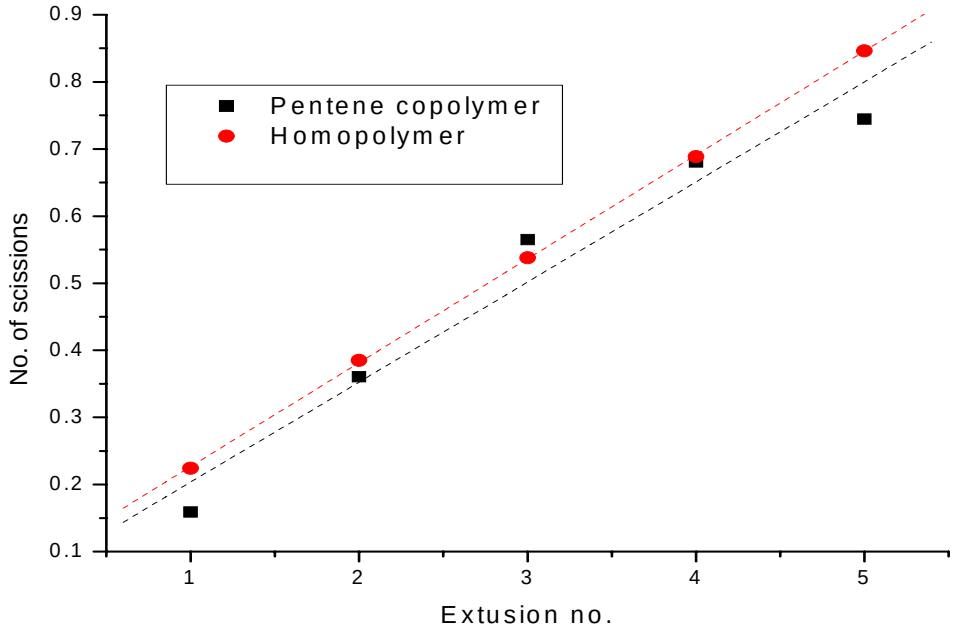

Figure 15: Number of chain scissions as a function of extrusion number showing a linear increase in the number of scissions with an increase in the number of extrusions.

The chain scission number is an average value of how many chain scissions have taken place per chain.

In this area there was virtually a linear increase in the number of chain scissions with the increasing number of extrusion for both samples. The chain scissions may, however, also be calculated as a function of molar mass. This can be performed using the chain-scission distribution function (CSDF).

8.5.1 The chain scission distribution function model

Recently, Prof S.V Canevarolo of the Department of Material Science at the *Universidade Federal de Sao Carlos* in Brazil developed the chain scission distribution function (CSDF)

model. This model can be used to predict the molecular weight dependence of the scission process during extrusion. He defined the chain scission distribution function as:

$$CSDF = Log (N_s + 1) \quad (8.5)$$

where: N_s is the number of chain scissions

The CSDF curve is indicative of the amount of scission taking place per molecule. In polyethylene, where both branching and scission may occur, the model gives an indication of the relative amounts of chain branching and chain scission taking place during extrusion. This model is available on request*.

8.5.2 Explanation of the mathematical basis of the CSDF model

All data manipulations for this model were carried out in Excel, using a special macro developed by Prof Canevarolo*. The first step was to export the two molar mass distribution curves (initial and after scission) from the Waters Millennium® software to Excel. This was carried out by obtaining the raw data in ASCI format, which is converted in Excel into a normal spreadsheet. The mathematical model is based on the concentration method. The equations were derived by Canevarolo and used to develop the concentration model.

Several authors define the average amount of chain scissions that takes place during extrusion as:

$$N_s = \frac{\overline{Mn_{(0)}}}{\overline{Mn_{(D)}} - 1} \quad (8.6)$$

This provides an average value for the amount of scission that occurs during an extrusion but provides no information on the amount of scission taking place in each fraction. The latter can now be extended to every original molecular weight fraction, to get scission values for each fraction:

$$N_s = \frac{Mn_{(0)}}{Mn_{(D)} - 1} \quad (8.7)$$

The chain scission distribution function is defined by (see also Section 7.5.1):

* The model was obtained from Prof Canevarolo (caneva@power.ufscar.br)

CSDF = Log (N_s + 1) (8.8)

We now define two parameters, C_0^T and C_0^T as the initial and final total weight concentration of the polymer eluted from the SEC instrument. Assuming that there is no loss of polymer, the following will apply:

$$C_0^T = C_D^T \tag{8.9}$$

This can now be written as:

$$\int_{MW_0^i}^{MW_0^F} \varphi(MW)d(MW) = \int_{MW_D^i}^{MW_D^F} \psi(MW)d(MW) \tag{8.10}$$

where φ(MW) is defined as the initial molar mass distribution curve and ψ(MW) the final molar mass distribution curves. Their integrals will be equivalent to the initial and final concentrations of the samples.

From this, every point in each of the partial cumulative concentration curves can be represented by:

$$c_0^{MW_0} = \int_{MW_0^i}^{MW_o} \varphi(MW)d(MW) \tag{8.11}$$

$$c_D^{MW_D} = \int_{MW_D^i}^{MW_D} \varphi(MW)d(MW) \tag{8.12}$$

where $c_0^{MW_0}$ is the initial cumulative concentration curve and $c_D^{MW_D}$ the final cumulative concentration curve

A requirement of the concentration is that two corresponding curves have the same partial cumulative concentrations, therefore:

$$C_0^{MW_o} = C_D^{MW_D} \tag{8.13}$$

Substituting the equations yield:

$$C_0^{MW_o} = \int_{MW_D^i}^{MW_D} \varphi(MW)d(MW) \qquad (8.14)$$

Equation 8.14 is the basis of the CSDF model and for each reference $C_D^{Mw_D}$, the MW_D value that satisfies this equation must be found. The CSDF can be calculated using equations 2 and 3.

8.5.3 Interpretation of the chain scission distribution function

If the degradation is mainly due to scission, then the molecular weight distribution curves shift to the low molecular weight side, resulting in positive CSDF values. If chain branching is the main degradation mechanism, then the molecular weight distribution curve will shift to the higher molecular weight side. In the branching area, the chain scission distribution function will yield negative values. This is mostly due to the reaction of a radical (formed by chain scission) with unsaturated groups in the polymer.

The slope of the CSDF curve can be related directly to the type of degradation: a curve with no slope is indicative of random (molecular weight independent) scission, whilst a linear curve with the slope not equal to zero is indicative of molecular weight dependent scission. In polypropylene (where only scission occurs and crosslinking effects during extrusions is generally negligible), the slope is generally **molar mass independent** in the low molecular weight region and **molar mass dependent** in the high molecular weight region. In the high molecular weight region, the higher the molecular weight, the higher the number of chain scissions per molecule.

8.5.3.1 Benefits of using the CSDF model

The CSDF model is a useful tool for evaluating the stability of a polyolefin resin towards thermo-mechanical degradation. For example, the effect of extrusion conditions on a polyolefin sample can be determined using this model. The model uses normal refractive index data in its calculations, so standard SEC measurements can be used in these evaluations.

8.5.4 Calculating the CSDF of polypropylene and propylene-1-pentene

The CSDF functions of the polypropylene homopolymer and the propylene-1-pentene copolymers were calculated using this program. Results are shown in Figure 16.

The CSDF curves of the polypropylene and the propylene-1-pentene copolymer samples displayed similar shapes. The curves were positive, indicating the absence of crosslinking reactions. In the molar mass region around log MW = 4-4.5, the scission process is virtually independent of molar mass (low gradient). Above log MW = 4.5, the scission process is highly molar mass dependent. There is an increase in the gradient of the curve with increasing molar mass. At high molar masses, the scission process is therefore very molar mass dependent, while at lower molar masses, the process is molar mass independent.

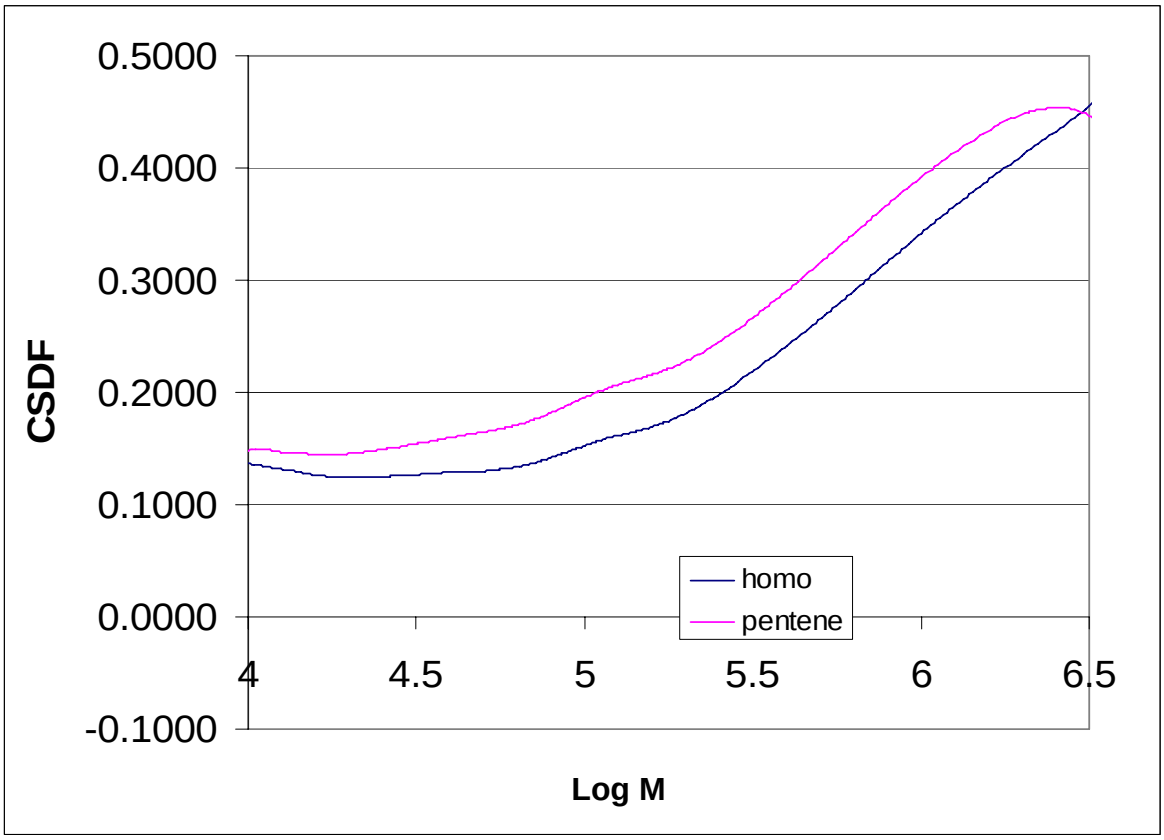

Figure 16: Number of chain scissions as a function of molar mass of polypropylene and propylene-1pentene.

8.6 Fractionation of unextruded and extruded propylene-1-pentene samples

Multiple extrusions of the polypropylene samples resulted in a significant decrease in the polymer molar mass and molar mass averages. After five extrusions, the M_w values of the homopolymer and the copolymer both decreased by 43%. This will ultimately result in a decrease in the mechanical properties of the polymer, which could result in a failure in the end-use applications. However, as no changes were detected in the infrared spectra (no increase in carbonyl index, apparent crystallinity and pentene content of the bulk polymer) and the DSC crystallisation curves (% crystallinity and melting points), these techniques were not able to detect any significant changes in the polymer. A comparison of the fractions obtained from the unextruded and extruded samples may, however, provide information on the changes in chemical composition during multiple extrusions.

TREF fractionation:

The fractionation of the multiply extruded propylene-1-pentene sample, before extrusions and after five extrusions, was compared. In Figure 17 the yields of each fraction for the two polymers are compared.

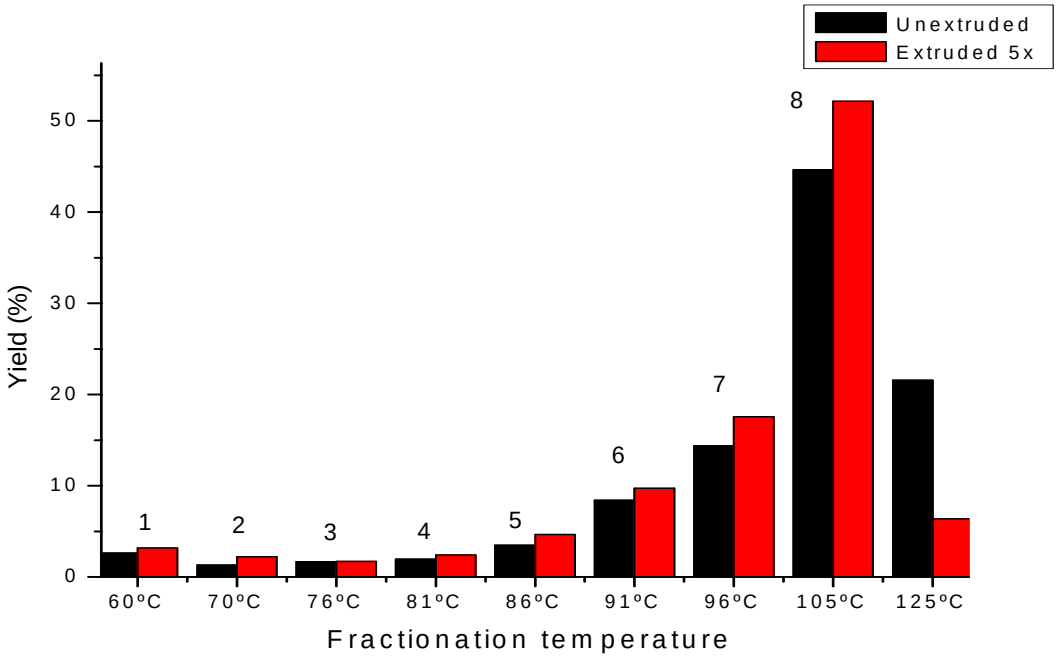

Figure 17: Effect of multiple extrusions on the yield of the different fractions of the propylene-1-pentene copolymer.

From Figure 17 it can be seen that there was a significant change in the yield of especially the higher crystallinity fractions. The yield of fraction 9 decreased dramatically (from 22% to approximately 6,4%). The yields of fractions 8 and 7 increased, while the lower crystallinity fractions also showed a slight increase. It would, therefore, appear as if the multiple extrusion process results in a significant change in the crystallisability of the higher crystallinity fractions in solution. This result is different from the DSC crystallisability, which did not show any significant change with an increase in the number of extrusions.

8.6.1 SEC analysis of the TREF fractions of the unextruded and extruded propylene-1-pentene samples

The molar masses of the fractions were determined. In Figure 18 an overlay of the molar masses of the fractions of the unextruded polymer can be seen. In Figure 19 the molar mass distribution curves of the extruded propylene-1-pentene sample can be seen.

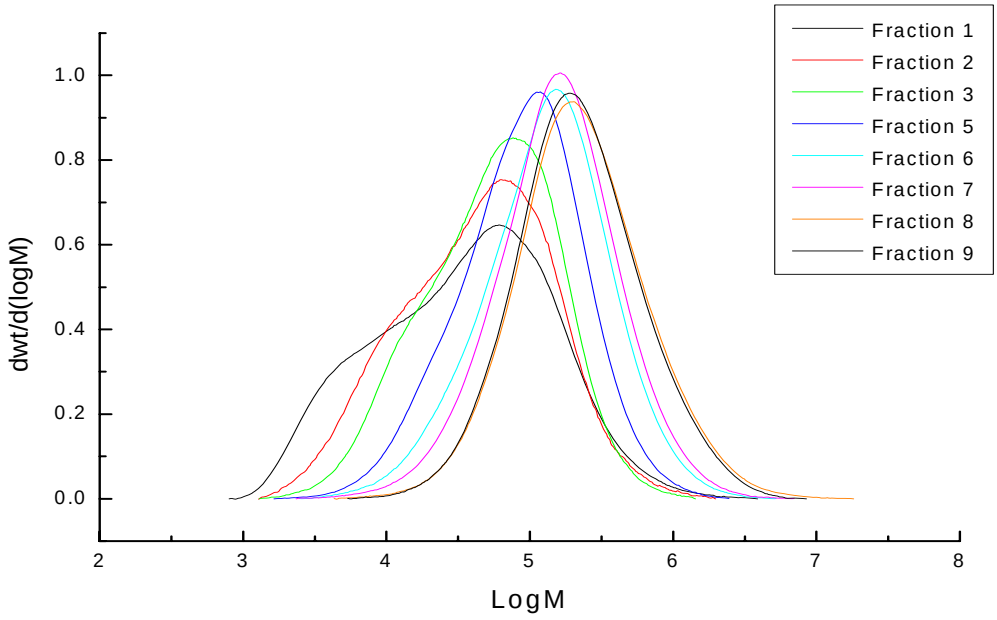

Figure 18: Molar mass distribution curves of the fractions of the unextruded propylene-1-pentene polymer.

Figures 18 and 19 show that the shapes of the molar mass distribution curves are similar for the fractions of the unextruded and extruded samples. However, the molar mass distribution curves of the degraded sample have moved to lower molar masses, as is evident from the shift in log M values on the high molar mass side. The curves also appeared to be narrower than for the unextruded sample. The high crystallinity fractions of both the unextruded samples generally had the highest M_z values (Figure 20).

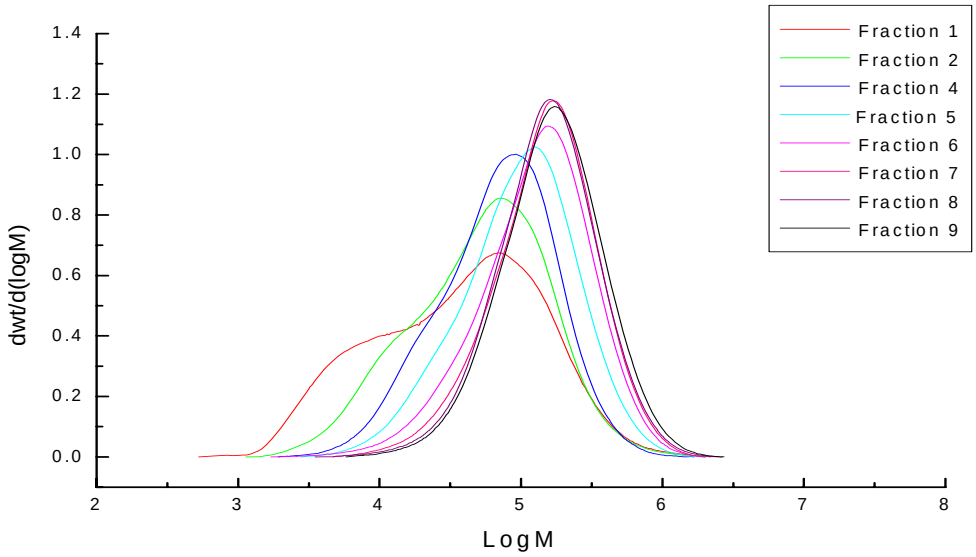

Figure 19: Molar mass distribution curves of the fractions of the extruded propylene-1-pentene polymer (extruded 5x).

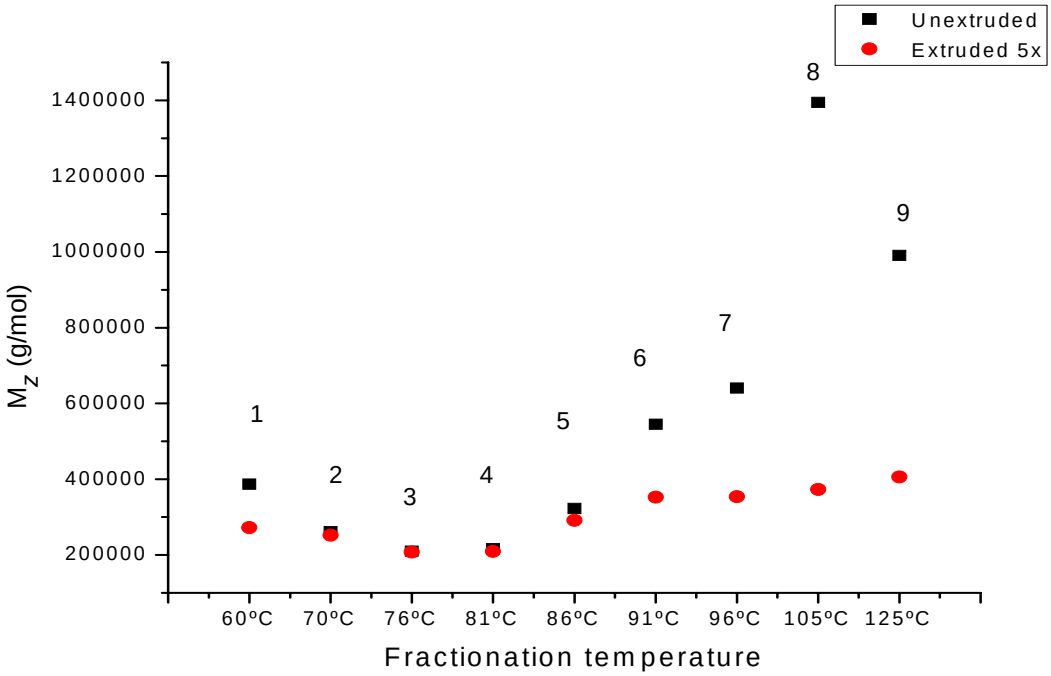

Figure 20: Effect of multiple extrusions on the M_z values of the propylene-1-pentene fractions showing a significant shift in the M_z values of especially the higher crystallinity fractions.

The M_z values of the lower crystallinity fractions showed a very small change with multiple extrusions. The higher crystallinity (and higher molar mass) fractions, however, showed a very significant change with multiple extrusions, and the two highest molar mass fractions showed the most significant change in M_z. A similar effect is also seen for the M_w values.

Fractions 8 and 9 showed the most significant changes in M_w values (Figure 21). Fractions 6 and 7 also showed a significant reduction with molar mass. However, from fractions 1 to 5, the reduction in molar mass was much smaller.

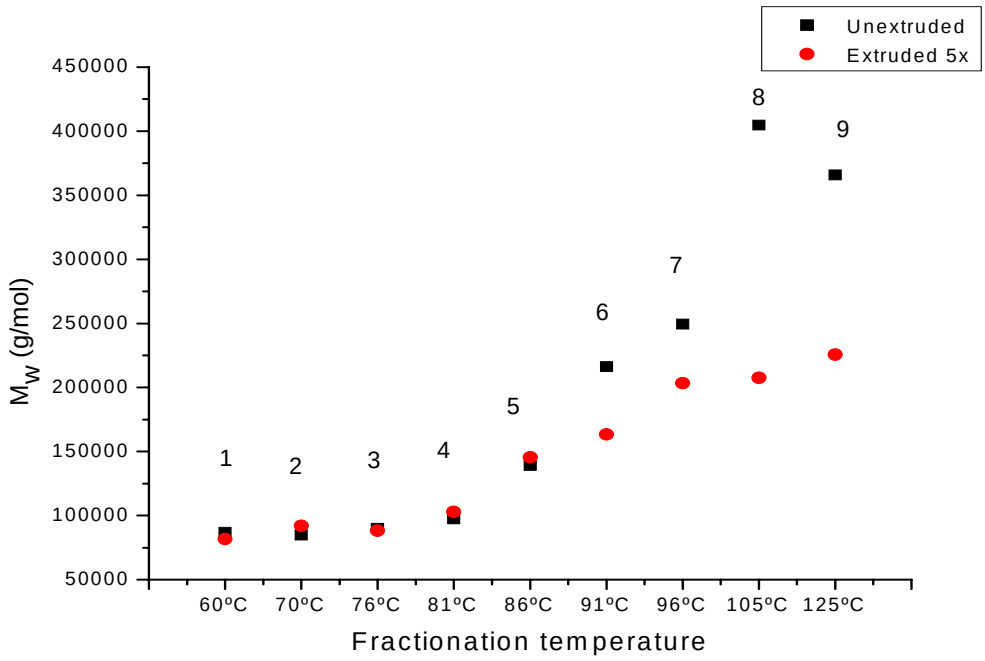

Figure 21: Effect of multiple extrusions on the M_w values of the fractions showing that the M_w of the lower crystallinity fractions are virtually unaffected.

The effect of multiple extrusions on the polydispersity index values can be seen in Figure 22.

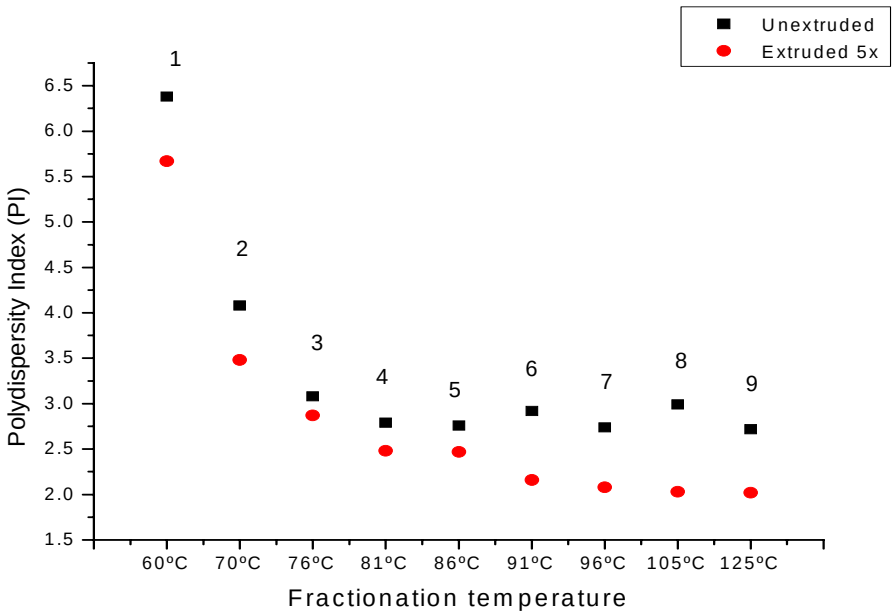

Figure 22: Effect of multiple extrusions on the polydispersity index values of the fractions.

Investigating an overlay of the molar mass distributions of the different fractions, it can be seen that the material crystallising below 60 ºC (first crystallisation temperature = fraction 1) was virtually unaffected by the extrusion process. Similar molar mass average values and molar mass distribution curve shapes were found (Figure 23). The M_z value of the fraction decreased slightly, resulting in a slight narrowing of the molar mass distribution curve.

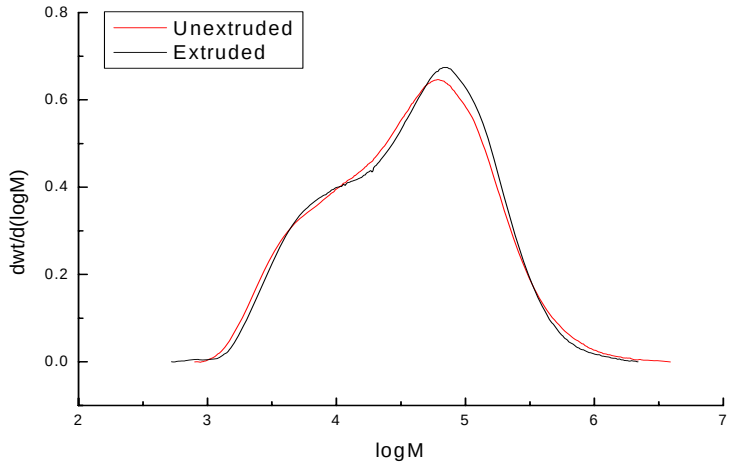

Figure 23: Effect of multiple extrusions on the molar mass distribution curve of fraction 1 showing a small effect on the molar mass distribution.

Even in fraction 5, only a small change was detected in the molar mass distribution curves (Figure 24).

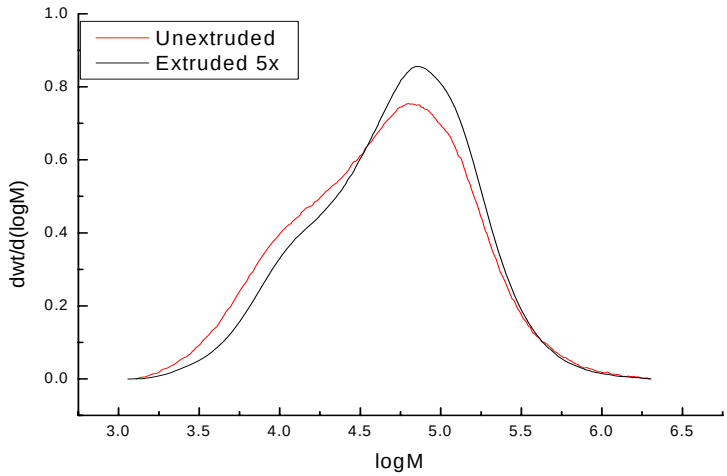

Figure 24: Effect of multiple extrusions on the molar mass distribution curve of fraction 5.

The molar mass distribution curves of fractions 6, 7, 8 and 9, however, showed a more significant change with multiple extrusions. In Figure 25, the effect of multiple extrusions on the molar mass distribution curves of fractions 7 and 8 can be seen.

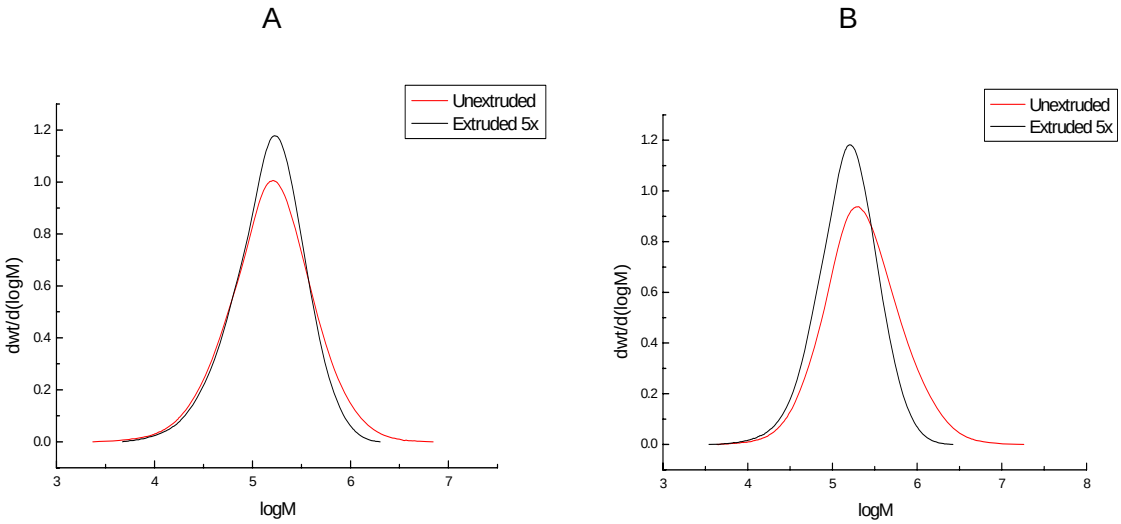

Figure 25: Effect of multiple extrusions on the molar mass distribution curves of fraction 7 (A) and 8 (B) showing a significant change on the molar mass distributions of these two fractions.

Fractions 7 and 8 showed very significant reductions on the high molar mass side. According to the theory of Bueche [14], the longer chains will preferentially degrade through the scission process. From the TREF results it is evident that the molar masses of the fractions crystallising below 60 ºC are affected to a very small extent, while the high crystallinity (and consequently higher molar mass) fractions are significantly affected. A polymer degraded by thermo-mechanical scission can, therefore, be considered as consisting of a blend of fractions of highly scissioned material and material that is virtually unaffected by the extrusion process.

8.6.2 DSC analysis of the TREF fractions of the unextruded and extruded samples

DSC analyses were performed on the fractions of the unextruded and extruded samples. The melting points of the different fractions can be seen in Figure 26. In both the unextruded and extruded samples, there was virtually a linear increase in the melting points of the fractions with an increase in fractionation temperature, confirming that TREF is virtually a diluent melting experiment [16]. Only fraction 1 deviated from this straight line, due to the very low crystallinity of this fraction (highly branched material). The melting points of the unextruded

fractions were similar to that of the extruded sample, confirming that the elution temperature in TREF is independent of molar mass, but rather dependent on the crystallinity.

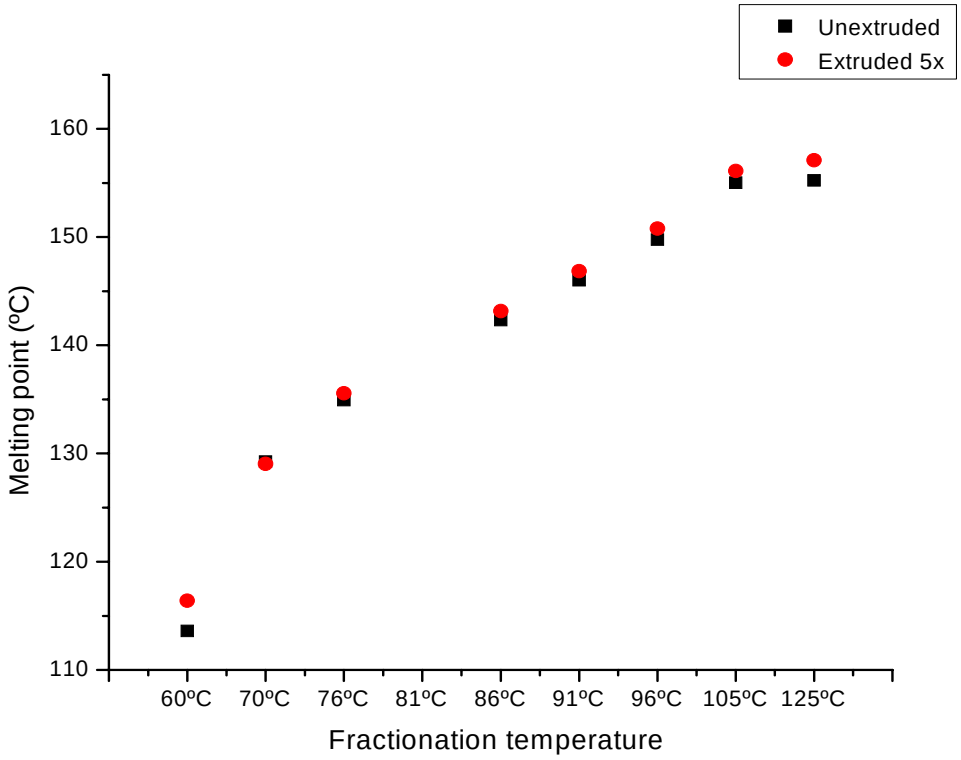

Figure 26: Effect of multiple extrusions on the melting points of the fractions of the extruded and unextruded propylene-1-pentene samples.

The crystallinity of the fractions was also investigated. The fractions were well separated according to crystallinity. Generally, the crystallinity of the fractions of the degraded and the undegraded polymers were similar (Figure 27).

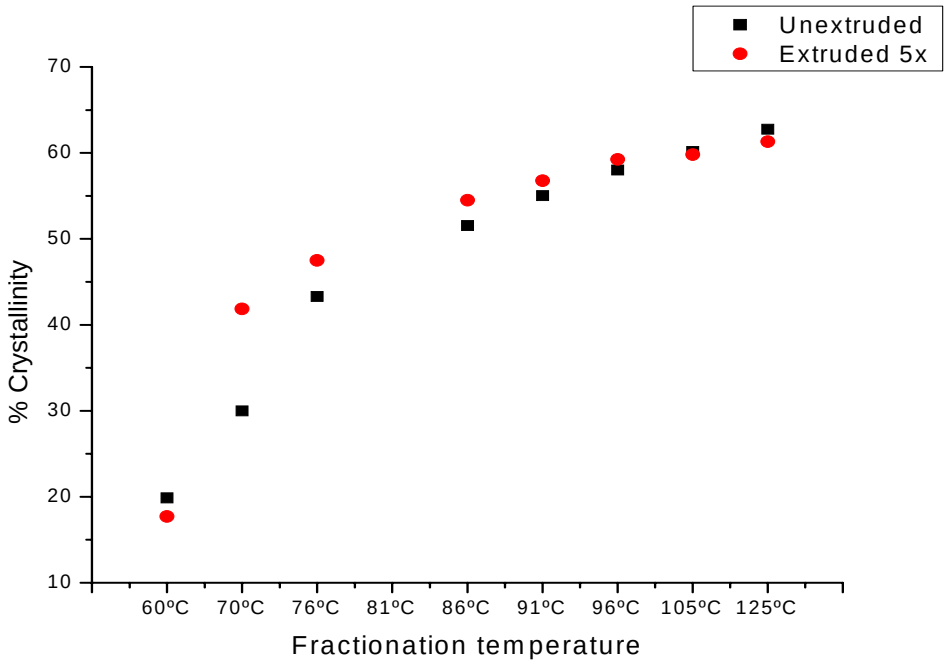

Figure 27: Effect of multiple extrusions on the crystallinity of the fractions showing that crystallinities of the fractions were generally comparable.

The fact that the crystallinity of the fractions did not change significantly during multiple extrusions indicates that there was no significant change in the chemical composition distribution of a fraction crystallising at a certain temperature. Therefore, the overall branching distribution of the material crystallising in a fraction did not change. This was confirmed by the overall observation that the crystallinity of the bulk polymer did not change with multiple extrusion. Also, the FTIR spectrum of the bulk polymer indicated that there was no decrease in the pentene content of the samples with degradation. Therefore, the extrusion process under oxygen deficient conditions was non-specific to the pentene group. This differs from the oxidative degradation process, where the pentene concentration decreases with degradation, and the crystallinity increases slightly with degradation.

It can, therefore, be concluded that the chain scission process resulted in a reduction in the molar mass of most of the fractions. The scission process, however, did not influence the crystallinity or the melting points of the different fractions, and the fractionation process was, therefore, not influenced by the molar mass.

The fractionation process, however, showed that the molar mass averages of the high molar mass fractions were influenced to a more significant extent than the lower molar mass fraction. The fraction obtained at 60 ºC showed virtually no decrease in molar mass. The

shape of the molar mass curves was also similar for the unextruded and the extruded (5x) samples.

8.7 Oven aging of the multiply-extruded samples

SEC, FTIR and DSC analyses indicated that there were only small differences between the behaviour of the propylene homopolymer and the propylene-1-pentene copolymer after multiple extrusions. The question now arises as to whether the multiple extrusions (chain scission in the absence of oxygen) will sensitise the polymers towards further oxidative degradation.

The samples extruded 3 and 5 times were pressed into plaques of constant thickness and subjected to thermal aging at 70 ºC. Samples were removed regularly for further analysis by DSC and SEC.

The carbonyl index values determined by FTIR shows that the pentene sample, extruded 5 times, degraded significantly faster than the same sample extruded 3 times (Figure 28). The homopolymer degraded slower, again with the sample extruded 5 times degrading faster than the same sample extruded only 3 times.

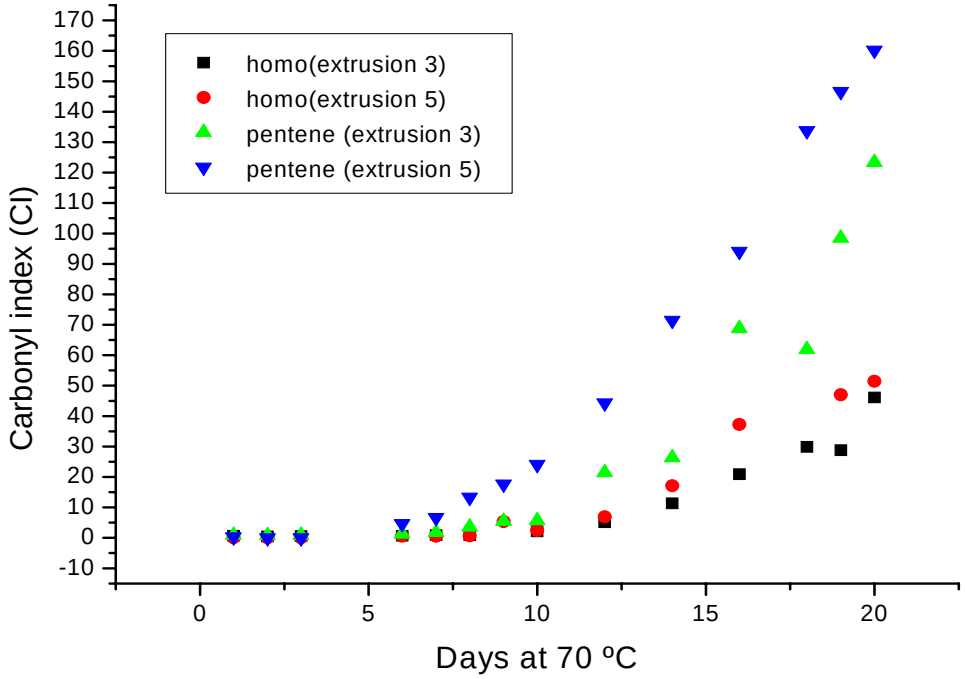

Figure 28: Effect of aging of multiply-extruded samples on the increase in carbonyl index. (The propylene-1-pentene sample (extruded 5 times) degraded the fastest.)

The M_w values, determined by size exclusion chromatography, indicated that the gradient of degradation for the two propylene-1-pentene samples (extruded 3x and 5x) were steeper than for the two homopolymer extruded samples (Figure 29).

Note: These analyses were performed on a Polymer Labs PL 220 instrument, using PSS HT columns. These results may, therefore, differ from the results obtained from following the multiple extrusions (analyses performed on a Waters 2000 Alliance instrument).

The DSC results indicated little change in crystallinity, while the melting point decreases with progressing degradation (Figure 30).

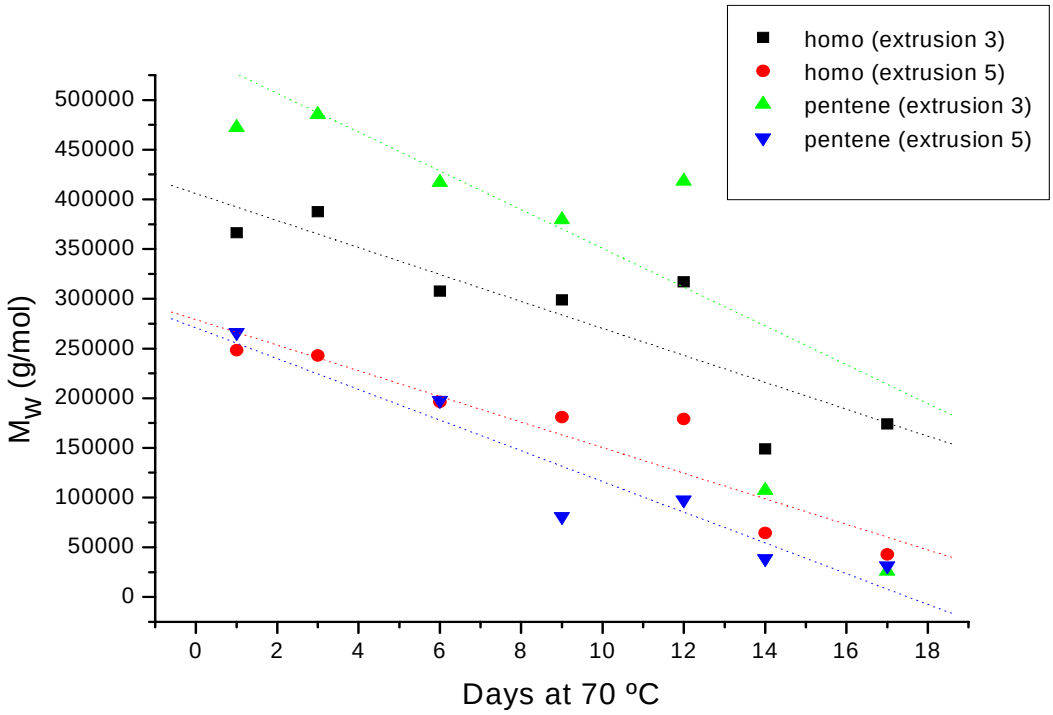

Figure 29: Decrease in molar mass of the multiply-extruded samples with time, aged at 70 ºC. (The two pentene samples showed a more steep decrease in molar mass.)

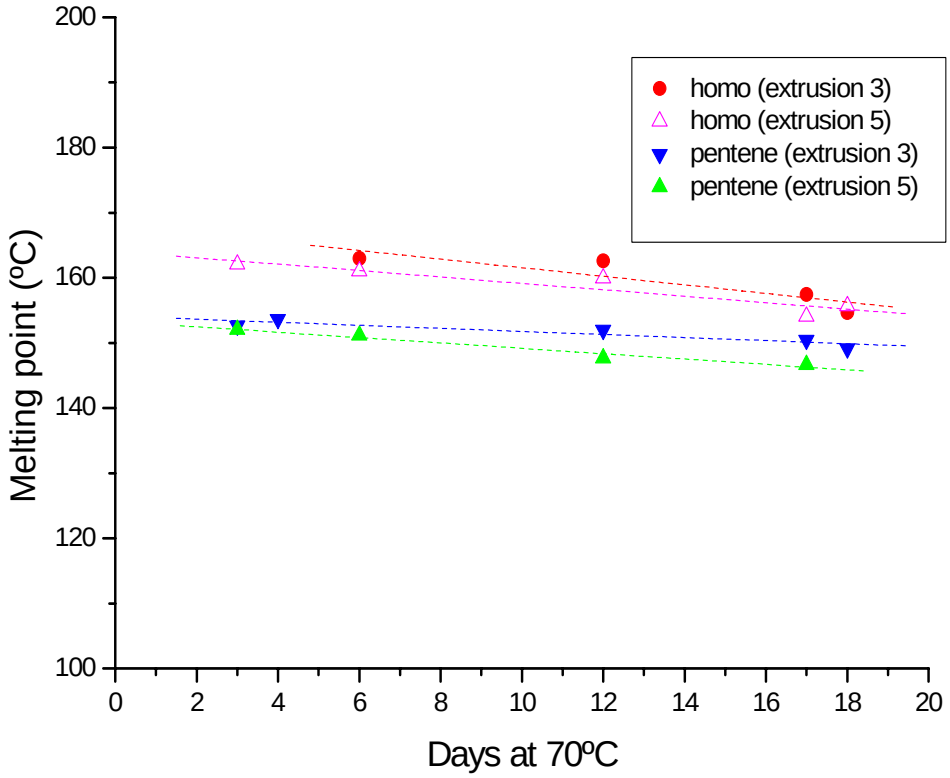

Figure 30: Decrease in the melting point of the multiply-extruded samples with time, aged at 70 ºC.

These results indicated that although the degradation process was not influenced significantly by the molar mass, the multiple extrusion process resulted in a sensitisation of the polymer towards thermo-oxidative degradation. This implies that although no increases were detected in the hydroperoxides and the carbonyl contents, the polymers were still sensitised towards degradation.

8.8 Conclusions

The overall objective of this section was to investigate the processing stability and degradation (effect of multiple extrusions) on unstabilised polypropylene homopolymer and propylene-1-pentene copolymer samples (one of each) using FTIR, SEC and DSC. A commercially-produced polypropylene homopolymer sample and a propylene-1-pentene sample were evaluated for processing stability using the multiple extrusion technique, whereby the polymers were extruded 5 times on a Brabender Plasticorder under the same conditions. There was no detectable difference in the degree of extrusion instability of the propylene homopolymer and propylene-1-pentene copolymer. FTIR results indicated that

there was no significant increase in the carbonyl indices of both samples during multiple extrusions. The oxygen deficient conditions in the extruder, therefore, only resulted in scission (decrease in the molar mass averages), without the formation of significant amounts of carbonyl functionalities. Under these test conditions, the two polymers also showed similar decreases in molar mass averages. The polydispersities of both samples narrowed significantly with an increasing number of extrusions. The M_z (indicative of the higher molar mass material) showed a more significant decrease compared to the M_n value (which is indicative of the low molar mass part of the molar mass distribution). The decrease in polydispersity was, therefore, mostly due to the decrease in the M_z value (scission of the longer chains).

In a comparison of the homopolymer and the propylene-1-pentene copolymer under multiple extrusions it was seen that the reduction in molar mass was independent of the initial molar mass and crystallinity. It was also independent of the incorporation of comonomer (similar behaviour exhibited by the homopolymer and the copolymer).
The DSC behaviour of the two samples was also similar, with virtually no change after 5 extrusions. Rheology evaluations showed that the zero shear viscosity decreased with an increase in the number of extrusions. A reasonable correlation was found between the zero shear viscosity and the M_w values obtained from SEC. The calculated polydispersity indices decreased with increasing extrusion number. This is in line with the polydispersity values calculated from SEC.

The second objective was to compare the TREF fractions of an unextruded propylene-1-pentene sample and to compare that with the fractions of a sample extruded 5 times. It was possible to fractionate an extruded sample by TREF in a similar fashion to a non-extruded sample. Generally the extruded and unextruded samples could be fractionated into fractions of similar crystallinities and melting points. The SEC results indicated that the multiply-extruded sample can be fractionated into fractions of highly scissioned material, with significantly lower polydispersities and fractions of lower scissioned material with less significant changes in the molar mass properties.

Aging of the multiple-extruded samples showed that the pentene copolymer samples (extruded 3 times and 5 times) degraded faster than the comparable homopolymer samples. The higher extrusion number (extrusion 5) for each sample degraded faster than the lower extrusion number sample (extrusion 3). This phenomenon could be seen from both the FTIR (carbonyl index) and molar mass values. Although there was no carbonyl formation detected

during multiple extrusions, the multiple extrusion process sensitised the samples for further degradation.

8.9 References

[1] Epacher, E., Tolveth, J., Stoll, K.; Pukansky, B., *Journal of Applied Polymer Science* **1999**, 74, 1595-1605

[2] Canevarolo, S., Babetto, C., *Advances in Polymer Technology* **2002**, 21, 243-249

[3] Canevarolo, S., *Polymer Degradation and Stability* **2000**, 709, 71-76

[4] Shlyapnikov, Y.A., Kyrushkin, S.G., Mar'in, A.P., *Antioxidative stabilisation of Polymers* **1996**, Taylor and Francis. ISBN 0 7484 0577 1

[5] Moss, S., Zweifel, H., *Polymer Degradation and Stability* **1989**, 25, 217-245

[6] Hinsken, H., Moss, S., Paquet, J-R., Zweifel, H., *Polymer Degradation and Stability* **1991**, 34, 279-293

[7] Tochácek, J., Sedlar, J., *Polymer Degradation and Stability* **1993**, 41,177-184

[8] Marshall, N., PhD thesis, University of Sussex, **December 2001**

[9] Zahavich, A.T.P., Latto, B., Takacs, E., Vlachopoulos, J., *Advances in Polymer Science* **1997**, 16, 11-24

[10] Yoncheng, Y., *Polymer Degradation and Stability* **1993**, 39, 193-198

[11] Santos, A.S.F., Agnelli, J.A.M., Trevisan, D.W., Manrich, S.; *Polymer Degradation and Stability* **2002**, 77, 441-447

[12] Kartalis, C.N., Papaspyrides, C.D., Pfaendner, R., Hoffmann, K., Herbst, H., *Journal of Applied Polymer Science* **1999**, 73, 1775-1785

[13] Mead, D.W., *Journal of Applied Polymer Science* **1995**, 57, 151-173

[14] Bueche, F., *Journal of Applied Polymer Science* **1960**, IV issue 10, 101-106

[15] Gonzales-Gonzales, V.A., Neira-Velasquez, G., Angulo-Sanchez, J.L., *Polymer Degradation and Stability* **1998**, 60, 33-42

[16] Mirabella, F.M., *Journal of Polymer Science Part B: Polymer Physics* **2001**, 39, 2819-2832

[17] Mucha, M., Kryzewski, K., *Colloid and Polymer Science* **1980**, 258, 743-752

Chapter Nine

Conclusions

9.1 Introduction

The overall conclusions of this thesis will now be discussed in terms of the four original main objectives, listed in Chapter 1.

Objective 1:

The main objective of this study was to investigate the use of hyphenated (SEC-FTIR) and fractionation techniques (CRYSTAF and TREF) in studying polyolefin degradation. These studies were carried out to compliment the classical techniques (SEC, FTIR and DSC) in studying degradation in polypropylene. A second objective of this section was to study the spatial heterogeneity of the degradation process in a degraded polypropylene homopolymer sample.

During degradation of polypropylene, changes are observed in the molar mass, chemical composition and chemical composition distribution. The classical techniques provided only information on changes in molar mass and chemical composition during the degradation process. Up to now, very little information existed on the changes in chemical composition during the degradation process. CRYSTAF is a relatively new technique for studying the chemical composition distribution of a polyolefin sample.

For this study, a commercial polypropylene homopolymer sample was degraded under different conditions to be representative of different stages of degradation. SEC analysis showed that the molar mass decreased significantly with progressing degradation. FTIR analysis indicated that the carbonyl index increased with an increase in the level of degradation.

The SEC-FTIR analysis technique was optimised for the analysis of the polypropylene homopolymer sample. SEC-FTIR impressively revealed that the degradation products were not uniformly distributed over the molar mass region. A high concentration of degradation products was found in the low molar mass end of the molar mass distribution. CRYSTAF analysis indicated that the chemical composition distribution became significantly broader with an increase in the level of degradation. There was a significant decrease in the crystallisation temperature. The soluble fraction also increased significantly with an increase in the level of degradation.

It was possible to fractionate a degraded sample using prep-TREF fractionation. Prep-TREF fractionation was able to fractionate the degraded sample into fractions of different carbonyl content. With increasing levels of degradation, a non-statistical distribution of carbonyl groups was found. The degraded polymer was fractionated into: 1) fractions of low crystallinity with low molar mass and high carbonyl content and 2) fractions of high crystallinity, high molar mass and low carbonyl content. CRYSTAF analysis of these TREF fractions showed that the lowest crystallinity fraction consisted of non-crystallisable, highly degraded material. The fractions of higher crystallinity had sharp crystallisation peaks, typical of isotactic polypropylene.

The spatial heterogeneity of a thick, degraded polypropylene homopolymer sample was studied by microtoming the sample into thin layers. SEC analysis revealed a dramatic increase in the molar mass from the surface of the sample (highly degraded) to the middle of the sample (less degraded). FTIR analysis revealed a decrease in the carbonyl index from the surface towards the middle of the sample. CRYSTAF analysis showed a significant difference in chemical composition distribution between a surface layer and a layer close to the middle of the sample.

Objective 2:

The second main objective was to study the degradation behaviour of an unstabilised commercial polypropylene homopolymer sample (produced using a Ziegler-Natta catalyst system) and contrast the degradation behaviour with that of commercial propylene-1-pentene samples. Another objective was to study the effect of pentene incorporation on the polymer microstructure.

For this study, the thermo-oxidative degradation behaviours of two commercial propylene-1-pentene samples were evaluated and contrasted with the degradation behaviour of a polypropylene homopolymer sample, manufactured under the same conditions. The degradation behaviour of the three samples was evaluated at 70 ºC and 90 ºC. NMR indicated no differences in tacticity between the undegraded homopolymer and copolymer samples. The catalyst residues were also similar, so differences in the degradation behaviour were not due to differences in the level of the catalyst residues. The crystallinities and melting points of the propylene-1-pentene samples were, however, found to be lower than those of the polypropylene homopolymer sample. The melting curves of the two copolymer samples were also broader compared to the homopolymer sample.

It was found that the propylene-1-pentene samples degraded significantly faster than a polypropylene homopolymer sample, degraded under the same conditions. Although the degradation at 90 ºC was significantly faster that at 70 ºC, the trends in the carbonyl indices, molar mass averages, apparent crystallinities and melting points were similar. With an increasing level of thermal degradation, an increase was found in the carbonyl index, while the molar mass decreased significantly. The FTIR results revealed a faster increase in the carbonyl index of the two propylene-1-pentene copolymers, compared to the homopolymer sample. SEC also indicated a faster decrease in all the molar mass averages of the copolymer samples compared to the homopolymer sample. The hydroperoxide concentration in the copolymer samples also increased at a faster rate. FTIR analysis also indicated an increase in the apparent crystallinity with an increase in degradation time, and a decrease in the melting temperature with increasing degradation.

SEC-FTIR was again used to determine the distribution of degradation products as a function of molar mass. The highest concentration of degradation products was again found in the low molar mass region.

The CRYSTAF curves of the three samples were investigated as a function of degradation time. Similar to the previous chapter, the CCD curves broadened, the crystallisation temperature decreased, and the soluble fraction increased with increasing levels of degradation. The CRYSTAF curves of sample P2 (a propylene-1-pentene random copolymer sample containing 2,9 weight% pentene) showed the most significant change with an increasing level of degradation. Compared to the homopolymer and P1 samples (a propylene-1-pentene random copolymer sample containing 1,7 weight% pentene), the CCD broadened the most, the soluble fraction increased the most and the crystallisation temperature decreased the most.

TREF analysis was performed on an undegraded P2 sample to investigate the effect of pentene incorporation on the polymer microstructure. The degraded sample was also fractionated and it was found that the carbonyl indices of all fractions in the degraded sample were significantly higher compared to the undegraded sample. Molar masses of all fractions in the degraded sample were significantly lower compared to the fractions of the undegraded sample. The TREF analysis of the undegraded sample indicated that all fractions contained pentene. Most of the pentene was incorporated in the shorter chains. The broadening of the chemical composition distribution (seen in CRYSTAF) was confirmed to be due to the incorporation of various levels of carbonyl and hydroperoxide groups in the fractions.

CRYSTAF analysis of the fractions of the degraded and the undegraded sample showed that the CCDs of the fractions in the degraded polymer was significantly different from the fractions of the undegraded sample (typically broader CCD).

A thick polypropylene-1-pentene sample was microtomed into layers to determine the degradation profile. It was shown that the layers close to the surface were highly degraded. They had a significantly higher carbonyl concentration and lower molar mass than layers deeper into the sample. The CRYSTAF results again indicated that the most degraded layer had the broadest chemical composition distribution

Objective 3:

The third main objective was to study the degradation behaviour of laboratory-synthesised propylene-1-pentene samples. Polypropylene copolymer samples, containing up to 8% pentene, were synthesised in the laboratory and then evaluated for their thermo-oxidative stability. SEC results indicated that the molar masses of the undegraded samples were all within the same order of magnitude (between 68,000 and 96,000). DSC analysis of the undegraded samples indicated that the crystallinities of the propylene-1-pentene samples were significantly lower than that of the polypropylene homopolymer, synthesised under similar conditions. CRYSTAF also showed a significant difference in crystallisation behaviour between the undegraded samples. FTIR and SEC results indicated that samples degraded according to pentene content. SEC-FTIR analysis indicated that, again, most of the degradation products were concentrated in the low molar mass region.

Objective 4:

The fourth objective was to evaluate the multiple extrusion behaviour of a polypropylene homopolymer and contrast the behaviour with that of a propylene-1-pentene sample.

The multiple extrusion behaviour of a commercial propylene-1-pentene sample and a homopolymer sample was contrasted using a Brabender twin-screw laboratory extruder. The molar mass decreased significantly with an increasing number of extrusions. There was no increase in the carbonyl index and no changes in the pentene content and the crystallinity of these samples with degradation. It was shown that the multiple extrusion behaviour of the propylene-1-pentene and the polypropylene homopolymer samples were similar. This was in contrast with the thermo-oxidative behaviour. Comparing the effect of multiple extrusions on

the molar mass averages, a larger drop in the M_z values was found compared to the other molar mass averages. The M_n values showed a much smaller decrease with degradation. The decrease in the polydispersity index was shown to be primarily due to the decrease in the M_z values (longer chains). CRYSTAF analysis showed a small drop in the crystallisation temperature with degradation. Prep-TREF analysis showed that it was possible to fractionate a multiple extruded sample into fractions of highly scissioned (large drop in molar mass) and less scissioned (smaller drop in molar mass) material. The low crystallinity fractions were found to have a small drop in M_z and M_w values, while the higher crystallinity fractions showed a more significant reduction with multiple extrusions. The thermal properties of the fractions were found to be similar for the unextruded and the extruded sample.

The model developed by Prof Canevarolo (referenced in Chapters 3 and 8) indicated molar mass dependent scission over most of the molar mass distribution range and similar CSDF functions for the polypropylene homopolymer and copolymer.

9.2 Overall conclusions and recommendations for future work

The main aim of this project was to use novel analytical approaches to study degradation in polypropylene in order to provide more information on the degradation processes. In this dissertation it was shown that the use of SEC-FTIR, CRYSTAF and TREF fractionation will complement the results obtained by classical techniques like FTIR, DSC and SEC. Up to now, information was only obtained on the changes in chemical composition and molar mass with degradation. These values were only average values and it was not possible to make conclusions regarding the distribution of degradation products as a function of molar mass or changes in the chemical composition as a function of degradation time.

SEC-FTIR provide information on the distribution of the main degradation products (carbonyl containing degradation products) as a function of molar mass. CRYSTAF was also shown to be useful in studying degradation, as the changes in chemical composition distribution with degradation could be studied. It was shown that the propylene-1-pentene copolymers had a significantly different CRYSTAF behaviour (chemical composition distribution change) compared to the polypropylene homopolymer studied in this dissertation. With the methods developed in this study, it is now possible to obtain information on the changes in chemical composition as a function of molar mass and chemical composition distributions, in addition to the data obtained by the classical techniques during degradation in a polypropylene homopolymer or copolymer sample.

The current study has opened several potential fields of study. It is recommended that the current investigation be extended to the stabilised propylene-1-pentene systems. Stabilisers are incorporated into the amorphous phases in polyolefin samples, and it would be interesting to compare stabilised samples at different stages of degradation to see if there are any differences between the stabilised systems and the unstabilised systems.

With the methods now proven to be useful in studying polymer degradation (SEC-FTIR, CRYSTAF and TREF), several other polymer systems which were not covered in this study, could be investigated. A potential area may be the determination of the degradation behaviour of ethylene-propylene random copolymer systems. Ethylene-propylene random copolymers are produced commercially by numerous manufacturers.

Polyethylene degradation (thermo-oxidative degradation and thermo-mechanical degradation) is another potential field of study. Polyethylenes are typically more resistant to degradation compared to polypropylene, but will still degrade under the influence of external factors.

The information obtained in this dissertation may also enable studies into improving the stability of polymer systems. It was already shown that the incorporation of a small quantity of ethylene into a polypropylene sample (random ethylene-propylene sample) may improve the stability significantly.

Fractionation of a polyolefin sample (PP or PE) may be carried out, and these fractions may be degraded and studied individually to gain a deeper understanding of the contribution of each fraction towards the overall stability of the polymer.

A recently developed CRYSTAF detector (IR4 detector manufactured by Polymer Char) it may now be possible to evaluate the carbonyl absorption during the CRYSTAF run. Initial testing was carried out and looks promising. This may eliminate the need to use \TREF fractionation to obtain carbonyl distribution data.

The influence of metallocene catalysts on polyolefin stability is also another field of interest. For example, a propylene-1-pentene copolymer made with a metallocene catalyst will have a more even distribution of pentene as a function of molar mass (narrower chemical composition distribution as a function of molar mass compared to a Ziegler-Natta catalysed system.